Diabetic Retinopathy:

Economic Evaluation and Cellular Functions

Julia Ho Yee, TING

A thesis submitted for the degree of

Doctor of Philosophy

University of Technology, Sydney

2008

CERTIFICATE OF AUTHORSHIP/ORIGINALITY

I certify that the work in this thesis has not previously been submitted for a degree nor has it been submitted as part of requirements for a degree except as fully acknowledged within the text.

I also certify that the thesis has been written by me. Any help that I have received in my research work and the preparation of the thesis itself has been acknowledged. In addition, I certify that all information sources and literature used are indicated in the thesis.

Julia Ho Yee, Ting

B Medical Science (Hons)

B Business

Acknowledgement

This thesis would not be possible without my supervisors, who are always so reassuring and supportive. ***Professor Donald Martin*** from the Fondation « Nanosciences aux limites de la nanoélectronique », Université Joseph Fourier, TIMC-GMCAO, La Tronche, France, who always have interesting solutions to all my problems. And ***Associate Professor Marion Haas*** from Centre for Health Economics Research and Evaluation, Faculty of Business, University of Technology, Sydney, who is always ever so helpful to answer my millions of questions.

I would like to thank ***Mr. Michael Simpson*** from Royal Blind Society for his valuable input into the costing of blindness; the ***Royal Australian and New Zealand College of Ophthalmologists*** (RANZCO) for allowing me to view the "Ophthalmology Workforce Model" report developed by Access Economic Pty Ltd for RANZCO (2006). I would also like to thank ***DR Murray Killingsworth*** from Electron Microscopy Laboratory, South Western Area Pathology Service, Liverpool, NSW, Australia for processing, sectioning and TEM imaging of the polyelectrolyte capsules. ***Mr. Paul Fanos*** and ***Greg Dalsanto*** from the UTS Science workshop, who built and repaired many vital experimental equipments; and ***DR Hedayetul Islam*** who made the titanium and titanium nitride thin films.

I would like to give my deepest gratitude to our Bionano group. ***DR Stella Valenzuela***, who juggle four hundred million things but is still able to look out and look after us; ***DR Loraine Holley*** who never seize to amaze me with her ability to learn completely new things; ***DR Bruce Cornell*** – the fountain of knowledge especially that related to physics. My fellow PhD students, **DR *Dakrong Pissuwan***, ***Kanthi Lewis*** and ***Joshua Chou*** who boast the morale in our laboratory.

The support staffs from the old Department of Health Sciences, the current Department of Medical and Molecular Biosciences (***Phil Lawerence***, ***Mike Johnson*** and ***June Treerat***) as well as Technical Services (***Bill Booth***) are excellent. They have made my research life much easier.

I would also like to thank my fellow colleagues from our stifling office (***Michelle Little***, ***Dorothy Curnow***, ***Monique Windley***, ***Ben Blacklow*** and ***Francesca Marcon***) who shared my joys and pains of being a postgraduate student and part time academic.

And last but not least, I like to thank my family and friends. Thank you **Mum** and **Dad**, for putting up with me while I pursue my studies. I would like to thank my fiancé, **Alex**, for all his emotional support and part-time slavery. And thank you ***Amy + Henry, Alice, Tonhi, Fran, Sophie + TC, Thidz, Lisa, Christine*** and **Victor** for bringing a smile to my face when all seem too difficult.

Lastly, I would also like to apologise to all my family and friends for neglecting them during my PhD candidature.

Publications arising from this thesis

Ting, J., Martin, D. & Haas, M. 2007, 'A Markov Model of Diabetic Retinopathy Progression for the Economic Evaluation of a Novel DR Prognostic Device', CHERE Working Paper, vol. 2007, no. 14.

Ting, J. & Martin, D. 2006, 'Basic and Clinical Aspects of Gene Therapy for Retinopathy Induced by Diabetes', Current Gene Therapy, vol. 6, no. 2, pp. 193-214.

Table of Content

List of Figures

List of Tables

List of Abbreviations

3D	Three Dimensional	**DR**	Diabetic Retinopathy
3T3-L1	Mouse Embryonic Adipose-Like Fibroblast	**HRQoL**	Health Related Quality Of Life
AFM	Atomic Force Microscopy	**ECM**	Extracellular Matrix
AGE	Advanced Glycation End Product	**EDTA**	Ethylenediaminetetraacetic Acid
AIHW	Australian Institute Of Health And Welfare	**EGTA**	Ethylene Glycol Tetraacetic Acid
ALP	Alkaline Phosphatase	**ESEM**	Environmental Scanning Electron Microscope
ANOVA	Analysis Of Variance	**FAK**	Focal Adhesion Kinase
Ar	Argon gas	**FBS**	Fetal Bovine Serum
BMI	Body Mass Index	**FGF**	Fibroblast Growth Factors
BSA	Bovine Serum Albumin	**FITC**	Fluorescein isothiocyanate
CAM	Cell Adhesion Molecules	**FPG**	Fasting Plasma Glucose
CFDA	5-Carboxyfluorescein diacetate	$\mathbf{Hb_{A1c}}$	Glycosylated Hemoglobin
CVD	Cardiovascular Disease	**HBS**	HEPES buffered Saline
DM	Diabetes Mellitus	**HCl**	Hydrochloric acid
DMEM	Dulbecco's Modified Eagle's Medium	**HCS 2/8**	Human Chondrocyte Cell
DNA	Deoxyribonucleic Acid	**HEK 293**	Human Embryonic Kidney 293 Cells

HUVEC	Human Umbilical Vein Endothelial Cells	**nSTDR**	Non-Sight Threatening Diabetic Retinopathy
ICER	Incremental Cost Effectiveness Ratio	**OAA**	Optometrists Association Australia
IGT	Impaired Glucose Tolerance	**OGTT**	Oral Glucose Tolerance Test
IL-8	Interleukin-8	**PAA**	Poly(Acrylic Acid)
LBL	Layer-By-Layer	**PAH**	Poly(Allylamine Hydrochloride)
LY	Life Years	**PBAC**	Pharmaceutical Benefits Advisory Committee
MA	Micro-Aneurysm	**PBS**	Phosphate Buffered Saline
MBS	Medicare Benefit Schedule	**PBS**	Pharmaceutical Benefits Schedule
ME	Maculopathy	**PDDA**	Poly(Diallyldimethylammonium Chloride)
mfERG	Multifocal Electroretinogram	**PDGF**	Platelet-Derived Growth Factor
MSAC	Medical Services Advisory Committee	**PD-L**	PEriodontal Ligament Cells
N_2	Nitrogen gas	**PDR**	Proliferative Diabetic Retinopathy
NaCl	Sodium Chloride	**PE**	Polyelectrolyte
NaOH	Sodium hydroxide	**PEI**	Polyethylenimine
NHMRC	National Health And Medical Research Council	**PEM**	Polyelectrolyte Multi-Layers
nPDR	Non-Proliferative Diabetic Retinopathy	**PE-PAH**	Polyelectrolyte Capsule With PAH As The Start Coating Material

PE-PSS	Polyelectrolyte Capsule With PSS As The Start Coating Material	**SWAP**	Short Wavelength Automated Perimetry
PI	Propidum Iodide	**SY**	Sight Years
pKa	Acid Dissociation Constant	**TCP**	Tissue Culture Plastic
pNPP	Alkaline Phosphatase Yellow	**TGF**	Transforming Growth Factor
pre-DM	Pre-Diabetes Mellitus	**Ti**	Titanium
pre-DR	Pre-Diabetic Retinopathy	**TiN**	Titanium Nitride
PSS	Poly(Sodium 4-Styrene Sulfonate)	**TiN120**	Titanium Nitride Thin Film Made With 120 Watts
QALY	Quality Adjusted Life Years	**TiN190**	Titanium Nitride Thin Film Made With 190 Watts
QoL	Quality Of Life	**TNF α**	Tumour Necrosis Factor A
Ra	Average Roughness	**UKPDS**	UK Prospective Diabetes Study
RAW	Mouse Leukaemic Monocyte Macrophage	**VEGF**	Vascular Endothelial Growth Factor
RCT	Randomized Controlled Trial	**VIPP**	Vision Impairment Prevention Program
RMS	Root Mean Square Of Roughness	**WESDR**	Wisconsin Epidemiological Study Of Diabetic Retinopathy
RNAse	Ribonuclease		
STDR	Sight Threatening Diabetic Retinopathy		

Abstract

This thesis reports an investigation from the “bedside” back to the “bench”. That is, from the economic evaluation of a medical intervention to basic research and development of a contractility assay. The underlying theme of this thesis is cellular contractility, which was stimulated from our laboratory’s work in the microvascular complications of Diabetic Retinopathy (DR).

The health economic perspective of this thesis evaluates the cost effectiveness and cost utility of DR prognosis using the prog-DR test. This novel prognostic test developed in our laboratory relies on the contractile response of blood vessels to detect subjects with high risk of developing DR. Markov modeling based on information in the literature was used to estimate the outcomes of a hypothetical population. The costs, health and utility outcomes of DR were compared to the potential outcomes if the prog-DR test was used. The model show that the prog-DR test can improve the health of the hypothetical population as measured in the number of life years (LY), sight years (SY) and quality-adjusted life years (QALY). The prog-DR test was more cost effective than the benchmark of annual or bi-annual screening and the incremental cost effectiveness ratio (ICER) appears to be at an acceptable level. Scenario and sensitivity analysis also show that the cost effectiveness of the prog-DR test can be improved by (i) better blood glucose management post prog-DR test, (ii) targeted screening (as opposed to population-wide screening) and (iii) reduced costs of both screening and management of DM and DR.

The physiological perspective of the thesis aimed to develop a contractility assay for DR that was based on a 3D scaffold, which was affordable, easy to make and mimicked the three dimensional physiological environment of blood vessels. The contractility assay was developed using a 3D, hollow scaffold (PE-PAH capsule) and involved (i) the selection of the optimal core material, (ii) optimisation of the manufacturing process, (iii) characterisation of the scaffold and (iv) ensuring that cells can be grown on it. The cyto-biocompatibility of the candidate polyelectrolyte Poly(Sodium 4-Styrene Sulfonate) (PSS) and Poly(Allylamine Hydrochloride) (PAH) in the thin films format were investigated using three different cell lines and the effects of these thin films were also

compared to titanium and titanium nitride thin films. In essence, PSS and PAH are not cytotoxic and was used to develop the contractile scaffold, PE-PAH capsule. This scaffold is relative elastic and the contractile force exerted by the 3T3-L1 cells was calculated based on the deformation of the PE-PAH capsule. The contractility assay was sufficiently sensitive to detect the nano-Newton magnitude of force developed by individual cells and discriminated the change in force due to disruption of the F-actin cytoskeleton by forskolin and cytochalasin D.

Chapter 1: Introduction

Diabetes Mellitus (DM) is a complicated disease; both genetic and environmental factors contribute to its development. DM can be classified as Type I or Insulin Dependent Diabetes Mellitus where the pancreatic beta cells are unable to secrete sufficient amounts of insulin for normal body function; and Type II or Non-insulin Dependent Diabetes Mellitus where the body is unable to respond appropriately to the action of insulin. In both types of DM there is a chronic elevation of blood glucose concentration, which damages many of the body's systems, in particular, blood vessels and nerves. Such damage has the potential to result in many debilitating complications such as cardiovascular disease, nephropathy, neuropathy and retinopathy.

Diabetic Retinopathy (DR) is a progressive micro-vascular complication of both Type I and II Diabetes Mellitus (DM). In essence, retinal blood vessels are damaged by high blood glucose and they become leaky and occluded, forming micro-aneurysm in the non-proliferative stage. The retina tries to compensate for these unhealthy blood vessels by growing new ones (angiogenesis) in the proliferative stage. However the proliferating blood vessels are not healthy and often cause more damage in the retina. That has devastating effects on vision, causing patients to see specks and spots; and if the macula becomes damaged or the retina detaches, the patient might become blind.

Quality of life for those who suffer from DM and diabetic co-morbidities are reduced (Brown et al. 2000; Coffey et al. 2002; Holmes et al. 2000). The loss in vision is one of the most feared disabilities/illnesses (Borland, Donaghue & Hill 1994; Lau et al. 2004). In comparison to hearing loss, the loss of vision is more likely to affect psychological health and even lead to suicide (De Leo et al. 1999).

The AusDiab Study Group found that 15.3% of Diabetics have DR (Tapp et al. 2003). In 1998 the Commonwealth Government committed $2.3 for the Vision Impairment Prevention Program (VIPP) to reduce the incidence and provide management of DR (Commonwealth Department of Health and Ageing 2002). Yet, according to the Diabesity study 7.4% of the Australian population are

Diabetics and 16.4% are pre-Diabetic and these numbers are expected to rise (Dunstan et al. 2001).

It was estimated that the Diabetes Mellitus costs Australians up to $6 billion each year (Colagiuri et al. 2003) which accounts for 5% of the total burden of disease (Marks, Coyne & Pang 2001). DR is one of the most common cause of blindness in the working-age (30-69) group (Constable 1999; Donnelly et al. 2000), which greatly reduces the workforce participation and leads to a loss in productivity (Ng, Jacobs & Johnson 2001).

Therefore DR has immense economic, societal and personal impacts. Consequently, in seeking a better understanding in DR in order to try to prevent and cure DR there are numerous research studies undertaken from all around the globe, including Australia, the UK, US as well as China and Japan. Those research studies range from basic sciences on cellular functions, epidemiology studies, genetic pre-disposition studies, clinical research and health economic studies on potential prevention and treatment regimes.

The pathophysiological process of DR may be described as the inability of the retinal blood vessels to control blood flow (Antonetti et al. 1998; Deng et al. 1999; Hughes et al. 2004) because high blood glucose damage the endothelial cells which line the retinal blood vessels and pericytes, the support cells that wrap around the endothelial cells. Endothelial cells are responsible for the integrity and permeability of the blood-retina barrier whereas Pericytes are responsible for the control of growth, contraction and survival of endothelial cells, especially under stress conditions (Hammes et al. 2002).

When the endothelial cells are damaged the permeability of the retinal vessels is increased. The increase in endothelial permeability allows fluid accumulation (oedema), protein and blood leakage into the vitreous (hemorrhages). These leakages and endothelial dysfunction then contribute to the occlusion and obliteration of the capillaries, thereby decreasing the permeability and perfusion to the site of damage, causing ischemia and cell death. The death of endothelial cells may lead to the formation of acellular capillaries whereas ischemia may result in neovascularisation.

Damage to and death of pericytes may lead to endothelial cell migration, growth and dysfunction (Hellstrom et al. 2001)and the absence of pericytes correlates with endothelial hyperplasia, increase capillary diameter and abnormal endothelial morphology (Hellstrom et al. 2001). Unlike other organs, there are a high number of pericytes in the retina microvasculature (Frank, Turczyn & Das 1990), which suggests the functional importance of these cells to the retina. The pericyte-to-endothelial cell ratio is 1:1 in the retina, as compared to a ratio of 1:10 in other microvasculature beds (Chakravarthy & Gardiner 1999)

Although many DR pathophysiological pathways have been identified, and numerous potential targets for the prevention and treatment have been found (Ting & Martin 2006), a cure for DR or DM is yet to be developed. There are various hypotheses which explain the damaging effects of DM which can restrict blood vessels from contracting and relaxing (Bandopadhyay et al. 2001; Gillies & Su 1993; Wheatcroft et al. 2003) and may ultimately lead to cell apoptosis (Artwohl et al. 2003; Li et al. 1997; Podesta et al. 2000). Those detrimental effects may be brought about by oxidation damage (Baynes & Thorpe 1999; Obrosova et al. 2003; Wen et al. 2002), direct activation of protein kinase C via synthesis of diacylglycerol from glucose (Ido, Carling & Ruderman 2002; Lee et al. 1989; Setter, Campbell & Cahoon 2003), advanced glycation end product (AGE) formation (Chen, Jiang & Tang 2003; Stitt et al. 2004; Yamagishi et al. 2002), damages through the Polyol Pathway and hypertension (Dosso, Leuenberger & Rungger-Brandle 1999; Wallow et al. 1993)

Occlusion caused by the formation of micro-thromboses which may block retinal capillaries (Boeri, Maiello & Lorenzi 2001; Wautier 1986) and leukostasis, the adhesion and attraction of leukocytes, which may cause inflammation in retinal capillaries (Miyamoto et al. 1998; Wautier 1986; Weill et al. 1995; Zhang, Gerhardinger & Lorenzi 2002) have been shown to cause changes in the microvasculature (Danis & Wallow 1987; Wallow et al. 1991) hence affect the ability of blood vessels to control blood flow.

Although there are many theories for the pathological development of DR, there is one underlying common theme or physiological mechanism. That underlying physiological mechanism is cellular contraction, and which is the focus for the

physiological studies described in this thesis. The work in our laboratory as well as in others has shown that cellular contractile function is affected by high glucose. For example, high glucose alter the contractile function of retinal pericyte (Aiello et al. 1994; Gillies & Su 1993; McGinty et al. 1999) and endothelial cells (Gillies et al. 1997) .

These research studies prompted our laboratory to develop the prog-DR prognostic test for DR which is currently under patent (Martin & Markhotina 2002) and further discussed in the Chapter 5. The test is based on the physiological premise that under normal conditions, retinal blood vessels observed by a fundoscope are able to contract and relax when stressed with specific drugs. Damaged retinal blood vessels have attenuated responses to the specific drugs, and hence microvascular disease such as DR can be identified using a physiological response rather than from a chemical blood test.

There are other clinical tools which can be used to predict the progression of DR, such as the multifocal electroretinogram (mfERG), vascular caliber analysis and short wavelength automated perimetry (SWAP). As reviewed by Hood (2000) and Lai et al (2007), mfERG is a form of electroretinogram where the focal electrical activity in multiple areas in the retina, predominately, photoreceptors (rods and cones), inner retinal cells (bipolar and amacrine cells), and the ganglion cells are examined. This application is very useful to assess retinal function/dysfunction and to identify the site of abnormality, whether the damage was cone receptor, bipolar cells or ganglion cells in original as reviewed by Hood (2000). Many authors have reported the use of mfERG to identify diabetic persons with or without non-proliferative DR (Bearse et al. 2004a; Bearse et al. 2004b; Bronson-Castain et al. 2007) as well as diabetic without retinopathy (Fortune, Schneck & Adams 1999; Han et al. 2004a; Han et al. 2004b; Han et al. 2004c) and it has been shown that through modeling, the development of DR within 1 (Han et al. 2004d) and 3 years (Ng et al. 2008) can be predicted.

Vascular caliber analysis is the use of non-invasive retinal imaging technique to measure and examine the arteriolar and venular calibers. It can be used to identify persons with diabetes with or without retinopathy because diabetes is

associated with dilated retinal arteriolar and venular calibers and the increasing severity of DR is associated with the further dilation of retinal venular caliber (Kifley et al. 2007; Nguyen et al. 2008; Tikellis et al. 2007).

SWAP is a form of perimetry, a visual field test which systematically measure the differential light sensitivity in the visual field by the detection of the presence of test targets on a defined background. SWAP is designed to assess the function of short-wavelength-sensitive mechanisms in the eye by using a two-color increment threshold procedure (blue-on-yellow). It has used to monitor the visual function of diabetic patients with various degree of retinopathy (Bengtsson, Hellgren & Agardh 2008; Han et al. 2004a; Remky et al. 2003) and maculopathy (Remky et al. 2003).

These clinical tools are very useful in their own right; however, the prog-DR test is likely to have additional advantages. The prog-DR test is more useful for the early detection of DR as compared to SWAP because it can detect pathological development before visual function is affected. In comparison to mfERG, the prog-DR test examines the direct source of pathophysiology, the blood vessels, whereas mfERG measures predominately the function of the electrically active tissues of the retina. As reviewed by Bearse et al (2006), the site of functional abnormalities detected by mfERG precedes the development of retinopathy, which enhance early diagnosis, but as reviewed Lai et al (2007) mfERG results may also be altered by the presence of cataract, different refractive errors and axial length presence in the patient. Vascular caliber analysis and the prog-DR test can bypass this pitfall as retinal imaging is not greatly affected by the presence of cataract, different refractive error and axial length.

The early detection of DR in vascular caliber analysis is based on structural changes in the retinal blood vessels, where retinal arteriolar and venular vessels are permanently widen. The prog-DR test may be more favourable as it is based on the acute functional changes in the retinal blood vessels which is likely to precede permanent structural changes, therefore allowing earlier detection of pathological developments.

This thesis describes my investigations of two important aspects of the prog-DR test for DR developed in our laboratory. The first aspect is a health economic evaluation of whether DR prognosis, such as via the use of the prog-DR test, is worthwhile. The second aspect is the development of an assay that allows for the physiological evaluation of the mechanisms that affect the contractility of the retinal microvascular cells.

To investigate the first aspect of my investigation, an economic evaluation was performed, which forms the health economic perspective of this thesis. In essence, a cost-effectiveness and cost-utility analysis were performed by comparing the costs, health and utility outcomes of DR to the potential outcomes if the prog-DR test was used. These outcomes were estimated through Markov modeling and are described in detail in chapter 2 and 3 of the thesis.

The investigation in the second aspect of my thesis was addressed by studies involving microvascular cells from bovine retinae. Although microvascular cells can be extracted and experimented on, more often than not these cells remain in their 3 dimensional vascular forms before spreading into a mono-layer. These cells also have a preference to form 3D structures or tubules in collagen and Matrigel in a process regulated by various growth factors such as Platelet-derived growth factor (PDGF), Vascular endothelial growth factor (VEGF), Transforming growth factor (TGF), Fibroblast growth factors (FGF), as well as angiopoietin, integrins, cadherin and so on as reviewed by Distler et al (2003).

Pericytes are known to be morphologically heterogeneous, biochemically and physiologically heterogeneous (Shepro & Morel 1993). Pericytes are heterogeneous in their expression of smooth muscle isoform of alpha-actin (Nehls & Drenckhahn 1991) and ion channel activities (Matsushita & Puro 2006) depending on their location on the micro-vessel. Endothelial cells also differ in response to acetylcholine and histamine (Huang et al. 2000) as well as to shear stress (Hong et al. 2006). That is, blood vessel contraction and relaxation is a team effort from heterogeneous units and heterogeneous responses. Therefore, assays of vascular function, specifically for cell contraction, which

involve a large number of cells enhance an understanding of the real physiological environment that has been developed from single-cell responses.

It became apparent that there is a need to perform research of the vascular cells in a 3 dimensional format for optimal results that closely resemble the natural state of these cells. Hence the physiological perspective of this thesis revolved around the investigation for potential surfaces and structures for this purpose.

The two questions being investigated in this thesis can be thought to be on opposite ends of the spectrum of biomedical research. That spectrum is commonly considered as “bench-to-bedside”. The “bedside” stage of clinical research is of course when a medical production is made available to the patients. The “bench” is when fundamental research is carried out in the laboratory, to further understand the disease and or the mechanism of the intervention. The health economic perspective can be thought as the “bedside” stage. In this section of the thesis, cost effectiveness and cost utility of the prog-DR test, the novel device for DR prognosis based on the basis of vascular *contractility,* were evaluated. It involved the modeling of DR progression, cost and utility. The “physiological” perspectives can be thought to be the “bench” stage and it aimed to develop a 3D scaffold which resembled the native physiological condition of vascular cell were designed specifically for *contraction* experiments. It involved cyto-biocompatibility testing of the candidate material and the engineering of this 3D scaffold. Although these two approaches or bodies of work are very different and utilize completely different skill sets and methods, these were carried out to investigate the clinical consequences and physiological basis for the common underlying theme of *cellular contraction*.

References

Aiello, L.P., Robinson, G., Lin, Y., Nishio, Y. & King, G. 1994, 'Identification Of Multiple Genes In Bovine Retinal Pericytes Altered By Exposure To Elevated Levels Of Glucose By Using Mrna Differential Display', *Proceedings Of The National Academy Of Sciences Of The United State Of America*, Vol. 91, pp. 6231-6235.

Antonetti, D., Barber, A., Khin, S., Lieth, E., Tarbell, J. & Gardner, T. 1998, 'Vascular Permeability In Experimental Diabetes Is Associated With Reduced Endothelial Occludin Content: Vascular Endothelial Growth Factor Decreases Occludin In Retinal Endothelial Cells.' *Diabetes*, Vol. 47, No. 12, pp. 1953-1959.

Artwohl, M., Graier, W., Roden, M., Bischof, M., Freudenthaler, A., Waldhausl, W. & Baumgartner-Parzer, S. 2003, 'Diabetic LDL Triggers Apoptosis In Vascular Endothelial Cells.' *Diabetes*, Vol. 52, No. 5, P. 1240.

Bandopadhyay, R., Orte, C., Lawrenson, J.G., Reid, A.R., De Silva, S. & Allt, G. 2001, 'Contractile Proteins In Pericytes At The Blood-Brain And Blood-Retinal Barriers', *Journal Of Neurocytology*, Vol. 30, No. 1, pp. 35-44.

Baynes, J. & Thorpe, S. 1999, 'Role Of Oxidative Stress In Diabetic Complications: A New Perspective On An Old Paradigm', *Diabetes*, Vol. 48, No. 1, pp. 1-9.

Bearse, J.M.A., Adams, A.J., Han, Y., Schneck, M.E., Ng, J., Bronson-Castain, K. & Barez, S. 2006, 'A Multifocal Electroretinogram Model Predicting The Development Of Diabetic Retinopathy', *Progress In Retinal And Eye Research*, Vol. 25, No. 5, pp. 425-448.

Bearse, M.A., Jr., Han, Y., Schneck, M.E. & Adams, A.J. 2004a, 'Retinal Function In Normal And Diabetic Eyes Mapped With The Slow Flash Multifocal Electroretinogram', *Investigative Ophthalmology & Visual Science*, Vol. 45, No. 1, pp. 296-304.

Bearse, M.A., Jr., Han, Y., Schneck, M.E., Barez, S., Jacobsen, C. & Adams, A.J. 2004b, 'Local Multifocal Oscillatory Potential Abnormalities In Diabetes And Early Diabetic Retinopathy', *Investigative Ophthalmology & Visual Science*, Vol. 45, No. 9, pp. 3259-3265.

Bengtsson, B., Hellgren, K.-J. & Agardh, E. 2008, 'Test-Retest Variability For Standard Automated Perimetry And Short-Wavelength Automated Perimetry In Diabetic Patients', *Acta Ophthalmologica* Vol. 86, No. 2, pp. 170-176.

Boeri, D., Maiello, M. & Lorenzi, M. 2001, 'Increased Prevalence Of Microthromboses In Retinal Capillaries Of Diabetic Individuals.' *Diabetes*, Vol. 50, pp. 1432-1439.

Borland, R., Donaghue, N. & Hill, D. 1994, 'Illnesses That Australians Most Feared In 1986 And 1993', *Australian Journal Of Public Health*, Vol. 18, No. 4, pp. 366-369.

Bronson-Castain, K.W., Bearse, M.A., Jr., Han, Y., Schneck, M.E., Barez, S. & Adams, A.J. 2007, 'Association Between Multifocal ERG Implicit Time Delays And Adaptation In Patients With Diabetes', *Investigative Ophthalmology & Visual Science*, Vol. 48, No. 11, pp. 5250-5256.

Brown, G., Brown, M., Sharma, S., Brown, H., Gozum, M. & Denton, P. 2000, 'Quality Of Life Associated With Diabetes Mellitus In An Adult Population', *Journal Of Diabetes And Its Complications*, Vol. 14, No. 1, pp. 18-24.

Chakravarthy, U. & Gardiner, T. 1999, 'Endothelium-Derived Agents In Pericyte Function/Dysfunction', *Progress In Retinal And Eye Research*, Vol. 18, No. 4, pp. 511-527.

Chen, B., Jiang, D. & Tang, L. 2003, 'Advanced Glycation End Products Induce Apoptosis And Expression Of Apoptotic Genes In Cultured Bovine Retinal Capillary Pericytes', *Chinese Journal Of Ophthalmology.*, Vol. 39, No. 4, pp. 224-247.

Coffey, J.T., Brandle, M., Zhou, H., Marriott, D. & Al, E. 2002, 'Valuing Health-Related Quality Of Life In Diabetes', *Diabetes Care*, Vol. 25, No. 12, P. 2238.

Colagiuri, S., Colagiuri, R., Conway, B., Grainger, D. & Davey, P. 2003, *Diabco$T Australia: Assessing The Burden Of Type 2 Diabetes In Australia*, Canberra.

Commonwealth Department Of Health And Ageing 2002, *National Diabetes Strategy: Vision Impairment Prevention Program*, Priorities And Quality Branch, Commonwealth Department Of Health And Ageing, Viewed 29/10/2003 2003 <http://www.dhac.gov.au/pq/diabetes/vipp.htm>.

Constable, I. 1999, 'Diabetic Retinopathy: Pathogenesis, Clinical Features And Treatment', In J. Turtle, T. Kaneko & S. Osato (Eds), *Diabetes In The New Millennium.*, Endocrinology And Diabetes Research Foundation, University Of Sydney, Sydney, pp. 365-385.

Danis, R. & Wallow, I. 1987, 'Microvascular Changes In Experimental Branch Retinal Vein Occlusion', *Ophthalmology*, Vol. 94, No. 10, pp. 1213-1221.

De Leo, D., Hickey, P.A., Meneghel, G. & Cantor, C.H. 1999, 'Blindness, Fear Of Sight Loss, And Suicide', *Psychosomatics*, Vol. 40, pp. 339-344.

Deng, D., Evans, T., Mukherjee, K., Downey, D. & Chakrabarti, S. 1999, 'Diabetes-Induced Vascular Dysfunction In The Retina: Role Of Endothelins', *Diabetologia*, Vol. 42, No. 10, pp. 1228-1234.

Distler, J., Hirth, A., Kurowska-Stolarska, M., Gay, R., Gay, S. & Distler, O. 2003, 'Angiogenic And Angiostatic Factors In The Molecular Control Of Angiogenesis', *Radiopharmacology*, Vol. 47, No. 3, P. 149.

Donnelly, R., Emslie-Smith, A., Gardner, I. & Morris, A. 2000, 'ABC Of Arterial And Venous Disease. Vascular Complications Of Diabetes.' *British Medical Journal*, Vol. 320, pp. 1062-1066.

Dosso, A.A., Leuenberger, P.M. & Rungger-Brandle, E. 1999, 'Remodeling Of Retinal Capillaries In The Diabetic Hypertensive Rat', *Investigative Ophthalmology & Visual Science*, Vol. 40, No. 10, pp. 2405-2410.

Dunstan, D., Zimmet, P., Welborn, T., Sicree, R., Armstrong, T., Atkins, R., Cameron, A., Shaw, J., Chadban, S. & On Behalf Of The Ausdiab Steering Committee 2001, *Diabesity And Associated Disorders In Australia - 2000: The Accelerating Epidemic. The Australian Diabetes, Obesity And Lifestyle Report.*, International Diabetes Institute, Melbourne.

Fortune, B., Schneck, M.E. & Adams, A.J. 1999, 'Multifocal Electroretinogram Delays Reveal Local Retinal Dysfunction In Early Diabetic Retinopathy', *Investigative Ophthalmology & Visual Science*, Vol. 40, No. 11, pp. 2638-2651.

Frank, R., Turczyn, T. & Das, A. 1990, 'Pericyte Coverage Of Retinal And Cerebral Capillaries', *Investigative Ophthalmology & Visual Science*, Vol. 31, No. 6, pp. 999-1007.

Gillies, M. & Su, T. 1993, 'High Glucose Inhibits Retinal Capillary Pericyte Contractility In Vitro', *Investigative Ophthalmology & Visual Science*, Vol. 34, No. 12, pp. 3396-3401.

Gillies, M., Su, T., Stayt, J., Simpson, J., Naidoo, D. & Salonikas, C. 1997, 'Effect Of High Glucose On Permeability Of Retinal Capillary Endothelium In Vitro.' *Investigative Ophthalmology & Visual Science*, Vol. 38, No. 3, pp. 635-642.

Hammes, H., Lin, J., Renner, O., Shani, M., Lundqvist, A., Betsholtz, C., Brownlee, M. & Deutsch, U. 2002, 'Pericytes And The Pathogenesis Of Diabetic Retinopathy.' *Diabetes*, Vol. 51, No. 10, pp. 3107-3112.

Han, Y., Adams, A.J., Bearse, M.A., Jr. & Schneck, M.E. 2004a, 'Multifocal Electroretinogram And Short-Wavelength Automated Perimetry Measures In Diabetic Eyes With Little Or No Retinopathy', *Arch Ophthalmol*, Vol. 122, No. 12, pp. 1809-1815.

Han, Y., Bearse, M.A., Jr., Schneck, M.E., Barez, S., Jacobsen, C. & Adams, A.J. 2004b, 'Towards Optimal Filtering Of "Standard" Multifocal Electroretinogram (Mferg) Recordings: Findings In Normal And Diabetic Subjects', *Br J Ophthalmol*, Vol. 88, No. 4, pp. 543-550.

Han, Y., Bearse, M.A., Jr., Schneck, M.E., Barez, S., Jacobsen, C.H. & Adams, A.J. 2004c, 'Multifocal Electroretinogram Delays Predict Sites Of Subsequent Diabetic Retinopathy', *Investigative Ophthalmology & Visual Science*, Vol. 45, No. 3, pp. 948-954.

Han, Y., Schneck, M.E., Bearse, M.A., Jr., Barez, S., Jacobsen, C.H., Jewell, N.P. & Adams, A.J. 2004d, 'Formulation And Evaluation Of A Predictive Model To Identify The Sites Of Future Diabetic Retinopathy', *Investigative Ophthalmology & Visual Science*, Vol. 45, No. 11, pp. 4106-4112.

Hellstrom, M., Gerhardt, H., Kalen, M., Li, X., Eriksson, U., Wolburg, H. & Betsholtz, C. 2001, 'Lack Of Pericytes Leads To Endothelial Hyperplasia And Abnormal Vascular Morphogenesis', *Journal Of Cell Biology*, Vol. 153, No. 3, pp. 543-554.

Holmes, J., Mcgill, S., Kind, P., Bottomley, J., Gillam, S. & Murphy, M. 2000, 'Health-Related Quality Of Life In Type 2 Diabetes (T2ARDIS-2)', *Value In Health*, Vol. 3, No. S1, pp. 47-51.

Hong, D., Jaron, D., Buerk, D.G. & Barbee, K.A. 2006, 'Heterogeneous Response Of Microvascular Endothelial Cells To Shear Stress', *American Journal Of Physiology - Heart And Circulatory Physiology*, Vol. 290, No. 6, pp. H2498-2508.

Hood, D.C. 2000, 'Assessing Retinal Function With The Multifocal Technique', *Progress In Retinal And Eye Research*, Vol. 19, No. 5, pp. 607-646.

Huang, T.Y., Chu, T.F., Chen, H.I. & Jen, C.J. 2000, 'Heterogeneity Of $[Ca^{2+}]_I$ Signaling In Intact Rat Aortic Endothelium', *FASEB Journal*, Vol. 14, No. 5, pp. 797-804.

Hughes, S.-J., Wall, N., Scholfield, C.N., Mcgeown, J.G., Gardiner, T.A., Stitt, A.W. & Curtis, T.M. 2004, 'Advanced Glycation Endproduct Modified Basement Membrane Attenuates Endothelin-1 Induced $[Ca^{2+}]_I$ Signalling And Contraction In Retinal Microvascular Pericytes', *Molecular Vision*, Vol. 10, pp. 996-1004.

Ido, Y., Carling, D. & Ruderman, N. 2002, 'Hyperglycemia-Induced Apoptosis In Human Umbilical Vein Endothelial Cells: Inhibition By The AMP-Activated Protein Kinase Activation.' *Diabetes*, Vol. 51, No. 1, P. 159.

Kifley, A., Wang, J.J., Cugati, S., Wong, T.Y. & Mitchell, P. 2007, 'Retinal Vascular Caliber, Diabetes, And Retinopathy', *American Journal Of Ophthalmology*, Vol. 143, No. 6, pp. 1024-1026.

Lai, T.Y.Y., Chan, W.-M., Lai, R.Y.K., Ngai, J.W.S., Li, H. & Lam, D.S.C. 2007, 'The Clinical Applications Of Multifocal Electroretinography: A Systematic Review', *Survey Of Ophthalmology*, Vol. 52, No. 1, pp. 61-96.

Lau, J., Lee, V., Fan, D., Lau, M. & Michon, J. 2004, 'Attitudes Towards And Perceptions Of Visual Loss And Its Causes Among Hong Kong Chinese Adults', *Clinical And Experimental Ophthalmology*, Vol. 32, No. 3, pp. 243-250.

Lee, T., Hu, K., Chao, T. & King, G. 1989, 'Characterization Of Endothelin Receptors And Effects Of Endothelin On Diacylglycerol And Protein Kinase C In Retinal Capillary Pericytes', *Diabetes*, Vol. 38, No. 12, pp. 1643-1646.

Li, W., Yanoff, M., Liu, X. & Ye, X. 1997, 'Retinal Capillary Pericyte Apoptosis In Early Human Diabetic Retinopathy', *Chinese Medical Journal*, Vol. 110, No. 9, pp. 659-663.

Marks, G.C., Coyne, T. & Pang, G. 2001, *Type 2 Diabetes Costs In Australia: The Potential Impact Of Changes In Diet, Physical Activity And Levels Of Obesity*, Australian Food And Nutrition Monitoring Unit, Canberra.

Martin, D.K. & Markhotina, N. 2002, 'Novel Screens To Identify Agents That Modulate Retinal Blood Vessel Function And Pericyte Function And Diagnostic And Therapeutic Application Therefore', World WO03103771.

Matsushita, K. & Puro, D.G. 2006, 'Topographical Heterogeneity Of KIR Currents In Pericyte-Containing Microvessels Of The Rat Retina: Effect Of Diabetes', *Journal Of Physiology*, Vol. 573, No. Pt 2, pp. 483–495.

Mcginty, A., Scholfield, C.N., Liu, W.-H., Anderson, P., Hoey, D.E.E. & Trimble, E.R. 1999, 'Effect Of Glucose On Endothelin-1-Induced Calcium Transients In Cultured Bovine Retinal Pericytes', *Journal Of Biological Chemistry*, Vol. 274, No. 36, pp. 25250-25253.

Miyamoto, K., Hiroshiba, N., Tsujikawa, A. & Ogura, Y. 1998, 'In Vivo Demonstration Of Increased Leukocyte Entrapment In Retinal Microcirculation Of Diabetic Rats', *Investigative Ophthalmology & Visual Science*, Vol. 39, No. 11, pp. 2190-2194.

Nehls, V. & Drenckhahn, D. 1991, 'Heterogeneity Of Microvascular Pericytes For Smooth Muscle Type Alpha- Actin', *Journal Of Cell Biology*, Vol. 113, No. 1, pp. 147-154.

Ng, J.S., Bearse, M.A., Jr., Schneck, M.E., Barez, S. & Adams, A.J. 2008, 'Local Diabetic Retinopathy Prediction By Multifocal ERG Delays Over 3 Years', *Investigative Ophthalmology & Visual Science*, Vol. 49, No. 4, pp. 1622-1628.

Ng, Y., Jacobs, P. & Johnson, J. 2001, 'Productivity Losses Associated With Diabetes In The U.S.' *Diabetes Care*, Vol. 24, No. 2, pp. 257-261.

Nguyen, T.T., Wang, J.J., Sharrett, A.R., Islam, F.M.A., Klein, R., Klein, B.E.K., Cotch, M.F. & Wong, T.Y. 2008, 'Relationship Of Retinal Vascular Caliber With Diabetes And Retinopathy', *Diabetes Care*, Vol. 31, No. 3, pp. 544-549.

Obrosova, I., Minchenko, A., Vasupuram, R., White, L., Abatan, O., Kumagai, A., Frank, R. & Stevens, M. 2003, 'Aldose Reductase Inhibitor Fidarestat Prevents Retinal Oxidative Stress And Vascular Endothelial Growth Factor Overexpression In Streptozotocin-Diabetic Rats.' *Diabetes*, Vol. 52, No. 3, pp. 864-871.

Podesta, F., Romeo, G., Liu, W., Krajewski, S., Reed, J., Gerhardinger, C. & Lorenzi, M. 2000, 'Bax Is Increased In The Retina Of Diabetic Subjects And Is Associated With

Pericyte Apoptosis In Vivo And In Vitro.' *American Journal Of Pathology*, Vol. 156, No. 3, pp. 1025-1032.

Remky, A., Weber, A., Hendricks, S., Lichtenberg, K. & Arend, O. 2003, 'Short-Wavelength Automated Perimetry In Patients With Diabetes Mellitus Without Macular Edema', *Graefe's Archive For Clinical And Experimental Ophthalmology*, Vol. 241, No. 6, pp. 468-471.

Setter, S.M., Campbell, R.K. & Cahoon, C.J. 2003, 'Biochemical Pathways For Microvascular Complications Of Diabetes Mellitus', *Annals Of Pharmacotherapy*, Vol. 37, No. 12, pp. 1858-1866.

Shepro, D. & Morel, N. 1993, 'Pericyte Physiology', *FASEB Journal*, Vol. 7, No. 11, pp. 1031-1038.

Stitt, A.W., Hughes, S.-J., Canning, P., Lynch, O., Cox, O., Frizzell, N., Thorpe, S.R., Cotter, T.G., Curtis, T.M. & Gardiner, T.A. 2004, 'Substrates Modified By Advanced Glycation End-Products Cause Dysfunction And Death In Retinal Pericytes By Reducing Survival Signals Mediated By Platelet-Derived Growth Factor', *Diabetologia*, Vol. 47, No. 10, pp. 1735-1746.

Tapp, R.J., Shaw, J.E., Harper, C.A., De Courten, M.P., Balkau, B., Mccarty, D.J., Taylor, H.R., Welborn, T.A. & Zimmet, P.Z. 2003, 'The Prevalence Of And Factors Associated With Diabetic Retinopathy In The Australian Population', *Diabetes Care*, Vol. 26, No. 6, pp. 1731-1737.

Tikellis, G., Wang, J., Tapp, R., Simpson, R., Mitchell, P., Zimmet, P., Shaw, J. & Wong, T. 2007, 'The Relationship Of Retinal Vascular Calibre To Diabetes And Retinopathy: The Australian Diabetes, Obesity And Lifestyle (Ausdiab) Study', *Diabetologia*, Vol. 50, No. 11, pp. 2263-2271.

Ting, J. & Martin, D. 2006, 'Basic And Clinical Aspects Of Gene Therapy For Retinopathy Induced By Diabetes', *Current Gene Therapy*, Vol. 6, No. 2, pp. 193-214.

Wallow, I., Bindley, C., Linton, K. & Rastegar, D. 1991, 'Pericyte Changes In Branch Retinal Vein Occlusion', *Investigative Ophthalmology & Visual Science*, Vol. 32, No. 5, pp. 1455-1463.

Wallow, I., Bindley, C., Reboussin, D., Gange, S. & Fisher, M. 1993, 'Systemic Hypertension Produces Pericyte Changes In Retinal Capillaries', *Investigative Ophthalmology & Visual Science*, Vol. 34, No. 2, pp. 420-430.

Wautier, J. 1986, 'Role Of Erythrocytes In Thromboembolism Pathology', *Annales De Medecine Interne (Paris)*, Vol. 137, No. 6, pp. 477-479.

Weill, D., Wautier, J., Dosquet, C., Wautier, M., Carreno, M. & Boval, B. 1995, 'Monocyte Modulation Of Endothelial Leukocyte Adhesion Molecules', *Journal Of Laboratory And Clinical Medicine*, Vol. 125, No. 6, pp. 768-774.

Wen, Y., Skidmore, J.C., Porter-Turner, M.M., Rea, C.A., Khokher, M.A. & Singh, B.M. 2002, 'Relationship Of Glycation, Antioxidant Status And Oxidative Stress To Vascular Endothelial Damage In Diabetes', *Diabetes, Obesity And Metabolism*, Vol. 4, No. 5, pp. 305-308.

Wheatcroft, S., Kearney, M., Shah, A., Grieve, D., Williams, I., Miell, J. & Crossey, P. 2003, 'Vascular Endothelial Function And Blood Pressure Homeostasis In Mice Overexpressing IGF Binding Protein-1.' *Diabetes*, Vol. 52, No. 8, P. 2075.

Yamagishi, S.-I., Amano, S., Inagaki, Y., Okamoto, T., Koga, K., Sasaki, N., Yamamoto, H., Takeuchi, M. & Makita, Z. 2002, 'Advanced Glycation End Products-Induced Apoptosis And Overexpression Of Vascular Endothelial Growth Factor In Bovine Retinal Pericytes', *Biochemical And Biophysical Research Communications*, Vol. 290, No. 3, pp. 973-978.

Zhang, J., Gerhardinger, C. & Lorenzi, M. 2002, 'Early Complement Activation And Decreased Levels Of Glycosylphosphatidylinositol-Anchored Complement Inhibitors In Human And Experimental Diabetic Retinopathy', *Diabetes*, Vol. 51, pp. 3499-3504.

Health Economic Perspective

Related publications:

Ting, J., Martin, D. & Haas, M. 2007, 'A Markov Model of Diabetic Retinopathy Progression for the Economic Evaluation of a Novel Dr Prognostic Device', CHERE Working Paper, vol. 2007, no. 14,

Chapter 2: Introduction to The Health Economic Perspective

2.1 Economics and Health Economics

Economics is a study of the allocation of resources, based on the assumption that resources are scarce. It includes macro-economics which addresses issues such as the spending of public funds, interest and unemployment rates, and micro-economics which covers such topics as demand and supply within markets, trade-offs (opportunity costs) between alternative sets of decisions as well as economic efficiencies. Opportunity cost can be defined as the loss in the value of the next best alternative forgone as the result of making a decision. Health and health services are topics which can be studied using economic theories and techniques. Health economics is therefore the study of resource allocation for health related products or policies. As described by Jefferson, Demicheli et al (2000), health economics can involve the examination of fiscal spending in health care systems, the relationship between socio-economic impacts on health, the study of demand and supply of health care products and or services as well as evaluations of the use of resources and consequences of alternate health interventions.

Health and health services have some interesting features which make them different from other good and services. In the microeconomic model of supply and demand for a commodity, the goal of the consumer is to maximize utility, which is demonstrated by a willingness to pay a certain price for a certain quantity of products (demand). The producer's goal is to maximize profit; to meet this objective the producer will sell a quantity of product at a certain price (supply). When market demand equals market supply, equilibrium is reached. In the economy of health and health care however, while the consumer aims to maximize utility, his or her willingness to pay and price inelasticity for some health interventions (especially if it is life-saving) is not matched by any other product or services in the market. That is, an individual is more likely to be willing to pay a sum well above his or her normal earnings to save his/her life (and probably that of a close relative, such as a spouse or child). It is likely that this attitude is driven partly by the fundamental relationship between health, health care and survival and partly by the fact that many health interventions

cannot be substituted by other goods and services. For example, food is also a fundamental need but when the price of one food item increases, individuals are able to substitute another (cheaper) item, which is likely to confer the same or similar amounts of utility, whereas if the price of open-heart surgery increases, a person who needs such surgery cannot substitute a cheaper intervention such as dialysis or anti-hypertensive drugs.

The high cost of producing and consuming health care is one of the main reasons that all developed countries have some form of subsidized health care system in place. Such systems do not represent conventional producers. That is, the objective of "producers" of health care is not always to maximize profits. Some producers, such as pharmaceutical companies have a profit maximizing objective, but the overall objective of public health products and services, whether in the form of public hospitals or subsidized vaccination schemes is to maximize the utility (i.e. health and well-being) of their citizens.

However, in common with other products and services, the health care sector has limited resources. When resources are scarce, inevitably, the provision of one intervention ultimately displaces the provision of another. Hence, there is a need to be able to make informed decisions as to what, how and when an intervention should be provided. It is for this reason that health economics and in particular economic evaluation is an important input to decision making in health.

2.2 Economic Evaluation

Economic evaluation is the systematic and comparative analysis of the costs and consequences of alternate strategies or course of actions. The evaluation must assess the costs and consequences of two or more alternate strategies or course of actions so that we can measure the benefits foregone by choosing the different course of actions that is opportunity costs.

The aim of economic evaluation is to inform the resource allocation decision process; that is to provide information which will enable decisions to be made about which products or services will provide the most value or improvement in health with the limited resources available. In other words, to assess which product or service will give the biggest "bang for the buck" or has the least opportunity cost. It should be noted however, that economic evaluations are one of many potential inputs to the decision making process. For example as reviewed by Sax (1990), issues such as society's opinion, the views of special advocacy groups, existing policies, expert advice and the philosophy of the government at the time will also influence the decision making process. Thus, the decision making process may not always be straight forward.

The issue of equity (especially equity of access) is also very important in health care as many consider the provision of care a universal right, as under Jonsen's (1986) "rule of rescue", people have a psychological "imperative to rescue identifiable individuals facing avoidable death" and as stated by Bochner (1994) 'a perceived duty to save endangered life where possible'. For example, provision of health care centres in rural areas may not be cost effective due to low rates of utilisation and difficulty in attracting staff to work in them, but it is considered appropriate that the population living in these areas have access to such care. Consider a very expensive intervention; the questions for the decision maker will include: should it be subsidized and made available if it is a patient's last chance for survival? What if the success rate of this intervention is extremely low or the side-effects very painful or may render the patient disabled? If the tradeoffs involve the provision of another intervention which may save other lives, should it still be subsidized and made available? What if the alternate intervention would only ease the comfort of others?

Although economic evaluation cannot answer all these questions, it is nevertheless a critical and objective analytical tool, producing results which are likely to aid the decision making process. As evidence-base medicine gains popularity, the use of economic evaluations by decision makers is becoming more common. For example, In Europe, the trend is for economic evaluations to be used more broadly in most countries Eberhardt, Stoklossa et al. (2005). In Australia, the Pharmaceutical Benefits Advisory Committee (PBAC) which advises the Minister for Health on whether a new drug should be subsidized by the government, requires an economic evaluation to form part of the submission document (Pharmaceutical Benefits Advisory Committee 1996), as does the Medical Services Advisory Committee (MSAC). These committees also consider the safety and clinical effectiveness of the health intervention.

An economic evaluation can take the form of a cost-minimisation analysis which is useful if the consequences of the alternate course of action are identical or very similar so that the aim is to search for the least costly alternative. It can also take the form of a cost effectiveness analysis which is often used if the costs and consequences of the alternate strategies differ in magnitude. The consequences of alternate strategies may also be converted into dollar amounts in a cost-benefit analysis so that health interventions with different relevant consequences (e.g life years, reduction in blood pressure, pain-free days) can be compared. Otherwise, the consequences may also be measured as Quality Adjusted Life Years (QALYs) in cost-utility analysis.

The economic evaluation undertaken in this thesis involves the prog-DR test developed in our laboratory. This test is a novel, non-invasive prognostic procedure which detects damage to the retinal vasculature before the development of clinical symptoms. Pre-clinical studies indicate that the test has the capability to detect the damaging effects of high blood glucose on retinal micro-vessels, thus allowing the prog-DR procedure to be used to identify individuals with diabetes and pre-diabetes who are at high risk of developing Diabetic Retinopathy (DR).

Various studies have already emphasized the importance of the early detection of DR (Brown, Pedula & Summers 2003; Ciulla, Amador & Zinman 2003; Clark

et al. 2000; Lloyd et al. 1995). However, the prog-DR procedure is a prognostic device, that is, it identifies high-risk individuals before they develop DR, thus providing an opportunity to prevent the development of DR. The test is not designed to diagnose individuals who already have DR and who may already require treatment. Therefore, although early DR detection may be cost effective, it does not automatically follow that DR prognosis is also cost effective. Hence, the aim of this study is to perform an economic evaluation of the prog-DR procedure using both cost-effectiveness and cost-utility analyses.

Ideally, an economic evaluation would be undertaken in conjunction with a randomized controlled trial (RCT) or some other controlled clinical evaluation of the prog-DR test, where the costs incurred and health progress (including the health-related quality of life) of patients would be followed and recorded. However, as DR is a chronic condition, an RCT would be very expensive and lengthy. In such situations, it is useful to use a modeling approach to first analyse the situation with already known information before committing to an expensive RCT. Models are built as simplified reflections of the real world and have been described as “the third way of doing science”. The development and use of models is both affordable and efficient in terms of time. For example, in 1978, an economic evaluation of end-stage renal disease modeled the effects on mortality of alternative programs (dialysis versus donor programs) (Doessel 1978). Recently, an economic evaluation of the Australian National Cervical Screening Program (comparing alternative screening intervals and age ranges) has been completed using Markov modeling (Anderson, Haas & Shanahan 2008).

The model built to undertake cost-effectiveness and cost-utility analyses of the prog-DR test can be broken down into three components: the modeling of health outcomes, costs and utility. The modeling of health outcomes or “effects” was carried out using a Markov Model, which is in essence is a decision tree with a time dimension. It takes a hypothetical population and divides them into different health states based on the natural progression of the disease and the probabilities of transitions into or between different health states. The different health states of DR include pre-diabetes, diabetes mellitus, micro-aneurysm (a clinical symptom in DR), mild non-proliferative DR (nPDR), severe nPDR,

proliferative DR (PDR), maculopathy, blindness and death, but for the interest of cost-effectiveness analysis, life-years and sight-years were also estimated.

Traditionally, the effects of an intervention are measured based on its impact on mortality. However, morbidity is also important as health is more than just being alive – the quality of the life lived is important. The measurement of health-related quality of life of individuals following interventions has been recognized as important since the 1950s as reviewed by Snoek (2000). Quality of life measurement is important for comparing different health interventions for several reasons: the primary effects of different health interventions may be very different; a health intervention may have several outcomes of interest; and different outcomes may have a differential impact on the quality of life of a patient. Therefore, combining different outcomes into a comparable composite quality of life score allows different health interventions to be compared.

Health related quality of life (HRQoL) is usually measured, using questionnaires, as a profile of health, covering physical, mental, emotional and social aspects of health. Well known measures of HRQoL include the SF36 and the EuroQol. For the purposes of incorporating HRQoL into economic evaluations, measures of HRQoL were adapted to measure “utility”, that is, a single score incorporating both length and quality of life. Utility is defined as a measure of the relative level of satisfaction a person might receive from a product or service, or in this case, health care. For example, the EuroQoL has been adapted to form a utility instrument called the EQ-5D (The EuroQol Group 1990), which classifies or score patients based on attributes of mobility, self-care, usual activity, pain/discomfort and anxiety/depression. The Quality of Well-Being scale (QWB) (Kaplan & Anderson 1988) scores patients based on attributes such as mobility, physical activity, social activity and symptom-problem complex. The scores (weights) obtained from these instruments range from 0 (death) to 1 (perfect health), but can also be negative if the condition is considered worse than death. The time patients spend in a particular health state (usually a year) is then weighted by the associated utility score to yield a gain or loss in Quality Adjusted Life Years (QALYs). Using measure such as QALYs, the combined impact on the quantity and quality of life of a health intervention, such as the prog-DR test can be estimated.

Costs attributed to an intervention include both health and non-health costs. In this case, health costs included the cost of using the prog-DR test (consultation and consumable costs) as well as future medical costs for blood glucose management and eye examinations (incurred because the prog-DR test identifies people who are both pre-diabetic and diabetic and their need for other interventions). Non-health costs associated with the identification of pre-diabetes, diabetes and/or DR need to be included in the costs of introducing the test; for example, disability pensions, rent assistance and mobility allowances are non-health costs which may be incurred due to disability (blindness) which results from these conditions. It should be noted that, in this case, price does not equal the value or opportunity cost of the provision of these goods or services because the health care sector is not a perfectly competitive and transparent market. Nevertheless, the prices are paid by public funding and are the best data available.

The details of the model with its three components are described in chapter 3 of this thesis, which is also published as a CHERE working paper (Ting, Martin & Haas 2007) http://www.chere.uts.edu.au/pdf/wp2007_14.pdf. The results of the cost-effectiveness and cost-utility analyses are reported in chapter 4 of this thesis.

References

Anderson, R., Haas, M. & Shanahan, M. 2008, 'The Cost-Eeffectiveness of Cervical Screening in Australia: What Is The Impact Of Screening At Different Intervals Or Over A Different Age-Range?' *Australian and New Zealand Journal of Public Health*, vol. 32, no. 1, pp. 43-52.

Bochner, F., Martin, E., Burgess, N., Somogyi, A. & Garry, M. 1994, 'Controversies In Treatment: How Can Hospitals Ration Drugs?' *British Medical Journal*, vol. 308, no. 6933, pp. 901-905.

Brown, J., Pedula, K. & Summers, K. 2003, 'Diabetic Retinopathy: Contemporary Prevalence In A Well-Controlled Population', *Diabetes Care*, vol. 26, no. 9, pp. 2637-2642.

Ciulla, T.A., Amador, A.G. & Zinman, B. 2003, 'Diabetic Retinopathy And Diabetic Macular Edema: Pathophysiology, Screening, And Novel Therapies', *Diabetes Care*, vol. 26, no. 9, p. 2653.

Clark, C., Fradkin, J.E., Hiss, R.G., Lorenz, R., Vinicor, F. & Warren-Boulton, E. 2000, 'Promoting Early Diagnosis and Treatment of Type 2 Diabetes: The National Diabetes Education Program', *The Journal of the American Medical Association* vol. 284, no. 3, pp. 363-365.

Doessel, D.P. 1978, 'Economic Analysis and End-Stage Renal Disease - An Australian Study', *Economic Analysis and Policy*, vol. 8, no. 2, pp. 21-36.

Eberhardt, S., Stoklossa, C. & von der Schulenburg, J.-M.G. 2005, *Euromet 2004 : The Influence Of Economic Evaluation Studies On Health Care Decision Making : A European Survey*, IOS Press,, Amsterdam ; Washington, DC :.

Jefferson, T., Demicheli, V. & Mugford, M. 2000, *Elementary Economic Evaluation In Health Care*, 2nd ed edn, BMJ books, London

Jonsen, A. 1986, 'Bentham In A Box: Technology Assessment And Health Care Allocation', *Law, Medicine and Health Care*, vol. 14, pp. 172-174.

Kaplan, R.M. & Anderson, J.P. 1988, 'A General Health Policy Model: Update And Applications.' *Health Services Research*, vol. 23, no. 2, pp. 203-233.

Lloyd, C.E., Klein, R., Maser, R.E., Kuller, L.H., Becker, D.J. & Orchard, T.J. 1995, 'The progression of retinopathy over 2 years: The Pittsburgh Epidemiology of Diabetes Complications (EDC) Study', *Journal of Diabetes and its Complications*, vol. 9, no. 3, pp. 140-148.

Pharmaceutical Benefits Advisory Committee 1996, *1995 Guidelines for the Pharmaceutical Industry on Preparation of Submissions to the Pharmaceutical Benefits Advisory Committee: including major submissions involving economic analyses*.

Sax, S. 1990, *Health Care Choices and the Public Purse*, Allen and Unwin, Sydney.

Snoek, F. 2000, 'Quality Of Life: A Closer Look At Measuring Patients' Well-Being', *Diabetes Spectrum* vol. 13, pp. 24-28.

The EuroQol Group 1990, 'EuroQol - A New Facility For The Measurement Of Health-Related Quality Of Life', *Health Policy*, vol. 16, no. 3, pp. 199-208.

Ting, J., Martin, D. & Haas, M. 2007, 'A Markov model of Diabetic Retinopathy Progression for the Economic Evaluation of a novel DR prognostic device', *CHERE Working Paper*, vol. 2007, no. 14.

Chapter 3: A Markov model of Diabetic Retinopathy Progression

Diabetic Retinopathy (DR) is a debilitating complication of diabetes, where the micro-vascular network of the retina becomes damaged, unable to control blood flow, and, as the condition worsens, start to proliferate. It is also one of the leading causes of blindness in the western world both for people of working age and those aged over 65 (Bamashmus, Matlhaga & Dutton 2004).

There is evidence that both Diabetes Mellitus (DM) and DR may be prevented or at least their progression slowed. Results from the Da Qing Impaired Glucose Tolerance (IGT) study (Pan et al. 1997), the Malmo Feasibility Study (Eriksson & Lindgarde 1991) and the Finnish Diabetes Prevention Study (Tuomilehto et al. 2001), indicate that progression from pre-DM, a condition of impaired fasting glucose and or impaired glucose tolerance, to DM may be slowed by weight reduction, sufficient exercise and/or appropriate diet. The UKPDS (Kohner et al. 2001; Stratton et al. 2001; UK Prospective Diabetes Study Group 1998) and WESDR (Batchelder & Barricks 1995) studies also provide evidence that strict control of blood glucose, blood pressure and weight can slow the progression of DR.

Currently, a diagnosis of DR is made following dilated fundus examination, performed by optometrists or ophthalmologists. However, DR and DM are often not diagnosed until the disease is advanced when sight is likely to have already been affected. Although laser treatment may be used to slow the progression to blindness in these advanced stages, these treatments also permanently damage the retina. Thus it seems logical that preventing the development of DR or identifying it early will increase the likelihood that an individual will retain sight, maintain a good quality of life and avoid the discomfort and cost of treatment (Javitt et al. 1994).

Our laboratory has developed a novel, non-invasive prognostic device aimed at identifying the earliest stages of DR (Markhotina, Liu & Martin 2007; Martin & Markhotina 2002). This innovation (prog-DR) can detect the damaging effects of high blood glucose on the retinal microvasculature, before the development of

clinical symptoms. It is expected that this test will be able to identify pre-diabetics as well as undiagnosed diabetics who have not developed DR.

Despite the intrinsic appeal of this technology, it is important to systematically assess the associated outcomes and costs. Although a randomised controlled trial, including an economic evaluation would be the most powerful means of determining the value of the test, such trials require large amounts of time and infrastructure and are expensive. To circumvent these limitations and to study the feasibility of the test before committing to a randomised clinical trial, models are often used to simulate real-world conditions, to forecast future outcomes, as well as predict outcomes when conditions such as prevalence rates, compliance to medications, costs etc are variable, especially in chronic diseases such as diabetes (Clarke et al. 2004; Eastman et al. 1997; Lamotte et al. 2002; The CDC Diabetes Cost-effectiveness Group 2002; Zhou et al. 2005b). Although there are various models of interventions for DM (Clarke et al. 2004; Eastman et al. 1997; Lamotte et al. 2002; The CDC Diabetes Cost-effectiveness Group 2002; Zhou et al. 2005a) and/or DR (Dasbach et al. 1991; Davies et al. 2002; Harper et al. 2003; Sharma et al. 2001; Vijan, Hofer & Hayward 2000), these often fail to include patient behaviour such as diet, exercise patterns and response to treatment and screening recommendations (i.e. compliance) nor do they include pre-DM as a state in the model.

Economic evaluations are used to assess the costs and consequences of alternative interventions, in this case, comparing a prognostic test for DR with no test. Such evaluations fall into four categories: cost minimisation, cost utility, cost benefit or cost effectiveness analyses. The aim of this paper is to describe the development of a Markov model designed to estimate the costs and consequences of pre-DR screening.

3.1 Methods

The Markov model was built in Microsoft Excel 2003 Professional edition on an IBM Intel Celeron computer. Markov models are used to describe random processes that evolve over time. The most common application of Markov models in health is to characterize all the possible prognoses for a given group of patients. This entails modeling the progress over time of a notional group of patients through a finite number of health states. Patients are initially placed into one of the health states, and the probabilities of transition to the other states in the model are defined within a given time period, known as a Markov cycle.

3.1.1 Markov Progression Model

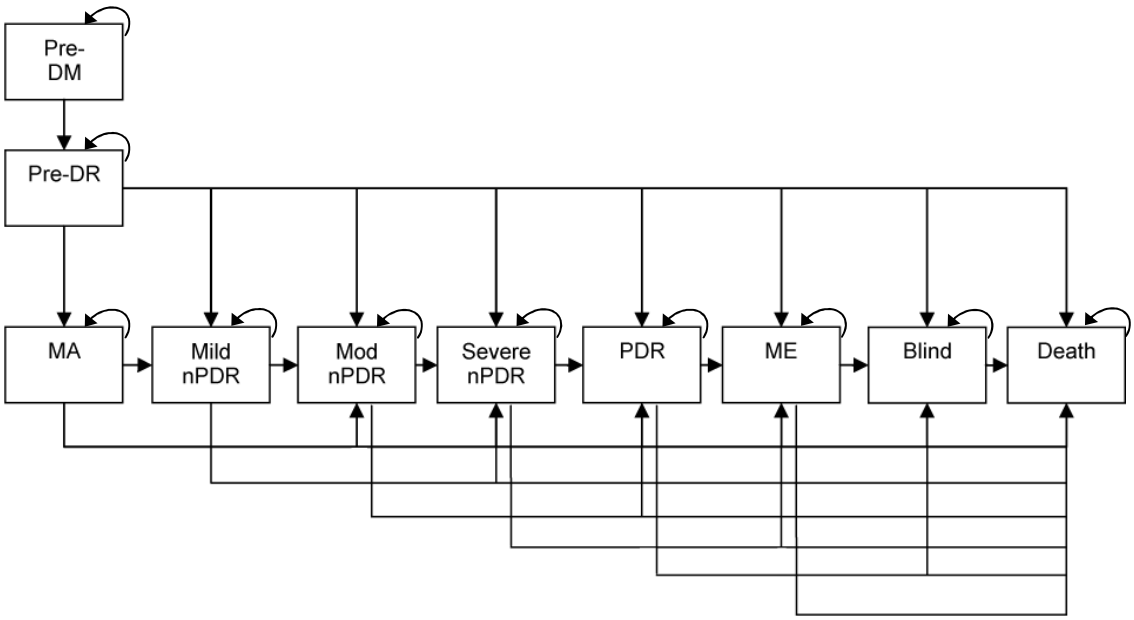

Figure 3.1: The progression of DR: Pre-DM is pre-diabetes; Pre-DR is pre diabetic retinopathy that is a diabetic stage without DR; MA is micro-aneurysm, nPDR is non-proliferative DR; PDR is proliferative DR and ME is macular edema. The severity of the stages increases from left to right.

The natural progression of DR is shown in Figure 3.1. The ideal scenario would be to prevent DM and DR, which would involve diagnosis at the pre-DM and pre-DR stage, before the development of symptomatic damage to sight associated with DM and/or DR. The aim of early diagnosis is to enable patients to modify their lifestyle and/or undergo medical interventions earlier, thus increasing the probability of preventing or slowing the progression to DM and DR. Although there have been reports of cases of regression of DR as a result of interventions, the reported incidence is low(Kawasaki et al. 2006); hence the model assumes a uni-directional flow of progression, and the transition of the disease is only to more advanced stages. However, subjects may skip one or more stages and move into more advanced stages.

Although this pre-symptomatic screening test can also identify non-diagnosed DM and hence may have implications for the development of other complications of diabetes such as renal failure and cardiovascular disease (CVD), these were not included in the model. This is because the primary aim of the screening test is the prevention of DR. There is a positive association between the severity of DR and other co-morbidities of diabetes such as cardiovascular disease (Klein et al. 1999; van Hecke et al. 2005b) ; however, these associations are not always straightforward. For example, the probability of individuals with diabetes developing cardiovascular disease is better explained by the presence of factors such as hypertension (van Hecke et al. 2005a), and nephropathy (Torffvit et al. 2005) whereas the severity of retinopathy has been shown to be associated with a decreased probability of developing CVD (Lovestam-Adrian, Hansson-Lundblad & Torffvit 2007). Diabetic nephropathy, which is also a micro-vascular complication of diabetes, shows more consistent association with the severity of DR (Rossing, Hougaard & Parving 2002; Villar et al. 1999) however, glycemic (Powrie et al. 1994; Villar et al. 1999) and blood pressure control (Schrier et al. 2002; Stephenson et al. 1995) are still important predictors (in conjunction with the presence of retinopathy) of nephropathy.

As a Markov model uses transition probabilities and most clinical studies present the data as hazard rates of progression, these were converted to transitional probabilities ($P_{transition}$) for this model by using the formula below, where *r* is the hazard rate and *t* is time:

$$P_{transition} = 1 - e^{\left(\frac{-r}{t}\right)}$$

The rationale for the above formula is based on a solution from the Kolmogorov's forward equation, applied to probability theory (Grimmett & Stirzaker 1992). The standard probability of transitions in a multi- discrete state model is as shown below, where *γ1,2* is the constant rate of transition from one state to another in a given *t* period.

$$P(t) = 1 - e^{(-\gamma 1,2t)}$$

The constant rate used in this thesis, is based on reported hazard rate, which is the marginal probability of default in cumulated in a given period. As the period of data collection is different for most studies, the hazard rate was averaged into the transition time of the Markov model (1 year). Note that the transition probabilities were not adjusted for age due to the lack of age-specific information.

3.1.1.1 The Hypothetical Population

As the diagnostic test is intended to be performed by optometrists or ophthalmologists, the cohort of interest was created by using the number of people who attended an optometrist or ophthalmologist for a comprehensive or brief initial consultation (Medicare Benefit Schedule (MBS) codes 10900 or 10916 respectively) in 2005 (3,017,424 people) (Medicare Australia 2005). The cohort was divided into two groups based on eligibility for the pre-DR test.

To be eligible, an individual must not have already been diagnosed with DM or DR. Undiagnosed diabetics with DR can be identified by dilated fundus microscopy, a procedure recommended by the Optometrists Association of Australia (OAA) (Optometrists Association Australia 2005) for those suspected of DR or DM. The OAA also recommends that patients diagnosed with DR be referred to their general practitioner for further investigation. Therefore, individuals eligible for the pre-DR test include normal subjects, undiagnosed diabetics without DR and pre-diabetics. The latter two groups progress through the model.

Using Australian epidemiological data, the percentage of the hypothetical population who are eligible and progress through the model is shown in Table 3.1. The prevalence rates of pre-diabetes, diagnosed and undiagnosed diabetes were based on the Diabesity study (Dunstan et al. 2001); the prevalence rate for Diabetic Retinopathy was based on the study by Tapp et al (2003).

	Number of patients excluded	Number of patients included
Total number of examinations by optometrists in Australia 2005		3,017,424
Patients with Diabetes Mellitus[*]	114,662	
Patients with undiagnosed Diabetes Mellitus with Diabetic Retinopathy[†]	7,109	
Subtotal of optometrist examinations eligible for new prog-DR test		2,895,653
Patients with normal findings	2,296,260	
Cohort of Patients entering the Markov Model		**599,393**
Cohort Composition		
Patients with pre-diabetes[‡]		491,840
Patients with undiagnosed Diabetes Mellitus without Diabetic Retinopathy[§]		107,553

Table 3.1: Method of determining the number of patients in the cohort for evaluation by the Markov Model. The prevalence rate of diagnosed Diabetes Mellitus[*] and pre-Diabetes[‡] were based on the Diabesity study (Dunstan et al. 2001), the prevalence rate of undiagnosed Diabetes Mellitus with [†] and without Diabetic Retinopathy [§] were based were based on the Diabesity study (Dunstan et al. 2001) and on the study by Tapp et al (2003).

3.1.1.2 Pre-diabetic progressions and lifestyle characteristics

Studies have found that pre-diabetics have a very high probability of developing DM. The Da Qing IGT study (1997) as well as other clinical studies have shown that increases in weight or Body Mass Index (BMI) accelerate the progression to diabetes, whilst adhering to a healthy diet and undertaking regular exercise can slow the progression (Edelstein et al. 1997; Tuomilehto et al. 2001).

This model takes into account some of these real-life decisions or characteristics of pre-diabetics; one such decision is their choice of diet and exercise patterns which are assumed to be related to their body mass index (BMI). According to the Diabesity Study, 59.6% of the diabetic population in Australia is overweight (BMI above 25); therefore 40.4% can be considered lean.

It was assumed that lean subjects have similar diet and exercise patterns to respondents to the 2003 NSW Health Survey, where sufficient exercise for a non- over weight person was defined as 2.5 hours of physical activity per week and a “healthy” diet was defined as one which includes sufficient consumption of fibre (Centre for Epidemiology and Research & NSW Department of Health 2004). For overweight subjects, it was assumed that four hours of physical activity per week is sufficient, and an appropriate diet include a reduced intake of fat, saturated fat and an increased intake of fiber(2001). However, as subjects are currently not diagnosed with pre-DM, it is assumed that they will undertake a pattern of “healthy” diet and exercise at the same rate as lean subjects because they do not receive any information which would predispose them to attempt a more challenging diet and exercise pattern. Based on these data, the lifestyle characteristics of the cohort were estimated and are summarized in Table 3.2.

Lifestyle / Health	None [‡]	Diet [§]	Exercise [‖]	Diet & exercise [#]
Lean [*]	44.3043%	= 19.3–8.704%	= 45-8.704%	=19.3 x 45%
		= 10.5957%	= 36.3957%	= 8.7043%
Over-weight [†]	25.5200%	= 12-8.52%	= 71-8.52%	=12 x 71%
		= 3.4800%	= 62.4800%	=8.5200%

Table 3.2: lifestyle characteristics of lean and overweight subjects. *Data based on the NSW Health Survey (2003) (NSW Health Department Funding and Systems Policy Branch 2003); [†] Data based on the study by Tuomilehto, Lindstrom, et al., (2001) (Tuomilehto et al. 2001). [‡] the residual percentage; [§] calculated by subtracting the achievement rate for both diet and exercise from that of diet; [‖] calculated by subtracting the achievement rate for both diet and exercise from that of exercise; [#] calculated by multiplying the achievement of diet by that of exercise. Numbers are rounded to four decimal places

The transitional probabilities to DM are based on the Da Qing IGT study (Pan et al. 1997); the probabilities are dependent on the BMI and lifestyle characteristics of individuals, so that for the same lifestyle characteristic, lean subjects have a reduced probability of progression. For example, lean subjects with an appropriate diet, sufficient exercise or both, have progression probabilities of 0.0770, 0.0496 and 0.0688, whereas the progression probabilities for overweight subjects are 0.1033, 0.1127 and 0.1167.

3.1.1.3 Diabetic progressions and lifestyle characteristics

For diabetics, the progression to more severe stages is dependent on two factors. The first is the choice of blood glucose control method, which is usually based on the severity of abnormal blood glucose levels. According to the DiabCo$t study (Colagiuri et al. 2003) 1% of diabetics do not actively attempt to control their blood glucose; 32.7% control their glucose levels through diet and exercise, 59.6% use hypoglycemic tablets and 6.7% use insulin alone or in combination with other hypoglycemic medications.

The second factor influencing progression is compliance with the chosen blood glucose control method; it is assumed that those who comply achieve strict control of blood glucose levels, whereas those who do not comply achieve conventional control. According to a study by Rubin (2005) compliance is lowest for behavioral types of control (diet and exercise) at 5.7%, highest for simple tablet consumption at 61-85% and moderate for insulin injections (62-64%).

Individuals who are either a non-diagnosed pre-diabetic or non-diagnosed diabetic do not have any information which would enable them to manage their blood glucose levels. The model assumes that their management regime consists of diet and exercise. However, under the current screening protocol, around 10.58% of non-diagnosed diabetics will be identified each year (Dunstan et al. 2001). This information is incorporated into the model.

3.1.1.4 Non-sight threatening DR (nSTDR)

The transitional probabilities for the stages of DR - defined as microaneurysm (MA), mild non-proliferative DR (nPDR) and moderate nPDR - were derived from the UKPDS (UK Prospective Diabetes Study Group 1998). Despite the availability of many other excellent studies on DR progression, the UKPDS was chosen as it was based on the more common type of DM (Type 2), involved a large number of participants (over 3800) and was conducted over a long period of time (up to 10yrs).

The UKPDS showed that progression from the early stages of DR was influenced by the level of blood glucose control achieved. That is, a strict blood glucose control regime (aimed at achieving an FPG of less than 6 mmol/L), slowed the rate of progression compared with conventional blood glucose control methods. These rates of progression were converted to annual transition probabilities and distributed among the stages of diabetic retinopathy. The distribution was based on the assumption that progression to the next stage of severity is twice that to the stage after and so on. The transition probabilities are summarized in Table 3.3.

For progression to macular oedema, the transition probabilities were based on the WESDR (Klein et al. 1995) as the UKPDS does not include these data. The WESDR cohort was similar to the conventional control group in the UKPDS, as the majority of the cohort had a glycosylated hemoglobin (Hb_{A1c}) percentage above 7%. As the incidence of macular oedema (maculopathy) was 6.7 times more frequent for those with higher HbA (Klein et al. 1995), the transitional probabilities for the intensive blood glucose control were divided by this amount.

	Pre-DR	MA only	mild nPDR	mod nPDR	severe nPDR	PDR	ME
Pre-DR	#	0.0194	0.0097	0.0049	0.0024	0.0012	0.0020
		(0.0234)	(0.0117)	(0.0058)	(0.0029)	(0.0015)	(0.0131)
MA only	0	#	0.0200	0.0100	0.0050	0.0025	0.0034
			(0.0242)	(0.0121)	(0.0061)	(0.0030)	(0.0230)
mild nPDR	0	0	#	0.0215	0.0107	0.0054	0.0043
				(0.0259)	(0.0130)	(0.0065)	(0.0288)
mod nPDR	0	0	0	#	0.0251	0.0125	0.0074
					(0.0302)	(0.0151)	(0.0496)
severe nPDR					#	0.0376	0.0030
						(0.0453)	(0.0198)
PDR						#	0.0033
							(0.0220)

Table 3.3: The transition probabilities for non-sight threatening DR with intensive control and conventional blood glucose control (represented in brackets). # represents the residual probability and numbers are rounded to four decimal places.

3.1.1.5 Sight-threatening DR (STDR)

As DR progresses, more of the retina becomes damaged and the risk of sight being affected increases. The stages at which sight is most likely to be threatened include severe nPDR, PDR and macular edema. The transitional probabilities for severe nPDR and PDR were derived from the UKPDS (UK Prospective Diabetes Study Group 1998), and the progression to macular oedema was based on the WESDR. A summary of the transitional probabilities is shown in Table 3.3.

For these sight threatening stages, the progression to more advanced stages is influenced by more than the control of blood glucose. It may also be affected by the need for laser treatment and compliance with monitoring and treatment recommendations.

Panretinal and focal laser photocoagulation can be used to restore some eyesight and slow the deterioration of the retina. As the laser treatment also causes irreversible damage to the retina, due to laser burns, the procedure is not always recommended. Identification of the need for treatment is facilitated by compliance with the recommendations for monitoring compiled by the National Health and Medical Research Council (NHMRC) (National Health and Medical Research Council 1997). For example, if the need for laser treatment was not identified (eg if diabetes was not diagnosed) or the intervention not carried out, the transitional probability of remaining in the current stage (no progression) is reduced to zero and the probability of transition to more advanced stages is increased; conversely, identified need and a high level of compliance with the intervention would result in a zero rate of deterioration and/or probability of progression (if the treatment was successful).

For the purpose of the model, the probability that laser treatment is needed was based on the UKPDS (UK Prospective Diabetes Study Group 1998) which showed the number of people who received laser treatment. It is likely that a person will have both eyes treated. Australian hospital data (Yi et al. 2003) was used to estimate the average number of eyes treated per patient, which was found to be 1.586 eyes per patient. The adjusted annual probability for

treatment was then distributed across different stages of STDR based on the utilization proportion for each stage (Kohner et al. 2001). The annual probabilities for laser treatment for intensive control are 0.0001, 0.0025 and 0.0172 for severe nPDR, PDR and ME; and 0.0002, 0.0034 and 0.0232 for conventional control respectively.

The likelihood of individuals complying with these recommendations was based on the study by Schoenfeld, Greene, Wu, et al., (2001), which showed that 64.8% of the diabetic population fully complied with the diabetes vision care guidelines for eye examinations (Aiello et al. 1998); 11.1% per cent attended examinations but did not undertake all recommended tests (partial compliance), and the remaining 24.1% did not attend an eye examination at all (zero compliance).

The probability of treatment is zero for individuals who do not comply with the NHMRC recommendations for eye examinations- such an individual would not be identified as needing treatment in the first place. Conversely, the probability of treatment is one for those who fully complied with the recommendations. As the NHMRC (National Health and Medical Research Council 1997) recommends three to twelve eye examinations per year for maculopathy and four to six eye examinations per year for severe nDR and PDR, it is assumed that a minimum of three or four examinations per year is sufficient to decide whether laser treatment is required. As partial compliance means that individuals have at least one examination per year, it is estimated that there is at least a one in four chance (or one in three for maculopathy) that the need for laser treatment will be identified and the same chance that an individual will comply with treatment recommendations. The effects of additional eye examinations were tested in the sensitivity analysis.

The success rate for laser treatments was derived from Australian hospital data (Bamroongsuk et al. 2002), based on the assumption that the laser treatment was deemed successful if no further treatment was required. It should be noted however that further treatment may not be required or provided due to other reasons such as no observed improvement with the treatment regime or non-compliance of patients. As no data about these possibilities were available, the

sensitivity of the incremental cost-effectiveness ratio (ICER) to variations of the success rate was tested. In the model, base-case success rates for laser treatments are set at 64.9% for severe nPDR and PDR and 48.8% for macular edema.

3.1.1.6 Blindness and Death

The transitional probabilities of progressing to blindness were based on studies by Janghorbani, Jones and Allison (2000), Lawson, Hunt and Kohner (1985) and the UKPDS (UK Prospective Diabetes Study Group 1998). The UKPDS (UK Prospective Diabetes Study Group 1998) shows that the transitional probability of progressing to blindness is 1.16 times higher for those with conventional blood glucose control than for those who achieve strict control. As the subjects in the blindness studies are similar to the conventional blood glucose control group with blood glucose levels above 6 mmol/L and HbA above 7% (Janghorbani, Jones & Allison 2000; Lawson, Hunt & Kohner 1985), the transitional probabilities to blindness were divided by 1.16 to yield the intensive transition probabilities. These are summarized in Table 3.4.

	Intensive control	Conventional control
Pre-DR (no DR)	0.0171	0.0199
MA only	0.0171	0.0199
mild nPDR	0.0427	0.0497
mod nPDR	0.0427	0.0497
severe nPDR	0.0427	0.0497
PDR	0.0544	0.0633
ME	0.0783	0.0908

Table 3.4: The transition probabilities to blindness from different stage of DR. Numbers are rounded to four decimal places.

The transitional probabilities of progressing to death were based on a study by Cusick, Meleth, Agron, et al (2005) for Type 2 diabetics. As the ratio of deaths due to diabetes and other causes is 1:1.53 (UK Prospective Diabetes Study Group 1998), the transitional probabilities of dying were divided by this ratio to differentiate between the two types of mortality.

In the UKPDS, it was shown that the mortality rate associated with conventional blood glucose control is 1.085 time higher than for intensive control (UK Prospective Diabetes Study Group 1998). As the subjects in the study by Cusick, Meleth, Agron, et al. (2005) were similar to the conventional blood glucose control group in the UKPDS, the transition probabilities were divided by 1.085 to yield the transition probabilities for those with intensive blood glucose control. The transition probabilities to death are summarized in Table 3.5.

It should be noted that it is these transitions probabilities that are likely to ultimately affect the outcomes of life years and sight years estimated in the model.

	Intensive control		Conventional control	
	DM related	Others	DM related	Others
Pre-DR	0.0207	0.0148	0.0224	0.0146
MA only	0.0207	0.0148	0.0224	0.0146
mild nPDR	0.0207	0.0148	0.0224	0.0146
mod nPDR	0.0284	0.0204	0.0309	0.0201
severe nPDR	0.0320	0.0229	0.0347	0.0226
PDR	0.0332	0.0238	0.0360	0.0235
ME	0.0332	0.0238	0.0360	0.0235
Blind	0.0332	0.0238	0.0360	0.0235

Table 3.5: Transitional probabilities to death by diabetes-related complications and other causes. Numbers are rounded to four decimal places.

3.1.2 Health utility measurement (determining QALY scores)

Quality-adjusted life years (QALYs) and other measures of utility have been developed as a means of valuing the trade-off between length of life and health-related quality of life. A number of approaches such as standard gamble, time trade-off or rating scales can be used to produce scores which represent the valuation attached to a number of health states. The health states cover dimensions such as mobility, pain/discomfort, self-care, psychological state and ability to perform usual activities. Scores are assigned to different health states so that full health has a score of one and death a score of zero.

Results from a study by Brown, Brown, Sharma, et al., (1999) provided utility values for a range of visual acuities associated with DR. Both the time trade-off and standard gamble methods were used in this study but the time trade-off results was used as these were similar to what is agreed on by researchers (Brown, Brown & Sharma 2000; Hoskins 2000; Javitt 2000) .A study by Fong, Sharza, Chen, et al., (2002) provided information on the range of visual acuity for different stages of DR and data from the worst eye was used. The weighted average utility scores were derived using a combination of information from these two studies and are shown in Table 3.6.

	QoL score
Pre-DR (no DR)	0.8402
MA only	0.8402
mild nPDR	0.8360
moderate nPDR	0.8182
severe nPDR	0.8182
PDR	0.8137
Maculo	0.7800
Blind	0.6400

Table 3.6: The Quality of Life Scores for different stages of Diabetic Retinopathy. Numbers are rounded to four decimal places

3.1.3 Cost data

Type 2 Diabetes Mellitus is a costly disease. Not only do individuals and society incur direct and non-direct health care costs, patients and their carers may also lose income and society productivity (Colagiuri et al. 2003). In this model, a range of health care costs was considered. These were discounted at 3% per annum (Mathers, Vos & Stevenson 1999; Murray & Lopez 1996) and varied between 5% and 7% in the sensitivity analysis.

3.1.3.7 Blood glucose management

The 2005 Pharmaceutical Benefits Schedule (PBS) (Department of Health and Ageing 2005) report lists the blood glucose indicators, insulin and other hypoglycemic medication available in Australia, including the prices paid by consumers. It is assumed that individuals purchase 53 weeks' worth of medications and medical consumables each year (one for each week of the year and one week's worth of back-up). The intake of hypoglycemic medications recommended by the Australian medicines handbook (Handbook 2004) was used in the model and it is assumed that blood glucose was measured once per day.

The Australian government collects pharmaceutical usage information via Medicare Australia, and this information is available online: (http://www.medicareaustralia.gov.au). The Australian government also funds a National Diabetes Services Scheme (NDSS) which subsidizes syringes and insulin pens which registered diabetics can access. Based on these data, the weighted average annual cost for insulin alone or in combinations with other hypoglycemic medications was estimated to be $5,329.72 – $6,793.82 per year, $81.92 - $169.91 per year for hypoglycaemic tablets and $342.40 per year for blood glucose indicators.

In order to use these pharmaceutical products, prescriptions and re-assessment of dosage are needed. The Medicare Benefit Schedule (MBS) (Department of Health and Ageing 2004), recommends that diabetics visit a general practitioner twice a year; it was assumed that one standard (MBS 2620) and one long

consultation (MBS 22622) would be needed (Department of Health and Ageing 2004). This adds $59 to the cost of blood glucose management.

3.1.3.8 Eye examinations

The MBS price for an eye examination is $60.25 (MBS 10914) (Department of Health and Ageing 2004), and the frequencies of eye examinations were based on NHMRC recommendations for diabetics (National Health and Medical Research Council 1997). For those with PDR and ME, fluorescein angiography in one or both eyes is recommended by the NHMRC. The costs of retinal photography, multiple exposures of 1 or both eyes with intravenous dye injection (MBS code 11215 or 11218) are $104.35 and $128.90 respectively (Department of Health and Ageing 2004); the weighted average cost per person of $127, based on usage of these services in the year beginning June 2004 (published on the Medicare website), was used.

The likelihood of compliance with the Australian NHMRC recommendations was based on the study by Schoenfeld, Greene, Wu, et al., (2001), which shows that 65% of the diabetic population fully comply with the diabetes vision care guidelines for eye examinations in America (Aiello et al. 1998). Eleven per cent attended examinations but did not undertake all recommended tests (partial compliance), and the remaining 24% did not attend an eye examination at all (zero compliance).

As the NHMRC recommends one eye examination every two years for nSTDR, and the model cycles annually, partial compliance for these stages was taken as being equal to full compliance.

3.1.3.9 Laser treatment cost

Retinal photocoagulation or laser treatment for DR (MBS 42809) costs $382.80 per session of treatment (Department of Health and Ageing 2004); however, multiple sessions and follow-up treatment are often needed. Based on Australian hospital data (Bamroongsuk et al. 2002), individuals with either severe nPDR or PDR undergo panretinal laser treatment; 99.973% require multiple laser sessions and 35% require follow up treatment. As the median waiting and follow-up assessment time indicate that no more than 5 treatments sessions are possible each year, the proportion of eyes which underwent 1 – 5 laser sessions was estimated. The weighted average cost of laser treatment per eye was also estimated (including the cost for the excess eye consultations above the NHMRC recommendations) and multiplied by the average number of eyes treated per patient (Yi et al. 2003). This yielded an annual cost per patient of $1959.13.

Similar estimates were made for macular edema, but since both focal and panretinal photocoagulations were used, the weighted average of these treatments of $1604.43 were used in the calculation of the annual cost per patient.

3.1.3.10 Non-health cost of blindness

The direct non-health costs associated with blindness vary between countries as well as states within countries, as different infrastructure and support mechanisms are available. Expert opinion from Mr. M. Simpson from the Royal Blind Society (NSW) was used to estimate the costs of blindness (see Table 3.7).

3.1.4 Sensitivity Analysis

The influence of 11 parameters on life years, sight years, QALYs gained and the cost were evaluated. Univariate sensitivity analysis was performed by varying the parameters upwards and downwards by 10% (Appendix A, Table A.1). An elasticity test (the percentage change in outcome divided by the percentage change in parameter) of 0.8 or more was considered to be elastic.

Cost Type	Employed person	Unemployed
*CSTDA support **		
Employment	$479.94	
Advocacy, info, & print disability	$21.28	$21.28
Admin	$153.91	$153.91
Centrelink Welfare support †		
Disability Pension Payment	$10,847.20 - $12,922.20	$10,847.20 - &12,922.20
Pharmaceutical Supplement	$75.40 - $150.80	$75.40 - $150.80
Rent Assistance	$2,470.00 - $2615.60	$2,470.00 - $2615.60
Employment Entry Payment	$9633.00	
Energy/Household concession	$657.80	$657.80
Travel Concessions	$1,470.56 - $21,840.00	$1,470.56
Mobility Allowance	$1,856.40	
Others		
Occupational Therapy ‡	$3,354.62	$3,354.62
Work-related writing equip §	$1,583.00	
Total	$22,940.11 - $55,338.55	$19,050.77 - $21,416.77
Weighted Average ‖		$20,226.57 - $31,593.30

Table 3.7: Cost of Blindness. * the average annual cost per user in each support category under the Commonwealth State/Territory Disability Agreement (CSTDA) in New South Wales (NSW) (Australian Institute of Health and Welfare 2004); † Centrelink welfare support for single and coupled residents (Department of Human Services 2005); ‡ assume a visit to the therapist once a week at standard cost per visit (NSW Health Department Funding and Systems Policy Branch 2003); § cost of equipment such as Braille, talking watches and so on (Vision Australia 2005); ‖ according to expert opinion, 70% of the blind are unemployed or underemployed. Note that the prices were inflated to 2005 levels, based on weighted average inflation rate (Australian Bureau of Statistics 2006).

3.2 Discussion

The aim of this chapter was to describe a model built to estimate the cost and health outcomes of screening for DR. Once constructed, such a model can be modified to predict and/or take account of changes in costs and health outcomes associated with alterations to policies, practices and/or the health profile of the population. A Markov model was built using information from a variety of sources including clinical trials and epidemiological data. This type of model is a cohort or population based model; it does not take into consideration individual progression pathways, but rather the progression of the cohort. It is a relatively simple type of model, but appropriate for the modelling problem at hand (Barton, Bryan & Robinson 2004).

It is intended that the model will be modified and estimated assuming the prog-DR test is used as a standard prognostic procedure, thereby determining the value of this test. In reality, the prog-DR test will need to be further assessed to ensure its safety and efficacy. Once this has been established, a randomised clinical trial would provide the most accurate estimates of the effectiveness and cost-effectiveness of the test. At this stage, these steps are neither possible nor practical; thus a model is useful in predicting and forecasting possible costs and consequences.

Although models have been previously developed to evaluate interventions for DM (Clarke et al. 2004; Eastman et al. 1997; The CDC Diabetes Cost-effectiveness Group 2002; Zhou et al. 2005a) and DR (Vijan, Hofer & Hayward 2000), these were not ideal for this situation for various reasons. Firstly, the DM models include the progression of a wide range of complications such as CVD, nephropathy, neuropathy and the aspects of the model dealing with DR are often simplified to 3-4 stages (Eastman et al. 1997; The CDC Diabetes Cost-effectiveness Group 2002; Zhou et al. 2005a), considered only as a blindness endpoint (Clarke et al. 2004; Tilden et al. 2007) or clustered as a microvascular complication (Lamotte et al. 2002). Although this approach is reasonable for a broad view of DM, it is not sufficient for an in-depth study on DR progression. Also, as previously mentioned, DR is not the best predictor of the macrovascular and microvascular complications of DM and the association of

DR with these complications is not always straight forward. In this study, a conservative approach has been taken and the potential beneficial effects of early DR and pre-DM diagnosis on these complications were not included in the model.

Several in depth models on DR progression have been published (Dasbach et al. 1991; Davies et al. 2002; Harper et al. 2003; Sharma et al. 2001; Vijan, Hofer & Hayward 2000) and these are well equipped to examine the effects of early DR diagnosis. However, the differentiating ability of the intervention to be investigated in this study is its usefulness as a prognostic device for DM and DR; hence it is essential to also examine the pre-DR and pre-DM stages of DR progression.

Many reports have shown that patient response to and participation in screening and treatment regimes are of paramount importance for most diabetic interventions (Polak et al. 2003; Schoenfeld et al. 2001) as reviewed by Lerman (2005), yet these are not often addressed in DM and DR intervention models. For example, studies have shown that compliance to behaviour oriented glycemic control is much lower than for simple medications (Rubin 2005); only 16% of diabetic patients received the recommended annual screening in two consecutive years (Mukamel et al. 1999) and more than one third of patients do not follow screening guidelines (Schoenfeld et al. 2001). Therefore, patient behaviour such as compliance to screening and treatment recommendations and diet and exercise pattern during the pre-DM phase was included in this model as it seems likely that this would have major impact on the cost effectiveness of the prog-DR test.

Detailed results of the economic evaluation will be described in Chapter 4. However, in summary, the base case model predicts that a majority of the 599,393 individuals with undiagnosed diabetes and pre-diabetes who visit optometrists in a one year period, would progress to more severe stages of DR as shown in Figure 3.2 and that, on average, an individual would lose 0.03 QALYs (the average QALY score per person would decrease from 0.840 to 0.810) over a 10 year period. The model also predicts that a total cost of over $AUD4,090 million would be incurred by the health and welfare systems with

the cost of blindness being the most costly component (more than $3,296 million) followed by the cost for blood glucose management (more than $627 million).

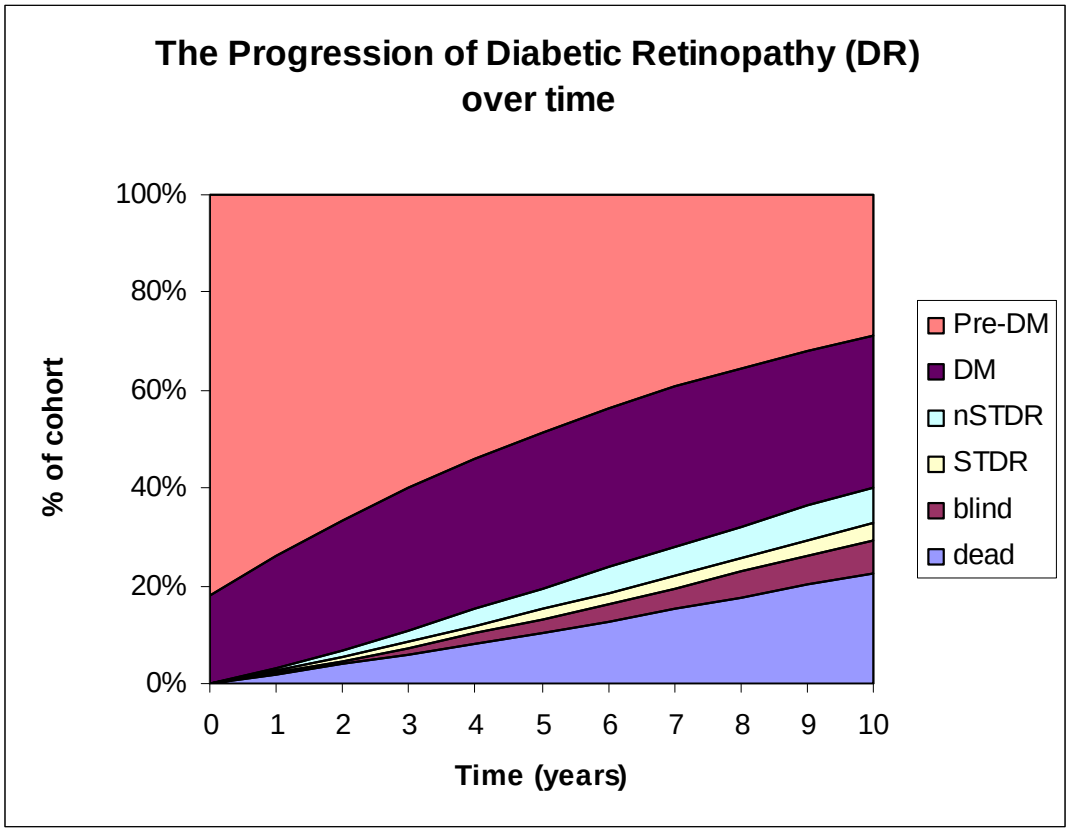

Figure 3.2: The cohort progression of DR over time. Pre-DM is pre-diabetes; DM is Diabetes Mellitus; nSTDR is non-sight threatening DR and STDR is sight threatening DR.

3.2.1 Limitations of the model

Markov models lack memory such that the transition probability is only dependent on the current state and not any previous states. This may not always be the case in "real life" situations; for example a patient who has been compliant with blood glucose management over a number of years is more likely to remain compliant, whereas a patient whose compliance has been erratic or who has been non-compliant is less likely to comply in the new cycle. This issue may have been overcome by introducing new states in the model which are dependent on previous actions; however this would complicate the model and is not practical as there are not sufficient data on compliance probabilities of DM and DR patients, based on previous compliance.

An inherent weakness of any model is that it assumes ceteris paribus, that is everything remains the same, when this is not always the case. For example, some of the data used in this model originated in the 1990s, and since then the management of DM, DR and blood glucose levels has improved due to better understanding of the disease process and development of improved medications. Patient behaviour, such as compliance to blood glucose management and eye examinations, which is important in determining the success of a diagnostic test, may also change over time. Out of pocket costs for visiting general practitioners, optometrists and or ophthalmologists were also not included as this not only changes overt time but very dependent on individual subjects. Therefore, a model is only as good as the assumptions made, and as reliable as the data it was built on.

An assumption which may not be realistic is that success in blood glucose management, (and therefore the reduced probability of progression), is dependent on the method used and rate of compliance. It implicitly assumes that patients will use the appropriate management method and that compliance automatically translates to success. Unfortunately, this is not always the case, as trial and error may be required to find the appropriate blood glucose management method or medication for a patient and depending on the severity of the disease, some patients may find it more or less difficult to successfully manage their blood glucose levels.

As mentioned, the model combines the results of research undertaken on populations living in UK (UK Prospective Diabetes Study Group 1998), China(Pan et al. 1997) and US (Klein et al. 1995) and includes subjects mostly over 30 years of age (Klein et al. 1995) whereas the hypothetical population is Australian and includes patients from all age groups. The assumption is that these data are comparable whereas they are in fact the best data available.

The health utility values are also limited to the data available. The model requires utility values specific to different states of DR; however most authors report utility values based on visual acuity (Brown et al. 1999; Sharma et al. 2003). Tung et al reported utility values for different stages of DR (Tung et al. 2005), however the sample size is relatively small (373), the response rate was

only 44% and the sample population had all been diagnosed with DM for over 10 years ; in contrast, many members of the hypothetical population would be newly diagnosed.

Therefore, the study by Fong et al (2002) on the visual acuity of DR patients at different stages was used to translate the utility values for different visual acuity levels of DR patients in the study by Brown et al (1999). It should be noted however, that the sample population in the Brown et al study had poor visual acuity (20/40 or worse) as the authors found that patients with good vision were unwilling to trade-off life years for perfect vision, making it difficult to use the time trade-off method to find the utility values. Also, as the authors suggested, patients with poor visual acuity may have already adapted to living with this handicap and hence may not consider a fall in visual acuity as having a major impact on their quality of life. Despite these two issues, the study by Brown et al provided the best available data showing that loss of vision has a detrimental effect on quality of life.

In summary, this Markov model for DR progression was able to estimate the DR states of a hypothetical cohort, including quality adjusted life years and costs, and can be used to predict potential changes to these outcomes if health policies and practices are modified. The model will be used to estimate the cost effectiveness and cost utility of the prog-DR screening test.

3.3 References

Aiello, L., Gardner, T., King, G., Blankenship, G., Cavallerano, J., Ferris, F. & Klein, R. 1998, 'Diabetic Retinopathy', *Diabetes Care*, vol. 21, no. 1, pp. 143-156.

Australian Bureau Of Statistics 2006, *Consumer Price Index, Australia*.

Australian Institute Of Health And Welfare 2004, *2003-2004 CSTDA NMDS User Data Cube*, <http://www.aihw.gov.au/disability/datacubes/index.cfm>.

Bamashmus, M., Matlhaga, B. & Dutton, G. 2004, 'Causes Of Blindness And Visual Impairment In The West Of Scotland', *Eye*, vol. 18, no. 3, pp. 257-261.

Bamroongsuk, P., Yi, Q., Harper, C.A. & Mccarty, D.J. 2002, 'Delivery Of Photocoagulation Treatment For Diabetic Retinopathy At A Large Australian Ophthalmic Hospital: Comparisons With National Clinical Practice Guidelines', *Clinical And Experimental Ophthalmology*, vol. 30, no. 2, pp. 115-119.

Barton, P., Bryan, S. & Robinson, S. 2004, 'Modelling In The Economic Evaluation Of Health Care: Selecting The Appropriate Approach', *Journal Of Health Services Research & Policy*, vol. 9, no. 2, P. 110.

Batchelder, T. & Barricks, M. 1995, 'The Wisconsin Epidemiologic Study Of Diabetic Retinopathy', *Archives Of Ophthalmology*, vol. 113, no. 6, pp. 702a-703a.

Brown, G., Brown, M. & Sharma, S. 2000, 'How Often Should Patients With Diabetes Be Screened For Retinopathy? [Letters]', *The Journal Of The American Medical Association*, vol. 284, no. 4, pp. 437-439.

Brown, M.M., Brown, G.C., Sharma, S. & Shah, G. 1999, 'Utility Values And Diabetic Retinopathy', *American Journal Of Ophthalmology*, vol. 128, no. 3, pp. 324-330.

Centre For Epidemiology And Research & NSW Department Of Health 2004, 'New South Wales Adult Health Survey 2003', *New South Wales Public Health Bulletin*, vol. 15, no. S4.

Clarke, P., Gray, A., Briggs, A., Farmer, A., Fenn, P., Stevens, R., Matthews, D., Stratton, I. & Holman, R. 2004, 'A Model To Estimate The Lifetime Health Outcomes Of Patients With Type 2 Diabetes: The United Kingdom Prospective Diabetes Study

(UKPDS) Outcomes Model (UKPDS no. 68)', *Diabetologia*, vol. 47, no. 10, pp. 1747-1759.

Colagiuri, S., Colagiuri, R., Conway, B., Grainger, D. & Davey, P. 2003, *Diabco$T Australia: Assessing The Burden Of Type 2 Diabetes In Australia*, Canberra.

Cusick, M., Meleth, A.D., Agron, E., Fisher, M.R., Reed, G.F., Knatterud, G.L., Barton, F.B., Davis, M.D., Ferris, F.L., III, Chew, E.Y. & Early Treatment Diabetic Retinopathy Study Research Group 2005, 'Associations Of Mortality And Diabetes Complications In Patients With Type 1 And Type 2 Diabetes: Early Treatment Diabetic Retinopathy Study Report no. 27 ', *Diabetes Care*, vol. 28, no. 3, pp. 617-625.

Dasbach, E., Fryback, D., Newcomb, P., Klein, R. & Klein, B. 1991, 'Cost Effectiveness Of Strategies For Detecting Diabetic Retinopathy.' *Medical Care*, vol. 29, pp. 20-39.

Davies, R., Roderick, P., Canning, C. & Brailsford, S. 2002, 'The Evaluation Of Screening Policies For Diabetic Retinopathy Using Simulation', *Diabetic Medicine*, vol. 19, no. 9, pp. 762-770.

Department Of Health And Ageing, A.G. 2004, *Medicare Benefit Schedule Book*.

Department Of Health And Ageing, A.G. 2005, *Schedule Of Pharmaceutical Benefits For Approved Pharmacists And Medical Practitioners*.

Department Of Human Services 2005, *Centrelink*.

Dunstan, D., Zimmet, P., Welborn, T., Sicree, R., Armstrong, T., Atkins, R., Cameron, A., Shaw, J., Chadban, S. & On Behalf Of The Ausdiab Steering Committee 2001, *Diabesity And Associated Disorders In Australia - 2000: The Accelerating Epidemic. The Australian Diabetes, Obesity And Lifestyle Report.*, International Diabetes Institute, Melbourne.

Eastman, R., Javitt, J., Herman, W., Dasbach, E., Zbrozek, A., Dong, F., Manninen, D., Garfield, S., Copley-Merriman, C., Maier, W., Eastman, J., Kotsanos, J., Cowie, C. & Harris, M. 1997, 'Model Of Complications Of NIDDM. I. Model Construction And Assumptions', *Diabetes Care*, vol. 20, no. 5, pp. 725-727.

Edelstein, S., Knowler, W., Bain, R., Andres, R., Barrett-Connor, E., Dowse, G., Haffner, S., Pettitt, D., Sorkin, J., Muller, D., Collins, V. & Hamman, R. 1997, 'Predictors

Of Progression From Impaired Glucose Tolerance To NIDDM: An Analysis Of Six Prospective Studies', *Diabetes*, vol. 46, no. 4, pp. 701-710.

Eriksson, K. & Lindgarde, F. 1991, 'Prevention Of Type 2 (Non-Insulin-Dependent) Diabetes Mellitus By Diet And Physical Exercise. The 6-Year Malmo Feasibility Study.' *Diabetologia*, vol. 34, no. 12, pp. 891-898.

Fong, D.S., Sharza, M., Chen, W., Paschal, J.F., Ariyasu, R.G. & Lee, P.P. 2002, 'Vision Loss Among Diabetics In A Group Model Health Maintenance Organization (HMO)', *American Journal Of Ophthalmology*, vol. 133, no. 2, pp. 236-241.

Grimmett, G. & Stirzaker, D. 1992, *Probability And Random Processes*, Oxford University Press, Oxford.

Handbook, A.M. 2004, *Australian Medicines Handbook*, Adelaide.

Harper, P.R., Sayyad, M.G., De Senna, V., Shahani, A.K., Yajnik, C.S. & Shelgikar, K.M. 2003, 'A Systems Modelling Approach For The Prevention And Treatment Of Diabetic Retinopathy', *European Journal Of Operational Research*, vol. 150, no. 1, pp. 81-91.

Hoskins, H. 2000, 'How Often Should Patients With Diabetes Be Screened For Retinopathy? [Letters]', *The Journal Of The American Medical Association*, vol. 284, no. 4, pp. 437-439.

Janghorbani, M., Jones, R.B. & Allison, S.P. 2000, 'Incidence Of And Risk Factors For Proliferative Retinopathy And Its Association With Blindness Among Diabetes Clinic Attenders', *Ophthalmic Epidemiology*, vol. 7, no. 4, pp. 225-241.

Javitt, J. 2000, 'How Often Should Patients With Diabetes Be Screened For Retinopathy? [Letters]', *The Journal Of The American Medical Association*, vol. 284, no. 4, pp. 437-439.

Javitt, J., Aiello, L., Chiang, Y., Ferris, F., Canner, J. & Greenfield, S. 1994, 'Preventive Eye Care In People With Diabetes Is Cost-Saving To The Federal Government. Implications For Health-Care Reform', *Diabetes Care*, vol. 17, no. 8, pp. 907-917.

Kawasaki, S., Hasegawa, O., Satoh, S., Saito, T., Ishio, H., Fukushima, H., Kato, S., Yamashita, H., Terauchi, Y. & Sekihara, H. 2006, 'Development And Progression Of

Retinopathy After Inpatient Management Of Diabetes.' *Internal Medicine*, vol. 45, no. 22, pp. 1267-1271.

Klein, R., Klein, B.E., Moss, S. & Cruickshanks, K. 1995, 'The Wisconsin Epidemiologic Study Of Diabetic Retinopathy Study XV: The Long Term Incidence Of Macular Edema', *Ophthalmology*, vol. 102, no. 1, pp. 7-16.

Klein, R., Klein, B.E.K., Moss, S.E. & Cruickshanks, K.J. 1999, 'Association Of Ocular Disease And Mortality In A Diabetic Population', *Archives Of Ophthalmology*, vol. 117, no. 11, pp. 1487-1495.

Kohner, E., Stratton, I., Aldington, S., Holman, R. & Matthews, D. 2001, 'Relationship Between The Severity Of Retinopathy And Progression To Photocoagulation In Patients With Type 2 Diabetes Mellitus In The UKPDS (UKPDS 52).' *Diabetic Medicine*, vol. 18, no. 3, pp. 178-184.

Lamotte, M., Annemans, L., Lefever, A., Nechelput, M. & Masure, J. 2002, 'A Health Economic Model To Assess The Long-Term Effects And Cost-Effectiveness Or Orlistat In Obese Type 2 Diabetic Patients', *Diabetes Care*, vol. 25, no. 2, pp. 303-308.

Lawson, P., Hunt, B. & Kohner, E. 1985, 'Medical Conditions In Patients With Diabetic Maculopathy', *Diabetic Medicine*, vol. 2, no. 4, pp. 245-250.

Lerman, I. 2005, 'Adherence To Treatment: The Key For Avoiding Long-Term Complications Of Diabetes', *Archives Of Medical Research*, vol. 36, no. 3, pp. 300-306.

Lovestam-Adrian, M., Hansson-Lundblad, C. & Torffvit, O. 2007, 'Sight-Threatening Retinopathy Is Associated With Lower Mortality In Type 2 Diabetic Subjects: A 10-Year Observation Study .' *Diabetes Research And Clinical Practice*, vol. 77, no. 1, pp. 141-147.

Markhotina, N., Liu, G.J. & Martin, D.K. 2007, 'Contractility Of Retinal Pericytes Grown On Silicone Elastomer Substrates Is Through A Protein Kinase A-Mediated Intracellular Pathway In Response To Vasoactive Peptides', *Nanobiotechnology, IET*, vol. 1, no. 3, pp. 44-51.

Martin, D.K. & Markhotina, N. 2002, 'Novel Screens To Identify Agents That Modulate Retinal Blood Vessel Function And Pericyte Function And Diagnostic And Therapeutic Application Therefore', World WO03103771.

Mathers, C., Vos, T. & Stevenson, C. 1999, *The Burden Of Disease And Injury In Australia Cat. no. PHE 17*, Canberra.

Medicare Australia 2005, *Medicare Benefits Schedule (MBS) Item Statistics Reports*, <http://www.medicareaustralia.gov.au>.

Mukamel, B.D., Bresnick, H.G., Wang, Q. & Dickey, F.C. 1999, 'Barriers To Compliance With Screening Guidelines For Diabetic Retinopathy', *Ophthalmic Epidemiology*, vol. V6, no. 1, pp. 61-72.

Murray, C. & Lopez, A. 1996, *The Global Burden Of Disease: A Comprehensive Assessment Of Mortality And Disability From Diseases, Injuries And Risk Factors In 1990 And Projected To 2020. volume 1*, Harvard School Of Public Health.

National Health And Medical Research Council 1997, *Management Of Diabetic Retinopathy*, National Health And Medical Research Council (NHMRC), Canberra.

NSW Health Department Funding And Systems Policy Branch 2003, *NSW Costs Of Care Standards 2003/04*.

Optometrists Association Australia 2005, *Diabetes Guidelines*.

Pan, X., Li, G., Hu, Y., Wang, J., Yang, W., An, Z., Hu, Z., Lin, J., Xiao, J., Cao, H., Liu, P., Jiang, X., Jiang, Y., Wang, J., Zheng, H., Zhang, H., Bennett, P. & Howard, B. 1997, 'Da Qing IGT Study: Effects Of Diet And Exercise In Preventing NIDDM In People With Impaired Glucose Tolerance', *Diabetes Care*, vol. 20, no. 4, pp. 537-544.

Polak, B.C.P., Crijns, H., Casparie, A.F. & Niessen, L.W. 2003, 'Cost-Effectiveness Of Glycemic Control And Ophthalmological Care In Diabetic Retinopathy', *Health Policy*, vol. 64, no. 1, pp. 89-97.

Powrie, J.K., Watts, G.F., Ingham, J.N., Taub, N.A., Talmud, P.J. & Shaw, K.M. 1994, 'Role Of Glycaemic Control In Development Of Microalbuminuria In Patients With Insulin Dependent Diabetes', *British Medical Journal*, vol. 309, no. 6969, pp. 1608-1612.

Rossing, P., Hougaard, P. & Parving, H.-H. 2002, 'Risk Factors For Development Of Incipient And Overt Diabetic Nephropathy In Type 1 Diabetic Patients: A 10-Year Prospective Observational Study', *Diabetes Care*, vol. 25, no. 5, pp. 859-864.

Rubin, R.R. 2005, 'Adherence To Pharmacologic Therapy In Patients With Type 2 Diabetes Mellitus', *The American Journal Of Medicine*, vol. 118, no. 5, Supplement 1, pp. 27-34.

Schoenfeld, E.R., Greene, J.M., Wu, S.Y. & Leske, M.C. 2001, 'Patterns Of Adherence To Diabetes Vision Care Guidelines: Baseline Findings From The Diabetic Retinopathy Awareness Program', *Ophthalmology*, vol. 108, no. 3, pp. 563-571.

Schrier, R.W., Estacio, R.O., Esler, A. & Mehler, P. 2002, 'Effects Of Aggressive Blood Pressure Control In Normotensive Type 2 Diabetic Patients On Albuminuria, Retinopathy And Strokes', *Kidney International*, vol. 61, no. 3, pp. 1086-1097.

Sharma, S., Hollands, H., Brown, G., Brown, M., Shah, G. & Sharma, S. 2001, 'The Cost-Effectiveness Of Early Vitrectomy For The Treatment Of Vitreous Hemorrhage In Diabetic Retinopathy', *Current Opinion In Ophthalmology*, vol. 12, no. 3, pp. 230-234.

Sharma, S., Oliver-Fernandez, A., Bakal, J., Hollands, H., Brown, G.C. & Brown, M.M. 2003, 'Utilities Associated With Diabetic Retinopathy: Results From A Canadian Sample', *British Journal Of Ophthalmology*, vol. 87, no. 3, pp. 259-261.

Stephenson, J., Fuller, J., Viberti, G., Sjolie, A. & Navalesi, R. 1995, 'Blood Pressure, Retinopathy And Urinary Albumin Excretion In IDDM: The EURODIAB IDDM Complications Study', *Diabetologia*, vol. 38, no. 5, pp. 599-603.

Stratton, I.M., Kohner, E.M., Aldington, S.J., Turner, R.C., Holman, R.R., Manley, S.E. & Matthews, D.R. 2001, 'UKPDS 50: Risk Factors For Incidence And Progression Of Retinopathy In Type II Diabetes Over 6 Years From Diagnosis', *Diabetologia*, vol. 44, no. 2, pp. 156-163.

Tapp, R.J., Shaw, J.E., Harper, C.A., De Courten, M.P., Balkau, B., Mccarty, D.J., Taylor, H.R., Welborn, T.A. & Zimmet, P.Z. 2003, 'The Prevalence Of And Factors Associated With Diabetic Retinopathy In The Australian Population', *Diabetes Care*, vol. 26, no. 6, pp. 1731-1737.

The CDC Diabetes Cost-Effectiveness Group 2002, 'Cost-Effectiveness Of Intensive Glycemic Control, Intensified Hypertension Control, And Serum Cholesterol Level Reduction For Type 2 Diabetes', *JAMA*, vol. 287, no. 19, pp. 2542-2551.

Tilden, D.P., Mariz, S., O'Bryan-Tear, G., Bottomley, J. & Diamantopoulos, A. 2007, 'A Lifetime Modelled Economic Evaluation Comparing Pioglitazone And Rosiglitazone For

The Treatment Of Type 2 Diabetes Mellitus In The UK.' *Pharmacoeconomics*, vol. 25, no. 1, pp. 39-54.

Torffvit, O., Lovestam-Adrian, M., Agardh, E. & Agardh, C.-D. 2005, 'Nephropathy, But Not Retinopathy, Is Associated With The Development Of Heart Disease In Type 1 Diabetes: A 12-Year Observation Study Of 462 Patients', *Diabetic Medicine*, vol. 22, no. 6, pp. 723-729.

Tung, T.-H., Chen, S.-J., Lee, F.-L., Liu, J.-H., Lin, C.-H. & Chou, P. 2005, 'A Community-Based Study For The Utility Values Associated With Diabetic Retinopathy Among Type 2 Diabetics In Kinmen, Taiwan', *Diabetes Research And Clinical Practice*, vol. 68, no. 3, pp. 265-273.

Tuomilehto, J., Lindstrom, J., Eriksson, J.G., Valle, T.T. & Al, E. 2001, 'Prevention Of Type 2 Diabetes Mellitus By Changes In Lifestyle Among Subjects With Impaired Glucose Tolerance', *The New England Journal Of Medicine*, vol. 344, no. 18, P. 1343.

UK Prospective Diabetes Study Group 1998, 'Intensive Blood-Glucose Control With Sulphonylureas Or Insulin Compared With Conventional Treatment And Risk Of Complications In Patients With Type 2 Diabetes (UKPDS 33)', *Lancet*, vol. 352, no. 9131, pp. 837-853.

Van Hecke, M.V., Dekker, J.M., Stehouwer, C.D.A., Polak, B.C.P., Fuller JH, Sjolie AK, Kofinis A, Rottiers R, Porta M & N, C. 2005a, 'Diabetic Retinopathy Is Associated With Mortality And Cardiovascular Disease Incidence: The EURODIAB Prospective Complications Study', *Diabetes Care*, vol. 28, no. 6, P. 1383.

Van Hecke, M.V., Dekker, J.M., Stehouwer, C.D.A., Polak, B.C.P., Fuller JH, Sjolie AK, Kofinis A, Rottiers R, Porta M & N, C. 2005b, 'Diabetic Retinopathy Is Associated With Mortality And Cardiovascular Disease Incidence: The EURODIAB Prospective Complications Study', *Diabetes Care*, vol. 28, no. 6, pp. 1383-1389.

Vijan, S., Hofer, T. & Hayward, R. 2000, 'Cost-Utility Analysis Of Screening Intervals For Diabetic Retinopathy In Patients With Type 2 Diabetes Mellitus', *The Journal Of The American Medical Association*, vol. 283, no. 7, pp. 889-896.

Villar, G., Garcia, Y., Goicolea, I. & Vazquez, J. 1999, 'Determinants Of Development Of Microalbuminuria In Normotensive Patients With Type 1 And Type 2 Diabetes.' *Diabetes Metabolism*, vol. 25, no. 3, pp. 246-254.

Vision Australia 2005, *Equipment Catalogue*.

Yi, Q., Bamroongsuk, P., Mccarty, D.J., Mukesh, B.N. & Harper, C.A. 2003, 'Clinical Outcomes Following Laser Photocoagulation Treatment For Diabetic Retinopathy At A Large Australian Ophthalmic Hospital', *Clinical And Experimental Ophthalmology*, vol. 31, no. 4, pp. 305-309.

Zhou, H., Isaman, D.J.M., Messinger, S., Brown, M.B. & Al, E. 2005a, 'A Computer Simulation Model Of Diabetes Progression, Quality Of Life, And Cost', *Diabetes Care*, vol. 28, no. 12, pp. 2856.

Zhou, H., Isaman, D.J.M., Messinger, S., Brown, M.B. & Al, E. 2005b, 'A Computer Simulation Model Of Diabetes Progression, Quality Of Life, And Cost', *Diabetes Care*, vol. 28, no. 12, pp. 2856-2863.

Chapter 4: Evaluation of a Novel Prognostic Procedure for Diabetic Retinopathy: Health Economics and Policy Implications

Diabetic Retinopathy (DR) is a chronic complication of both Types I and II Diabetes Mellitus (DM). It occurs when high levels of blood glucose damage the micro-vessels of the retina, causing the micro-vessels to become leaky, occluded and even proliferate. Chronic retinal damage has detrimental effects on sight and can lead to blindness.

A novel, non-invasive prognostic procedure (prog-DR) has been developed in our laboratory (Markhotina, Liu & Martin 2007; Martin & Markhotina 2002). The prognostic procedure detects the damaging effects of high blood glucose on the retinal microvasculature before the development of clinical symptoms. The prog-DR procedure measures the change in diameter or blood flow that is stimulated in the retinal microvasculature by the action of a stimulating compound that targets the microvasculature pericytes (Martin & Markhotina 2002). Pre-clinical studies indicate that the procedure provides the prognostic capability to detect the damaging effects of high blood glucose on the retinal microvasculature. Thus, prog-DR will allow earlier identification of individuals with pre-diabetes or diabetes.

In this paper we utilise a Markov model (Ting, Martin & Haas 2007) for DR progression to evaluate whether the use of prog-DR confers advantages and the extent to which this occurs for a hypothetical cohort of patients with either (a) undiagnosed diabetes without DR or (b) pre-diabetes.

4.1 Methods

4.1.1 Model structure and assumptions

The model of the patient cohort (Ting, Martin & Haas 2007) was constructed using (i) published studies on progression of pre-diabetes and DR; (ii) published studies on interventions examining the effects on clinical and quality of life outcomes of compliance with management of DR and blood glucose; (iii) scheduled medical fees and (iv) prognosis-related health-care and non-health care costs.

Unlike other models, it includes the pre-DM state because previous research has shown that individuals in this health state are at high risk of progressing to diabetes (Eriksson & Lindgarde 1991; Pan et al. 1997; Tuomilehto et al. 2001). The model also includes patient behaviour such as diet and exercise patterns and responses to treatment and screening recommendations (i.e. compliance probabilities).

All costs were estimated in 2005 Australian dollars and costs and outcomes were discounted at 3% (Gold et al. 1996; Mathers, Vos & Stevenson 1999; Murray & Lopez 1996). Total accumulated costs, sight-years, life-years and QALYs were estimated by simulating a hypothetical cohort and following them for 10 years.

The cohort consisted of 599,393 individuals with either undiagnosed diabetes without DR or pre-diabetes who visited an optometrist or ophthalmologist for either a comprehensive or brief initial consultation (Medicare Benefit Schedule (MBS) codes 10900 and 10916 respectively) in 2005 (Medicare Australia 2005). Without the use of prog-DR, such at-risk individuals would not be detected under current practice. Individuals already diagnosed with diabetes were not included as most patients with diabetes develop DR (Klein et al. 1998) and it was assumed that their risk of DR would have already be made known to them. The model assumed that the results of prog-DR would enable individuals to make decisions about modifying their lifestyle and initiate appropriate management measures (with the help of health care professionals) which in turn will change the probability of progression to more severe stages of DR.

Details of the assumptions made in modelling the cohort of patients and the sources of data are presented in Tables 4.1 and 4.2.

The model was used to evaluate the value for money of the prog-DR test via (*i*) a cost effectiveness analysis using sight years (SY) and life years (LY) gained as the measures of effectiveness, and (*ii*) a cost-utility analysis using quality adjusted life years (QALYs) as the measure of utility. The results are reported as Incremental Cost-Effectiveness Ratios (ICERs).

4.1.2 Scenario analysis

Scenario analysis was performed to investigate the effects of varying patient behavioural reactions to the prog-DR test. Different levels of compliance to NHMRC guidelines for DR and blood glucose management were examined and the scenarios are summarised in Table 4.3.

4.1.3 Sensitivity Analysis

We investigated the sensitivity of the outcomes generated by the Markov model by varying the input values by ±10% (summarised in Appendix B Tables B.1 and B.2). The sensitivity of the utility value for blindness was tested by lowering it from 0.64 to 0.26 which is the lower limit suggested in literature (Brown, Brown & Sharma 2000; Brown et al. 2001; Hoskins 2000; Javitt 2000).

	Pre-diabetics *Diet and exercise patterns*	***Diabetics*** *Blood glucose management*	***NHMRC guideline on Diabetic Retinopathy*** *eye examinations and treatments*
With prog-DR test	Similar to the overweight pre-diabetic subjects in the control group of the Diabetes Prevention Study who were given oral and written information about the appropriate diet and exercise (Tuomilehto et al. 2001) similar to that which a patient may receive at a visit to their GP.	Use of insulin, hypoglycemic medication and/or diet and exercise, either intensively (ie being able to maintain blood glucose at or lower than 6 mmol/L and HbA below 7%) or conventionally (ie blood glucose above 6 mmol/L and HbA above 7%) similar to the subjects in the UKPDS (UK Prospective Diabetes Study Group 1998)	Aware hence have the opportunity to comply with the recommendations.

Table 4.1: The differences in behaviour of diagnosed (with prog-DR test) and non-diagnosed (without test) subjects

	Pre-diabetics *Diet and exercise patterns*	***Diabetics*** *Blood glucose management*	***NHMRC guideline on Diabetic Retinopathy*** *eye examinations and treatments*
Without test	Similar to non-over weight respondents to the 2003 NSW Health Survey (Centre for Epidemiology and Research & NSW Department of Health 2004); this group will not receive any information which would predispose them to modify their existing diet and exercise patterns.	Maintain blood glucose levels conventionally by using diet and exercise only.	Unaware hence unable to follow.

Table 4.1: The differences in behaviour of diagnosed (with prog-DR test) and non-diagnosed (without test) subjects continue

Items for pre-DR screening	Cost †
Pre-DR test *	$59.50
Standard initial consultation (MBS item 2620) †	$21.00
OGTT pathology test (MBS item 66542) †	$19.30
Extended consultation on OGTT result and blood glucose management advice (MBS item 22622) †	$38.00
Total for pre-DR screening	$137.80

Table 4.2: The cost for pre-DR screening based on Australian Benefit Schedule (Department of Health and Ageing 2004). Costs associated with the screening test and follow-up diagnosis and treatment are included in the model. * It is expected that the cost of consumables and the skills and time required for this test would be similar to that needed for an optic fundi examination with intravenous dye (MBS code 11212) (Department of Health and Ageing 2004). †As screening will identify diabetics and pre-diabetics not yet diagnosed, the cost of referral to a general practitioner for an oral glucose tolerance test (OGTT) and subsequent management of the condition based on Medicare Benefit Schedule Book (Department of Health and Ageing 2004) were also included.

4.2 Results

4.2.1 Clinical and Costs Outcomes

The results indicate that using the prog-DR test would result in improved clinical outcomes. Over a ten year period, use of the prog-DR test resulted in an additional 9,961 life years, 25,629 sight years and 36,090 QALYs. Its use would also reduce the proportion of patients who progress to advanced stages of DR where sight is highly likely to be or is affected (Figure 4.1).

The use of prog-DR was associated with an increase in the median total accumulated cost (approximately an additional $1,794 ± 67 million), although this did not occur uniformly. While prog-DR resulted in a reduction in the accumulated cost of blindness by approximately $305 million (at the end of 10 years), increases in other costs such as those associated with the management of blood glucose and routine eye examinations offset this reduction.

4.2.2 Incremental Cost Effectiveness

The median incremental cost effectiveness ratio (ICER) was $180,080 ± 6,756 per life year gained, $69,991 ± 2,626 per sight year gained and $49,703 ± 1,865 per QALY gained. The relevance of these ICER values are illustrated in the Cost Effectiveness Analysis plot in Figure 4.2, which also reflects the implicit threshold values implied by PBAC decisions in 2005 prices. The “accept line” represents an ICER of $50,714, so that a new intervention with an ICER point which lies below this line is considered to be cost effective; the “reject line” represents the ICER of $94,705 so that interventions with an ICER point above this line are not considered cost effective. The area between these two lines can be interpreted as a “grey” area, so that interventions with ICER points here may or may not be judged to be cost effective.

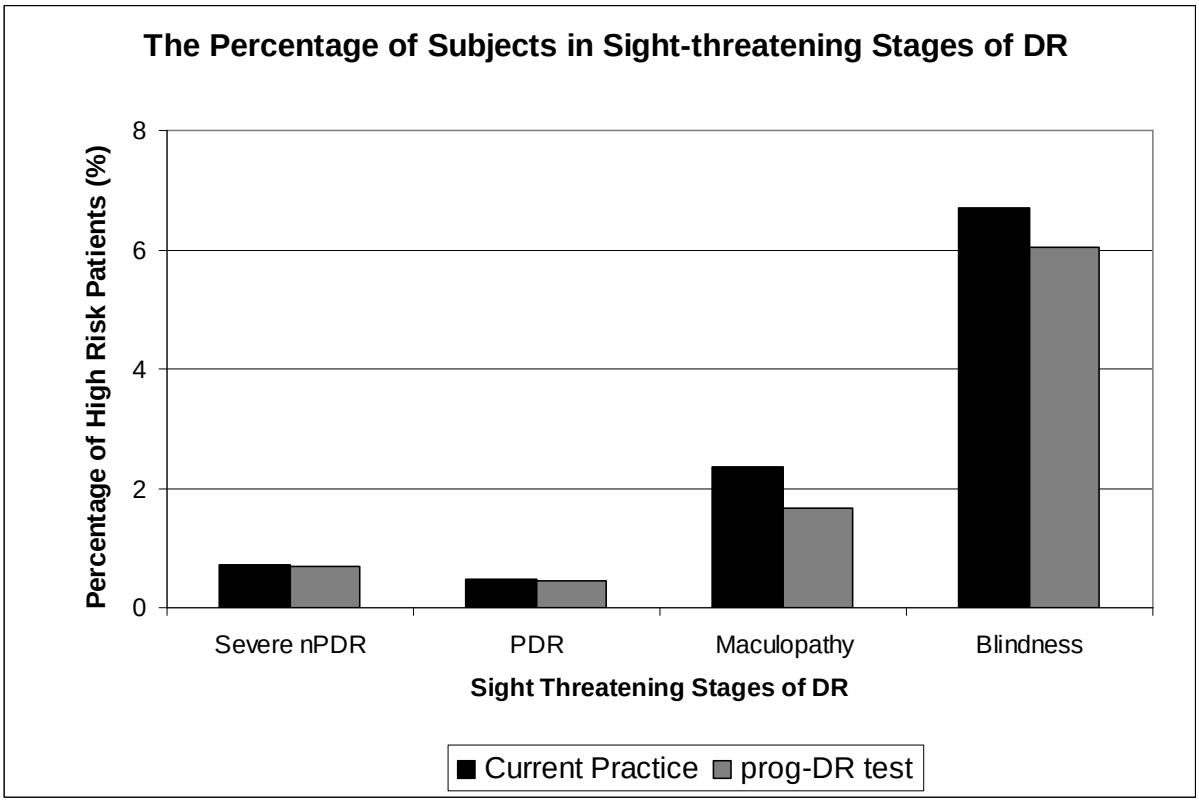

Figure 4.1: The percentage of subjects in sight threatening Stage of DR. Severe non-proliferative Diabetic Retinopathy (nPDR), Proliferative Diabetic Retinopathy (PDR), maculopathy and blindness are stages of Diabetic Retinopathy which can affect sight. The use of the prog-DR test reduced the percentage of subjects in these sight-threatening or threatened stages of Diabetic Retinopathy.

4.2.3 Scenario analysis

Scenario analysis was conducted to analyse the effects of different behavioural scenarios following pre-DR screening (see Table 4.3). In the best-case scenario (A), 100% compliance to blood glucose control and NHMRC eye examinations guidelines (National Health and Medical Research Council 1997) resulted in higher costs but also increases in the number of LYs, SYs and QALYs gained – producing an overall improvement in the ICERs for LYs, SYs and QALYs gained. In the worst scenario (H), while zero compliance to blood glucose control or NHMRC eye examination guidelines resulted in reductions in LY, SY and QALYs gained, there was also a significant reduction in costs – thus also producing an overall improvement in the ICERs (Figure 4.3).

Scenarios in which behaviours ranged between 0% and 100% compliance produced ICERS which fluctuate around the base case. These scenarios did not produce an ICER above the "reject line" of $94,705 nor did they cause a significant reduction (6% or more) in the probability of PBAC recommendation. The scenario analysis suggested that the cost effectiveness of the prog-DR test is not likely to be affected by the behaviour of patients post DR prognosis.

4.2.4 Sensitivity analysis

The sensitivity analysis showed that the cost per incremental QALY is sensitive to changes in (i) the need for laser treatment, (ii) discount rates, (iii) costs of blood glucose control, (iii) pre-DR screening costs and iv) total annual costs. That is, changes in these parameters increase the incremental cost per QALY beyond the threshold of $50,724 where the prog-DR test may not be considered cost-effective. However, when the probability model of PBAC recommendation developed by Harris et al (Harris et al. 2008b) was used, the ICER was only sensitive to increases in the cost of blood glucose control and total accumulated costs; that is, such increases reduced the probability of PBAC recommendations by more than 6%.

Cost per incremental QALY gained (AUD$)		**Adherence to NHMRC guidelines**		
		100%	Base case	0%
Adherence to Blood glucose control	100%	A: 45,827	B: 44,442	C: 41,598
	Base case	D: 52,903	**$49,703**	E: 50,120
	0%	F: 45,557	G: 46,124	H: 37,199

Table 4.3: Matrix of the scenarios examined with varying compliance to NHMRC guideline and blood glucose management. 100% adherence to blood glucose and NHMRC guidelines (National Health and Medical Research Council 1997) for eye examinations and treatments is considered the best behavioral scenario; the worst being 0% adherence to both parameters and the variations in adherence as scenarios in between.

4.3 Discussion

Using a Markov model to estimate DR progression from Pre-DM to death shows that the use of a pre-DR screening test results in increases in life years, sight years and QALYs gained, and a reduction in the percentage of subjects in sight-threatening stages of DR. This suggests that the use of the prog-DR test may ultimately increase longevity and improve sight and quality of life for individuals. The effect of the prog-DR test in increasing the longevity and quality of life of patients will also result in an increase in the total costs of testing and subsequent health care. This is likely to occur despite a reduction in the cost of blindness. Although productivity gains were not included in the model, it is reasonable to assume that individuals who live longer with a better quality of life will also be more likely to increase their productivity, thus contributing to the economic well-being of the community.

The results from this model can be regarded as conservative, as it does not take into account any potential reductions in the development of other complications of diabetes such as renal failure and cardiovascular disease (CVD) which may be associated with an early diagnosis of DM. Further, individual and societal benefits foregone due to the loss of sight, such as loss of income and productivity were not included in the model; it has been estimated that this may account for up to $52,348.40 per year (Australian Bureau of Statistics 2005, 2006). Further, whilst DM and DR are chronic conditions, the model was estimated over a 10 year period. Hence, it is likely that there would be greater increases in life years, sight years and QALYs if the model was continued over a longer period or until no members of the cohort were alive.

4.3.1 Limitations of the Model

There are a number of limitations to the model which need to be acknowledged. First, the model assumes that the prog-DR test is a perfect screening system, with 100% accuracy and no false positive or negative results. The extent to which this is true cannot be tested without further development of the test and, in particular, its use in animal and human clinical trials.

Second, it may not be realistic to assume that one-off screening of the whole hypothetical population will be possible within a one year timeframe as implied by the model. Even though the test takes only 15 minutes, there are additional barriers to DR screening as outlined by Keefe (2003). Third, the model assumes that all eligible individuals who consult an ophthalmologist or optometrist will have the test. This may not be realistic, as, despite the non-invasive nature of the test, not all ophthalmologists and optometrists may offer it and not all individuals will be willing to take it when offered. For a new diagnostic test to be utilised, the patient population needs to be made aware of its existence and choose to use it; and the potential providers of the test (ophthalmologists and optometrists) will also have to be able to offer the service. This seems unlikely to occur in just one year especially when unpublished data in the Ophthalmology workforce model developed by Access Economic Pty Ltd for RANZCO (2006), showed that there may be insufficient capacity in the ophthalmology workforce to meet the projected demand for services by 2014/2015.

Finally, as the subjects of the clinical studies from which the data were derived were all aged 45 years or over, the data used may not be an accurate representation of the general population. However, the model will be able to be updated when better data become available. For example, this may be possible if the proposed health smart card system is implemented; pre-DM, DM and DR progression information from patients will be able to be collected and made available in de-identified, electronic form for further research.

4.3.2 Is prog-DR cost-effective?

The cost per QALY gained for the prog-DR test ($49,703) is comparable to that estimated for annual or bi-annual DR screening US$56,435-121,932 (Vijan, Hofer & Hayward 2000), inflated to 2005 values (U.S. Department of Labor 2008) [1]. That is, compared to a benchmark, it appears to be cost-effective.

[1] Original 2000 values were US$49,760-107,510. CPI values from 2000 and 2005 were used to inflate this to 2005 value. Note that US dollar is currently worth more than Australian dollar.

However, the issue of cost-effectiveness of a particular intervention or technology can also be judged relative to a threshold. The Pharmaceutical Benefits Advisory Committee (PBAC) uses information about cost-effectiveness in making decisions about which medications should be subsidised in Australia (ie listed on the PBS). Although PBAC does not publish a threshold, the levels implied by previous reimbursement decisions made by the committee are to accept if the ICER is lower than $50,714 and reject if it is higher than $91,705 per life year gained (Australian Bureau of Statistics 2006; George, Harris & Mitchell 2001) [2]. The cost per QALY, LY and SY gained for the prog-DR test are graphed relative to these ICER thresholds in Figure 4.2.

Although the cost per additional life year gained using the prog-DR test ($180,080) was greater than the acceptable ICER implied by PBAC decisions, the cost per additional QALY gained ($49,703), was within the acceptable range and is the more appropriate comparator. This is because the QALY measure takes into account changes in both the quantity and quality of life which occur as a result of the prog-DR test.

It should be noted that the incremental cost effectiveness ratios do not represent the ultimate cut-off point for acceptable levels and it has been argued that such thresholds may not always be appropriate (Ubel et al. 2003). That is, medicines and technologies which exceed the implied ICER may still be recommended for listing on the Pharmaceutical Benefits Scheme but the chances of acceptance decreases as the ICER increases.

Although the ICER (measured as the cost per QALY gained) has a statistically significant effect on decisions made by the PBAC, many other factors influence the decision making of PBAC (George, Harris & Mitchell 2001) such as whether the disease in question is life threatening (Harris et al. 2008a), whether an alternate treatment available and in particular, the level of uncertainty in the data. For example, a medical intervention with a very low ICER may be rejected by PBAC if there are significant uncertainties about the assumptions

[2] Original 1998/1999 values were to accept if the ICER is lower than $42,000 and reject if it is higher than $76,000 per life year gained. CPI values from 1999-2005 were used to inflate these to 2005 values.

used in the economic evaluation, the benefits of the intervention or whether clinicians would implement the intervention a real-life setting.

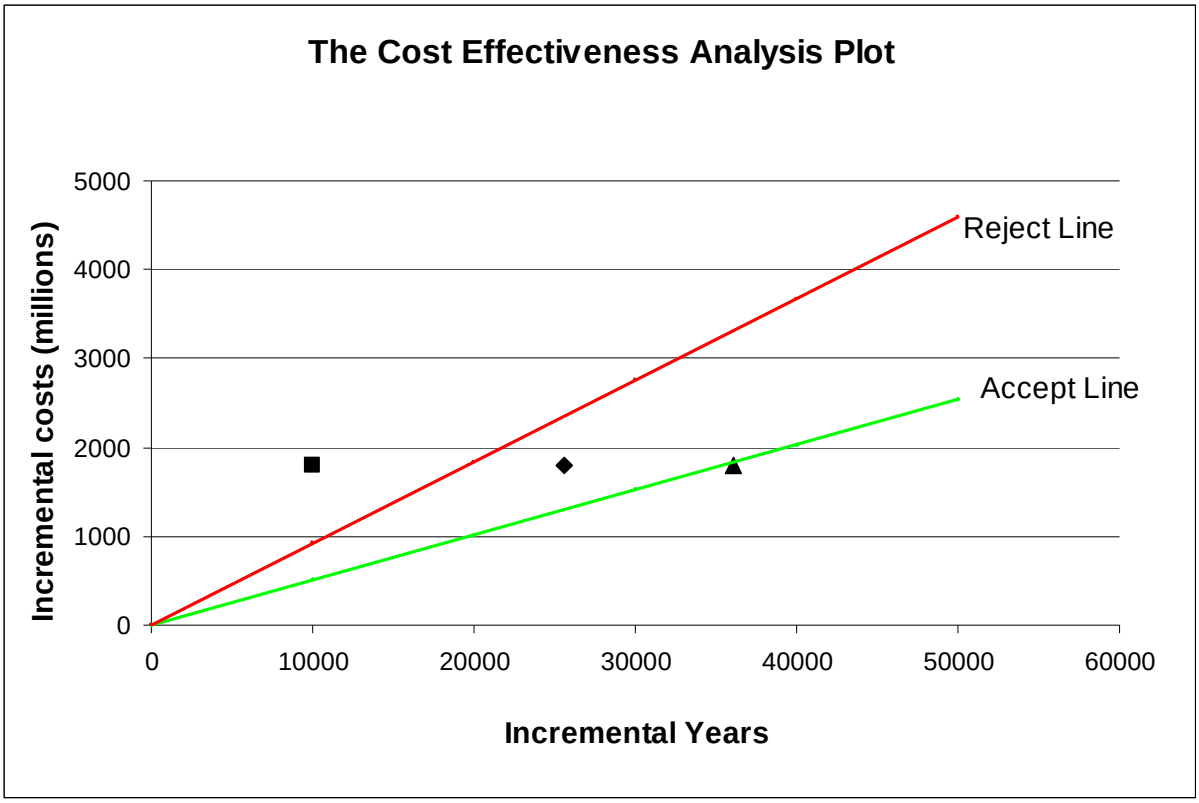

Figure 4.2: The Cost Effectiveness Analysis Plot For The Incremental QALY, Sight Year And Life Year Versus Incremental Costs. The accept line represent a cost per incremental life year of $50,714; the reject line represent a cost per incremental life year of $94,705; ▲ represents the median a cost per incremental quality adjusted life year, ◆ represents the median a cost per incremental sight year and ■ represents the median a cost per incremental life year

The model developed by Harris et al (2008) to predict the probability of PBAC recommendation was used to examine the likelihood of the prog-DR test being recommended for funding (Figure 4.3). Based on the prog-DR test having an incremental cost per QALY of $49,703, and the average ICER of PBAC submissions having a cost per QALY gained of $46,400, the predicted probability of PBAC recommending a medicine to be listed on the PBS, is approximately 10% for the prog-DR test and and 11% for the average PBAC submission. This indicates that the chances of the prog-DR test being recommended for funding is not significantly different from the average.

Although these probabilities of acceptance/recommendations are quite low, if the clinical significance of the intervention can be demonstrated, the probability rises to 33% which is below the average acceptance rate of submissions which include cost minimisation analysis (46%) but above the average acceptance rate of submissions which include cost effectiveness analysis (24%).

Harris et al (2008) also show that submissions increase their probability of recommendation (up to 22%) if they include a high level of relevant evidence, from good quality studies they conclude that the results of economic evaluations inform the decision making process but information on the cost per QALY gained (even if the technology is highly cost effective) alone is not sufficient.

In summary, the results of the economic evaluation of DR prognosis has demonstrated that the prog-DR test is cost effective relative to the bench mark of annual and bi-annual screening of DR and its ICER is within the acceptable range when both the quantity and quality of life is considered. However, the test is not cost effective relative to the average medicine submitted to the PBAC for consideration for listing on the PBS.

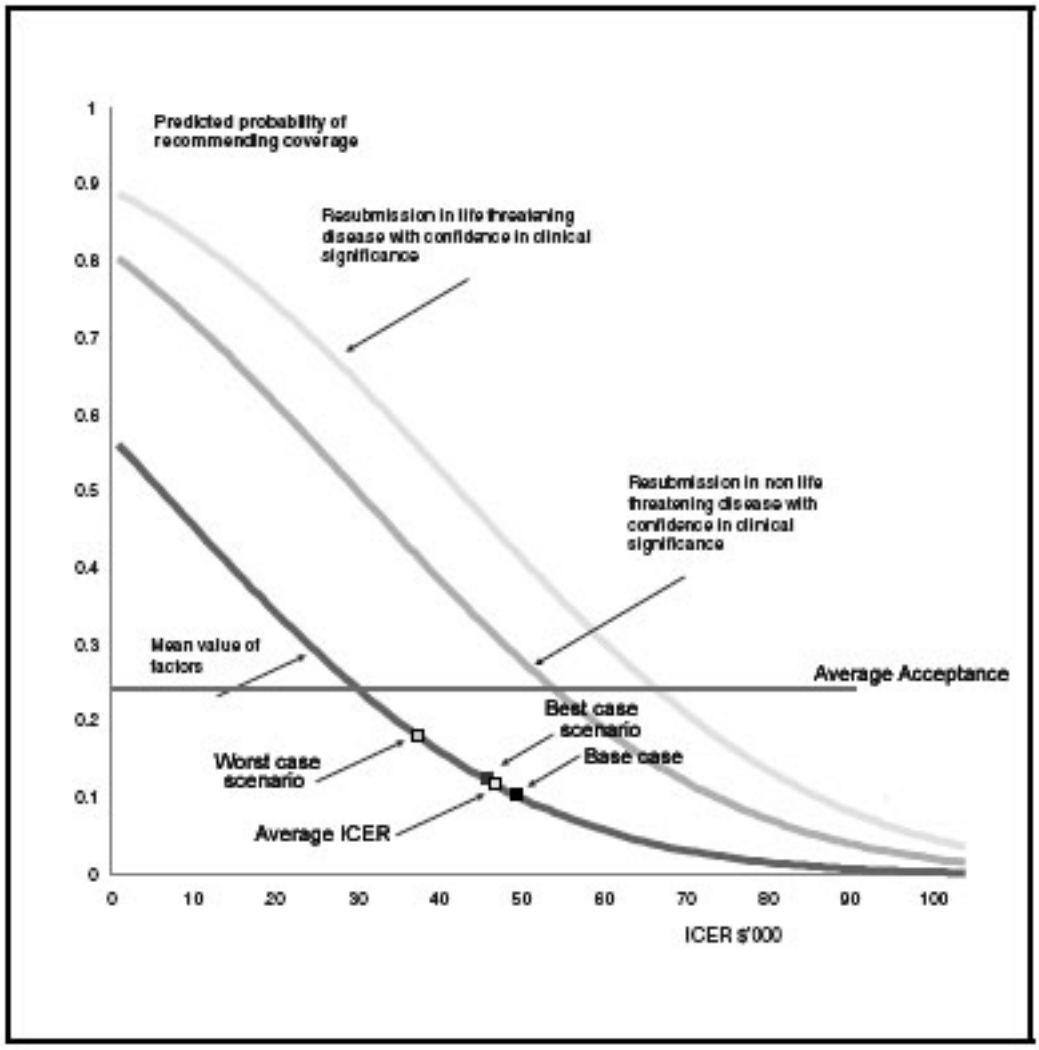

Figure 4.3: The Cost Effectiveness Analysis Plot Of The Incremental QALY And Costs In Different Case Scenarios. The "Average Acceptance" line represents the average acceptance rate of 0.24 for all cost effective analysis submitted to PBAC. "Average ICER" is $46,400, the "Base case" represents an ICER of $49,703 with the use of prog-DR test. As described in Table 4.3, the "Best case scenario" represents ICER if there was 100% compliance to blood glucose management and NHMRC guideline for eye examinations; the "Worst case scenario" represents no compliance to blood glucose management and NHMRC guideline for eye examinations. This Figure was adapted from Harris et al 2008.

4.3.3 Scenario analysis

In the scenario analysis, several scenarios resulted in improvements in the ICER (cost per QALY gained (see Table 4.3)). The worst behavioural scenario, where it is assumed that individuals do not comply at all with NHMRC guidelines for DR or blood glucose management, produced the largest reduction in the ICER; that is, it is the most cost-effective scenario. The best behavioural scenario (100% adherence to blood glucose management and 100% adherence to guideline for eye examinations and treatment) (National Health and Medical Research Council 1997) also produced an improvement in the ICER. The worst behavioural scenario is most cost effective because the reduction in costs is greater than that of the associated loss of QALYs; on the other hand, in the best behavioural scenario (or any scenario involving an increased adherence to guidelines) the increase in QALYs is not significantly greater than any concomitant increase in costs.

It is also worth noting that 100% adherence to blood glucose management always yields an increase in LYs, SYs and QALYs and an improvement in all ICERs but this is not the case for adherence to the NHMRC guidelines. This is an important finding: while it is already established that blood glucose control is the most important factor in the effective management of diabetes (Gaster & Hirsch 1998; UK Prospective Diabetes Study Group 1998), these results suggest that it is also a critical factor in the maintenance of quality of life and improving the cost effectiveness of interventions.

4.3.4 Sensitivity analysis

The sensitivity of the ICER to assumptions made about the parameters in the model was analysed using the implied threshold comparator as well as results from the probability model described by Harris et al (2008). The cost per QALY gained was sensitive to (i) changes in the need for laser treatment, and increases in (ii) the discount rate (iii) annual total cost iv) cost of pre-DR screening, (v) blood glucose control and (vi) cost of blindness. Changes in the value of these parameters produced ICERs above the $50,714 threshold but all were still below the $91,705 reject cut-off. Thus, it seems likely that screening for DR before the development of clinical symptoms is relatively cost effective. On the other hand, if the value of the parameters are changed according to the results from the probability model (Harris et al, 2008), the ICER is only sensitive to increases to blood glucose management and total accumulated costs, both of which result in a reduced probability of the prog-DR test being recommended for listing by the PBAC by more than 6%. These results suggest that costs (particularly the cost of blood glucose management and total accumulated costs) are the main drivers of the cost effectiveness of the prog-DR test,

4.3.5 Further research

The modelling approach described in this paper was used because it is more affordable and timely than a randomised clinical trial. However, in the event that the test is considered appropriate to develop further, clinical trials will be necessary to assess its safety and clinical effectiveness. Such information will also be useful to “fill in the gaps” in terms of the assumptions and other limitations of the model. For example, information which could not be included in the model about the rate of uptake of the test by both patients and providers, the costs and health-related quality of life affecting individuals at risk of developing DR and related complications such as renal failures and CVD events will be able to be collected as part of a clinical trial.

4.3.6 Conclusion

Overall, the results of this study suggest that the prog-DR test is a cost-effective screening tool. The cost-effectiveness may be improved by (i) better blood glucose management post prog-DR test, (ii) targeted screening (as opposed to population-wide screening) and (iii) reduced costs of both screening and management of DM and DR.

4.4 References

Australian Bureau Of Statistics 2005, *2005 Australian Year Book*.

Australian Bureau Of Statistics 2006, *Consumer Price Index, Australia*.

Brown, G., Brown, M. & Sharma, S. 2000, 'How Often Should Patients With Diabetes Be Screened For Retinopathy? [Letters]', *The Journal Of The American Medical Association*, vol. 284, no. 4, pp. 437-439.

Brown, M., Brown, G., Sharma, S., Kistler, J. & Brown, H. 2001, 'Utility Values Associated With Blindness In An Adult Population.' *British Journal Of Ophthalmology*, vol. 85, no. 3, P. 327.

Centre For Epidemiology And Research & NSW Department Of Health 2004, 'New South Wales Adult Health Survey 2003', *New South Wales Public Health Bulletin*, vol. 15, no. S4.

Department Of Health And Ageing, A.G. 2004, *Medicare Benefit Schedule Book*.

Eriksson, K. & Lindgarde, F. 1991, 'Prevention Of Type 2 (Non-Insulin-Dependent) Diabetes Mellitus By Diet And Physical Exercise. The 6-Year Malmo Feasibility Study.' *Diabetologia*, vol. 34, no. 12, pp. 891-898.

Gaster, B. & Hirsch, I.B. 1998, 'The Effects Of Improved Glycemic Control On Complications In Type 2 Diabetes', *Archives Of Internal Medicine*, vol. 158, no. 2, pp. 134-150.

George, B., Harris, A. & Mitchell, A. 2001, 'Cost-Effectiveness Analysis And The Consistency Of Decision Making: Evidence From Pharmaceutical Reimbursement In Australia (1991 To 1996)', *Pharmacoeconomics*, vol. 10, no. 11, pp. 1103-1109.

Gold, M., Siegel, J., Weinstein, M. & Russell, L. 1996, *Cost-Effectiveness In Health And Medicine*, Oxford University Press, New York.

Harris, A.H., Hill, S.R., Chin, G., Jing J.L. & Walkom, E. 2008a, 'The Role Of Value For Money In Public Insurance Coverage Decisions For Drugs In Australia: A Retrospective Analysis 1994-2004', *Medical Decision Making*, vol. 28, no. 5, P. 713(710).

Harris, A.H., Hill, S.R., Chin, G., Li, J.J. & Walkom, E. 2008b, 'The Role Of Value For Money In Public Insurance Coverage Decisions For Drugs In Australia: A Retrospective Analysis 1994-2004.' *Medical Decision Making*, vol. 28, no. 5, pp. 713-723.

Hoskins, H. 2000, 'How Often Should Patients With Diabetes Be Screened For Retinopathy? [Letters]', *The Journal Of The American Medical Association*, vol. 284, no. 4, pp. 437-439.

Javitt, J. 2000, 'How Often Should Patients With Diabetes Be Screened For Retinopathy? [Letters]', *The Journal Of The American Medical Association*, vol. 284, no. 4, pp. 437-439.

Keeffe, J. 2003, *Screening For Diabetic Retinopathy: A Planning And Resource Guide*, Centre For Eye Research Australia.

Klein, R., Klein, B.E.K., Moss, S.E. & Cruickshanks, K.J. 1998, 'The Wisconsin Epidemiologic Study Of Diabetic Retinopathy: XVII', *Ophthalmology*, vol. 105, no. 10, pp. 1801-1815.

Markhotina, N., Liu, G.J. & Martin, D.K. 2007, 'Contractility Of Retinal Pericytes Grown On Silicone Elastomer Substrates Is Through A Protein Kinase A-Mediated Intracellular Pathway In Response To Vasoactive Peptides', *Nanobiotechnology, IET*, vol. 1, no. 3, pp. 44-51.

Martin, D. & Markhotina, N. 2002, *Novel Screens To Identify Agents That Modulate Retinal Blood Vessel Function And Pericyte Function And Diagnostic And Therapeutic Application Therefore*, World, WO03103771.

Mathers, C., Vos, T. & Stevenson, C. 1999, *The Burden Of Disease And Injury In Australia*, AIHW.

Medicare Australia 2005, *Medicare Benefits Schedule (MBS) Item Statistics Reports*, <http://www.medicareaustralia.gov.au>.

Murray, C. & Lopez, A. 1996, *The Global Burden Of Disease: A Comprehensive Assessment Of Mortality And Disability From Diseases, Injuries And Risk Factors In 1990 And Projected To 2020. Volume 1*, Harvard School Of Public Health.

National Health And Medical Research Council 1997, *Management Of Diabetic Retinopathy*, National Health And Medical Research Council (NHMRC), Canberra.

Pan, X., Li, G., Hu, Y., Wang, J., Yang, W., An, Z., Hu, Z., Lin, J., Xiao, J., Cao, H., Liu, P., Jiang, X., Jiang, Y., Wang, J., Zheng, H., Zhang, H., Bennett, P. & Howard, B. 1997, 'Da Qing IGT Study: Effects Of Diet And Exercise In Preventing NIDDM In People With Impaired Glucose Tolerance', *Diabetes Care*, vol. 20, no. 4, pp. 537-544.

Ting, J., Martin, D. & Haas, M. 2007, 'A Markov Model Of Diabetic Retinopathy Progression For The Economic Evaluation Of A Novel DR Prognostic Device', *CHERE Working Paper*, vol. 2007, no. 14.

Tuomilehto, J., Lindstrom, J., Eriksson, J.G., Valle, T.T. & Al, E. 2001, 'Prevention Of Type 2 Diabetes Mellitus By Changes In Lifestyle Among Subjects With Impaired Glucose Tolerance', *The New England Journal Of Medicine*, vol. 344, no. 18, P. 1343.

U.S. Department Of Labor 2008, *Consumer Price Index*, Washington, D.C.

Ubel, P.A., Hirth, R.A., Chernew, M.E. & Fendrick, A.M. 2003, 'What Is The Price Of Life And Why Doesn't It Increase At The Rate Of Inflation?' *Archives Of Internal Medicine*, vol. 163, no. 14, pp. 1637-1641.

UK Prospective Diabetes Study Group 1998, 'Intensive Blood-Glucose Control With Sulphonylureas Or Insulin Compared With Conventional Treatment And Risk Of Complications In Patients With Type 2 Diabetes (UKPDS 33)', *Lancet*, vol. 352, no. 9131, pp. 837-853.

Vijan, S., Hofer, T.P. & Hayward, R.A. 2000, 'Cost-Utility Analysis Of Screening Intervals For Diabetic Retinopathy In Patients With Type 2 Diabetes Mellitus', *Journal Of The American Medical Association*, vol. 283, no. 7, pp. 889-896.

Physiological Perspective

Related publications:

Ting, J. & Martin, D. 2006, 'Basic and Clinical Aspects of Gene Therapy for Retinopathy Induced by Diabetes', Current Gene Therapy, vol. 6, no. 2, pp. 193-214

Chapter 5: Introduction to the Development of Microvascular Cell Contraction Assay

The prog-DR test developed in our laboratory and evaluated in the previous chapters is based on the premise that even slight damage (such as in the pre-diabetic stage) will affect the stimulated contraction of retinal microvasculature. The mechanism of prognosis is as shown in Figure 5.1; it involves the non-invasive application of a stress drug, which reaches maximum retinal drug concentration in 10 minutes.

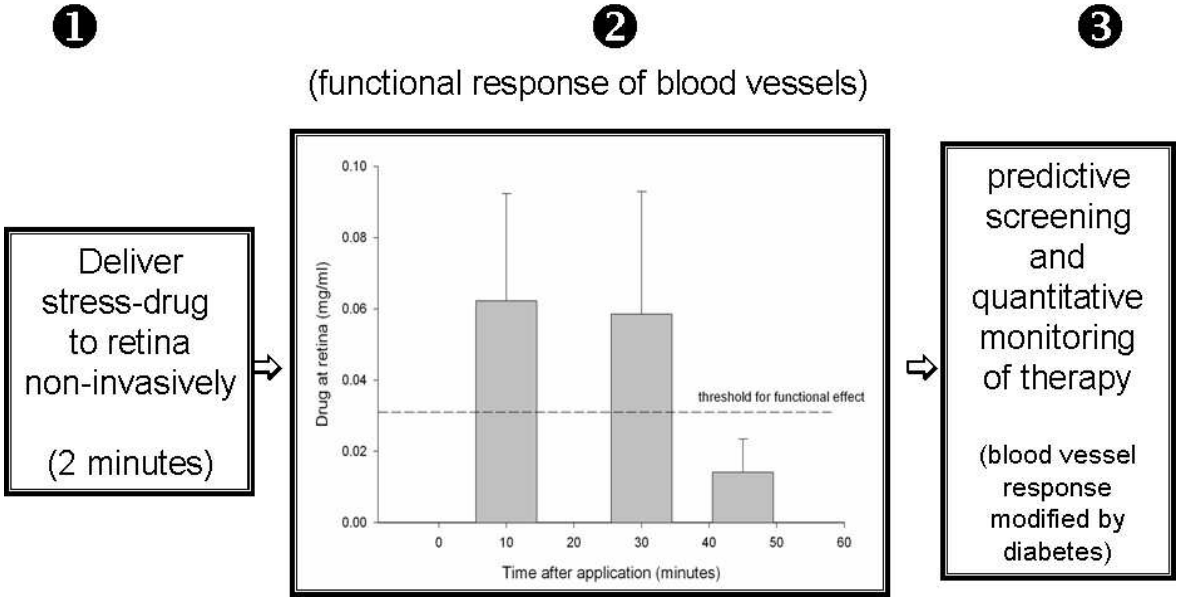

Figure 5.1: The Mechanism of the prog-DR test for DR prognosis.

The stress drug can cause contraction or relaxation of the retinal microvasculature which can be monitored by standard fundus microscopy as illustrated by Figure 5.2 where the retina of a live streptozotocin-diabetic rat was imaged using slit lamp microscopy. Damaged retinal microvasculature can be identified as these are unable to respond or the response would be attenuated (Martin & Markhotina 2002).

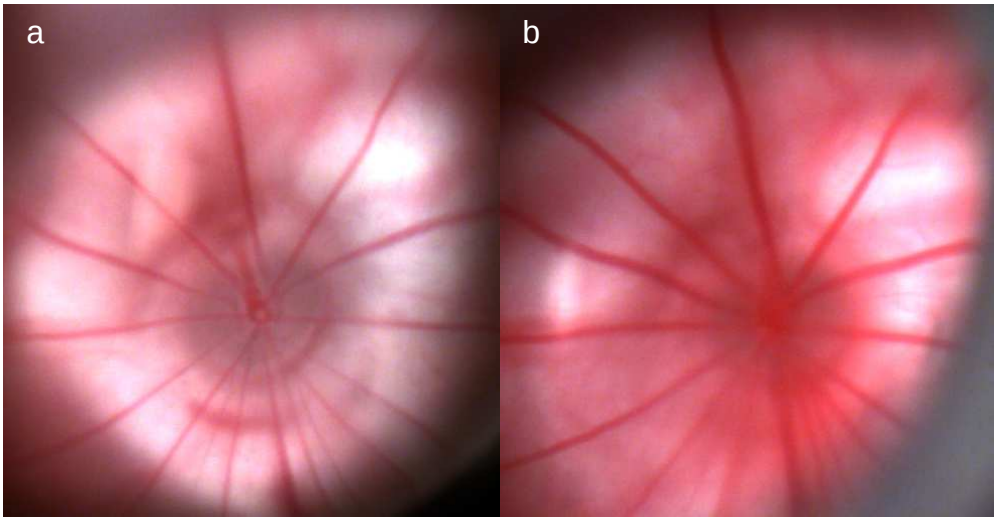

Figure 5.2: The retina of a live streptozotocin-diabetic rats before (a) and after (b) stress drug application as imaged by slit lamp microscopy.

In order to understand the physiological basis of the attenuated contractile response of damaged retinal vessels in the prog-DR test, an in-depth understanding of vascular contraction and relaxation is needed. Specifically, the contractile response of retinal vessels is due to the response of retinal micro-vascular endothelial cells and pericytes. Therefore, the contraction and relaxation physiology of these cells must be elucidated and characterized.

Endothelial cells line the lumen of micro-vessels and have tight junctions which form a physical blood-retinal barrier to protect the retinal circulation (Risau 1991). Pericytes are oval shaped cells which have multiple processes which encircle endothelial cells. These cells express contractile proteins such as smooth muscle protein, actin (Chan et al. 1986; DeNofrio, Hoock & Herman 1989; Nehls & Drenckhahn 1991), and have been shown to contract (Kelley et al. 1987; Matsugi, Chen & Anderson 1997; Murphy & Wagner 1994; Schor & Schor 1986) and reduce the diameter of blood vessels (Schönfelder et al. 1998). As reviewed by Hirschi and D'Amore (1996), there is an intricate relationship between retinal pericyte and endothelial cells. For example, pericytes inhibit the growth of endothelial cells (Orlidge & D'Amore 1987); endothelial cells affect the contraction of pericytes (Chakravarthy et al. 1992; Dodge, Hechtman & Shepro 1991; Ramachandran, Frank & Kennedy 1993).

In hyperglycemia, the contractility of pericyte is inhibited (Aiello et al. 1994; Gillies & Su 1993; McGinty et al. 1999) and in Diabetic Retinopathy pericytes are lost (Robinson et al. 1991). High blood glucose and fluctuations in blood glucose can cause endothelial cell dysfunction (Ceriello et al. 2008) and promote endothelial cell migration (Huang & Sheibani 2008). In diabetes, the balance and interaction between pericyte and endothelial are also impaired (Hammes et al. 2002) which can lead to neovascularisation. However, the exact mechanism of pericyte and endothelial dysfunction and death is yet to be fully understood.

My first approach was to undertake contractility studies on bovine and horse retinal microvascular cells based on Gitlin and D'Amore's (1983) method of cell extraction and Capetandes and Gerritsen's (1990) primary cell culture technique. A simple optimization process for the endothelial cell extraction was also found (refrigeration of the eyeballs overnight). It was noted that the pericytes undergo morphological changes over time (enlargement) and endothelial cells survival is dramatically reduced with standard passaging (with trypsin). Over one year was spent in isolating the bovine and horse retinal microvascular cells, with an extraction attempt every 2-4 weeks. Although there were numerous successful attempts, the success rate and yield of these cells also appears to be seasonal, with high success rate and yield in summer and spring, but very limited yield in winter and autumn.

Although the extraction of these microvascular cells was limited, it was observed by our laboratory that these cells have the tendency to retain their tubular/vasculature structure. Similar observations have been reported by other groups, as reviewed by Distler et al (2003). The growth of these cells on three dimensional systems have very different morphologies compared growth on two dimension glass coverslips (Kelly et al 1987), and in our experience, the response of such tubular "clumps" of cells to high potassium and glibenclamide is different from that of cells that have spread into monolayers (see Appendix C). Those observations emphasise the need to investigate the contraction of these cells in a three-dimensional (3D) format which resembles the natural physiological environment.

Microvascular pericytes are heterogeneous morphologically, biochemically and physiologically (Shepro & Morel 1993), differing in their expression of smooth muscle isoform of alpha-actin (Nehls & Drenckhahn 1991) and ion channel activities (Matsushita & Puro 2006). Microvascular endothelial cells are also heterogeneous in response to acetylcholine, histamine (Huang et al. 2000) and to shear stress (Hong et al. 2006). The heterogeneity of these cells means that the average or total response may be a better reflection of the real *in vivo* environment than if single-cell response were examined.

A literature search on the contraction of retinal microvascular cell reveals that most research was performed on two-dimensional surfaces. This ranges from morphological analysis (area changes) on tissue-culture surfaces (Murphy & Wagner 1994; Nagy et al. 1995; Pang et al. 1993), to silicone substrate on which cell contraction would wrinkle the silicone thin films on top of the silicone fluids (Kelley et al. 1988; Matsugi, Chen & Anderson 1997). Although cell contraction can be identified on these surfaces, such measurements do not reproduce the natural morphology for the cells.

Cell contraction involves the shortening of actin cables, changes in the area of the cell thereby pulling or compressing the substrate on which the cell is grown on. A change in cell area which does not transmit a mechanical force on to the substrate, such as in cell apoptosis (cell shrinkage) cannot be considered as cell contraction; hence cell area is not the ideal measurement for cell contraction. The wrinkling of silicone substrate allows the mechanical force transmitted from cell to substrate to be identified. However such a measurement is only semi-quantitative and silicone is cytotoxic which may affect the function of the cells grown on it.

Recent advances in nanotechnology and polymer chemistry have led to the development of more sophisticated and quantifiable methods to examine cell contraction. For example, on the substrates developed by du Roure et al (2005) and Park et al (2005), contraction of cells deflects the micro-pillars and micro-cantilevers, and when the elastic modulus of the micro-pillars and micro-cantilevers are known, the force exerted by cell contraction can be calculated.

However, these substrates are two dimensional and do not resemble the physiological environment, that is, these are not three dimensional.

Collagen can be used as a three dimensional substrate, and if the elasticity of the collagen is known, the force which is transmitted on to the substrate by cell contraction can also be quantified. Collagen substrates are often used to measure the chronic contraction of fibroblasts (Delvoye et al. 1991; Freyman et al. 2001; Kolodney & Wysolmerski 1992). Although this method to measure cell contraction is quantifiable and chemically similar to the physiological environment, collagen is expensive and the physical physiological environment of microvascular cells is actually tubular and hollow.

Although there is a range of substrates on which cell contraction can be measured, these are deficient in one way or the other; either being cytotoxic, expensive and or dissimilar to the physiological environment of a blood vessels. This prompted the need to develop an affordable, easy to make and use substrate which imitates the physiological environment of microvascular cells. That is, a substrate that is three-dimensional, tubular, hollow, and non-cytotoxic.

The aim of the physiological perspective of this thesis was to develop a 3D contractility assay that would be applicable to microvascular retinal cells. This assay was developed using several material substrates in order to find the most appropriate type of material and several cell-lines were used due to the primary microavascular cells being unavailable. However, the motivation and application was to construct an assay that is useful for the investigation of the physiological basis for the attenuated contractile response of damaged retinal vessels as illustrated by the prog-DR test.

Polyelectrolyte (PE) appears to be the ideal candidate, as these polyions or polymers with a charge are non-cytotoxic and relatively cheap (see Appendix D, Table D.1). PE has also been extensively used to make micro-size capsules and thin films, hence has been well characterized, and the layer-by-layer technique used to construct the polyelectrolyte capsule is very simple. Furthermore, these capsules have shown to be elastic and compressible

(Dubreuil, Elsner & Fery 2003; Gao et al. 2001; Lulevich, Andrienko & Vinogradova 2004).

For various reasons, the cell lines HEK-293, 3T3-L1 and SaOS-2 were used in the biomaterial testing section of this thesis (Chapter 6) as opposed to the retinal microvascular primary cells. Firstly, obtaining retinal microvascular primary cells was difficult as highlighted above. Secondly, these cell lines are readily available, easy to grow and manipulate for experimentation. The SaOS-2 is an epithelial and osteoblast like, Human Osteosarcoma cell line was chosen because this cell line has been extensively tested on in biomaterial research, and in particular, on polyelectrolyte coated surfaces (Tryoen-Tóth et al. 2002) which is the material of interest in this thesis. The 3T3-L1 is a pre-adipocyte like, Mouse Embryonic fibroblast cell line have also been tested on a range of biomaterial (Cyster et al. 2003; Leclerc et al. 2004; Mitchell et al. 2004) and it has the ability to contract (Ho, Grant & Barbenel 2002; Kono et al. 1991; Nobe et al. 2003) which is important for the for the testing of the developed contraction assay in Chapter 7. The neuronal like, Human Embryonic Kidney cell line, HEK-293 was also used to elucidate any cell specific response to the biomaterial being tested.

The strategy here was to first characterize the potential cytotoxic effects these polyelectrolytes have on cells, and then to build a three-dimensional structure for contraction assay. The characterization of cell response to polyelectrolyte thin films are described in Chapter 6 and the development of three-dimensional construction for contraction assay is described in Chapter 7.

5.1 References

Aiello, L.P., Robinson, G., Lin, Y., Nishio, Y. & King, G. 1994, 'Identification Of Multiple Genes In Bovine Retinal Pericytes Altered By Exposure To Elevated Levels Of Glucose By Using Mrna Differential Display', *Proceedings Of The National Academy Of Sciences Of The United State Of America*, Vol. 91, pp. 6231-6235.

Capetandes, A. & Gerritsen, M. 1990, 'Simplified Methods For Consistent And Selective Culture Of Bovine Retinal Endothelial Cells And Pericytes', *Investigative Ophthalmology & Visual Science*, Vol. 31, No. 9, pp. 1738-1744.

Ceriello, A., Esposito, K., Piconi, L., Ihnat, M., Thorpe, J., Testa, R., Bonfigli, A.R. & Giugliano, D. 2008, 'Glucose "Peak" And Glucose "Spike": Impact On Endothelial Function And Oxidative Stress', *Diabetes Research And Clinical Practice*, Vol. 82, No. 2, pp. 262-267.

Chakravarthy, U., Gardiner, T., Anderson, P., Archer, D. & Trimble, E. 1992, 'The Effect Of Endothelin 1 On The Retinal Microvascular Pericyte', *Microvascular Research*, Vol. 43, No. 3, pp. 241-254.

Chan, L., Li, W., Khatami, M. & Rockey, J. 1986, 'Actin In Cultured Bovine Retinal Capillary Pericytes: Morphological And Functional Correlation', *Experimental Eye Research*, Vol. 34, pp. 3396-3401.

Cyster, L.A., Parker, K.G., Parker, T.L. & Grant, D.M. 2003, 'The Effect Of Surface Chemistry And Nanotopography Of Titanium Nitride (TiN) Films On 3T3-L1 Fibroblasts', *Journal Of Biomedical Materials Research Part A*, Vol. 67A, No. 1, pp. 138-147.

Delvoye, P., Wiliquet, P., Leveque, J.-L., Nusgens, B.V. & Lapiere, C.M. 1991, 'Measurement Of Mechanical Forces Generated By Skin Fibroblasts Embedded In A Three-Dimensional Collagen Gel', Vol. 97, No. 5, pp. 898-902.

Denofrio, D., Hoock, T. & Herman, I. 1989, 'Functional Sorting Of Actin Isoforms In Microvascular Pericytes', *Journal Of Cell Biology*, Vol. 109, No. 1, pp. 191-202.

Distler, J., Hirth, A., Kurowska-Stolarska, M., Gay, R., Gay, S. & Distler, O. 2003, 'Angiogenic And Angiostatic Factors In The Molecular Control Of Angiogenesis', *Radiopharmacology*, Vol. 47, No. 3, pp. 149-161.

Dodge, A., Hechtman, H. & Shepro, D. 1991, 'Microvascular Endothelial-Derived Autacoids Regulate Pericyte Contractility', *Cell Motility And The Cytoskeleton*, Vol. 18, No. 3, pp. 180-188.

Du Roure, O., Saez, A., Buguin, A., Austin, R.H., Chavrier, P., Silberzan, P. & Ladoux, B. 2005, 'Force Mapping In Epithelial Cell Migration', *Proceedings Of The National Academy Of Sciences Of The United State Of America*, Vol. 102, No. 7, pp. 2390-2395.

Dubreuil, F., Elsner, N. & Fery, A. 2003, 'Elastic Properties Of Polyelectrolyte Capsules Studied By Atomic-Force Microscopy And RICM', *Soft Matter And Biological Physics*, Vol. 12, No. 2, pp. 215-221.

Freyman, T.M., Yannas, I.V., Yokoo, R. & Gibson, L.J. 2001, 'Fibroblast Contraction Of A Collagen-GAG Matrix', *Biomaterials*, Vol. 22, No. 21, pp. 2883-2891.

Gao, C., Donath, E., Moya, S., Dudnik, V. & MÃthwald, H. 2001, 'Elasticity Of Hollow Polyelectrolyte Capsules Prepared By The Layer-By-Layer Technique', *Soft Matter And Biological Physics*, Vol. 5, No. 1, pp. 21-27.

Gillies, M. & Su, T. 1993, 'High Glucose Inhibits Retinal Capillary Pericyte Contractility In Vitro', *Investigative Ophthalmology & Visual Science*, Vol. 34, No. 12, pp. 3396-3401.

Gitlin, J. & D'Amore, P. 1983, 'Culture Of Retinal Capillary Cells Using Selective Growth Media', *Microvascular Research*, Vol. 26, No. 1, pp. 74-80.

Hammes, H., Lin, J., Renner, O., Shani, M., Lundqvist, A., Betsholtz, C., Brownlee, M. & Deutsch, U. 2002, 'Pericytes And The Pathogenesis Of Diabetic Retinopathy.' *Diabetes*, Vol. 51, No. 10, pp. 3107-3112.

Hirschi, K.K. & D'Amore, P.A. 1996, 'Pericytes In The Microvasculature', *Cardiovascular Research*, Vol. 32, No. 4, pp. 687-698.

Ho, G., Grant, M. & Barbenel, J. 2002, 'Contractile Behaviour Of 3t3 Mouse Fibroblasts In Artificial Skin Substitutes: Effect Of Different Cell-Seeding Methods', *European Cells And Materials* Vol. 4, No. Supplement 2, pp. 55-56.

Hong, D., Jaron, D., Buerk, D.G. & Barbee, K.A. 2006, 'Heterogeneous Response Of Microvascular Endothelial Cells To Shear Stress', *American Journal Of Physiology - Heart And Circulatory Physiology*, Vol. 290, No. 9, pp. H2498-2508.

Huang, Q. & Sheibani, N. 2008, 'High Glucose Promotes Retinal Endothelial Cell Migration Through Activation Of Src, PI3K/Akt1/Enos, And Erks', *American Journal Of Physiology: Cell Physiology*, Vol. 295, No. 6, pp. C1647-C1657.

Huang, T.Y., Chu, T.F., Chen, H.I. & Jen, C.J. 2000, 'Heterogeneity Of $[Ca^{2+}]_I$ Signaling In Intact Rat Aortic Endothelium', *FASEB Journal*, Vol. 14, No. 5, pp. 797-804.

Kelley, C., D'Amore, P., Hechtman, H. & Shepro, D. 1987, 'Microvascular Pericyte Contractility In Vitro: Comparison With Other Cells Of The Vascular Wall', *Journal Of Cell Biology*, Vol. 104, pp. 483-490.

Kelley, C., D'Amore, P., Hechtman, H. & Shepro, D. 1988, 'Vasoactive Hormones And Camp Affect Pericyte Contraction And Stress Fibres In Vitro', *Journal Of Muscle Research And Cell Motility*, Vol. 9, No. 2, pp. 184-194.

Kolodney, M.S. & Wysolmerski, R.B. 1992, 'Isometric Contraction By Fibroblasts And Endothelial Cells In Tissue Culture: A Quantitative Study', *Journal Of Cell Biology*, Vol. 117, No. 1, pp. 73–82.

Kono, T., Tanii, T., Furukawa, M., Mizuno, N., Taniguchi, S., Ishii, M., Hamada, T. & Yoshizato, K. 1991, 'Effect Of Tretinoin On Collagen Gel Contraction Induced By Mouse 3T3 Fibroblasts', *Journal Of Dermatological Science*, Vol. 2, No. 1, pp. 45-49.

Leclerc, E., Furukawa, K.S., Miyata, F., Sakai, Y., Ushida, T. & Fujii, T. 2004, 'Fabrication Of Microstructures In Photosensitive Biodegradable Polymers For Tissue Engineering Applications', *Biomaterials*, Vol. 25, No. 19, pp. 4683-4690.

Lulevich, V.V., Andrienko, D. & Vinogradova, O.I. 2004, 'Elasticity Of Polyelectrolyte Multilayer Microcapsules', *The Journal Of Chemical Physics*, Vol. 120, No. 8, pp. 3822-3826.

Martin, D. & Markhotina, N. 2002, *Novel Screens To Identify Agents That Modulate Retinal Blood Vessel Function And Pericyte Function And Diagnostic And Therapeutic Application Therefore*, World.

Matsugi, T., Chen, Q. & Anderson, D. 1997, 'Contractile Responses Of Cultured Bovine Retinal Pericytes To Angiotensin II', *Archives Of Ophthalmology*, Vol. 115, No. 10, pp. 1281-1285.

Matsushita, K. & Puro, D.G. 2006, 'Topographical Heterogeneity Of KIR Currents In Pericyte-Containing Microvessels Of The Rat Retina: Effect Of Diabetes', *Journal Of Physiology*, Vol. 573, No. Pt 2, pp. 483–495.

Mcginty, A., Scholfield, C.N., Liu, W.-H., Anderson, P., Hoey, D.E.E. & Trimble, E.R. 1999, 'Effect Of Glucose On Endothelin-1-Induced Calcium Transients In Cultured Bovine Retinal Pericytes', *Journal Of Biological Chemistry*, Vol. 274, No. 36, pp. 25250-25253.

Mitchell, S.A., Poulsson, A.H.C., Davidson, M.R., Emmison, N., Shard, A.G. & Bradley, R.H. 2004, 'Cellular Attachment And Spatial Control Of Cells Using Micro-Patterned Ultra-Violet/Ozone Treatment In Serum Enriched Media', *Biomaterials*, Vol. 25, No. 18, pp. 4079-4086.

Murphy, D. & Wagner, R. 1994, 'Differential Contractile Response Of Cultured Microvascular Pericytes To Vasoactive Agents.' *Microcirculation*, Vol. 1, No. 2, pp. 121-128.

Nagy, Z., Kolev, K., Csonka, E., Pek, M. & Machovich, R. 1995, 'Contraction Of Human Brain Endothelial Cells Induced By Thrombogenic And Fibrinolytic Factors: An In Vitro Cell Culture Model', *Stroke*, Vol. 26, No. 2, pp. 265-270.

Nehls, V. & Drenckhahn, D. 1991, 'Heterogeneity Of Microvascular Pericytes For Smooth Muscle Type Alpha- Actin', *Journal Of Cell Biology*, Vol. 113, No. 1, pp. 147-154.

Nobe, H., Nobe, K., Fazal, F., De Lanerolle, P. & Paul, R.J. 2003, 'Rho Kinase Mediates Serum-Induced Contraction In Fibroblast Fibers Independent Of Myosin LC20 Phosphorylation', *American Journal Of Physiology - Cell Physiology*, Vol. 284, No. 3, pp. C599-606.

Orlidge, A. & D'Amore, P. 1987, 'Inhibition Of Capillary Endothelial Cell Growth By Pericytes And Smooth Muscle Cells', *Journal Of Cell Biology*, Vol. 105, pp. 1455-1462.

Pang, I., Shade, D., Tamm, E. & Desantis, L. 1993, 'Single-Cell Contraction Assay For Human Ciliary Muscle Cells. Effect Of Carbachol', *Investigative Ophthalmology & Visual Science*, Vol. 34, No. 5, pp. 1876-1879.

Park, J., Ryu, J., Choi, S.K., Seo, E., Cha, J.M., Ryu, S., Kim, J., Kim, B.-S. & Lee, S.H. 2005, 'Real-Time Measurement Of The Contractile Forces Of Self-Organized

Cardiomyocytes On Hybrid Biopolymer Microcantilevers', *Analytical Chemistry*, Vol. 77, No. 20, pp. 6571-6580.

Ramachandran, E., Frank, R. & Kennedy, A. 1993, 'Effects Of Endothelin On Cultured Bovine Retinal Microvascular Pericytes', *Investigative Ophthalmology & Visual Science*, Vol. 34, No. 3, pp. 586-595.

Risau, W. 1991, 'Induction Of Blood-Brain Barrier Endothelial Cell Differentiation', *Annals Of The New York Academy Of Sciences*, Vol. 633, pp. 405-419.

Robinson, W.G., Mccaleb, M.L., Feld, L.G., Michaelis, O.E., Laver, N. & Mercandetti, M. 1991, 'Degenerated Intramural Pericytes (Ghost Cells) In The Retinal Capillaries Of Diabetic Rats', *Current Eye Research*, Vol. 10, No. 4, pp. 339 - 350.

Schönfelder, U., Hofer, A., Paul, M. & Funk, R.H.W. 1998, 'In Situ Observation Of Living Pericytes In Rat Retinal Capillaries', *Microvascular Research*, Vol. 56, No. 1, pp. 22-29.

Schor, A.M. & Schor, S.L. 1986, 'The Isolation And Culture Of Endothelial Cells And Pericytes From The Bovine Retinal Microvasculature: A Comparative Study With Large Vessel Vascular Cells', *Microvascular Research*, Vol. 32, No. 1, pp. 21-38.

Shepro, D. & Morel, N. 1993, 'Pericyte Physiology', *FASEB Journal.*, Vol. 7, No. 11, pp. 1031-1038.

Tryoen-Tóth, P., Vautier, D., Haikel, Y., Voegel, J.-C., Schaaf, P., Chluba, J. & Ogier, J. 2002, 'Viability, Adhesion, And Bone Phenotype Of Osteoblast-Like Cells On Polyelectrolyte Multilayer Films', *Journal Of Biomedical Materials Research*, Vol. 60, No. 4, pp. 657-667.

Chapter 6: The Characterisation of Cell Response to Polyelectrolyte Thin Films

The chapter describes my investigations of the cyto-compatibility of PE thin films composed of PSS and PAH, using 3T3-L1, HEK-293 and SaOS-2 cells. These investigations included cytotoxicity testing, morphological evaluation, cell attachment and adhesion, extracellular matrix production, and cell proliferation evaluations. The SaOS-2 cells also have the advantage that the maturity or level of differentiation of this cell line can also be estimated in the form of Alkaline Phospatase activity and matrix mineralisation as reviewed by Christenson (1997) and Duplomb, Dagouassat et al (2007). Thus, the SaOS-2 cell-line allows some conclusions to be drawn concerning the influence of the thin films on cell function

Polyelectrolytes (PE), also called polyions are polymers with repeating units that are electrolytes or charged. There is a wide range of PE, including molecules such as polyethylenimine (PEI), poly(diallyldimethylammonium chloride) (PDDA), poly(allylamine hydrochloride) (PAH) and chitosan which are cationic, and poly(styrene sulfonate) (PSS), poly(acrylic acid) (PAA), dextran sulphate and gelatine are anionic. In this study, PSS and PAH thin films were used. The charge on these polymers allow for ionic interactions which create interesting and useful properties for these polymer chains. Firstly, it allows ionic bonding, thereby forming thin films with material of the opposite charge, which may be anything from plastic, glass, latex, even on to bacterial and mammalian cells (Georgieva et al. 2004; Neu et al. 2001). The layer-by-layer (LBL) technique (the alternate adsorption of polyions of opposite charges on to a material) also allows multi-layers of PE thin films (PEM) to be made. The alternate adsorption process needs to be employed as the mixing of polycations and polyanions will cause precipitations.

Polymer chains are usually randomly distributed in a solution. However, PE molecules and chains repel each other since they carry the same charge and therefore, changing the ionic strength of a solution will also change the conformational shape of the PE molecules and chains (Carrillo & Dobrynin 2007). It has been shown that the presence of salt in the making of thin films

will increase its thickness (Blomberg, Poptoshev & Caruso 2006; Gopinadhan et al. 2007; Tjipto, Quinn & Caruso 2005). Exposure to salt solutions once the PEM has been form can also have a swelling and smoothing effect on thin films (Dubas & Schlenoff 2001) and softening effects on capsules (Heuvingh, Zappa & Fery 2005; Lebedeva et al. 2005).

The change in pH also changes the conformation shape of PE molecule and chains (Milkova & Radeva 2007), so that the lowering of pH will increase PE film thickness (Elzbieciak, Kolasinska & Warszynski 2008; Halthur, Claesson & Elofsson 2004; Kolasinska, Krastev & Warszynski 2007) and increase the permeability of PE capsules (Antipov et al. 2002).

The simplicity, versatility and ability to be fine-tune of PE allows for tremendous potential for biomedical application such as micro-encapsulation, controlled drug release, biosensors as well as tissue engineering. It is the ultimate aim for this section of the thesis, to engineer a three dimensional platform for cell contraction assays (like an artificial capillary) using these PE. In order for this body of work to advance and to progress towards the goal of the thesis, it is essential that the biocompatibility of these thin films and or capsules are understood. As reviewed by Kirkpatrick, Bittinger et al. (1998), a biocompatible material must be non-cytotoxic, non-mutagenic, non-carcinogenic and be able perform its function whilst maintaining an appropriate host response. Appropriate host responses in general include a low or zero inflammatory response to the material, no increase in the risk of infection and no effect on the normal function of adjacent tissues and cells.

Titanium (Ti) and titanium nitride (TiN) thin films were also used as comparators for the SaOS-2 response to the PE thin films, and it has the advantages of (i) Ti has been well established as a biocompatible metal, (ii) Ti is inert, durable, and has good mechanical strength and corrosive-resistance, as reviewed by Lautenschlager and Monaghan (1993), (iii) TiN has good haemocompatibility (Dion et al. 1995; Dion et al. 1993) as well as good mechanical strength. Those biocompatibility advantages are some of the reasons why Ti and TiN have been used as a biomaterials for implants of bones and joints as well as dental implants, as reviewed by Schweitzer et al (1995), Mezger and Creugers (1992).

This also makes the characterisation of osteoblast-like cell behaviour on these thin films appropriate and relevant to my investigations leading up to the construction of a 3D assay for cell contractility.

Cyto-compatibility of the substrates was investigated in this thesis. The cyto-compatibility assessment included testing the effect of the substrate on cytotoxicity/viability and bio-function. Bio-function testing included morphological evaluation (cell shape and spread), cell attachment and adhesion, proliferation (growth and cell cycle). For the SaOS-2 cell line, the level of differentiation was also examined. Biocompatibility of the substrates in host animals was not investigated in this thesis since the substrates were developed for in vitro contractility testing.

There are four main factors which may influence the cyto-compatibility of a material: (i) chemical composition, (ii) zeta or surface potential, (iii) hydrophobicity and (iv) surface topography (such as roughness). The chemical compositions of the polyelectrolyte, titanium and titanium nitride thin films are known. Poly(sodium 4-styrenesulfonate) (PSS) have a negative zeta potential and it's thin film hydrophilic. Poly(allylamine hydrochloride) (PAH) have a positive zeta potential and it's thin film is hydrophobic. Several papers have shown that glass (Gu & Li 2000; Sze et al. 2003), Ti thin films (Cai et al. 2006; Nebea et al. 2007) and TiN colloids (Zhang et al. 2005) have a negative zeta potential at pH 7. There are already some information on hydrophobicity and surface topography of the titanium thin films, but these features tends to vary with different preparation and treatment methods (Lim & Oshida 2001). For example, Lim, Oshida et al (2001) found their Ti samples to be hydrophilic and water contact angles to be less than 45^{o} whilst Cai, Müller et al. (2005) found all their Ti samples to have a water contact angle of around 80^{o}.

Although there is some understanding on how these factors may influence cyto-compatibility, it is important to remember that different cells may react differently on the same material as reviewed by Pizzoferrato, Ciapetti et al. (1994). This was also clearly demonstrated by the study by Haris et al (2005) where fibroblast and osteoblast have different levels of spreading and adherence on the same titanium surface.

Table 6.1 summarises previous studies on the cyto-compatibility of PSS and PAH related thin films. As shown in this table, the cell behaviour or response was not always examined in depth. With the exception of the HUVECs, the other cell lines were commonly only tested for viability, morphology and initial attachment. For example, only the viability and morphology was examined for the motor-neurons (Vodouhe et al. 2005) and only the viability, morphology and initial attachment of fibroblasts were investigated (Mhamdi et al. 2006b). Furthermore, some studies have inter-changed the terms “initial attachment” (the first connection or interaction between cell and surface) and “adhesion” (the strength by which cells link with the surface). The former which begins within minutes of exposure of cells to the surface whereas the latter occur within hours as reviewed by Jäger et al (2007), requires the cells to be alive and involves a large range of proteins such as integrins, focal adhesion kinase as well as the formation of extracellular matrix. Hence, the process of cell adhesion is a lot more complex and different from initial attachment.

The aim of this study is to characterise the hydrophobicity and surface topography of the polyelectrolyte, titanium and titanium thin films and extensively characterise the cyto-compatibility of PE thin films composed of PSS and PAH using 3T3-L1 and HEK-293 cells. This study involves cytotoxicity testing, morphological evaluation, cell attachment and adhesion, extracellular matrix production, and cell proliferation evaluations.

Study	**Cell type**	**Cell behaviour examined**
Boura, Menu et al. (2003)	HUVEC	Viability Morphology (optical microscopy) Initial attachment Adhesion Proliferation Phenotype (Von Willebrand factor)
Boura, Muller et al. (2005)	HUVEC	Viability F-actin expression ICAM-1 expression Phenotype(Von Willebrand factor)
Boura, Kerdjoudj et al. (2006)	HUVEC	Morphology (Atomic Force microscopy) Integrins (β1) expression F-actin expression
Tryoen-Tóth, Vautier et al. (2002)	SaOS-2 PD-L	Viability Initial Attachment Phenotype (Alkaline Phosphatase (ALP) expression and activity) Cytokine production (Interleukin-8 (IL-8) and Tumour Necrosis Factor α (TNF α))
Lin, Wang et al.(2006)	Chondrocytes	Viability Morphology Initial attachment

Vautier, Karsten et al. (2002)	HCS-2/8	Viability Initial attachment Cytokine production (IL-8) F-actin expression Vinculin expression
Richert, Lavalle et al. (2002)	HCS-2/8	Adhesion
Mhamdi, Picart et al.(2006)	fibroblast	Viability Morphology Initial attachment
Vodouhê, Schmittbuhl et al. (2005)	Motor-neurons	Viability Morphology

Table 6.1: Summary of studies on cell response to PSS and PAH polyelectrolyte thin films

6.1 Methods

6.1.1 PE Thin films production

6.1.1.1 Polyelectrolyte (PE) thin films

24-well plates or 12mm round glass coverslips were coated with a combination of negatively charged PSS (Sigma 243051) and positively charged PAH (Sigma 283223). Thin films are formed on the wells or on the coverslips by shaking on a rocking platform for 20 minutes with 1mg/mL of PSS or PAH in 0.5M NaCl, follow washing with water. Multi-layered polyelectrolyte films were made by alternate coating of PSS and PAH.

The polyelectrolyte solutions were sterile filtered and water was sterilised by autoclave. The coating procedure was also carried out in a Class 1 laminar flow hood to ensure sterility of these thin films.

6.1.1.2 Titanium (Ti) and Titanium Nitride (TiN) thin films

Round glass coverslips (12mm in diameter) were coated with titanium and titanium nitride by direct current magnetron sputtering (Edward High Vacuum Ltd). The glass coverslips were placed in a pressure chamber and a turbo molecular pump was used to evacuate the air to below 5 x 10^{-6} Torr, as monitored using hot cathode ionization gauge. A MKS mass gas flow controller was used to feed Argon (Ar) and or Nitrogen (N_2) of ultrahigh purity into the chamber to a total pressure of 2.4 mTorr. The direct current magnetron generates a strong radiofrequency field which excites and ionise the Ar and/or N_2 gases. These ionised gases accelerates towards a Ti target of 9cm in diameter and 99.999% purity, charged using a MDX 1.5 kV power supply (120 Watts for TiN120, 190 Watts for the TiN190 and 150 Watts for the Ti thin films). The collision of ionised gases and titanium effectively knocks out titanium atoms at high velocity which deposits on the substrate.

For TiN thin films, N_2 partial pressure was kept constant at 0.4 mTorr, and the knocked out Ti atoms combines with the ionised N^+ to deposit TiN on to the substrate. N_2 was not used for Ti thin film deposition. The distance between the substrate (coverslips) and the titanium target was kept constant at 6cm.

These thin films were sterilised by soaking and washing in 70% ethanol, follow by washing with sterilised water. The thin films were allowed to dried and the ethanol fully evaporated before they are brought into contact with cells.

6.1.2 Thin film characterisation

6.1.2.1 Water contact Angle

The wettability of thin films were characterised by placing a droplet of water (10□L volume) on the thin films and the contact angle was measured using the following procedure. An image of the water droplet on the thin film was taken. The profile of the water droplet was digitised form that image using software to define the x and y co-ordinates on the outline of the water droplet. Microsoft® Office Excel 2003 was used to estimate the best fit (polynomial) equation for those co-ordinates of the digitised profile of the water droplet. This equation was then used to find the gradient of the curve at the edge of the water droplet in contact with the surface, and the arctangent angle (which represents the water contact angle) was calculated from that gradient.

6.1.2.2 Surface Roughness

The surface morphology of the thin films were analysed by atomic force microscopy (Dimension™ 3100). In brief, random 1x1μm areas of thin films were scanned in tapping mode. Nanoscope III was used to measure the surface roughness. Surface roughness measurements include root mean square of roughness (RMS), average roughness (Ra), and peak-heights.

6.1.1 Cell Culture

Cultures of Human Embryonic Kidney cells HEK-293 and mouse embryonic adipose like fibroblast cells 3T3-L1 were grown in 10% FBS in DMEM (Invitrogen 21063-045) and incubated at 37^{o}C, in a 5% CO_2 atmosphere. Cells were passaged using Trypsin-EDTA (Sigma T4299) for 5 minutes.

Cultures of SaOS-2 cells were grown in 15% FBS in McCoy's 5A medium (Invitrogen 12330-031) and incubated at 37^{o}C, 5% CO_2. Cells were passaged with Trypsin-EDTA (Sigma T4299) for 15 minutes.

6.1.2 Phase contrast microscopy

6.1.2.1 Cell Spread and Morphology

Cells were seeded at 5,000 cells per well in pre-coated 24 well plates (see section 6.1.1) and incubated for 1, 3, 5 and 7 days. These were then fixed and extracted with ice-cold 1:1 acetone:methanol and stained with 1% Coomassie Blue and imaged on the Nikon TE300 microscope using a digital camera (Leica DC300F) and Image Pro Plus version 5.1. The morphology of the cells was recorded and the areas occupied by the cells were also measured using Image Pro Plus version 5.1.

6.1.3 Fluorescent Microscopy

Cells were seeded at 100,000 cells per well in pre-coated coverslips (see section 6.1.1) and incubated at 37^{o}C in a 5% CO_2 atmosphere overnight, then fixed with 4% paraformaldehyde for 15 minutes; extracted with 0.1% Triton X-100 for a minute, and then blocked by incubation with 100mM glycine for 5 minutes then in 1% BSA for 20-30 minutes. The cells were then stained for actin with Alexa Fluor® 633 phalloidin (Invitrogen A22284) in 1% BSA for 20 minutes in the dark and mounted with ProLong® Gold anti-fade reagent (Invitrogen P36934) and coverslips were sealed with nail polish. The cells were then imaged using the Olympus TE300 fluorescent microscope under the x100 oil immersion objective.

6.1.4 Propidium Iodide (PI) Assay

A modified PI fluorescence assay (Dengler et al. 1995; Nieminen et al. 1992; Zhang et al. 1999) was used to determine cell numbers in the initial attachment, adhesion, proliferation and cytotoxicity assays. Briefly, cells were seeded into pre-coated 24 well plates (48 wells for cytotoxicity assay) and incubated at 37^{o}C in a 5% CO_2 atmosphere at the cell density and time as show in Table 6.2. The supernatant was then removed and frozen at least overnight. Cells were then thawed and incubated at 50ug/mL of PI (Sigma, 81845) in PBS for 30 minutes and the fluorescence intensity of each well was read at 520/620 by BioTek Synergy™ HT Multi-Mode Microplate Reader. The fluorescence intensity of

known cell number was used to create a standard curve and the cell numbers from experiments were determined.

For the initial attachment and adhesion assay, cells were washed gently with their corresponding culture medium to remove non-adhering cells before freezing. For the adhesion assays chemical dissociation of the cells was carried out by incubation for 5 minutes in Trypsin-EDTA (Sigma T4299) diluted 10 times in calcium free PBS. To test for the calcium dependency of cell adhesion in additional experiments, cells were also incubated in PBS that contained 1mM calcium chloride.

For the cytotoxicity assay, live cells were first incubated with PI in culture medium and the fluorescence intensity of each well was read to determine the number of dead/cytotoxic cells. Then the cells were frozen and read again to find the total cell number. Each variable was assayed in duplicates or triplicates and each assay was repeated at least three times.

Assay	Initial attachments	Adhesion	Proliferation	Cytotoxicity
Seeding Density (cells/well)	100,000	100,000	5,000	150,000
Time	3 hours	overnight	1, 3, 5 & 7	Overnight

Table 6.2: The cell density and time used in propidium iodide assays.

6.1.5 Alamar Blue Assay

Since the Ti and TiN thin films are not transparent, the propidium iodide assay cannot be used to determine cell number. The method used for assaying the numbers of cells on the Ti and TiN thin films was as follows. In brief, SaOS-2 cells were seeded at 100,000 cells per coated coverslip in 24-well plates for initial attachment, adhesion and viability assay as described above. However, because the SaOS-2 is not sufficiently metabolically active to be used with the alamar blue assay just 3 hours after seeding, for the initial attachment assay after the incubation with the medium containing cells for 3 hours, removal of this medium and washing with fresh medium, the SaOS-2 cells were allowed to incubate overnight. For the proliferation assay, cells were seeded at 50,000 cells per well. The live cells were incubated with 10% Alamar blue (Invitrogen, DAL1025) in cell culture media for 2 hours and the fluorescence intensity of the supernatant was read by BioTek Synergy™ HT Multi-Mode Microplate Reader. The fluorescence intensity of a known number of cells was used to create a standard curve, which allowed the cell numbers from experiments to be determined. Each variable was assayed in duplicates or triplicates and each assay was repeated at least three times.

6.1.6 Cell Cycle Analysis

SaOS-2 cells were seeded at 250,000 cells per 25cm^2 tissue culture flasks with or without polyelectrolyte coatings. After 1, 3, 5 and 7 days of incubation, cells were detached using Trypsin-EDTA (Sigma T4299) , washed twice with PBS and resuspended and incubated in PBS containing 0.1% Triton X-100, 0.1% Bovine Serum Albumin (BSA), 40µg/mL propidium iodide and 10µg/mL RNase A at 4^{o}C for a minimum of 30 minutes. The DNA content of these propidium iodide stained cells were analysed using the BD FACSCalibur^{TM} flowcytometer. Experiments were measured in duplicates and repeated three times. The WinMDI 2.8 software was used to generate flow cytometry data and the Cylchred 1.0.2 software was used to estimate the proportion of cells in the different stages of cell cycle.

6.1.7 Extracellular Matrix Collagen Assay

A modified method by Tullbery-Reinert and Jundt (1999) was used to quantify the presence of collagen on extracellular matrix. In brief, 100,000 cells were seeded onto pre-coated 6-well plates (see section 6.1.1) and grown for 5 to 7 days until at least 90% confluency was reached in the control well. The cells were gently lifted by incubation in 150□M EGTA and 0.1% Triton X-100 in Milli-Q water at 4^{o}C for 20-30 minutes and placed on to a rocking platform, with the speed set on medium, for 10 minutes to further dissociate the cells. The remaining matrix was then washed three times with PBS and cell dissociation was confirmed by microscopy. The matrix was then fixed with Bouin's Fluid for 30 minutes, washed with running tap water for 15 minutes, air dried and stained with Direct Red 80 (Sigma 43665) for 1 hour. The samples were then washed vigorously with water, and then with 10µM HCl three times to ensure all unbound dye was washed off. The bound dye was then dissociated by incubation with 100µM NaOH on a rocking platform for 30 minutes, and the absorbance of the supernatant was then read at 550nM on the BioTek Synergy™ HT Multi-Mode Microplate Reader. Coated 6-well plates without cells (but incubated with media for the same time as the cells) were treated exactly the same way and were used as background absorbance reading for the respective surfaces. Experiments were repeated three times and each variable was assayed in duplicate.

6.1.8 Alkaline Phosphatase (ALP) Activity Assay

SaOS-2 cells were seeded at 50,000 cells per well in 24-well plates. On the tenth day of culture, 5µL of the supernatant added to 195µL of Alkaline Phosphatase Yellow (pNPP) Liquid Substrate System (Sigma P7998) and the kinetic changes in absorbance at 405nm of the solution mixture was recorded for 30 minutes on the BioTek Synergy™ HT Multi-Mode Microplate Reader. Experiments were repeated twice and each variable were assayed in quadruplicates.

The ALP activity (IU/L) was calculated using the following formula, where $OD_{t=n}$ and $OD_{t=0}$ are absorbance at 405nm at the incubation times of n=30 minutes and 0 minutes; *RV* is the total reaction volume, ε is 18.75mM^{-1}cm^{-1}, *l* is the light path in cm and *SV* is the sample volume (5μL).

$$ALP\ activity = \frac{(OD_{t=n} - OD_{t=0}) \times 1000 \times RV}{4 \times \varepsilon \times l \times SV}$$

6.1.9 Von Kossa Assay

SaOS-2 cells were seeded at 5,000 cells per well in 24-well plates and grown for 10 days to full confluency. The cells were washed twice with PBS and fixed with 4% paraformaldehyde for 10 minutes. After fixation, the cells were washed again twice with distilled water and incubated with 5% silver nitrate under UV exposure for 40 minutes to stain for mineralised nodules. The cells were then washed thoroughly with distilled water and incubated with 5% sodium thiosulphate for 5 minutes and then washed again with distilled water. The mineralised nodules formed under basal condition were imaged at 10 times magnification on the Nikon TE300 microscope using a digital camera (Leica DC300F) and Image Pro Plus version 5.1. The images were analysed for the number and size of the mineral nodules using Image Pro Plus version 5.1 in a similar way as was reported by Nefussi, Ollivier et al 1997 (1997). The total mineralisation was estimated as the total area of all nodules presented per field. Results were normalised against control.

6.1.10 Statistical Analysis

All statistical analysis was carried out with SPSS 15.0, using one-way ANOVA with Tukey-Kramer procedure for multiple comparisons. The calcium dependency adhesion assays results were compared with independent Student's t-tests. A probability of $p<0.05$ was considered statistically significant.

6.2 Results

6.2.1 Thin films characterisation

Polyelectrolyte, titanium and titanium nitride thin films differ in chemical composition and hydrophobicity. As shown in Figure 6.1, PAH, TiN120 and TiN190 are relatively hydrophobic thin films with water contact angle over 80^{o}. PSS thin film and glass coverslips are significantly more hydrophilic, and titanium thin film is the most hydrophilic, so much so that the water droplet on the thin film forms a water contact angle of less than 10^{o}.

The surface morphology of the thin films are shown in Figure 6.3. Glass, PSS and PAH are relatively smooth with average roughness (Ra) and roughness measured in root mean square (RMS) below 1 nanometer, as shown in Figure 6.2. Ti and TiN thin films are significantly rougher than other surfaces as measured by RMS, but Ti thin films were not significantly rougher by Ra. TiN190 have two differently sized peaks or "bumps" as shown in Figure 6.3, and the minimum and maximum heights of these bumps are significantly different from the ones on Ti and TiN-120 thin films as shown in Table 6.3. The peaks and bumps on glass, PSS and PAH thin films were not measured as these surfaces were relatively smooth in comparison to the Ti and TiN thin films.

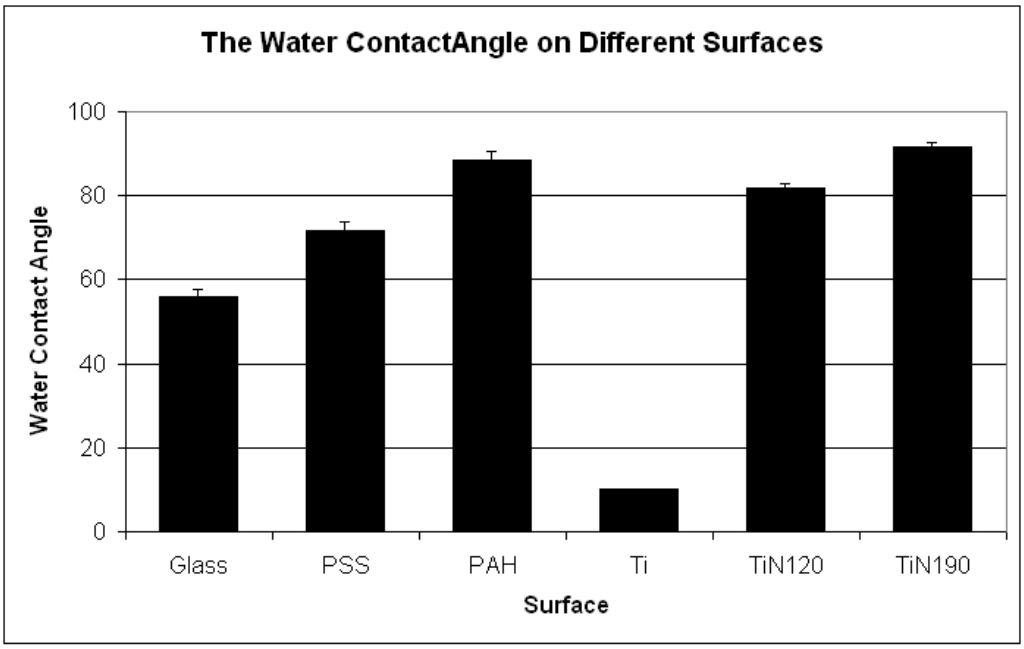

Figure 6.1: The water contact angle on different thin films. The results show the average from six independent measurements. Error bars represent the standard error.

Thin Film	Maximum vertical height of peaks	Minimum vertical height of peaks
Ti	11.3±1.85	2.88±0.55
TiN120	23.0±3.34	4.14±0.29
TiN190	45.9±3.34	20.0±1.9

Table 6.3: The size of peaks on different surfaces as measured by Atomic Force Microscopy. The results show the average from at least four independent scans and the error bars represent the stand error.

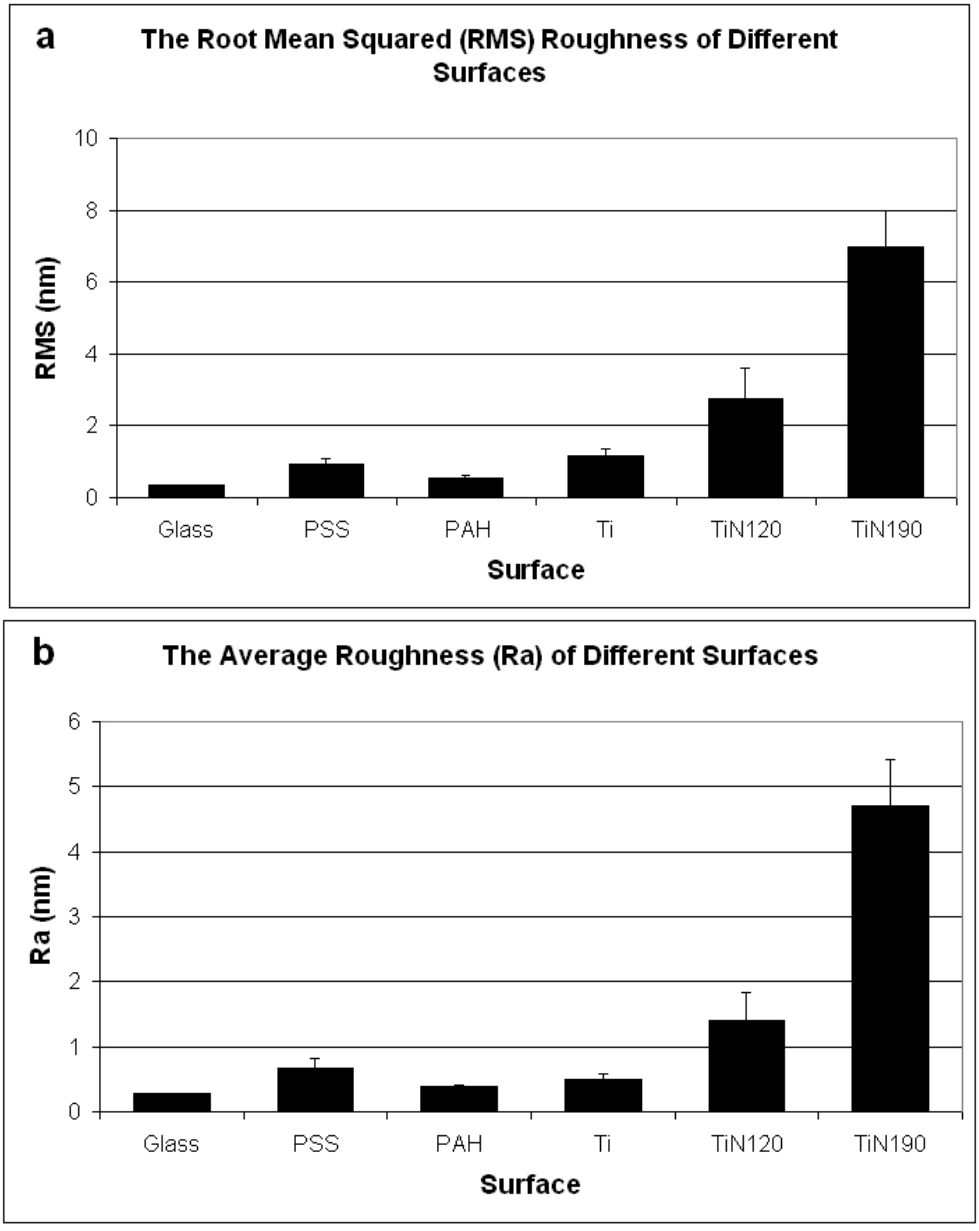

Figure 6.2: Surface Roughness of Different thin films as measured by Root Mean Square (RMS) roughness (a) and average roughness (Ra) (b). The results show the average from at least three independent scans on AFM. Error bars represent the standard error.

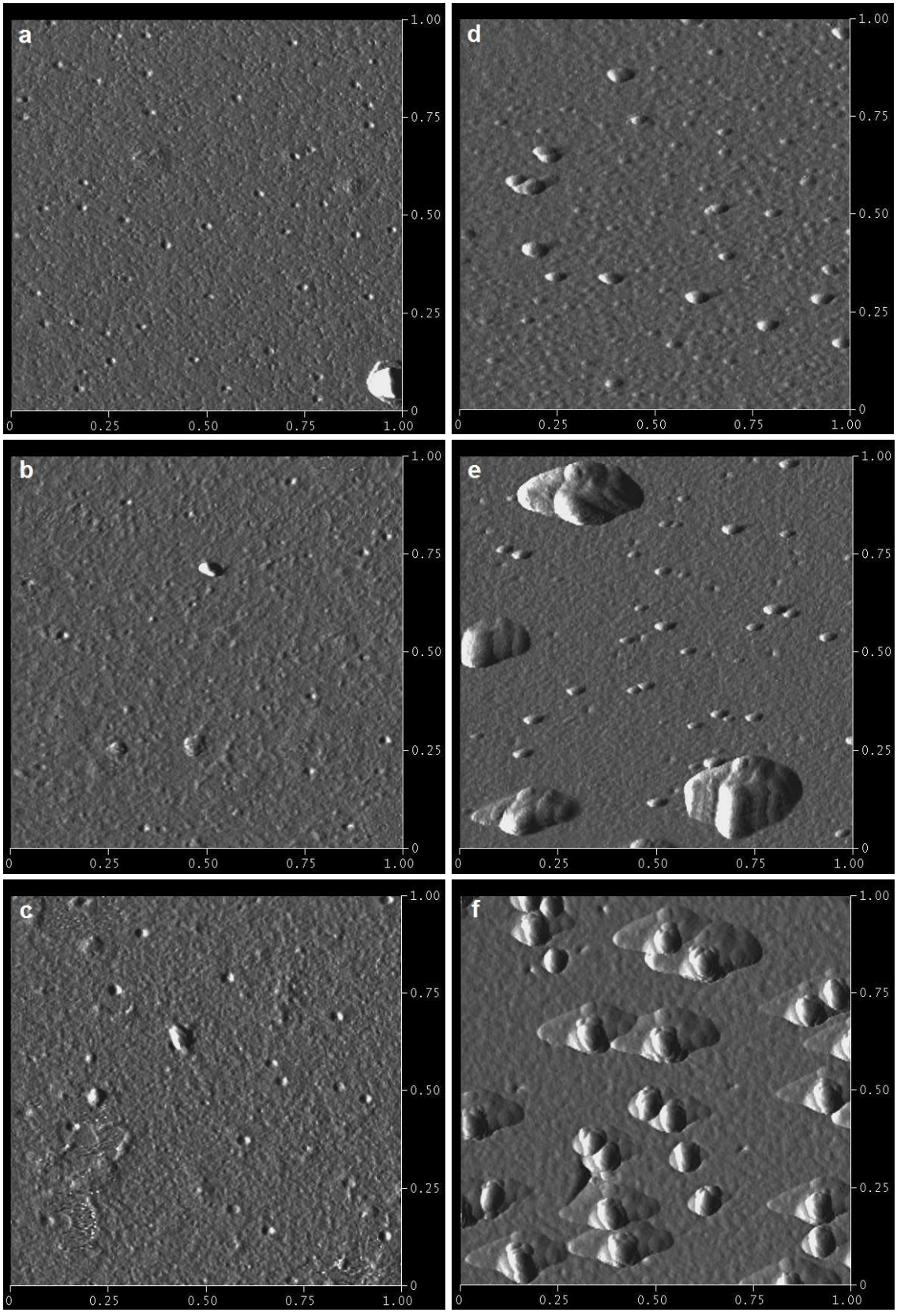

Figure 6.2: Atomic Force Microscopy images of glass coverslip (a), PSS (b), PAH (c), Ti (d), TiN120 (e) and TiN190 (f) thin films.

6.2.2 Cytotoxicity

The PI assay did not show cytotoxicity levels above normal (5%) for any of the cell lines, on any of the surfaces as shown in Figure 6.4 and Figure 6.5a. The Alamar blue assay of cell viability showed that there were significantly lower numbers of viable SaOS-2 cells on the TiN120 thin films as shown in Figure 6.5b.

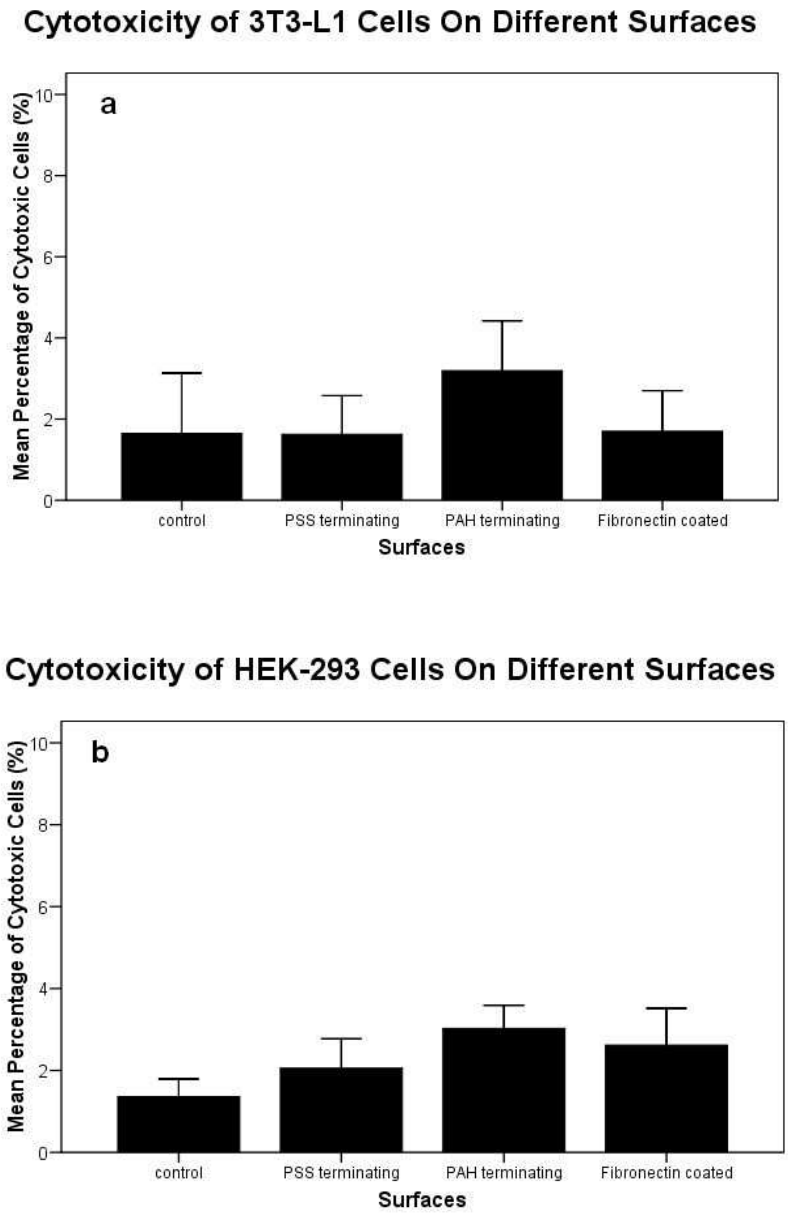

Figure 6.4: Cytotoxicity of 3T3-L1 (a) and HEK-293 cells (b). The percentage of cytotoxic cells was determined by PI assay as described in *Methods*. Error bars represent the standard error.

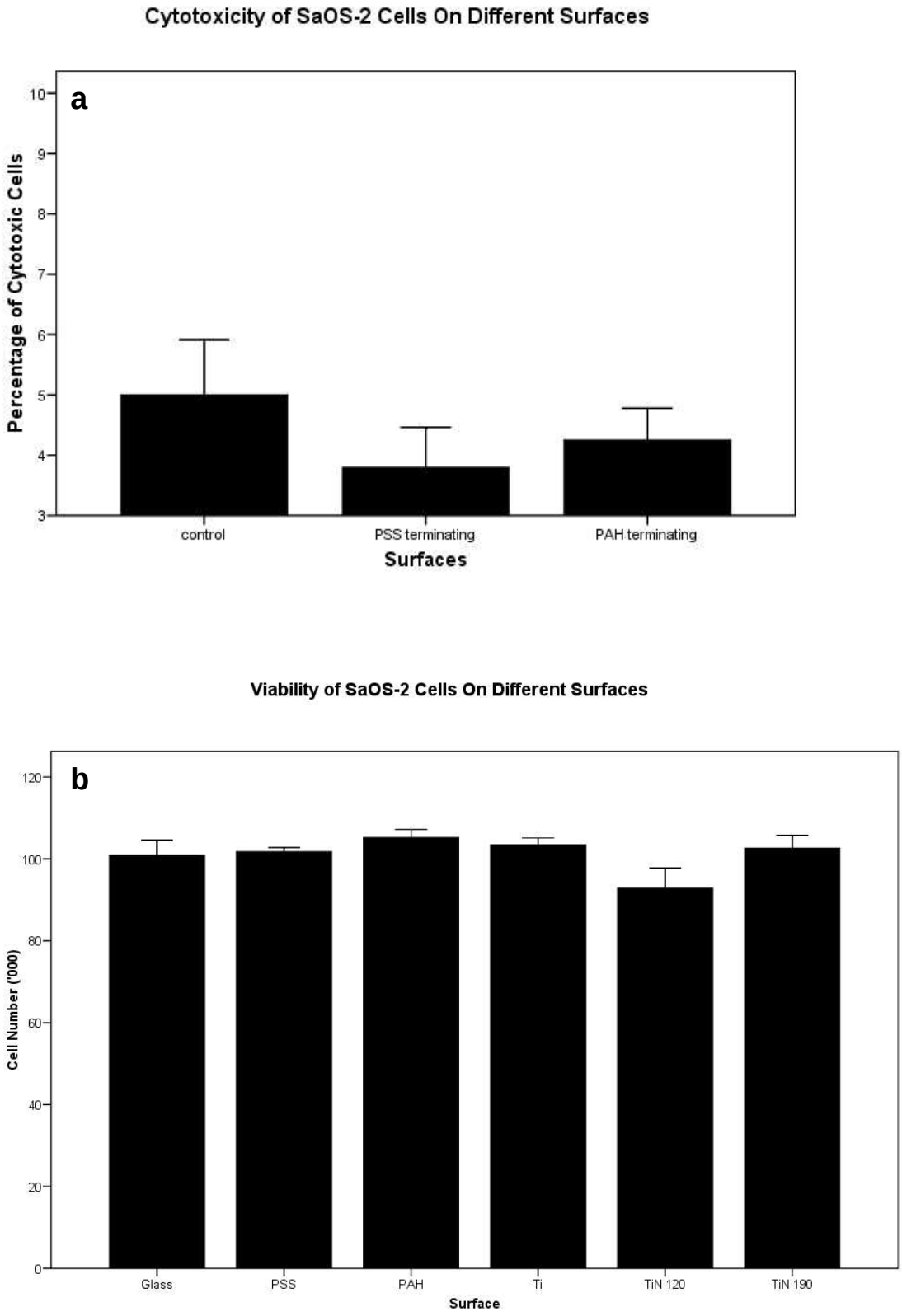

Figure 6.5: The cytotoxicity (a) and viability (b) of SaOS-2 cells on different thin films as determined by PI assay (a) and Alamar Blue assay (b). Cell number was determined by Alamar Blue assay as described in *Methods*. Error bars represent the standard error.

6.2.3 Proliferation and cell cycle

Although preliminary results from flowcytometry did not show significant differences in cell proliferation on day 3 (see Appendix E), the proliferation of 3T3-L1 cells were actually lower on PAH-terminating surfaces, with cell number significantly lower than all other surfaces by day 7 as shown in Figure 6.6. For the PSS-terminating thin films on other hand, cell number was significantly higher on multi-layered PSS-terminating films than to the PSS monolayer.

For the HEK-293 cells, cell number reaches maximum on day 5 for most of the surfaces, and overcrowding and the depletion of growth nutrients probably accounted for the reduction in cell number by day 7. The cell number on day 5 shows that there was significantly less on PAH thin film, however, cell number increases with the number of PE layers on these PAH terminating thin films. For PSS terminating thin films, PSS monolayer thin film had the highest number of cells. The addition of fibronectin coating on PEM also significantly changes the cell number compared to PEM alone except for 2PAHPSS PEM which had more 3T3-L1 cells on Day 7 without fibronectin.

The proliferation of SaOS-2 cells were analysed by Alamar blue assay and it showed that SaOS-2 cell number were significantly lower on PAH terminating surfaces on day 7 as shown in Figure 6.7a.

The proliferation of SaOS-2 cells on PAH thin films was also significantly lower than PSS, Ti and TiN190 thin films as shown in Figure 6.7b. The cell number on day 7 was highest and significantly higher on TiN190 thin films; followed by Ti which had significantly more cells than glass, PAH and TiN120 thin films.

Cell cycle of the SaOS-2 cells were measured by flowcytometry over several days, and there were some significant differences between the tissue culture plastic (TCP), PSS and PAH thin films on day 7 as shown in Figure 6.8. On day 7, there were significantly more cells on TCP in the G1 phase of cell cycle, significantly less cells on PAH thin films in the S phase than on PSS thin films, and more cells on PAH thin films in the G2 phase (where cells have doubled the amount of DNA). We were unable to repeat these on the Ti and TiN thin films as these were only available on small coverslips which does not yield sufficient cells for such analysis.

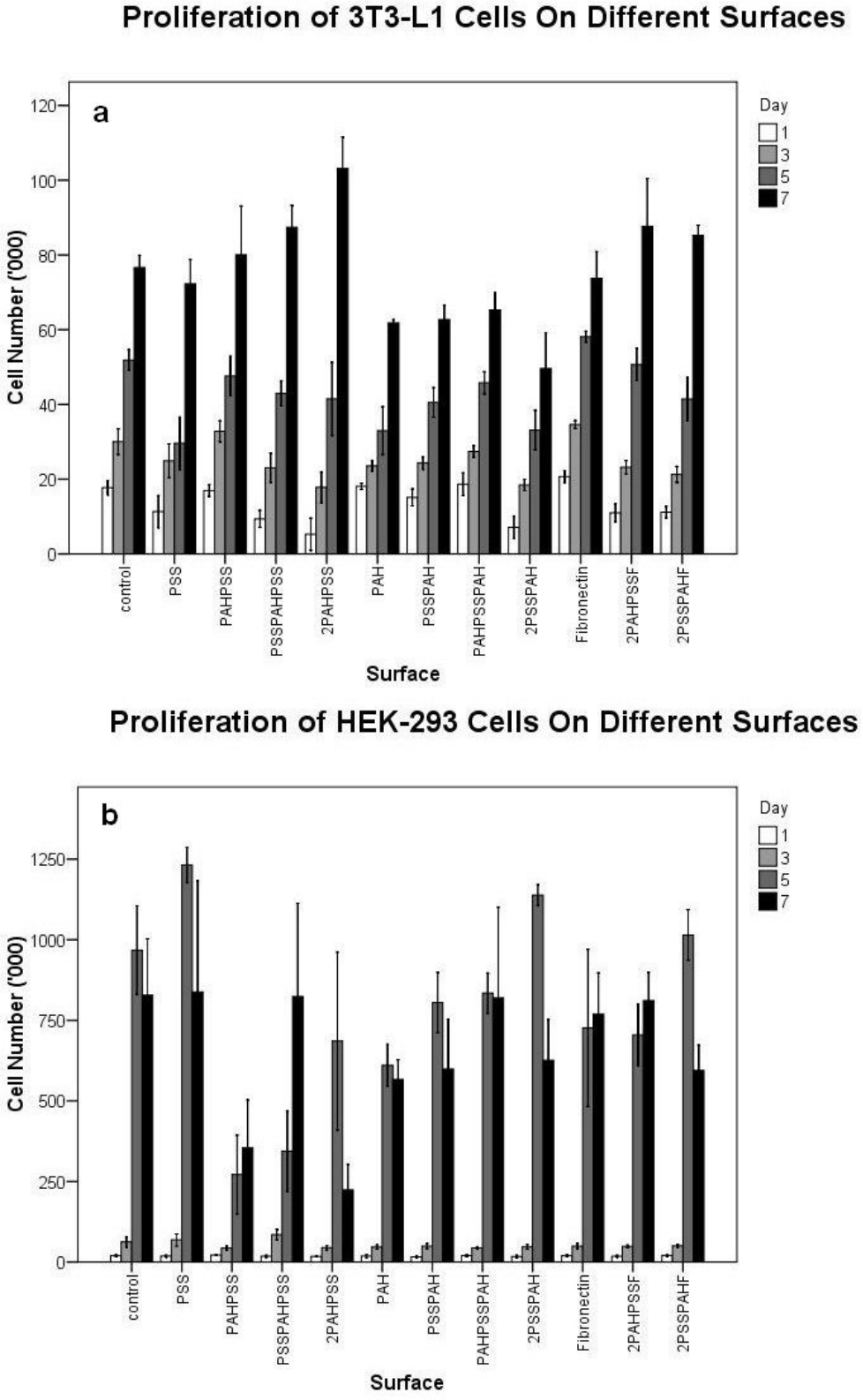

Figure 6.6: Proliferation of 3T3-L1 (a) and HEK-293 cells (b). Cell number was determined by PI assay as described in *Methods*. Error bars represent the standard error.

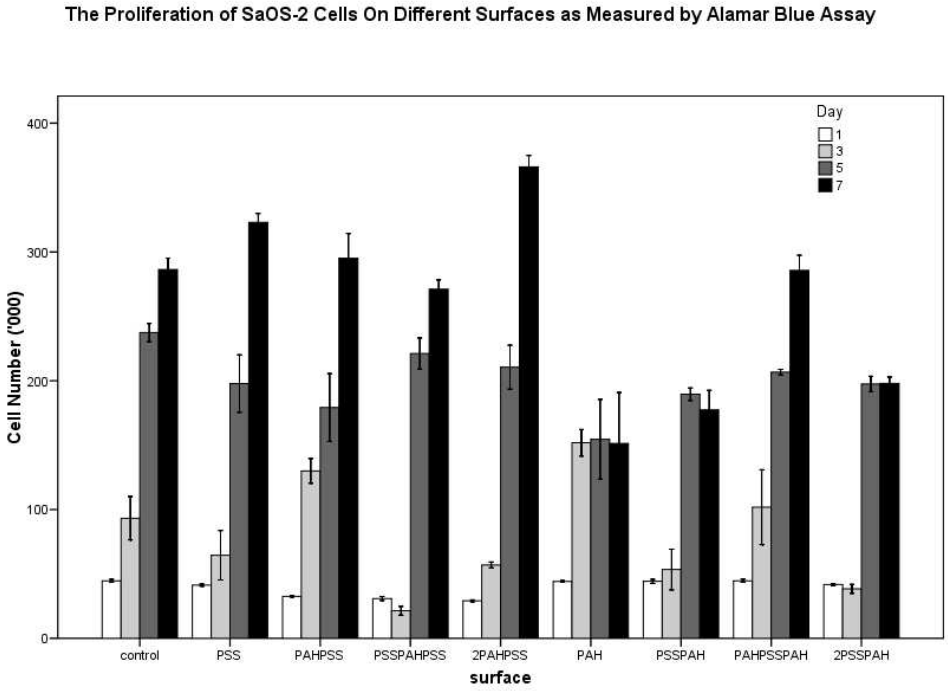

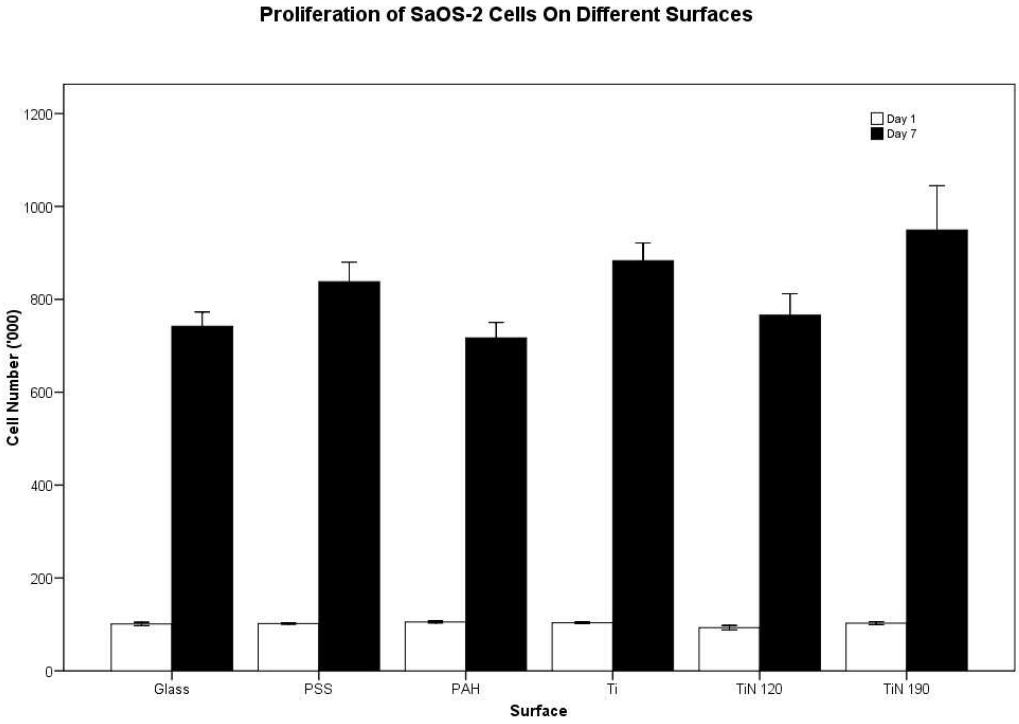

Figure 6.7: Proliferation of SaOS-2 Cells as measured using Alamar blue assay on polyelectrolyte thin films (a) as well as with Ti and TiN thin films (b). Error bars represent the standard error.

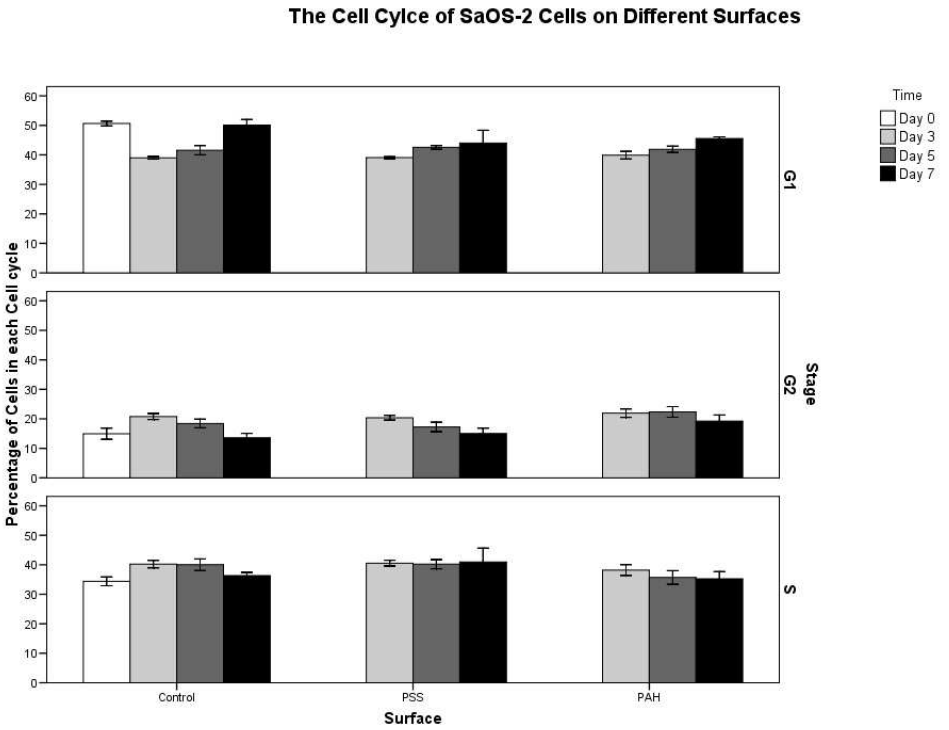

Figure 6.8: The proportion of SaOS-2 cells at different stages of cell cycle on TCP, PSS and PAH thin films at different time points as measured by flowcytometry. Error bars represent the standard error.

6.2.4 Morphology and F-actin Distribution

The morphology and the spread of the HEK-293 or 3T3-L1 cells did not appear different between PE thin films by phase contrast microscopy, but morphology and the spread of the SaOS-2 cells appeared to differ between polyelectrolyte thin films as shown in Figure 6.9, where the cells are elongated on PAH thin film. The spread of *individual* SaOS-2 cells were significantly different on day 1, where cells on PAH terminating surfaces occupy more area than cells on PSS terminating surfaces; and are significantly longer in length to both control and PSS terminating surfaces as shown in Figure 6.10. These differences were not observed on the Ti and TiN thin films nor for the HEK-293 and 3T3-L1 cells.

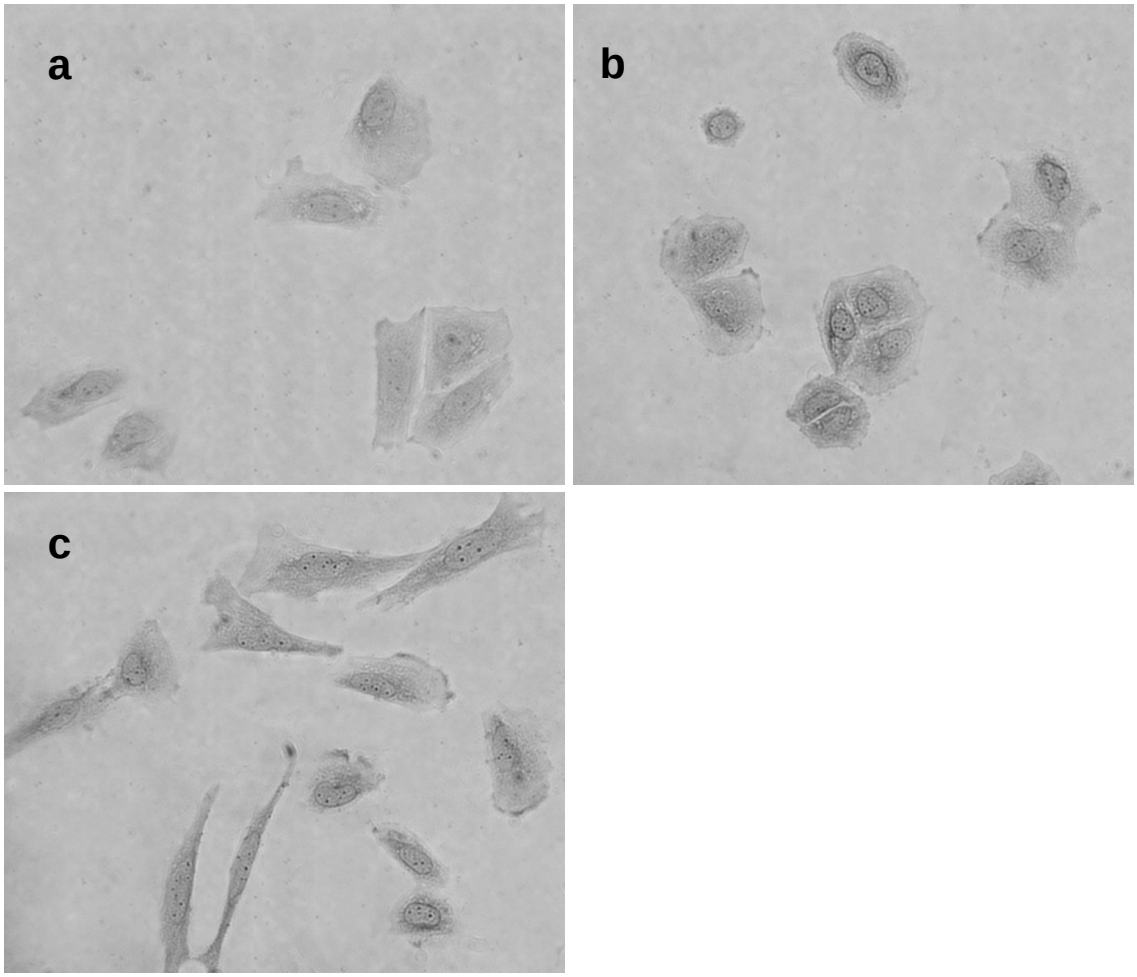

Figure 6.9: Morphology of SaOS-2 on tissue culture treated glass (a), PSS (b) and PAH (c). Cells were fixed by 4% paraformaldehyde and stained with 1% Coomassie Blue and imaged on the Nikon TE300 microscope on the x40 objective as described in *Methods*.

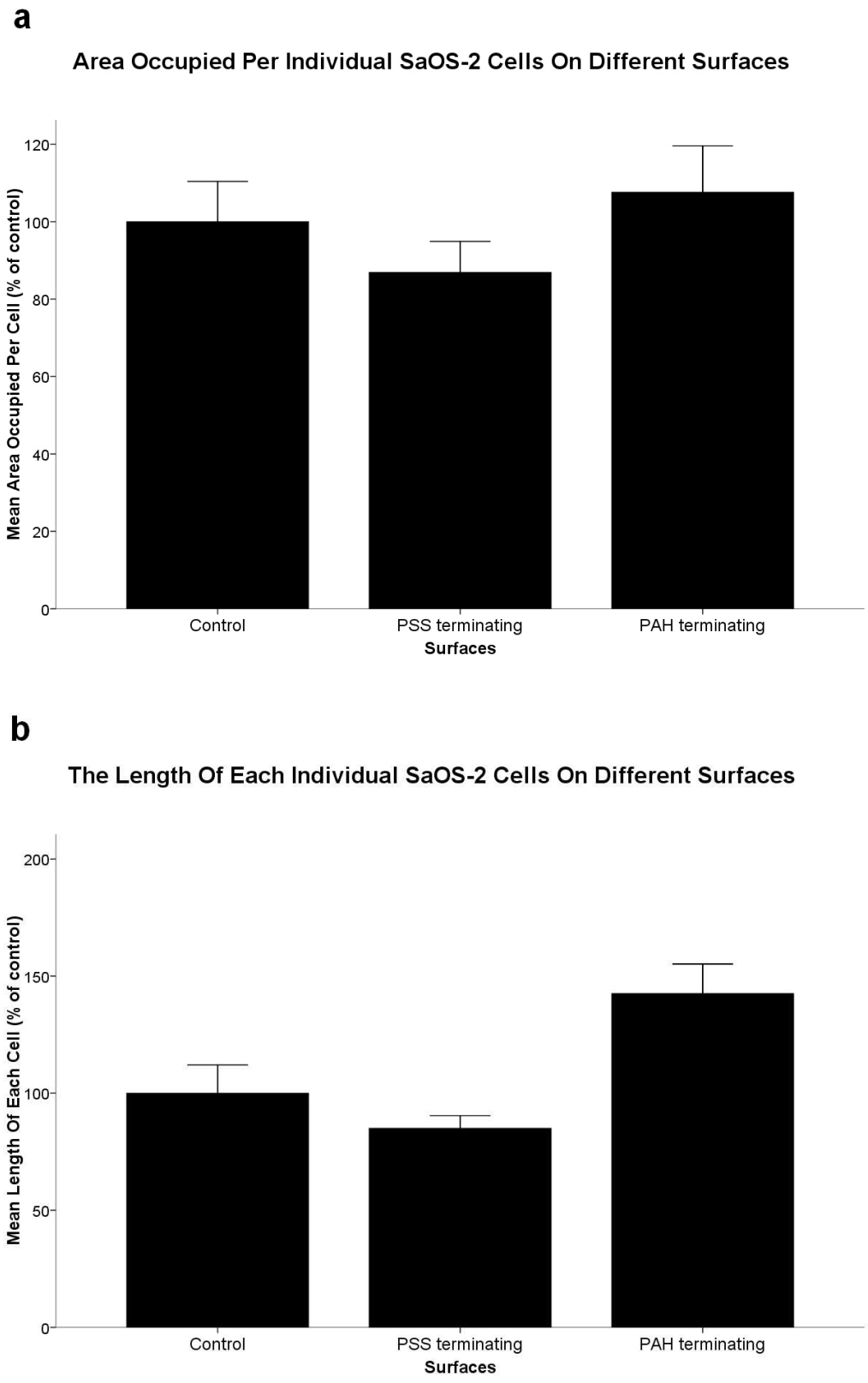

Figure 6.10: The area (a) and length (b) of each individual SaOS-2 cell TCP, PSS and PAH terminating thin films. Cells were fixed by 4% paraformaldehyde and stained with 1% Coomassie Blue and imaged on the Nikon TE300 microscope on the x40 objective as described in *Methods* and measured using Image Pro Plus 5.0. Error bars represent the standard error.

The actin distribution on the other hand appear to differ on different PE surfaces for the 3T3-L1, whereby the filaments appears to be thicker and more likely to run in parallel on the PAH terminating surfaces but are more diffuse on PSS terminating surfaces. These are shown in Figure 6.11.

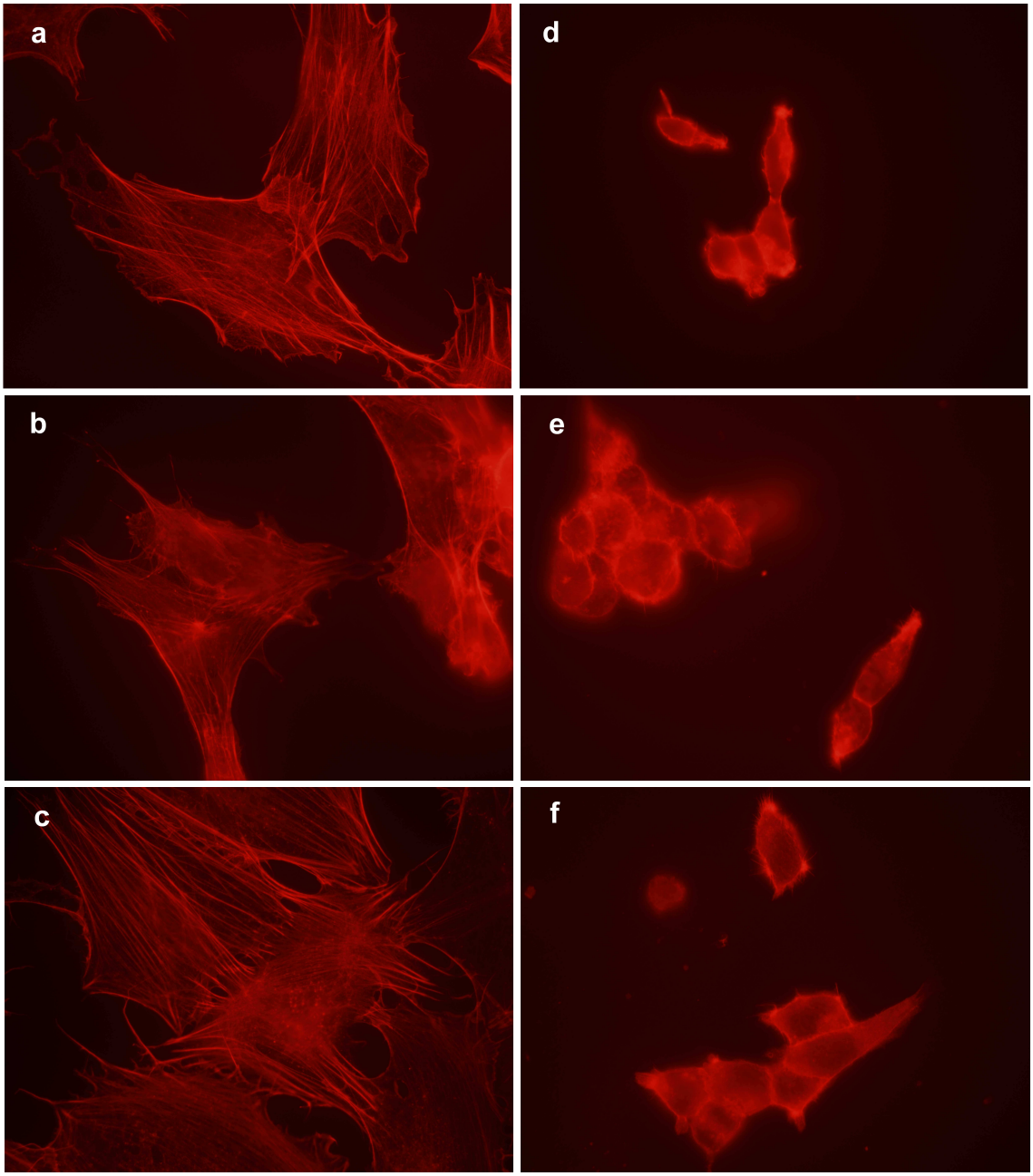

Figure 6.11: The F-actin distribution of 3T3-L1 (a,b,c) and HEK-293 (d,e,f) cells on tissue culture treated glass (a,d), PSS (b,e) and PAH (c,f) coated surfaces. The F-actin filaments were stained by Alexa Fluor® 633 phalloidin as described in *Method*, and imaged Olympus TE300 fluorescent microscope under the x100 oil immersion objective.

The actin distribution of SaOS-2 cells also appear to differ on different thin films where the filaments appears to be thicker and more likely to run in parallel on the PAH thin films. These are shown in Figure 6.12.

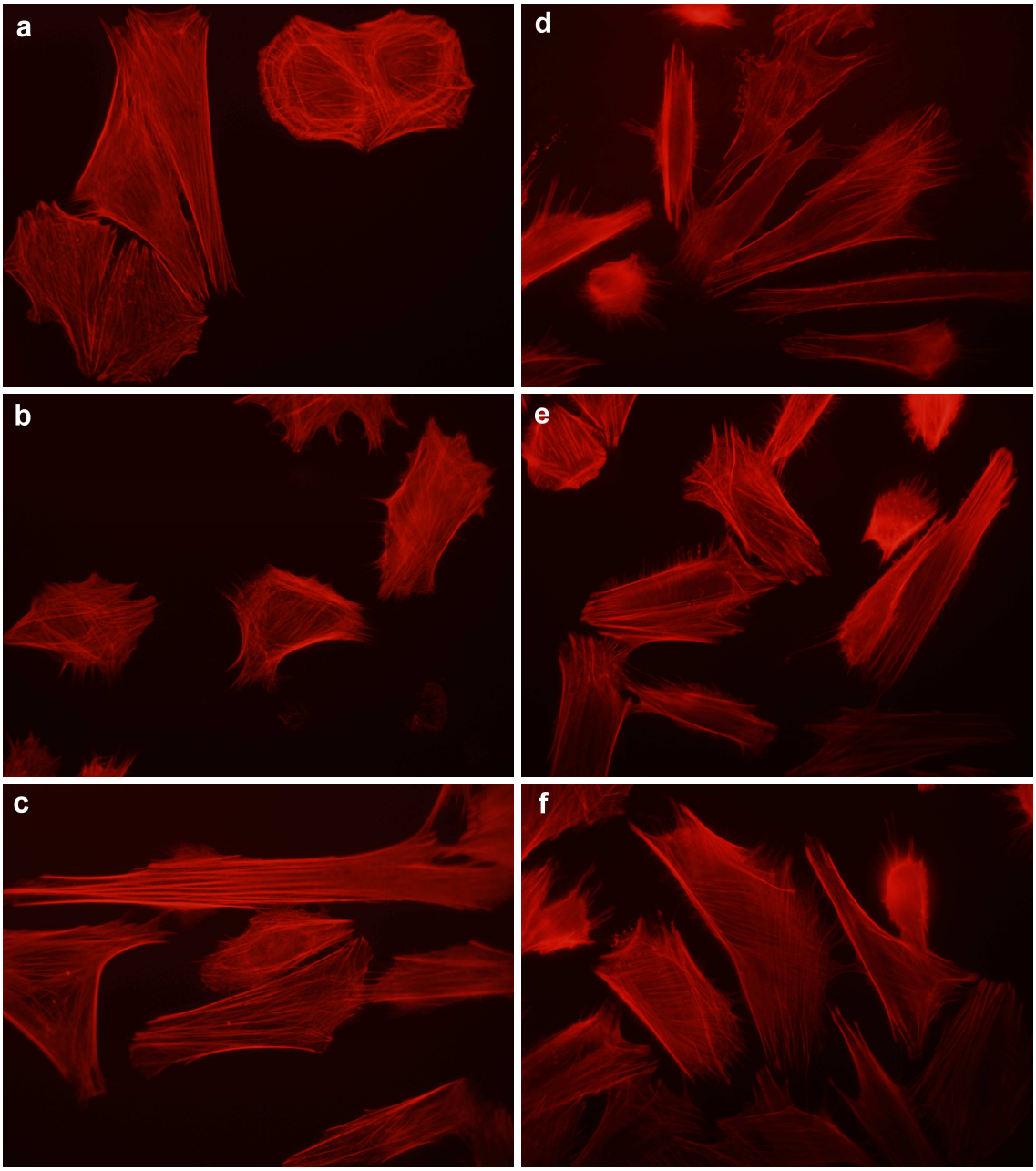

Figure 6.12: The actin morphology of SaOS-2 on tissue culture treated glass (a), PSS (b) PAH (c), Ti (d), TiN120 (e) and TiN190 (f) coated surfaces. The F-actin filaments were stained by Alexa Fluor® 633 phalloidin as described in *Method*, and imaged Olympus TE300 fluorescent microscope under the x100 oil immersion objective.

6.2.5 Initial attachment

The initial attachment of cells was measured by the two assay methods. The propidium iodide assay was used to analyse the cell number on different polyelectrolyte thin films whereas the alamar blue assay was used for the Ti and TiN thin films were involved. The initial attachments of the 3T3-L1 and HEK-293 cells as measured by the PI assay were significantly higher on PAH terminating surfaces as shown in Figure 6.13, even more so than fibronectin coated surfaces.

Also measured by the PI assay, Figure 6.14a show that there were significantly less SaOS-2 cells attached on PSS terminating surfaces. There were no significant differences between PSS terminating PEM with 1, 2, 3, or 4 polyelectrolyte layers (PSS, PAHPSS, PSSPAHPSS and 2PAHPSS) and the same applied to PAH terminating thin films.

Figure 6.14b shows that there are significantly more SaOS-2 cells on PAH and Ti thin films as compared to the control (glass) as measured by the alamar blue assay. The number of cells attached on Ti thin films was also significantly more than PSS and TiN120 thin films.

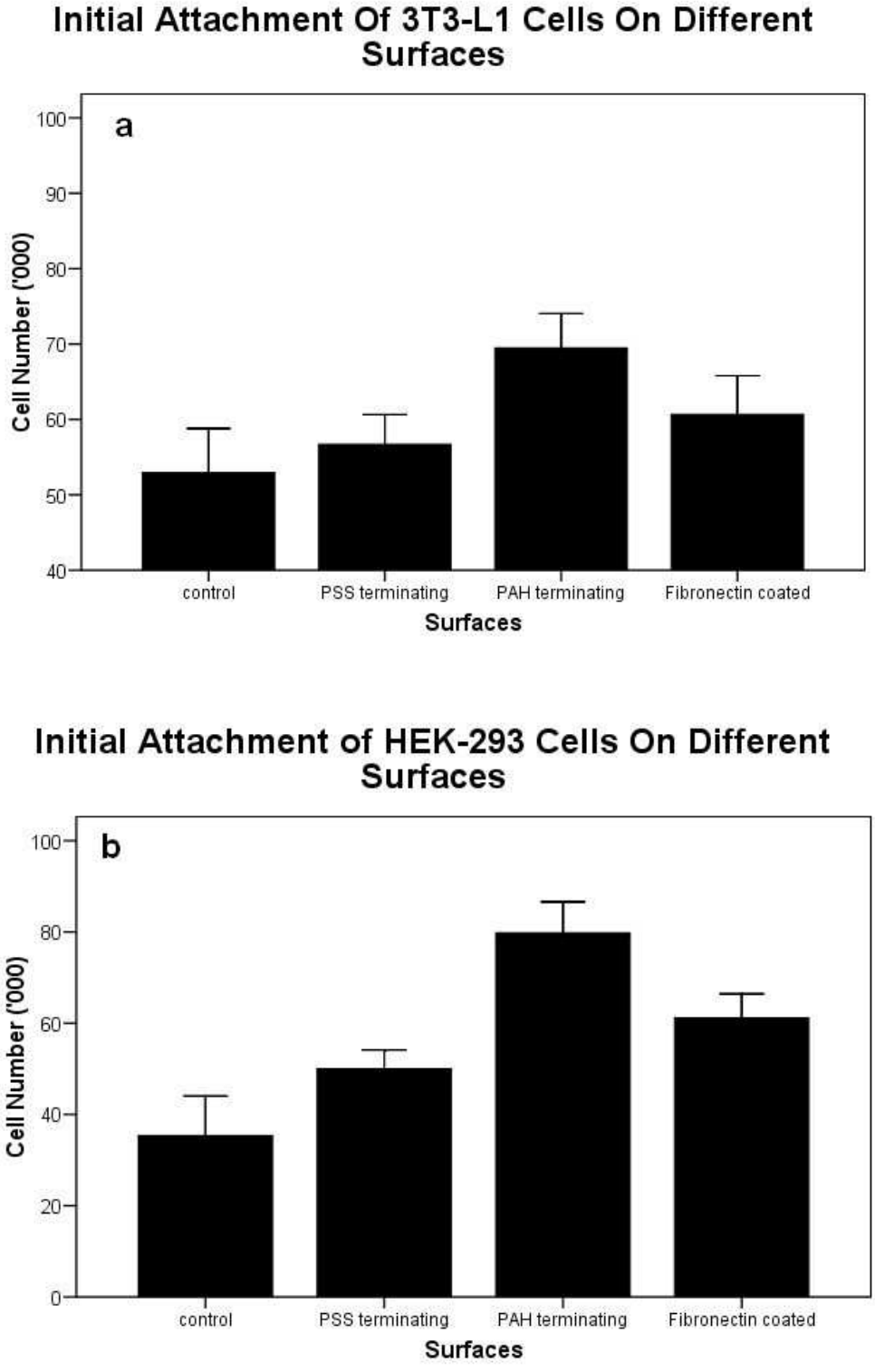

Figure 6.13: The initial attachment of 3T3-L1 (a) and HEK-293 cells (b). Cell number was determined by PI assay as described in *Methods*. Error bars represent the standard error.

a

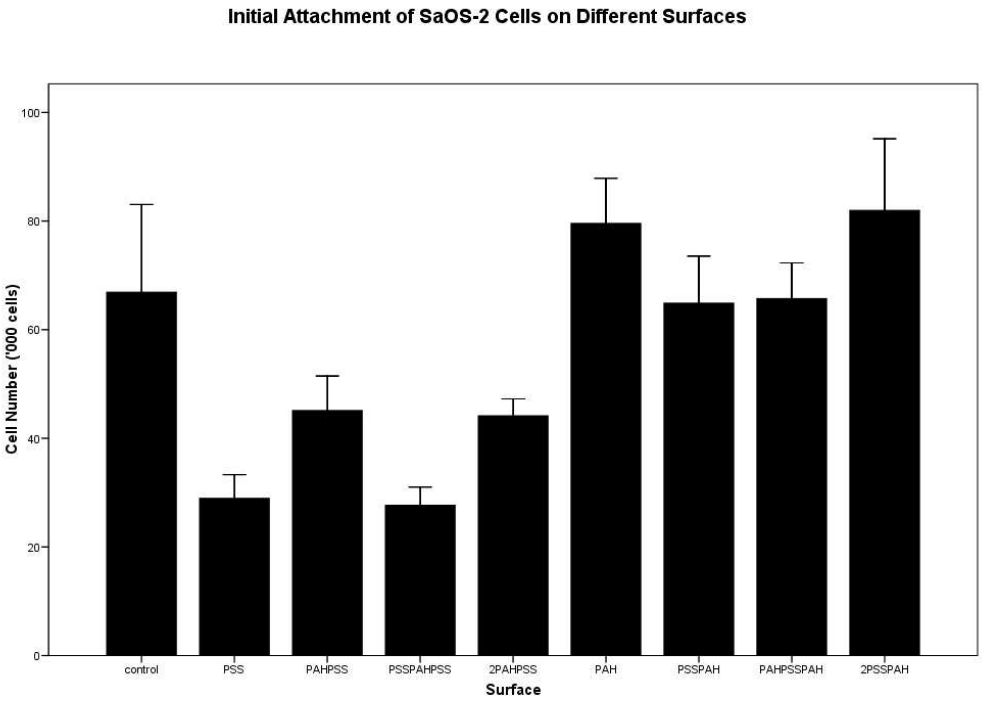

b

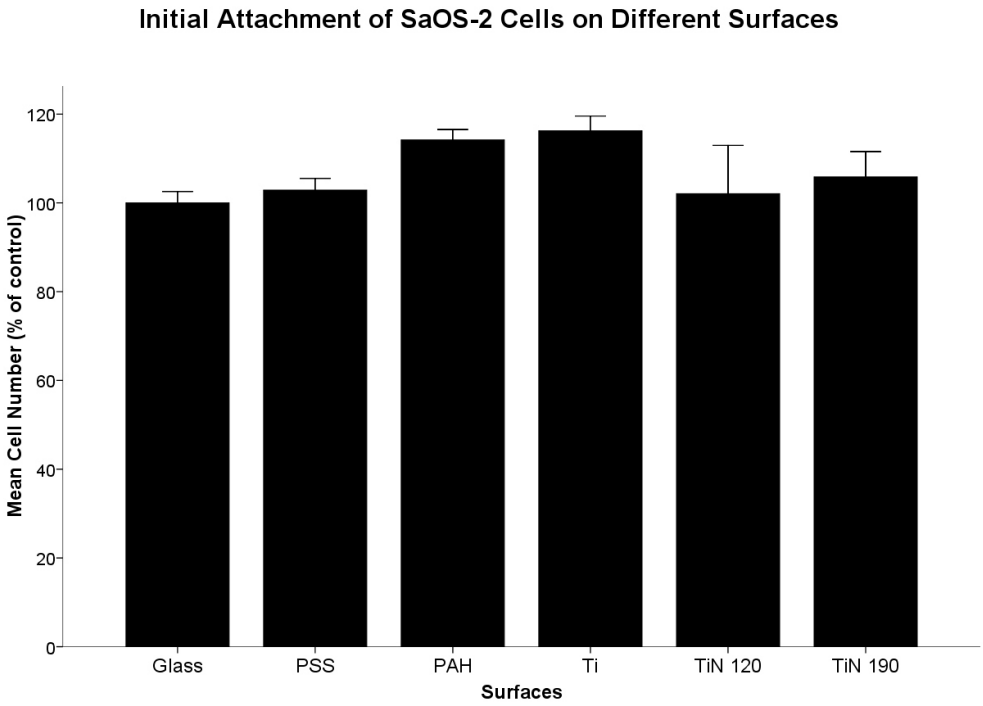

Figure 6.34: The initial attachment of SaOS-2 Cells as measured by PI assay (a) and Alamar Blue assay (b). Error bars represent the standard error.

6.2.6 Cell adhesion and Extracellular Matrix production

The adhesion of cells was significantly higher on PAH terminating surfaces for the 3T3-L1 and HEK-293 cell lines as shown in Figure 6.15. Although the adhesion of cells on PSS-terminating surfaces are generally low, the number of HEK-293 cell adhering is significantly higher on multi-layered PSS-terminating films than mono-layer as seen in Figure 6.15b.

The adhesion of HEK-293 cells was calcium dependent on PSS-terminating and fibronectin (alone) coated surfaces but not on tissue culture plastic and PAH terminating surfaces. The adhesion of 3T3-L1 cells are in general calcium dependent except on PAH terminating PEM of three and four layers (PAHPSSPAH and 2PSSPAH) and PSS terminating PEM of 4 layers (2PAHPSS). These are shown in Figure 6.16.

The relative levels of extracellular matrix (collagen) production by the 3T3-L1 and HEK-293 cells, as detected by the Direct-red staining show that cells on PAH have a significantly higher level of collagen in the extracellular matrix for both cell types as shown in Figure 6.17.

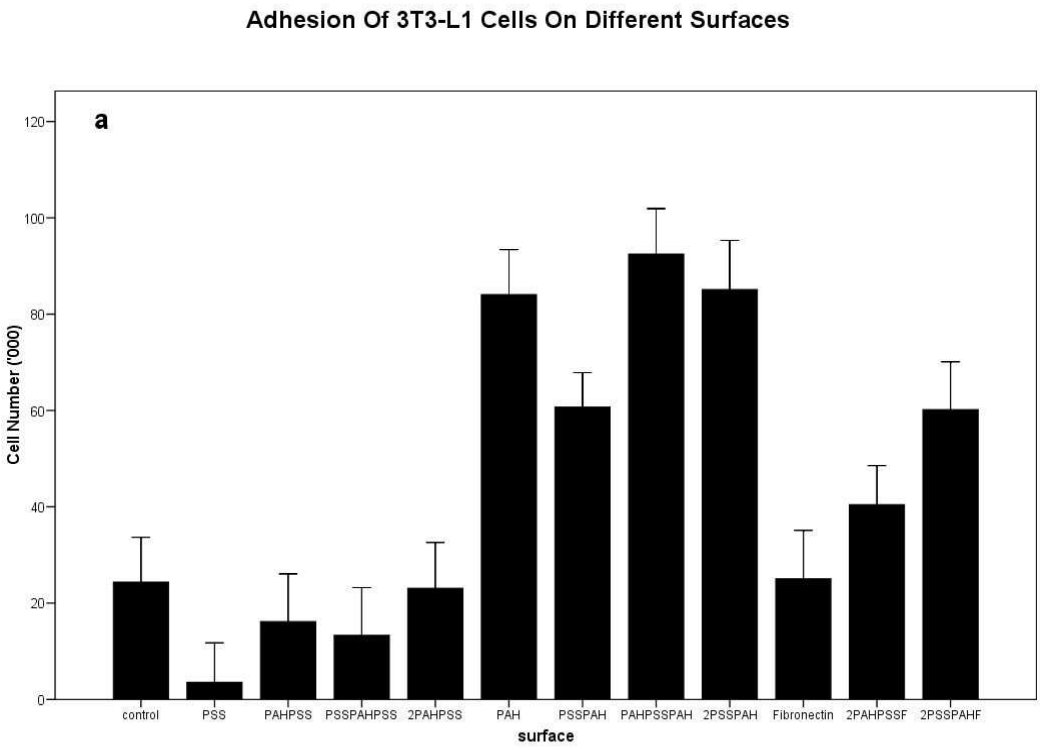

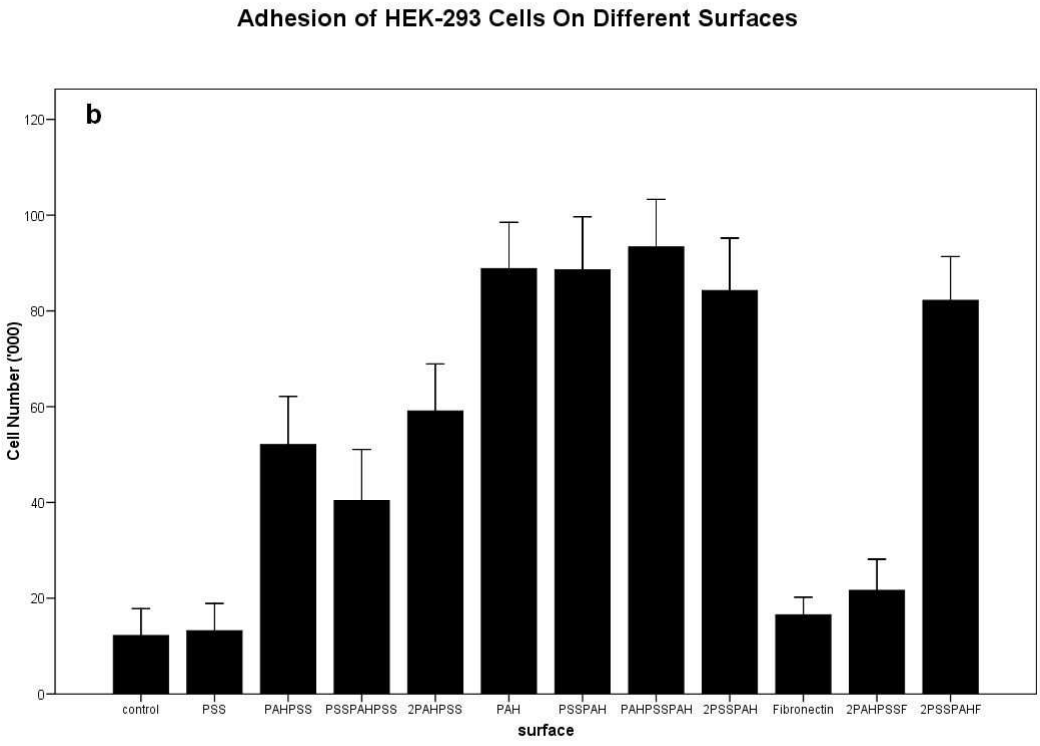

Figure 6.15: Adhesion of 3T3-L1 (a) and HEK-293 cells (b). Cell number was determined by PI assay as described in *Methods*. Error bars represent the standard error.

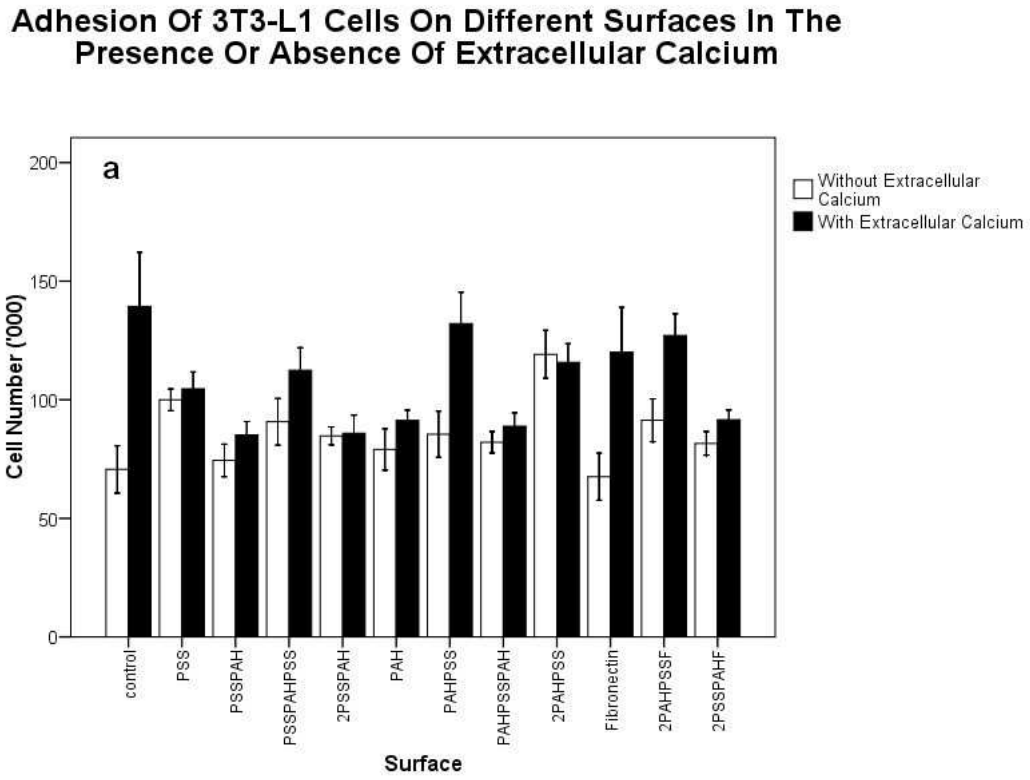

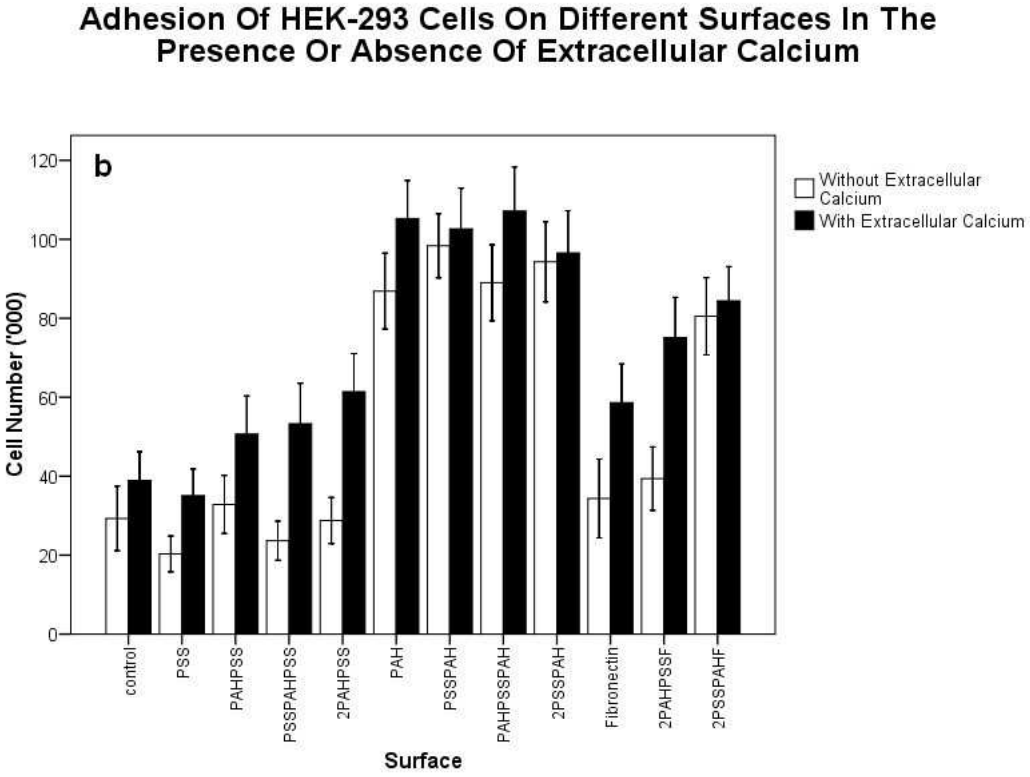

Figure 6.16: The Calcium Dependency of 3T3-L1 (a) and HEK-293 (b) Cell Adhesion on Different Surfaces. Cell number was determined by PI assay as described in *Methods*. Error bars represent the standard error.

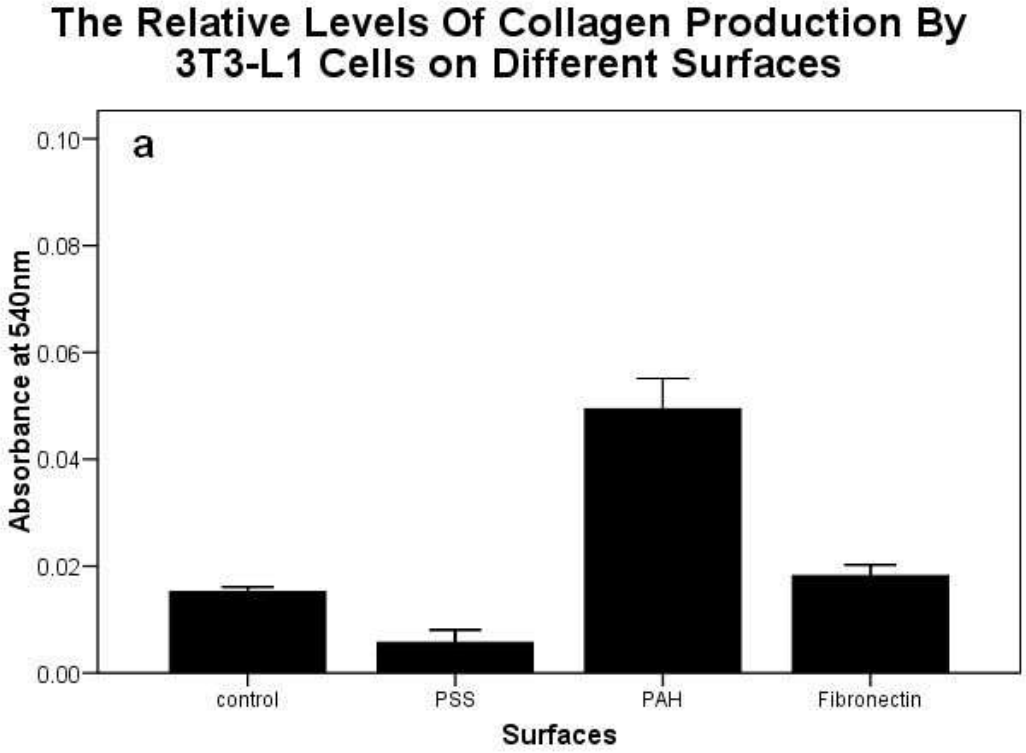

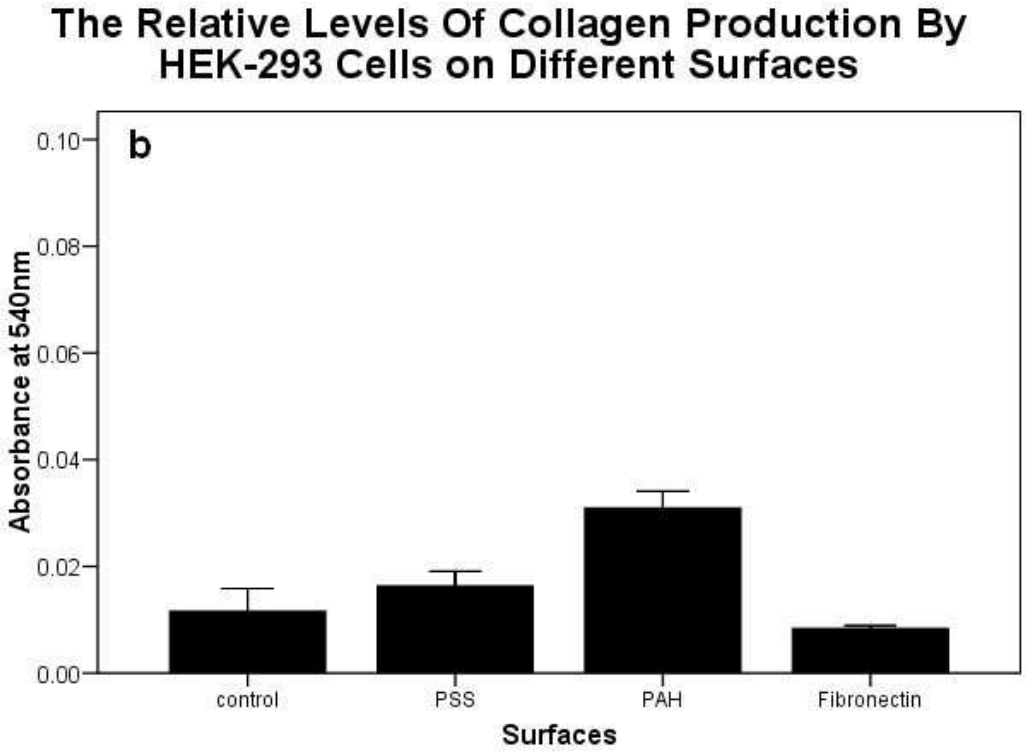

Figure 6.17: Relative Collagen Production by 3T3-L1 (a) and HEK-293 cells (b). The relative amount of collagen was determined by absorbance of Direct Red which peaks at 540nm. . Error bars represent the standard error.

Figure 6.18a shows that there were slightly more SaOS-2 cells adhering on the PAH terminating thin films than on PSS terminating thin films, and when the number of cells adhered were analysed in composite by the type of terminating polyelectrolyte (that is, PSS versus PAH terminating as oppose to the different polyelectrolyte combinations such as PAHPSS, PSSPAHPSS), there were significantly less cells adhering on PSS terminating thin films than PAH terminating thin films. However there were significant differences between PSS terminating thin films, especially PSSPAHSS which had significantly less adhering cells than PSS, and PAHPSS; PAH also had significantly more adhering cells than other PAH terminating PEM.

Figure 6.18b shows that the adhesion of SaOS-2 cells is significantly higher on PAH, Ti and TiN190 thin films compared to glass, PSS and TiN120 thin films.

The relative levels of extracellular matrix (collagen) production, as detected by the Direct-red staining show that cells on PAH have a significantly higher level of collagen in the extracellular matrix as shown in Figure 6.19.

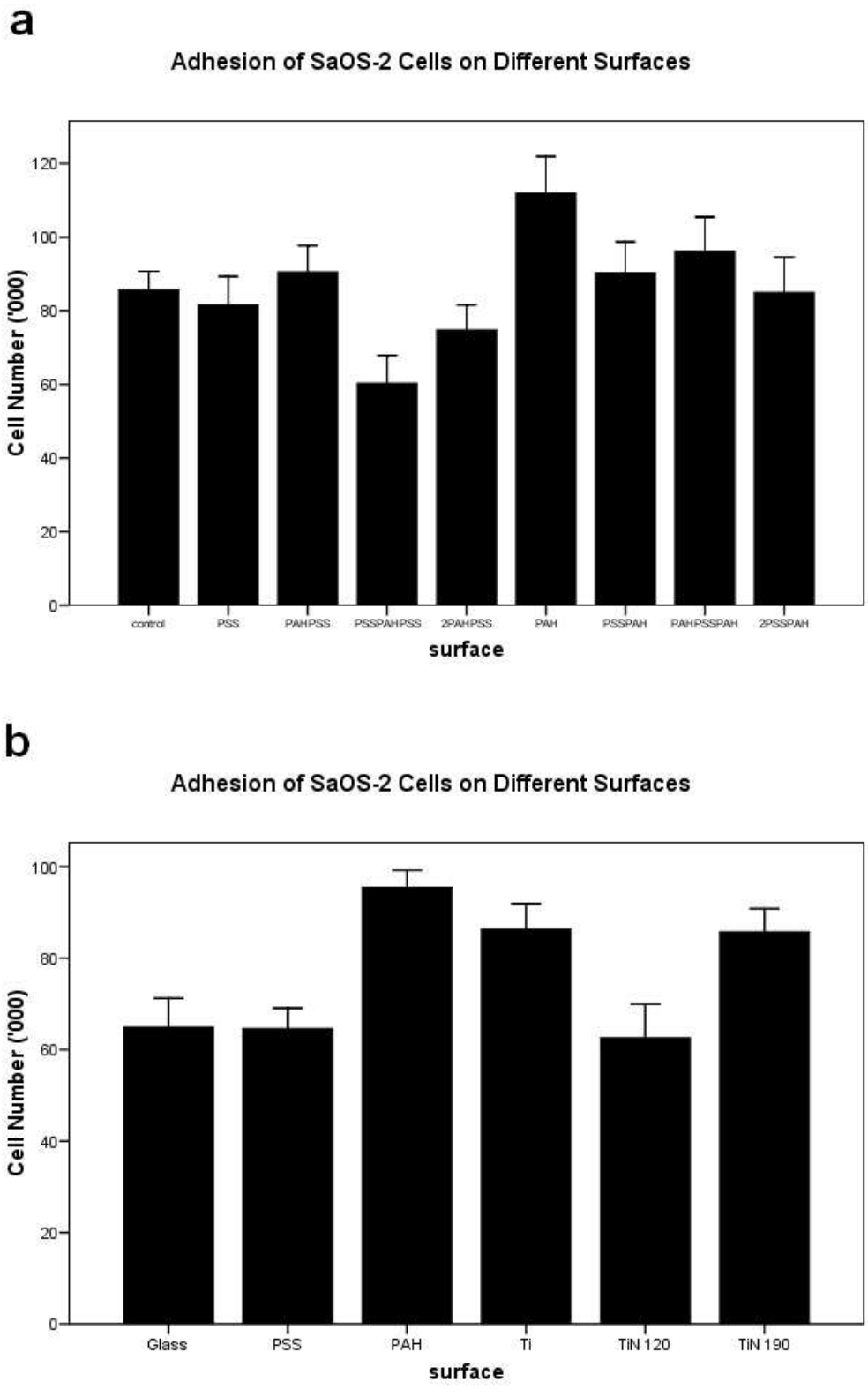

Figure 6.18: Adhesion of SaOS-2 cells as measured by PI assay (a) and Alamar Blue assay (b). Error bars represent the standard error.

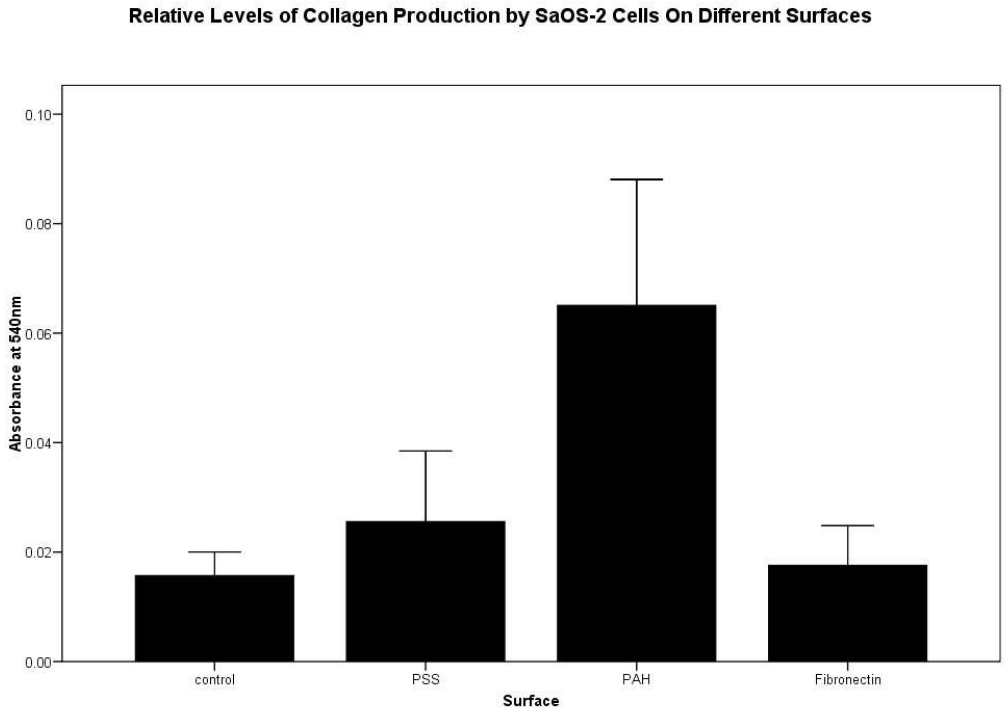

Figure 6.49: Relative Collagen Production by SaOS-2 Cells. The relative amount of collagen was determined by absorbance of Direct Red which peaks at 540nm. Error bars represent the standard error.

6.2.7 Cell Differentiation

The level of cell differentiation was measured by the Alkaline phosphatise (ALP) activity and the amount of mineralisation was measured by Von Kossa assay. As shown in Figure 6.20a, there was no significant difference between tissue culture plastic (control), PSS and PAH terminating thin films for the levels of ALP activity except between PAHPSS and PAH thin films.

Compared to Ti and TiN thin films, TiN thin films made with 190 volts (TiN190) had the highest and significantly higher levels of ALP activity, whilst TiN120 had significantly less ALP activity compared to TiN190 and other thin films as shown in Figure 6.20b.

The basal level of calcification or mineralisation was measured by the Von Kossa which stains calcified areas by silver nitrate staining. Figure 6.21 shows the total mineralisation (total area with nodules) per image field normalised to control, and it shows that the total mineralisation vary quite a lot between thin

films, but in general, PSS terminating thin films has higher (but not significantly) levels of mineralisation.

Interestingly, as shown in Figure 6.22a, the size or area of each mineral nodules on PAH terminating thin films are significantly larger than control and PSS terminating thin films, whilst these nodules on PSS terminating thin films are significantly smaller than control. However, the nodules on PSSPAHPSS appears to also be significantly larger than nodules other PSS terminating thin films. Nodules on PAH monolayer thing films follow by 2PSSPAH thin films are also significantly larger than nodules on other PAH terminating thin films.

The number of nodules on PAH monolayer thin films was also significantly less than PSS terminating thin films except for 2PAHPSS as shown in Figure 6.22b. However, the standard errors are quite large, that is, the number of nodules is not homogenous distributed.

a

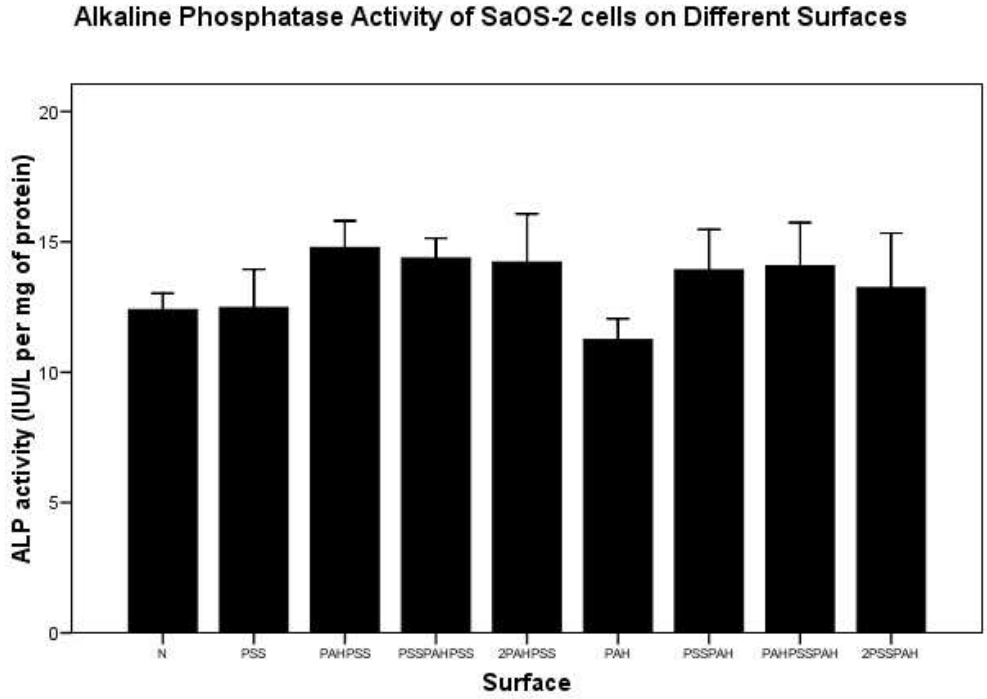

b

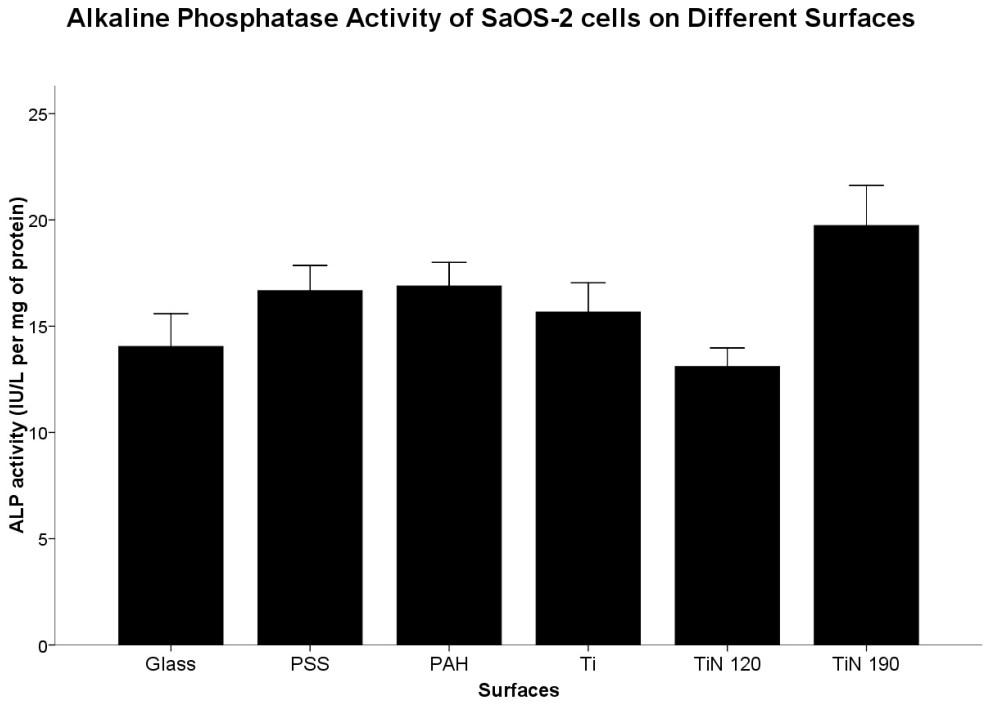

Figure 6.20: The level of alkaline phospatase activity of SaOS-2 cells on different thin films as measured on day 10. Error bars represent the standard error.

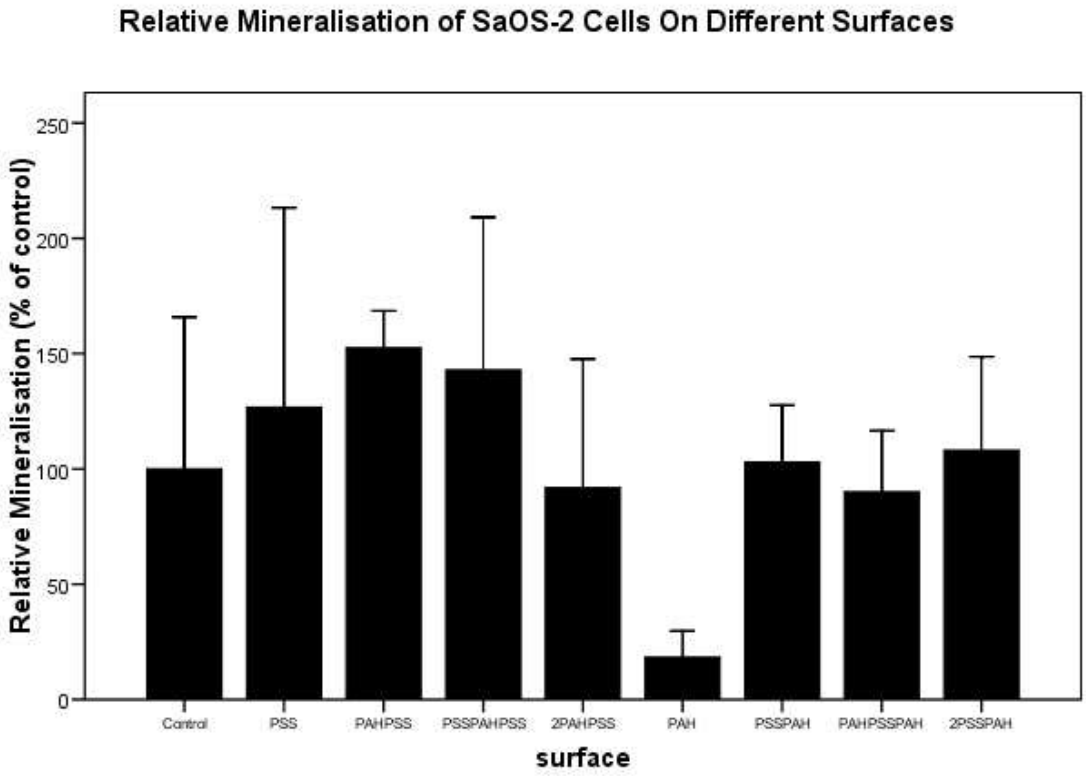

Figure 6.21: The relative mineralisation of SaOS-2 cells on different surfaces. Mineralised nodules were stained by silver nitrate as described in *Method* and calculated as the total area of all nodules in an image field. Error bars represent the standard error.

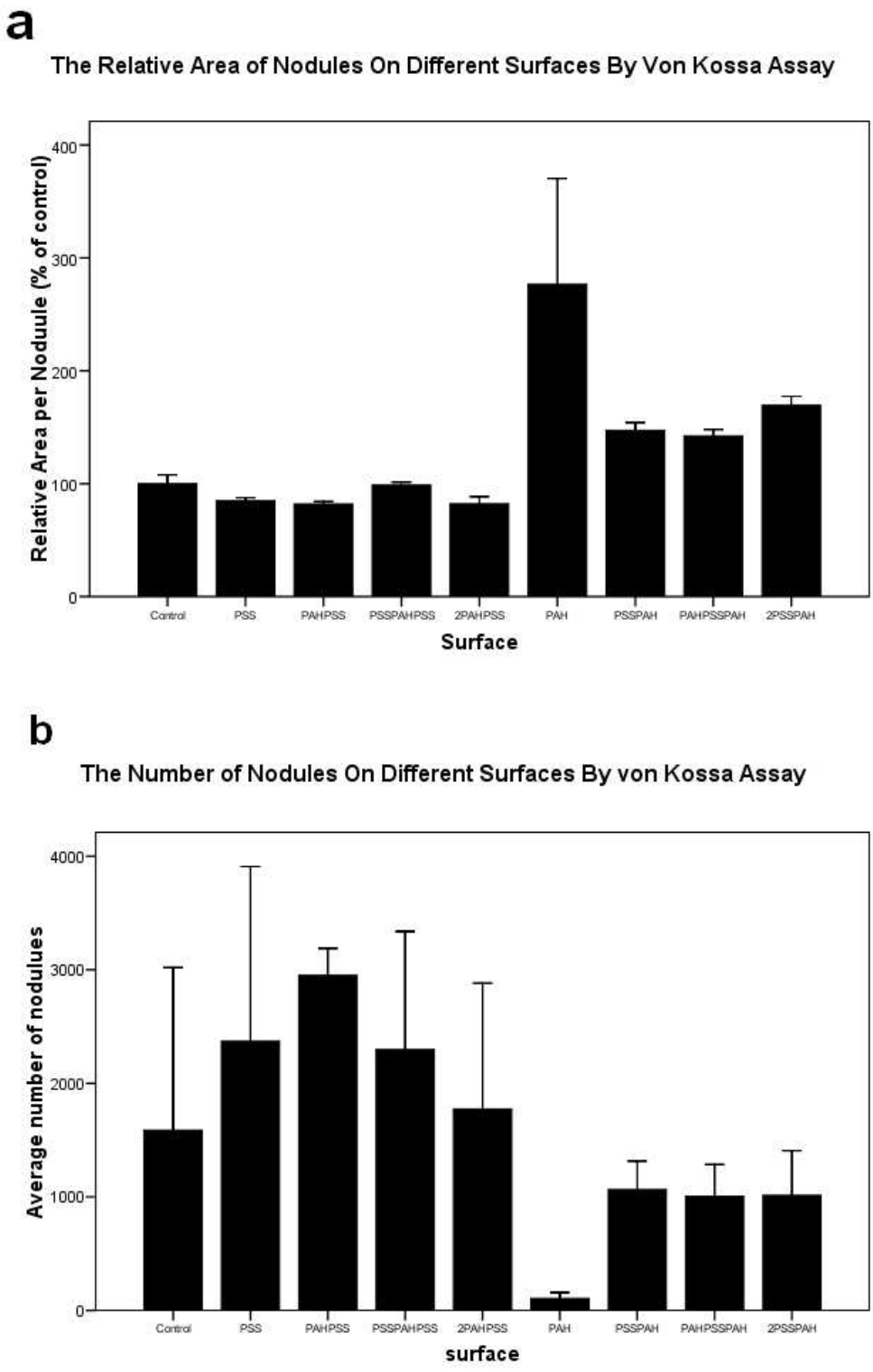

Figure 6.22: The area (a) and number (b) of mineralised nodules produced by SaOS-2 cells on different surfaces. Mineralised nodules were stained by silver nitrate as described in *Method* and the area per nodule were normalised against control. Error bars represent the standard error.

6.3 Discussion

6.3.1 Thin films characterisation

The PE thin films made in this study were composed of PSS a poly-anion which is hydrophilic and PAH, a poly-cation which is hydrophobic. It has been well established that the terminating or the outmost layer of the thin film determine its characteristic (Elzbieciak, Kolasinska & Warszynski 2008; Kolasinska & Warszynski 2005). That is, thin films with PSS as its terminating layer would have a negative surface zeta potential and is more hydrophilic than a thin film with PAH as its terminating layer, which would have a positive surface zeta potential and is hydrophobic (Kolasinska, Krastev & Warszynski 2007). The zeta potential of glass, PSS, PAH thin films, Ti and TiN colloids have been previously shown, therefore were not repeated in this study. Apart from PAH thin film which is cationic, the rest of the thin films have a negative zeta potential (Cai et al. 2006; Gu & Li 2000; Nebea et al. 2007; Sze et al. 2003; Zhang et al. 2005). However, it should be noted that zeta potential measurements reflect the average charge of the whole surface. It remains possible that the distribution of charges would not be homogenous on a rough or patterned surface as reviewed (Delgado et al. 2007; Zembala 2004) .

The wettability of these thin films also differs: TiN and PAH thin films being the most hydrophobic and Ti thin film being the most hydrophilic. There was also a difference in hydrophobicity between TiN120 and TiN190 which may be attributed to the different surface roughness. For example, it has been shown that a change in surface roughness can change the water contact angle of titanium and titanium alloy (Ponsonnet et al. 2003) as well as mineral particles (Ulusoy & Yekeler 2005).

Interestingly, titanium thin films have been conventionally found to be hydrophobic with a water contact angle of around 80^{o} (Cai et al. 2005), but have been occasionally reported as hydrophilic, which had been thought to be due to the differences in surfaces roughness (Lim et al. 2001; Lim & Oshida 2001). However, a recent study has reported that such difference in wettability is due to a phenomenon where there is a shift from hydrophobicity to a hydrophilic configuration by previously wetting of the titanium (Rupp et al. 2004). The

titanium thin films used in this study were sterilised with 70% ethanol, which therefore pre-wetted before exposure to cells and explains the low water contact angles that were measured.

Surface roughness of these PE thin films increase with the increase in the number of PE layers (Gong et al. 2005; Lowman & Buratto 2002) but has been found to be independent on the type of outer layer (Gong et al. 2005) and asymptotes to 4nm RMS roughness (Lowman & Buratto 2002). Glass, PSS and PAH thin films are relatively smooth surfaces (RMS<2nm), and this was expected as the maximum surface roughness (RMS) reported for 10 bi-layers of PSS and PAH thin films asymptote at 4nm (Lowman & Buratto 2002). Ti and TiN thin films on the other hand, are a lot rougher. On Ti thin films, there appear to be a scatter of small grains of 2.88 to 11.3nm in height. Similar scatter of grains also appears on TiN120 thin films, but there were also larger rhomboidal shaped structures (max height at 23 ± 3.3nm) which have a peak towards their medial plane. Similar rhomboid structures are seen on the TiN190 thin films, but these are even taller (maximum height at 45.99 ± 3.34nm). These surface features are different from what have been shown in the literature. For example, Xu, Ye et al (2006) showed a hemi-shere patterning on silicone but the sputtering was carried out in high N_2 atmosphere. At a lower partial pressure of N_2 (0.26 Torr), the Ti appears in waves when sputtered on to silicone. These are most likely to be due to the difference in the use of substrate (silicone versus glass in this instance) and different pressure (N_2 partial pressure is 0.4 mTorr) and power during deposition.

6.3.2 Cytotoxicity

The results show that (mono and multi-layers) PE thin films are not cytotoxic which is in agreement with what is already reported in the literature (Boura et al. 2003; Lin et al. 2006; Petra Tryoen-Tóth 2002; Vautier et al. 2002). This confirms that it may be feasible to grow cells on 3D structures made from PE for cell contraction assay.

The PI assay relied on the measurement of fluorescence intensity of the DNA-bound PI dye to determine cell number and cytotoxicity, hence could not be used for the Ti and TiN thin films. This is because these thin films are not transparent and will affect the accuracy of this optical measurement.

Alamar blue assay was used instead to measure the viability of the SaOS-2 cells when Ti and TiN thin films were used. This assay relies on the metabolic activity of live cells to chemically reduce a blue, non-fluorescent resazurin into a red fluorescent product which is released into the supernant. By measuring the absorbance or in this case, the fluorescence intensity of the supernant, the number of viable cells can be determined. This assay showed that there were significantly less viable cells on TiN120 thin films. This was not expected as TiN thin films have been shown to have enhanced the viability of cells in some cases, (Chien et al. 2008) and TiN has good haemocompatibility (Dion et al. 1995; Dion et al. 1993) . Furthermore, the thin film with exactly the same chemical composition (TiN190) did not show a reduction in cell viability.

There were only slight differences in the hydrophobicity of the two TiN thin films (both $>90^{o}$ in water contact angle), and the only other difference is the increased surface roughness of the TiN190 thin films. Although an increase in surface roughness has been shown to increase osteoblast cell density, such a difference was not seen on the first day after seeding (Kunzler et al. 2007). Some studies have attributed to the lowering of viability to the reduction of cell adhesion as reviewed (Bacáková et al. 2004). Although the cell adhesion was not as strong on TiN120 thin films, there was not a significant difference in initial attachment which seems to suggest that the reduction in cell viability reading may not be due to the reduction in cell number. As proliferation and ALP activity were significantly lower on TiN120, it may be hypothesised that the reduction in cell viability reading may be attributed to the reduction in metabolic activity (which leads to reduced dye conversion) of SaOS-2 cells on these thin films.

6.3.3 Cell cycle and Proliferation

It has been shown that cationic charges increases proliferation (De Rosa et al. 2004) and the relationship between cell growth rate and zeta potential (0 to +20) is sigmoidal (2004; Kishida et al. 1991). It has also been shown that the wettability of surfaces can effect cell growth (Altankov, Grinnell & Groth 1996; Kim et al. 2007; Ruardy et al. 1997) in cell-type dependent manner (Fuse et al. 2007; Ruardy et al. 1997). Hydrophobic surfaces often inhibit cell growth (Chang et al. 2005; Groth & Altankov 1996) whilst Choee et al (2004) and Kim et al (2007) have found that fibrobloast proliferation was highest on hydrophilic surfaces, with a water contact angle between 57^{o} on and 60^{o}. Based on these studies, it was expected that fibroblast (such as the 3T3-L1) proliferation should be highest on *cationic, hydrophilic* surfaces.

PAH thin films are cationic and hydrophobic whereas PSS thin films are anionic hydrophilic. The results of this study show that the cell number were actually significantly lower on PAH terminating surfaces compared to the PSS terminating surfaces for both cell types (day 7 for the 3T3-L1 and day 5 for the HEK-293 cells), which seems to suggest that water contact angle (wettability or hydrophobicity) of the PE thin films is the major factor contributing to cell proliferation, or at least a more important contributor than the charge of the thin film.

Increased surface roughness has also been shown to enhance the proliferation of Human Umbilical Vein Endothelial Cells (Chung et al. 2003) and osteoblast-like cells (Degasne et al. 1999; Schweikl et al. 2007), but to reduce the proliferation for fibroblasts (Kunzler et al. 2007; Schweikl et al. 2007). For neural cells, proliferation is only enhanced within a window of surface roughness (Fan et al. 2002). However, in this study cell number did not correlate with the number of PE layers (maximum 4 layers), hence it was postulated that the increase in surface roughness in this instance did not play a major role in the proliferation of the 3T3-L1 and HEK-293 cells on these PSS and PAH thin films.

Cell cycle analysis shows G2 arrest and a reduction in the proportion of SaOS-2 cells in the S phase of the cell cycle on PAH thin films as compared to PSS thin

films. The S phase of the cell cycle involves the synthesis of genetic material to allow cells to enter into the G2 phase where there is doubling of the amount of genetic material and preparation of the cells to move into mitosis. Therefore, reduction in the synthesis of genetic material and G2 arrest would lead to a reduction in cell proliferation. In fact, the PI and Alamar Blue assay showed that there are reduced numbers of SaOS-2cells on PAH thin films on day 7. This is similar to the results for the 3T3-L1 and HEK-293 cells.

Proliferation of SaOS-2 cells on TiN thin films showed varying results. As mentioned, cell proliferation was reduced on TiN120 thin films, whilst it was enhanced on TiN190. This is likely due to TiN190 being the rougher surface, which has been shown to sometimes increase osteoblast cell proliferation (Degasne et al. 1999; Kunzler et al. 2007; Marinucci et al. 2006), but not always (Cai, Bossert & Jandt 2006). Ti thin film also had high level of SaOS-2 cell proliferation, which is not surprising as it has been shown that hydrophilic surfaces enhance cell proliferation (Choee et al. 2004; Lee et al. 1998; Zelzer et al. 2008).

6.3.4 Morphology and F-actin distribution

There were no significantly differences in the morphology and spread of the of HEK-293 and 3T3-L1 cells as observed by phase contrast microscopy. Figure 6.10 showed that there were no significant differences between the total spread in the area occupied by SaOS-2 cell population, however, *individual* cells on PAH terminating thin films are elongated and occupy significantly more area than cells on PSS terminating thin films. Interestingly, this elongated morphology of the SaOS-2 cells resembles the less mature osteoblast cell line of MG-63.

However, intracellularly, the actin cytoskeleton of the cell has been found to be influenced by the wettability, zeta potential and roughness of the surface. For example, hepatocyte and fibroblasts are more likely to develop actin stress fibers on hydrophilic surfaces (Altankov, Grinnell & Groth 1996; Finke et al. 2007; Krasteva et al. 2001; Lee et al. 2003). The Actin cytoskeleton of osteoblast (Finke et al. 2007) and chondrosarcoma cells (HCS-2/8) (Vautier et al. 2002) is more developed on cationic polymer coated titanium. Increased

surface roughness has been found to induce the formation stress fibers of osteoblasts (Lipski et al. 2008; Salido et al. 2007) and long, thick actin fibers in parallel with the long axis of endothelial and pre-osteoblastic cells (Harris et al. 2005)

The 3T3-L1 cells in this study formed the F-actin cables on the PAH terminating surfaces whereas the F-actin distribution diffused on the PSS terminating surfaces. No changes were observed for the HEK-293 cells. As there were no obvious changes with increase in the number of PE layers, surface roughness in this instance did not play a significant role in altering F-actin distribution of the 3T3-L1 cells. These differences in F-actin distribution of 3T3-L1 on PAH terminating thin films is most likely be attributed to its positive zeta potential, as it has been shown that only hydrophilic surfaces enhance the development of F-actin stress fibers (Altankov, Grinnell & Groth 1996; Finke et al. 2007; Krasteva et al. 2001; Lee et al. 2003) whilst PAH terminating thin films are hydrophobic.

The F-actin in SaOS-2 cells was found to be thicker and the filaments were more parallel on PAH thin films than PSS thin films and glass which have similar surface roughness. These differences were not observed for the Ti and TiN thin films, which have a similar water contact angle to PAH thin films. This suggests that these morphological changes may be attributed to the cationic nature of the PAH thin films and not hydrophobicity and surface roughness.

These results indicate that PAH may be the preferred terminating layer for the 3D contraction system, as F-actin cables are thick and in an orientation which may allow contraction. It is interesting to note as well, that the change in F-actin distribution was not observed in the HEK-293 cells, which highlights the fact that different cells can behaviour very differently on the same surface (Harris et al. 2005; Lee et al. 1998; Lee et al. 2000).

6.3.5 Initial attachment

The initial attachment and adhesion assays results were also in agreement with the literature which found that the positively charge PAH yield a higher number of cells adhering (Boura et al. 2003; Lin et al. 2006; Mhamdi et al. 2006a; Tryoen-Tóth et al. 2002; Vautier et al. 2002). This is not surprising since

eukaryotic cells display a net negative surface charge (Camp & Capitano 2005), and hence are more likely to be attracted to a positively charged surface. The increase in zeta potential of a surface also increase cell attachment (Kishida et al. 1991) and more force is needed to pull-off cells from cationic (Poly(L-lysine) films (Richert et al. 2002) and glass beads from PAH terminating surfaces (Gong et al. 2005). This "stickiness" is preferable for the 3D contraction system as it may increase the chances of cells attaching and adhering, and confirms that PAH may be the preferred terminating layer for the 3D contraction system.

The enhancement of cell attachment on Ti thin films cannot be attributed to the same process as PAH terminating PEM, because Ti thin films are the opposite in zeta potential and wettability to PAH terminating PEM. Cell attachment was not enhanced for other thin films (TiN and PSS) with similar zeta potential. However, Ti thin films are unlike all the other thin films in this study, in that these are very hydrophilic. It has been traditionally thought that protein adsorption is higher on hydrophobic surfaces (Welin-Klintström, Askendal & Elwing 1993) including hydrophobic titanium (Jansson & Tengvall 2004) as was previously reviewed (Sadana 1992; Wahlgren & Arnebrant 1991). However, Grinnell & Feld (1982) found that in the presence of cells, there were actually more fibronectin associated with hydrophilic surfaces, and the biological activity of adsorbed fibronectin is much less active on hydrophobic surfaces (Grinnell & Feld 1981). In fact, a recent study by Wei et al (2007) showed a higher level of immunological detection of fibronectin on hydrophilic hexamethyldisiloxane surfaces than its hydrophobic counterparts. Therefore, the enhanced initial attachment on Ti thin films is likely to be attributed to the enhanced levels of adsorbed protein and biological activity due to its hydrophilicity.

However, it is important to note that there is a difference between initial attachment and adhesion. As reviewed by Jäger et a (2007), initial attachment involves the interaction of cells with the protein adsorbed surface during the first few minutes of contact whereas adhesion of cells involves the interaction of cells with the extracellular matrix which is produced within hours contact.

Increased surface roughness increases protein adsorption on to some (Dolatshahi-Pirouz et al. 2008; Rechendorff et al. 2006) but not all surfaces

(Cai, Bossert & Jandt 2006). Although fibronectin absorption is higher on hydrophilic surfaces (Wei et al. 2007), it has been reported that absorption of this negatively charged protein is much higher on PAH terminating (cationic and hydrophobic) surfaces than PSS terminating (anionic) surfaces (Ngankam, Mao & VanTassel 2004; Wittmer et al. 2007). That is, the adsorption of protein on polyelctrolyte thin films can be largely attributed to the electrostatic interaction between proteins and the surface (Ladam et al. 2000; Ladam et al. 2001; Ladam et al. 2002). This is clearly demonstrated by the difference in the levels protein adsorbed when the polarity of the PE molecules are altered with changes in ionic strength (Ladam et al. 2000; Ngankam, Mao & VanTassel 2004) and pH (Gergely et al. 2004) of the adsorption solution.

When the protein and the surface charges are opposites there is greater level of protein adsorption, and the adsorbed protein layer is much thicker and possibly even in multi-layers (Ladam et al. 2002). It is conceivable that during the first few minutes of exposure to cell culture medium, serum proteins which are essential for cell attachment, such as fibronectin and vitronectin (Steele et al. 1995; Steele et al. 2005; Thomas et al. 1997) are absorbed quicker and at greater amounts on to PAH terminating than PSS terminating surfaces.

Proteins adsorbed onto a solid surface are different from their soluble form and may undergo conformational and or orientation changes (Horbett 1993, 1994). As reviewed by Horbett (1994), these structural changes can alter the “biological activity” of the protein, perhaps by revealing or masking binding sites, so that for a similar level of protein absorbed, the binding capability can be drastically different (Lindon et al. 1986). For example, the “biological activity” of fibronectin, which is essential for cell attachment, has been shown to vary with different types of surfaces it is adsorbed on to (Grinnell & Feld 1982; Grinnell & Feld 1981). Fibronectin binds “end-on” to the positively charged PAH terminating surface to form a near-vertical conformation whereas PSS binds to the body of the fibronectin molecule to form a more horizontal conformation (Ngankam, Mao & VanTassel 2004). Potentially the enhanced initial attachment as well as adhesion may be attributed to the structural/orientation changes of cell attachment-related serum proteins absorbed on to PAH-terminating thin films.

Therefore, the effects of these PE thin films have on cells occurred within the first 3 hours of contact, if not earlier. The high cell number on the cationic PAH terminating surface in the initial attachment assay (see Figure 6.13 an 6.14) may be attributed to two factors. That is, the electrostatic interaction between cells with the surface and different level of absorbed of proteins, which may also undergo conformational and or orientation changes.

6.3.6 Cell adhesion and ECM

Cell adhesion is a complex and dynamic process which involves an array of different proteins as reviewed by various authors (Sniadecki et al. 2006; Thiery 2003; Worth & Parsons 2008; Zamir & Geiger 2001). However, it is certain that the adhesion of cells is influenced by the cells' ability to interact with extracellular matrix. As reviewed by Bacáková et al (2004), the basolateral aspect of the cell membrane expresses adhesion molecules, such as integrins, and selectins, and binds to molecules in the extracellular matrix such as fibronectin, vitronectin, collagen and laminin which can be adsorbed from serum. Therefore, the ability of cells to adhere and the strength of adhesion are influenced by the production extracellular matrix and expression of cell adhesion molecules (CAM).

SaOS-2 cell adhesion was elevated on PAH, Ti and TiN190 thin films as shown in Figure 6.18b. This was expected as high surface roughness (Khang et al. 2008; Lincks et al. 1998; Schweikl et al. 2007) such as TiN190 thin film, hydrophilic surfaces (Chang et al. 2005; Krasteva et al. 2001; Lee et al. 1998) such as Ti thin films have been shown to increase cell adhesion.

It has been shown that cationic surfaces enhance extracellular matrix production, especially collagen I and III (De Rosa et al. 2004). In fact, Figure 6.17 and 6.19 confirm that collagen production was significant higher on PAH terminating surfaces. The enhanced extracellular matrix production would allow for increase adhesive interaction with CAM. However, the adhesion of the SaOS-2 cells did not reflect the magnitude of enhancement in collagen production. It was expected that with such increased levels of collagen production (approximately 4 times more than tissue culture plastic), the adhesion of SaOS-2 would be greatly enhanced, yet there was not a

significantly difference between PAH thin film and tissue culture plastic. In fact, as shown in Figure 6.18a the adhesion of the SaOS-2 on PAH terminating surfaces was only significantly greater than PSS terminating surfaces and not to control. That is, SaOS-2 cells adhesion on PAH terminating surfaces was not significantly enhanced compared to tissue culture plastic for the 3T3-L1 and HEK-293 cells.

For the 3T3-L1 and HEK-293 cells, adhesion was greatly facilitated on the PAH teminating thin films by an average of three and seven times compared to TCP and five and two times more compared to PSS terminating thin films. There were no significantly differences in SaOS-2 adhesion between PAH terminating thin films and control and only an average of 1.25 times more cells on PAH terminating thin films than PSS terminating thin films. It appears that the PAH terminating thin films only produce a slight enhancing effect on cell adhesion, whereas PSS terminating thin films have a slight inhibitory effect on this particular cell line. Those results illustrate that the effects of thin films are very much cell dependent.

There were instances where the increased production in extracellular matrix did not enhance cell adherence. For example, El-Amin et al (2003) found that for primary human osteoblastic cells, higher levels of fibronectin, collagen, laminin and osteonectin (at 12 hours) did not enhance the number of adhering cells. It has also been shown that the surface on which cells are grown on can alter the expression of some CAM (Cenni et al. 1997; Chung et al. 2003; Shur et al. 2005). Specifically for PEM, β1-integrin and phosphorylated Focal Adhesion Kinase (FAK) residue tyrosine 397 (pY397) expression by endothelial (HUVECS) cells was found to be lowered on PAH monolayer thin films and not on multi-layered thin films (Boura 2005). One might speculate that the reduced expression of these CAM would reduce the interaction with extracellular matrix, therefore leading to a reduction of cell adhesion. However, that speculation is contrary to the results of this thesis (see Figure 6.15 and 6.18b). Potentially, the expression of integrins may have been desensitised due to the abundance of extracellular matrix similar to the down-regulation of integrins on laminin-enriched substrates (Delcommenne & Streuli 1995). It has also been shown that adherent cells have lower integrin expression than cells kept under

nonadherent conditions (Chen et al. 1992). Therefore, a reduction in integrin expressions such as on PAH terminating thin films can still accommodate for strong cell adhesion provided that there is sufficient surface/matrix for interaction.

The lack of enhancement of SaOS-2 adhesion on PAH terminating thin films when collagen production was increased may be attributed to a reduced expression of CAMs. In fact, it has been shown that β1 integrin expression is lower for cells grown on extracellular matrix compared to cells grown on tissue culture plastic (Delcommenne & Streuli 1995), and specifically for osteoblastic cells MG-63 and SaOS-2 cells, integrin expression is lower for adhering cells then cells which are kept in suspension (Chen et al. 1992).

There can be different intracellular signalling pathways to induce adhesion of the cells to the surfaces. The HEK-293 cells adhered using calcium dependent pathways on PSS terminating surfaces (Figure 6.16b) and the same applies to the 3T3-L1 cells (Figure 6.16a) except on the thicker PEM (3-4 layers). That is, the cells use mostly CAM which are resistant to proteolytic degradation (trypsin) and calcium dependent. This is not to say that the HEK-293 cells on PAH terminating surfaces and 3T3-L1 cells on thick PEM do not use calcium dependent CAM, but there is likely to be a significant increase in the expression of calcium independent CAM which allowed the cells to adhere in the absence of extracellular calcium. Potentially, HEK-293 calcium dependent CAM expression is sensitive to the surface charge of the substrate where as 3T3-L1 is sensitive to surface roughness.

The use of different adhesion pathways and different levels of collagen production by the same cell line clearly indicate that the PE thin films have affected ECM production. Many studies have already shown the importance of cell-ECM interaction and the cascade of effects such interactions can have on cells. For example, different substratum or extracellular matrix can cause morphological changes (Carri et al. 1992; Kelley et al. 1987; Senoo & Hata 1994), changed in the actin organisation (Mooney, Langer & Ingber 1995; Nagaki et al. 1995; Toral et al. 2007), cell proliferation (de Jong-Hesse et al. 2005; Senoo & Hata 1994) and function (Nagaki et al. 1995; Toral et al. 2007).

6.3.7 Cell Differentiation

The level of osteoblast maturity or differentiation can be measured by the ability of the cells to make bones. There are several markers for bone formation as reviewed by Christenson (1997) and Duplomb and Dagouassat et al (2007), and these include Collagen Type I which comprise of 90% of the bone matrix, procollagen I (precursor of Collagen Type I), Alkaline phosphatise (ALP), osteocalcin, osteopontin, osteonectin. The ability of osteoblasts to mineralised the extracellular matrix can also be visualised by Von Kossa technique which stains for phosphate and carbonate, or by alizarin red staining of calcium in the mineralised nodules as reviewed by Puchtler, Meloan and Terry (1968).

As the morphology of the SaOS-2 cells on PAH terminating thin films resemble the less mature osteblast cell line MG-63, it was suspected that the level of ALP activity in the supernant of SaOS-2 cells may be reduced. Yet, as shown in Figure 6.20a there were no significantly differences between polyelectrolyte thin films, which suggest that SaOS-2 cells are similarly differentiated on these different polyelectrolyte thin films. However, it has been shown that the secreted ALP are often localised in the extracellular matrix (Bonucci, Silvestrini & Bianco 1992; de Bernard et al. 1986) therefore, not detectable in this assay. Also, ALP is released by osteoblasts into the supernatant in a cell cycle dependent manner (Fedarko et al. 1990), therefore, the reduce proliferation, G2 arrest and reduced proportion of SaOS-2 cells entering into S-phase of the cell cycle on PAH thin films may have affected the ALP activity detected in this study.

The von Kossa assay was used to visualise the mineralisation of matrices as another indication of SaOS-2 differentiation. As shown in Figure 6.21, the total mineralisation was only significantly lower on PAH thin films, but not necessarily for all PAH terminating thin films. Although it has been well established that the silver nitrate in the von Kossa assay binds to the phosphates in the calcium deposits (Puchtler & Meloan 1978), it has also been suggested that it alone is not sufficient as a mineralisation indicator as it can give false positives (Bonewald et al. 2003)

Interestingly, as shown in Figure 6.22a and b, the size and number of these mineralised nodules are drastically different between PSS and PAH terminating thin films. The sizes of the nodules are significantly larger on PAH terminating thin films, but the number of nodules was also significantly reduced, which is drastically different from what is usually reported for mineralisation of matrices, whereby the size of each nodule increases with the number of nodules (Bonewald et al. 2003; Nefussi et al. 1997; Puchtler & Meloan 1978).

Although these results do not conclusively show that the SaOS-2 cells are more or less matured/differentiated on different polyelectrolyte surfaces, its suggests that PAH monolayer thin film reduce the level of mineralisation and ALP activity of SaOS-2 cells, and it demonstrates that SaOS-2 cells mineralise its matrices differently on the different polyelectrolyte thin films. The results with Ti and TiN thin films were used to helps us understand how such differences comes about.

The von Kossa assay was not used with the Ti and TiN thin films, as these thin films are coloured and opaque, which means the parameters used for imaging the mineralised nodules cannot be consistent. The ALP activity of the supernatant was therefore measured and it showed that TiN190 thin films had significantly higher levels of ALP activity whilst TiN120 had the lowest. It was not surprising that SaOS-2 cells on TiN190 had the highest levels of ALP activity, as TiN190 is the roughest thin film in this study, and it had been shown that surface roughness can alter osteoblast cell gene expression (Harle et al. 2004), often enhancing osteogenic phenotypes such as osteonectin, osteopontin expressions in primary osteoblasts (Marinucci et al. 2006) and osteocalcin and ALP activity in immortal osteoblast cell lines (Lincks et al. 1998).

The initial attachment and adhesion of SaOS-2 cells on TiN120 was low but not significantly different from control. However, there were significantly lower levels of viability and proliferation, which suggest that the reduced ALP activity was most likely to be attributed to the lower levels of metabolic activity as illustrated in by Figure 6.7 where the ability of the cells to metabolically convert alamar blue is much lower on TiN120.

In conclusion, the differences in zeta potential and hydrophobicity of the PSS and PAH polyelectrolyte thin films have elicited different response from the 3T3-L1, HEK-293 and SaOS-2 cells. In general, it seems that the cationic nature of the PAH thin films have enhanced initial attachment and adhesion of all cell lines, probably due to enhanced protein adsorption and protein orientation and ECM production. However, the hydrophobic nature of PAH has reduced proliferation of all cell lines. However, these speculations should be further investigated to elucidate whether these effects were the results of different or the combination PE thin film attributes (zeta potential and wettability).

The SaOS-2 cells produce different levels and types of on different PE thin films, whilst PAH thin films elongated and altered the F-actin distribution of SaOS-2 cells and inhibited their proliferation. The data also demonstrated that hydrophilic thin films such as Ti can enhance the proliferation of SaOS-2 cells as well as initial attachment and adhesion despite having an opposite zeta potential and wettability to PAH terminating PEM. A rough surface such as TiN190 on the other hand, can enhance adhesion, proliferation and level of differentiation (by ALP activity) of SaOS-2 cells.

For the end application of a 3D contraction system composed with PE, my results in this chapter indicate that PAH is the preferred terminating layer, as it enhances cell adhesion and the F-actin distribution of the 3T3-L1 cells appears to resemble a cell which may be contractile.

6.4 References

Altankov, G., Grinnell, F. & Groth, T. 1996, 'Studies On The Biocompatibility Of Materials: Fibroblast Reorganization Of Substratum-Bound Fibronectin On Surfaces Varying In Wettability.' *Journal Of Biomedical Materials Research*, vol. 30, no. 3, pp. 385-391.

Antipov, A.A., Sukhorukov, G.B., Leporatti, S., Radtchenko, I.L., Donath, E. & Möhwald, H. 2002, 'Polyelectrolyte Multilayer Capsule Permeability Control', *Colloids And Surfaces A: Physicochemical And Engineering Aspects*, vol. 198-200, pp. 535-541.

Bacáková, L., Filová, E., Rypácek, F., Švorcík, V. & Starý, V. 2004, 'Cell Adhesion On Artificial Materials For Tissue Engineering.' *Physiological Research*, vol. 53, no. Supplement 1, pp. S35-S46.

Blomberg, E., Poptoshev, E. & Caruso, F. 2006, 'Surface Interactions During Polyelectrolyte Multilayer Build-Up. 2. The Effect Of Ionic Strength On The Structure Of Preformed Multilayers', *Langmuir*, vol. 22, no. 9, pp. 4153-4157.

Bonewald, L.F., Harris, S.E., Rosser, J., Dallas, M.R., Dallas, S.L., Camacho, N.P., Boyan, B. & Boskey, A. 2003, 'Von Kossa Staining Alone Is not Sufficient To Confirm That Mineralization In Vitro Represents Bone Formation', *Calcified Tissue International*, vol. 72, no. 5, pp. 537-547.

Bonucci, E., Silvestrini, G. & Bianco, P. 1992, 'Extracellular Alkaline Phosphatase Activity In Mineralizing Matrices Of Cartilage And Bone: Ultrastructural Localization Using A Cerium-Based Method', *Histochemistry And Cell Biology*, vol. 97, no. 4, pp. 323-327.

Boura, C., Kerdjoudj, H., Moby, V., Vautier, D., Dumas, D., Schaaf, P., Voegel, J.C., Stoltz, J.F. & Menu, P. 2006, 'Initial Adhesion Of Endothelial Cells On Polyelectrolyte Multilayer Films', *Bio-Medical Materials And Engineering*, vol. 16, no. Supplment 4, pp. S115 - S121.

Boura, C., Menu, P., Payan, E., Picart, C., Voegel, J.C., Muller, S. & Stoltz, J.F. 2003, 'Endothelial Cells Grown On Thin Polyelectrolyte Mutlilayered Films: An Evaluation Of A New Versatile Surface Modification', *Biomaterials*, vol. 24, no. 20, pp. 3521-3530.

Boura, C., Muller, S., Voegel, J., Schaaf, P., Stoltz, J. & Menu, P. 2005, 'Behaviour Of Endothelial Cells Seeded On Thin Polyelectrolyte Multilayered Films: A New Biological Scaffold', *Clinical Hemorheoloy And Microcirculation*, vol. 33, no. 3, pp. 269-275.

Cai, K., Bossert, J. & Jandt, K.D. 2006, 'Does The Nanometre Scale Topography Of Titanium Influence Protein Adsorption And Cell Proliferation?' *Colloids And Surfaces B: Biointerfaces*, vol. 49, no. 2, pp. 136-144.

Cai, K., Frant, M., Bossert, J., Hildebrand, G., Liefeith, K. & Jandt, K.D. 2006, 'Surface Functionalized Titanium Thin Films: Zeta-Potential, Protein Adsorption And Cell Proliferation', *Colloids And Surfaces B: Biointerfaces*, vol. 50, no. 1, pp. 1-8.

Cai, K., Müller, M., Bossert, J., Rechtenbach, A. & Jandt, K.D. 2005, 'Surface Structure And Composition Of Flat Titanium Thin Films As A Function Of Film Thickness And Evaporation Rate', *Applied Surface Science*, vol. 250, no. 1-4, pp. 252-267.

Camp, J.P. & Capitano, A.T. 2005, 'Size-Dependent Mobile Surface Charge Model Of Cell Electrophoresis', *Biophysical Chemistry*, vol. 113, no. 2, pp. 115-122.

Carri, N.G., Rubin, K., Gullberg, D. & Ebendal, T. 1992, 'Neuritogenesis On Collagen Substrates. Involvement Of Integrin-Like Matrix Receptors In Retinal Fibre Outgrowth On Collagen', *International Journal Of Developmental Neuroscience*, vol. 10, no. 5, pp. 393-405.

Carrillo, J.Y. & Dobrynin, A.V. 2007, 'Molecular Dynamics Simulations Of Polyelectrolyte Adsorption', *Langmuir*, vol. 23, no. 5, pp. 2472-2482.

Cenni, E., Granchi, D., Ciapetti, G., Verri, E., Cavedagna, D., Gamberini, S., Cervellati, M., Di Leo, A. & Pizzoferrato, A. 1997, 'Expression Of Adhesion Molecules On Endothelial Cells After Contact With Knitted Dacron', *Biomaterials*, vol. 18, no. 6, pp. 489-494.

Chang, E.-J., Kim, H.-H., Huh, J.-E., Kim, I.-A., Seung Ko, J., Chung, C.-P. & Kim, H.-M. 2005, 'Low Proliferation And High Apoptosis Of Osteoblastic Cells On Hydrophobic Surface Are Associated With Defective Ras Signaling', *Experimental Cell Research*, vol. 303, no. 1, pp. 197-206.

Chen, D., Magnuson, V., Hill, S., Arnaud, C., Steffensen, B. & Klebe, R. 1992, 'Regulation Of Integrin Gene Expression By Substrate Adherence', *Journal Of Biological Chemistry*, vol. 267, no. 33, pp. 23502-23506.

Chien, C., Liu, K., Duh, J., Chang, K. & Chung, K. 2008, 'Effect Of Nitride Film Coatings On Cell Compatibility', *Dental Materials*, vol. 24, no. 7, pp. 986-993.

Choee, J.-H., Lee, S.J., Lee, Y.M., Rhee, J.M., Lee, H.B. & Khang, G. 2004, 'Proliferation Rate Of Fibroblast Cells On Polyethylene Surfaces With Wettability Gradient', *Journal Of Applied Polymer Science*, vol. 92, no. 1, pp. 599-606.

Christenson, R. 1997, 'Biochemical Markers Of Bone Metabolism: An Overview', *Clinical Biochemistry*, vol. 1997, no. 30, P. 8.

Chung, T.-W., Liu, D.-Z., Wang, S.-Y. & Wang, S.-S. 2003, 'Enhancement Of The Growth Of Human Endothelial Cells By Surface Roughness At Nanometer Scale', *Biomaterials*, vol. 24, no. 25, pp. 4655-4661.

De Bernard, B., Bianco, P., Bonucci, E., Costantini, M., Lunazzi, G., Martinuzzi, P., Modricky, C., Moro, L., Panfili, E. & Pollesello, P. 1986, 'Biochemical And Immunohistochemical Evidence That In Cartilage An Alkaline Phosphatase Is A Ca2+-Binding Glycoprotein
10.1083/Jcb.103.4.1615', *Journal Of Cell Biology*, vol. 103, no. 4, pp. 1615-1623.

De Jong-Hesse, Y., Kampmeier, J., Lang, G.K. & Lang, G.E. 2005, 'Effect Of Extracellular Matrix On Proliferation And Differentiation Of Porcine Lens Epithelial Cells', *Graefe's Archive For Clinical And Experimental Ophthalmology*, vol. 243, no. 7, pp. 695-700.

De Rosa, M., Carteni, M., Petillo, O., Calarco, A., Margarucci, S., Rosso, F., De Rosa, A., Farina, E., Grippo, P. & Peluso, G. 2004, 'Cationic Polyelectrolyte Hydrogel Fosters Fibroblast Spreading, Proliferation, And Extracellular Matrix Production: Implications For Tissue Engineering', *Journal Of Cellular Physiology*, vol. 198, no. 1, pp. 133-143.

Degasne, I., Basle, M.F., Demais, V., Hure, G., Lesourd, M., Grolleau, B., Mercier, L. & Chappard, D. 1999, 'Effects Of Roughness, Fibronectin And Vitronectin On Attachment, Spreading, And Proliferation Of Human Osteoblast-Like Cells (Saos-2) On Titanium Surfaces', *Calcified Tissue International*, vol. 64, no. 6, pp. 499-507.

Delcommenne, M. & Streuli, C.H. 1995, 'Control Of Integrin Expression By Extracellular Matrix', *Journal Of Biological Chemisty*, vol. 270, no. 45, pp. 26794-26801.

Delgado, A.V., González-Caballero, F., Hunter, R.J., Koopal, L.K. & Lyklema, J. 2007, 'Measurement And Interpretation Of Electrokinetic Phenomena', *Journal Of Colloid And Interface Science, Elkin 06, International Electrokinetics Conference, June 25-29, Nancy, France*, vol. 309, no. 2, pp. 194-224.

Dengler, W., Schulte, J., Berger, D., Mertelsmann, R. & Fiebig, H. 1995, 'Development Of A Propidium Iodide Fluorescence Assay For Proliferation And Cytotoxicity Assays', *Anti-Cancer Drugs*, vol. 6, pp. 552-532.

Dion, I., Baquey, C., Candelon, B. & Monties, J. 1995, 'Hemocompatibility Of Titanium Nitride', *International Journal Of Artificial Organs*, vol. 15, no. 10, pp. 617-621.

Dion, I., Rouais, F., Trut, L., Baquey, C., Monties, J. & Havlik, P. 1993, 'Tin Coating: Surface Characterization And Haemocompatibility.' *Biomaterials*, vol. 14, no. 3, pp. 169-176.

Dolatshahi-Pirouz, A., Rechendorff, K., Hovgaard, M.B., Foss, M., Chevallier, J. & Besenbacher, F. 2008, 'Bovine Serum Albumin Adsorption On Nano-Rough Platinum Surfaces Studied By QCM-D', *Colloids And Surfaces B: Biointerfaces*, vol. 66, no. 1, pp. 53-59.

Dubas, S.T. & Schlenoff, J.B. 2001, 'Swelling And Smoothing Of Polyelectrolyte Multilayers By Salt', *Langmuir*, vol. 17, no. 25, pp. 7725-7727.

Duplomb, L., Dagouassat, M., Jourdon, P. & Heymann, D. 2007, 'Concise Review: Embryonic Stem Cells: A New Tool To Study Osteoblast And Osteoclast Differentiation', *Stem Cells*, vol. 25, no. 3, pp. 544-552.

El-Amin, S.F., Lu, H.H., Khan, Y., Burems, J., Mitchell, J., Tuan, R.S. & Laurencin, C.T. 2003, 'Extracellular Matrix Production By Human Osteoblasts Cultured On Biodegradable Polymers Applicable For Tissue Engineering', *Biomaterials*, vol. 24, no. 7, pp. 1213-1221.

Elzbieciak, M., Kolasinska, M. & Warszynski, P. 2008, 'Characteristics Of Polyelectrolyte Multilayers: The Effect Of Polyion Charge On Thickness And Wetting Properties', *Colloids And Surfaces A: Physicochemical And Engineering Aspects Organized Molecular Films Selected Papers From LB12 - The 12th International Conference On Organized Molecular Films, July 1-5, 2007, Krakow, Poland*, vol. 321, no. 1-3, pp. 258-261.

Fan, Y.W., Cui, F.Z., Hou, S.P., Xu, Q.Y., Chen, L.N. & Lee, I.-S. 2002, 'Culture Of Neural Cells On Silicon Wafers With Nano-Scale Surface Topograph', *Journal Of Neuroscience Methods*, vol. 120, no. 1, pp. 17-23.

Fedarko, N., Bianco, P., Vetter, U. & Robey, P.G. 1990, 'Human Bone Cell Enzyme Expression And Cellular Heterogeneity: Correlation Of Alkaline Phosphatase Enzyme Activity With Cell Cycle', *Journal Of Cellular Physiology*, vol. 144, no. 1, pp. 115-121.

Finke, B., Luethen, F., Schroeder, K., Mueller, P.D., Bergemann, C., Frant, M., Ohl, A. & Nebe, B.J. 2007, 'The Effect Of Positively Charged Plasma Polymerization On Initial Osteoblastic Focal Adhesion On Titanium Surfaces', *Biomaterials*, vol. 28, no. 30, pp. 4521-4534.

Fuse, Y., Hirata, I., Kurihara, H. & Okazaki, M. 2007, 'Cell Adhesion And Proliferation Patterns On Mixed Self-Assembled Monolayers Carrying Various Ratios Of Hydroxyl And Methyl Groups', *Dental Materials Journal*, vol. 26, no. 6, pp. 814-819.

Georgieva, R., Moya, S., Donath, E. & Baumler, H. 2004, 'Permeability And Conductivity Of Red Blood Cell Templated Polyelectrolyte Capsules Coated With Supplementary Layers', *Langmuir*, vol. 20, no. 5, pp. 1895-1900.

Gergely, C., Bahi, S., Szalontai, B., Flores, H., Schaaf, P., Voegel, J.-C. & Cuisinier, F.J.G. 2004, 'Human Serum Albumin Self-Assembly On Weak Polyelectrolyte Multilayer Films Structurally Modified By Ph Changes', *Langmuir*, vol. 20, no. 13, pp. 5575-5582.

Gong, H., Garcia-Turiel, J., Vasilev, K. & Vinogradova, O.I. 2005, 'Interaction And Adhesion Properties Of Polyelectrolyte Multilayers', *Langmuir*, vol. 21, no. 16, pp. 7545-7550.

Gopinadhan, M., Ivanova, O., Ahrens, H., Gunther, J.-U., Steitz, R. & Helm, C.A. 2007, 'The Influence Of Secondary Interactions During The Formation Of Polyelectrolyte Multilayers: Layer Thickness, Bound Water And Layer Interpenetration', *Journal Of Physical Chemistry B*, vol. 111, no. 29, pp. 8426 -8843.

Grinnell, F. & Feld, M. 1982, 'Fibronectin Adsorption On Hydrophilic And Hydrophobic Surfaces Detected By Antibody Binding And Analyzed During Cell Adhesion In Serum-Containing Medium', *Journal Of Biological Chemistry*, vol. 257, no. 9, pp. 4888-4893.

Grinnell, F. & Feld, M.K. 1981, 'Adsorption Characteristics Of Plasma Fibronectin In Relationship To Biological Activity', *Journal Of Biomedical Materials Research*, vol. 15, no. 3, pp. 363-381.

Groth, T. & Altankov, G. 1996, 'Fibroblast Spreading And Proliferation On Hydrophilic And Hydrophobic Surfaces Is Related To Tyrosine Phosphorylation In Focal Contacts', *Journal Of Biomaterials Science, Polymer Edition*, vol. 7, pp. 297-305.

Gu, Y. & Li, D. 2000, 'The Zeta-Potential Of Glass Surface In Contact With Aqueous Solutions', *Journal Of Colloid And Interface Science*, vol. 226, no. 2, pp. 328-339.

Halthur, T.J., Claesson, P.M. & Elofsson, U.M. 2004, 'Stability Of Polypeptide Multilayers As Studied By In Situ Ellipsometry: Effects Of Drying And Post-Buildup Changes In Temperature And Ph', *Journal Of American Society*, vol. 126, no. 51, pp. 17009-17015.

Harle, J., Salih, V., Olsen, I., Brett, P., Jones, F. & Tonetti, M. 2004, 'Gene Expression Profiling Of Bone Cells On Smooth And Rough Titanium Surfaces', *Journal Of Materials Science: Materials In Medicine*, vol. 15, no. 11, pp. 1255-1258.

Harris, L., Patterson, L., Bacon, C., Gwynn, I. & Richards, R. 2005, 'Assessment Of The Cytocompatibility Of Different Coated Titanium Surfaces To Fibroblasts And Osteoblasts', *Journal Of Biomedical Materials Research Part A*, vol. 73A, no. 1, pp. 12-20.

Heuvingh, J., Zappa, M. & Fery, A. 2005, 'Salt Softening Of Polyelectrolyte Multilayer Capsules', *Langmuir*, vol. 21, no. 7, pp. 3165-3171.

Horbett, T.A. 1993, 'Chapter 13 Principles Underlying The Role Of Adsorbed Plasma Proteins In Blood Interactions With Foreign Materials', *Cardiovascular Pathology*, vol. 2, no. 3, Supplement 1, pp. 137-148.

Horbett, T.A. 1994, 'The Role Of Adsorbed Proteins In Animal Cell Adhesion', *Colloids And Surfaces B: Biointerfaces*, vol. 2, no. 1-3, pp. 225-240.

Jäger, M., Zilkens, C., Zanger, K. & Krauspe, R. 2007, 'Significance Of Nano- And Microtopography For Cell-Surface Interactions In Orthopaedic Implants.' *Journal Of Biomedicine And Biotechnology*, vol. 2007, no. 8, pp. 9036-9055.

Jansson, E. & Tengvall, P. 2004, 'Adsorption Of Albumin And Igg To Porous And Smooth Titanium', *Colloids And Surfaces B: Biointerfaces*, vol. 35, no. 1, pp. 45-51.

Kelley, C., D'Amore, P., Hechtman, H. & Shepro, D. 1987, 'Microvascular Pericyte Contractility In Vitro: Comparison With Other Cells Of The Vascular Wall', *Journal Of Cell Biology*, vol. 104, pp. 483-490.

Khang, D., Lu, J., Yao, C., Haberstroh, K.M. & Webster, T.J. 2008, 'The Role Of Nanometer And Sub-Micron Surface Features On Vascular And Bone Cell Adhesion On Titanium', *Biomaterials*, vol. 29, no. 8, pp. 970-983.

Kim, S.H., Ha, H.J., Ko, Y.K., Yoon, S.J., Rhee, J.M., Kim, M.S., Lee, H.B. & Khang, G. 2007, 'Correlation Of Proliferation, Morphology And Biological Responses Of Fibroblasts On LDPE With Different Surface Wettability', *Journal Of Biomaterials Science, Polymer Edition*, vol. 18, pp. 609-622.

Kirkpatrick, C., Bittinger, F., Wagner, M., Kohler, H., Van Kooten, T., Klein, C. & Otto, M. 1998, 'Review Paper:Current Trends In Biocompatibility Testing', *Proceedings Of The I MECH E Part H Journal Of Engineering In Medicine*, vol. 212, pp. 75-84.

Kishida, A., Iwata, H., Tamada, Y. & Ikada, Y. 1991, 'Cell Behaviour On Polymer Surfaces Grafted With non-Ionic And Ionic Monomers', *Biomaterials*, vol. 12, no. 8, pp. 786-792.

Kolasinska, M., Krastev, R. & Warszynski, P. 2007, 'Characteristics Of Polyelectrolyte Multilayers: Effect Of PEI Anchoring Layer And Posttreatment After Deposition', *Journal Of Colloid And Interface Science*, vol. 305, no. 1, pp. 46-56.

Kolasinska, M. & Warszynski, P. 2005, 'The Effect Of Support Material And Conditioning On Wettability Of PAH/PSS Multilayer Films', *Bioelectrochemistry Proceedings Of The International Workshop On Surface Modification For Chemical And Biochemical Sensing, SMCBS'2003*, vol. 66, no. 1-2, pp. 65-70.

Krasteva, N., Groth, T., Fey-Lamprecht, F. & Altankov, G. 2001, 'The Role Of Surface Wettability On Hepatocyte Adhesive Interactions And Function.' *Journal Of Biomaterials Science -- Polymer Edition*, vol. 12, no. 6, pp. 613-627.

Kunzler, T.P., Drobek, T., Schuler, M. & Spencer, N.D. 2007, 'Systematic Study Of Osteoblast And Fibroblast Response To Roughness By Means Of Surface-Morphology Gradients', *Biomaterials*, vol. 28, no. 13, pp. 2175-2182.

Ladam, G., Gergely, C., Senger, B., Decher, G., Voegel, J., Schaaf, P. & Cuisinier, F. 2000, 'Protein Interactions With Polyelectrolyte Multilayers: Interactions Between Human Serum Albumin And Polystyrene Sulfonate/Polyallylamine Multilayers.' *Biomacromolecules*, vol. 1, no. 4, pp. 674-687.

Ladam, G., Schaaf, P., Cuisinier, F.J.G., Decher, G. & Voegel, J.-C. 2001, 'Protein Adsorption Onto Auto-Assembled Polyelectrolyte Films', *Langmuir*, vol. 17, no. 3, pp. 878-882.

Ladam, G., Schaaf, P., Decher, G., Voegel, J.-C. & Cuisinier, F.J.G. 2002, 'Protein Adsorption Onto Auto-Assembled Polyelectrolyte Films', *Biomolecular Engineering*, vol. 19, no. 2-6, pp. 273-280.

Lautenschlager, E. & Monaghan, P. 1993, 'Titanium And Titanium Alloys As Dental Materials.' *International Dental Journal*, vol. 43, no. 3, pp. 243-253.

Lebedeva, O.V., Kim, B.-S., Vasilev, K. & Vinogradova, O.I. 2005, 'Salt Softening Of Polyelectrolyte Multilayer Microcapsules', *Journal Of Colloid And Interface Science*, vol. 284, no. 2, pp. 455-462.

Lee, J.H., Khang, G., Lee, J.W. & Lee, H.B. 1998, 'Interaction Of Different Types Of Cells On Polymer Surfaces With Wettability Gradient', *Journal Of Colloid And Interface Science*, vol. 205, no. 2, pp. 323-330.

Lee, J.H., Lee, S.J., Khang, G. & Lee, H.B. 2000, 'The Effect Of Fluid Shear Stress On Endothelial Cell Adhesiveness To Polymer Surfaces With Wettability Gradient', *Journal Of Colloid And Interface Science*, vol. 230, no. 1, pp. 84-90.

Lee, S.J., Khang, G., Lee, Y.M. & Lee, H.B. 2003, 'The Effect Of Surface Wettability On Induction And Growth Of Neurites From The PC-12 Cell On A Polymer Surface', *Journal Of Colloid And Interface Science*, vol. 259, no. 2, pp. 228-235.

Lim, Y., Oshida, Y., Andres, C. & Barco, M. 2001, 'Surface Characterizations Of Variously Treated Titanium Materials', *International Journal Of Oral Maxillofacial Implants*, vol. 16, no. 3, pp. 333–342.

Lim, Y.J. & Oshida, Y. 2001, 'Initial Contact Angle Measurements On Variously Treated Dental/Medical Titanium Materials.' *Bio-Medical Materials & Engineering*, vol. 11, no. 4, P. 325.

Lin, Y., Wang, L., Zhang, P., Wang, X., Chen, X., Jing, X. & Su, Z. 2006, 'Surface Modification Of Poly(L-Lactic Acid) To Improve Its Cytocompatibility Via Assembly Of Polyelectrolytes And Gelatin', *Acta Biomaterialia*, vol. 2, no. 2, pp. 155-164.

Lincks, J., Boyan, B.D., Blanchard, C.R., Lohmann, C.H., Liu, Y., Cochran, D.L., Dean, D.D. & Schwartz, Z. 1998, 'Response Of MG63 Osteoblast-Like Cells To Titanium And Titanium Alloy Is Dependent On Surface Roughness And Composition', *Biomaterials*, vol. 19, no. 23, pp. 2219-2232.

Lindon, J., Mcmanama, G., Kushner, L., Merrill, E. & Salzman, E. 1986, 'Does The Conformation Of Adsorbed Fibrinogen Dictate Platelet Interactions With Artificial Surfaces?' *Blood*, vol. 68, no. 2, pp. 355-362.

Lipski, A., Pino, C., Haselton, F., Chen, I. & Shastri, V. 2008, 'The Effect Of Silica Nanoparticle-Modified Surfaces On Cell Morphology, Cytoskeletal Organization And Function.' *Biomaterials*, vol. 29, no. 28, pp. 3836-3846.

Lowman, G.M. & Buratto, S.K. 2002, 'Nanoscale Morphology Of Polyelectrolyte Self-Assembled Films Probed By Scanning Force And Near-Field Scanning Optical Microscopy', *Thin Solid Films*, vol. 405, no. 1-2, pp. 135-140.

Marinucci, L., Balloni, S., Becchetti, E., Belcastro, S., Guerra, M., Calvitti, M., Lilli, C., Calvi, E.M. & Locci, P. 2006, 'Effect Of Titanium Surface Roughness On Human Osteoblast Proliferation And Gene Expression In Vitro', *International Journal Of Oral Maxillofacial Implants*, vol. 21, no. 5, pp. 719-725.

Mezger, P.R. & Creugers, N.H.J. 1992, 'Titanium Nitride Coatings In Clinical Dentistry', *Journal Of Dentistry*, vol. 20, no. 6, pp. 342-344.

Mhamdi, L., Picart, C., Lagneau, C., Othmane, A., Grosgogeat, B., Jaffrezic-Renault, N. & Ponsonnet, L. 2006a, 'Study Of The Polyelectrolyte Multilayer Thin Films' Properties And Correlation With The Behavior Of The Human Gingival Fibroblasts', *Materials Science And Engineering: C*, vol. 26, no. 2-3, pp. 273-281.

Mhamdi, L., Picart, C., Lagneau, C., Othmane, A., Grosgogeat, B., Jaffrezic-Renault, N. & Ponsonnet, L. 2006b, 'Study Of The Polyelectrolyte Multilayer Thin Films' Properties And Correlation With The Behavior Of The Human Gingival Fibroblasts', *Materials Science And Engineering: C*, vol. 26, no. 2-3, pp. 273-281

Milkova, V. & Radeva, T. 2007, 'Effect Of Chain Length And Charge Density On The Construction Of Polyelectrolyte Multilayers On Colloidal Particles', *Journal Of Colloid And Interface Science*, vol. 308, no. 2, pp. 300-308.

Mooney, D., Langer, R. & Ingber, D. 1995, 'Cytoskeletal Filament Assembly And The Control Of Cell Spreading And Function By Extracellular Matrix', *Journal Of Cell Science*, vol. 108, no. 6, pp. 2311-2320.

Nagaki, M., Shidoji, Y., Yamada, Y., Sugiyama, A., Tanaka, M., Akaike, T., Ohnishi, H., Moriwaki, H. & Muto, Y. 1995, 'Regulation Of Hepatic Genes And Liver Transcription Factors In Rat Hepatocytes By Extracellular Matrix', *Biochemical And Biophysical Research Communications*, vol. 210, no. 1, pp. 38-43.

Nebea, B., Finkeb, B., Lüthena, F., Bergemanna, C., Schröderb, K., Rychlya, J., Liefeithc, K. & Ohlb, A. 2007, 'Improved Initial Osteoblast Functions On Amino-Functionalized Titanium Surfaces', *Biomolecular Engineering*, vol. 24, no. 5, pp. 447-454.

Nefussi, J., Ollivier, A., Oboeuf, M. & Forest, N. 1997, 'Rapid nodule Evaluation Computer-Aided Image Analysis Procedure For Bone nodule Quantification', *Bone*, vol. 20, no. 1, pp. 5-16.

Neu, B., Voigt, A., Mitlöhner, R., Leporatti, S., Gao, C., Donath, E., Kiesewetter, H., Möhwald, H., Meiselman, H. & Bäumler, H. 2001, 'Biological Cells As Templates For Hollow Microcapsules.' *Journal Of Microencapsulation*, vol. 18, no. 3, pp. 385-395.

Ngankam, A.P., Mao, G. & Vantassel, P.R. 2004, 'Fibronectin Adsorption Onto Polyelectrolyte Multilayer Films', *Langmuir*, vol. 20, no. 8, pp. 3362-3370.

Nieminen, A.-L., Gores, G.J., Bond, J.M., Imberti, R., Herman, B. & Lemasters, J.J. 1992, 'A novel Cytotoxicity Screening Assay Using A Multiwell Fluorescence Scanner', *Toxicology And Applied Pharmacology*, vol. 115, no. 2, pp. 147-155.

Petra Tryoen-Tóth, D.V., Youssef Haikel, Jean-Claude Voegel, Pierre Schaaf, Johanna Chluba, Joëlle Ogier, 2002, 'Viability, Adhesion, And Bone Phenotype Of Osteoblast-Like Cells On Polyelectrolyte Multilayer Films', *Journal Of Biomedical Materials Research*, vol. 60, no. 4, pp. 657-667.

Pizzoferrato, A., Ciapetti, G., Stea, S., Cenni, E., Arciola, C.R., Granchi, D. & Lucia 1994, 'Cell Culture Methods For Testing Biocompatibility', *Clinical Materials*, vol. 15, no. 3, pp. 173-180.

Ponsonnet, L., Reybier, K., Jaffrezic, N., Comte, V., Lagneau, C., Lissac, M. & Martelet, C. 2003, 'Relationship Between Surface Properties (Roughness, Wettability) Of Titanium And Titanium Alloys And Cell Behaviour', *Materials Science And Engineering: C*, vol. 23, no. 4, pp. 551-560.

Puchtler, H., Meloan, S. & Terry, M. 1968, 'On The History And Mechanism Of Alizarin And Alizarin Red S Stains For Calcium', *Journal Of Histochmistry And Cytochemistry*, vol. 17, no. 2, pp. 110-124.

Puchtler, H. & Meloan, S.N. 1978, 'Demonstration Of Phosphates In Calcium Deposits: A Modification Of Von Kossa's Reaction', *Histochemistry And Cell Biology*, vol. 56, no. 3, pp. 177-185.

Rechendorff, K., Hovgaard, M.B., Foss, M., Zhdanov, V.P. & Besenbacher, F. 2006, 'Enhancement Of Protein Adsorption Induced By Surface Roughness', *Langmuir*, vol. 22, no. 26, pp. 10885-10888.

Richert, L., Lavalle, P., Vautier, D., Senger, B., Stoltz, J.-F., Schaaf, P., Voegel, J.-C. & Picart, C. 2002, 'Cell Interactions With Polyelectrolyte Multilayer Films', *Biomacromolecules*, vol. 3, no. 6, pp. 1170-1178.

Ruardy, T.G., Moorlag, H.E., Schakenraad, J.M., Van Der Mei, H.C. & Busscher, H.J. 1997, 'Growth Of Fibroblasts And Endothelial Cells On Wettability Gradient Surfaces', *Journal Of Colloid And Interface Science*, vol. 188, no. 1, pp. 209-217.

Rupp, F., Scheideler, L., Rehbein, D., Axmann, D. & Geis-Gerstorfer, J. 2004, 'Roughness Induced Dynamic Changes Of Wettability Of Acid Etched Titanium Implant Modifications', *Biomaterials*, vol. 25, no. 7-8, pp. 1429-1438.

Sadana, A. 1992, 'Protein Adsorption And Inactivation On Surfaces. Influence Of Heterogeneities', *Chem. Rev.*, vol. 92, no. 8, pp. 1799-1818.

Salido, M., Vilches, J., Gutiérrez, J. & Vilches, J. 2007, 'Actin Cytoskeletal Organization In Human Osteoblasts Grown On Different Dental Titanium Implant Surfaces.' *Histology And Histopathology*, vol. 22, no. 12, pp. 1355-1364.

Schweikl, H., Muller, R., Englert, C., Hiller, K.-A., Kujat, R., Nerlich, M. & Schmalz, G. 2007, 'Proliferation Of Osteoblasts And Fibroblasts On Model Surfaces Of Varying Roughness And Surface Chemistry', *Journal Of Materials Science: Materials In Medicine*, vol. 18, no. 10, pp. 1895-1905.

Schweitzer, J., Zemmel, N., Drake, D., Morgan, R., Bill, T. & Edlich, R. 1995, 'New Instruments, Bone Liners, And Tray For Finger Joint Arthroplasty', *Journal Of Long Term Effects Of Medical Implants*, vol. 5, no. 2, pp. 147-153.

Senoo, H. & Hata, R. 1994, 'Extracellular Matrix Regulates And L-Ascorbic Acid 2-Phosphate Further Modulates Morphology, Proliferation, And Collagen Synthesis Of Perisinusoidal Stellate Cells', *Biochemical And Biophysical Research Communications*, vol. 200, no. 2, pp. 999-1006.

Shur, I., Zilberman, M., Benayahu, D. & Einav, S. 2005, 'Adhesion Molecule Expression By Osteogenic Cells Cultured On Various Biodegradable Scaffolds', *Journal Of Biomedical Materials Research Part A*, vol. 75A, no. 4, pp. 870-876.

Sniadecki, N., Desai, R., Ruiz, S. & Chen, C. 2006, 'Nanotechnology For Cell-Substrate Interactions', *Annals Of Biomedical Engineering*, vol. 34, no. 1, pp. 59-74.

Steele, J.G., Dalton, B.A., Johnson, G. & Underwood, P.A. 1995, 'Adsorption Of Fibronectin And Vitronectin Onto Primaria(TM) And Tissue Culture Polystyrene And Relationship To The Mechanism Of Initial Attachment Of Human Vein Endothelial Cells And BHK-21 Fibroblasts', *Biomaterials*, vol. 16, no. 14, pp. 1057-1067.

Steele, J.G., Johnson, G., Mcfarland, C., Dalton, B.A., Gengenbach, T.R., Chatelier, R.C., Underwood, P.A. & Griesser, H.J. 2005, 'Roles Of Serum Vitronectin And Fibronectin In Initial Attachment Of Human Vein Endothelial Cells And Dermal Fibroblasts On Oxygen- And Nitrogen-Containing Surfaces Made By Radiofrequency Plasmas', *Journal Of Biomaterials Science, Polymer Edition*, vol. 6, pp. 511-532.

Sze, A., Erickson, D., Ren, L. & Li, D. 2003, 'Zeta-Potential Measurement Using The Smoluchowski Equation And The Slope Of The Current-Time Relationship In Electroosmotic Flow', *Journal Of Colloid And Interface Science*, vol. 261, no. 2, pp. 402-410.

Thiery, J.P. 2003, 'Cell Adhesion In Development: A Complex Signaling Network', *Current Opinion In Genetics & Development*, vol. 13, no. 4, pp. 365-371.

Thomas, C.H., Mcfarland, C.D., Jenkins, M.L., Rezania, A., Steele, J.G. & Healy, K.E. 1997, 'The Role Of Vitronectin In The Attachment And Spatial Distribution Of Bone-Derived Cells On Materials With Patterned Surface Chemistry', *Journal Of Biomedical Materials Research*, vol. 37, no. 1, pp. 81-93.

Tjipto, E., Quinn, J.F. & Caruso, F. 2005, 'Assembly Of Multilayer Films From Polyelectrolytes Containing Weak And Strong Acid Moieties', *Langmuir*, vol. 21, no. 19, pp. 8785-8792.

Toral, C., Mendoza-Garrido, M.E., Azorín, E., Hernández-Gallegos, E., Gomora, J.C., Delgadillo, D.M., Solano-Agama, C. & Camacho, J. 2007, 'Effect Of Extracellular Matrix On Adhesion, Viability, Actin Cytoskeleton And K^+ Currents Of Cells Expressing Human Ether À Go-Go Channels', *Life Sciences*, vol. 81, no. 3, pp. 255-265.

Tryoen-Tóth, P., Vautier, D., Haikel, Y., Voegel, J.-C., Schaaf, P., Chluba, J. & Ogier, J. 2002, 'Viability, Adhesion, And Bone Phenotype Of Osteoblast-Like Cells On Polyelectrolyte Multilayer Films', *Journal Of Biomedical Materials Research*, vol. 60, no. 4, pp. 657-667.

Tullberg-Reinert, H. & Jundt, G. 1999, 'In Situ Measurement Of Collagen Synthesis By Human Bone Cells With A Sirius Red-Based Colorimetric Microassay: Effects Of Transforming Growth Factor ÃŸ2 And Ascorbic Acid 2-Phosphate', *Histochemistry And Cell Biology*, vol. 112, no. 4, pp. 271-276.

Ulusoy, U. & Yekeler, M. 2005, 'Correlation Of The Surface Roughness Of Some Industrial Minerals With Their Wettability Parameters', *Chemical Engineering And Processing*, vol. 44, no. 5, pp. 555-563.

Vautier, D., Karsten, V., Egles, C., Chluba, J., Schaaf, P., Voegel, J.-C. & Ogier, J. 2002, 'Polyelectrolyte Multilayer Films Modulate Cytoskeletal Organization In Chondrosarcoma Cells', *Journal Of Biomaterials Science, Polymer Edition*, vol. 13, pp. 712-731.

Vodouhe, C., Schmittbuhl, M., Boulmedais, F., Bagnard, D., Vautier, D., Schaaf, P., Egles, C., Voegel, J.-C. & Ogier, J. 2005, 'Effect Of Functionalization Of Multilayered Polyelectrolyte Films On Motoneuron Growth', *Biomaterials*, vol. 26, no. 5, pp. 545-554.

Vodouhê, C., Schmittbuhl, M., Boulmedais, F., Bagnard, D., Vautier, D., Schaaf, P., Egles, C., Voegel, J.-C. & Ogier, J. 2005, 'Effect Of Functionalization Of Multilayered Polyelectrolyte Films On Motoneuron Growth', *Biomaterials*, vol. 26, no. 5, pp. 545-554.

Wahlgren, M. & Arnebrant, T. 1991, 'Protein Adsorption To Solid Surfaces', *Trends In Biotechnology*, vol. 9, no. 1, pp. 201-208.

Wei, J., Yoshinari, M., Takemoto, S., Hattori, M., Kawada, E., Liu, B. & Oda, Y. 2007, 'Adhesion Of Mouse Fibroblasts On Hexamethyldisiloxane Surfaces With Wide Range Of Wettability', *Journal Of Biomedical Materials Research Part B: Applied Biomaterials*, vol. 81B, no. 1, pp. 66-75.

Welin-Klintström, S., Askendal, A. & Elwing, H. 1993, 'Surfactant And Protein Interactions On Wettability Gradient Surfaces', *Journal Of Colloid And Interface Science*, vol. 158, no. 1, pp. 188-194.

Wittmer, C.R., Phelps, J.A., Saltzman, W.M. & Van Tassel, P.R. 2007, 'Fibronectin Terminated Multilayer Films: Protein Adsorption And Cell Attachment Studies', *Biomaterials*, vol. 28, no. 5, pp. 851-860.

Worth, D.C. & Parsons, M. 2008, 'Adhesion Dynamics: Mechanisms And Measurements', *The International Journal Of Biochemistry & Cell Biology*, vol. 40, no. 11, pp. 2397-2409.

Xu, X.-Q., Ye, H. & Zou, T. 2006, 'Characterization Of DC Magnetron Sputtering Deposited Thin Films Of Tin For SBN/Mgo/Tin/Si Structural Waveguide', *Journal Of Zhejiang University - Science A*, vol. 7, no. 3, pp. 472-476.

Zamir, E. & Geiger, B. 2001, 'Molecular Complexity And Dynamics Of Cell-Matrix Adhesions', *J Cell Sci*, vol. 114, no. 20, pp. 3583-3590.

Zelzer, M., Majani, R., Bradley, J.W., Rose, F.R.A.J., Davies, M.C. & Alexander, M.R. 2008, 'Investigation Of Cell-Surface Interactions Using Chemical Gradients Formed From Plasma Polymers', *Biomaterials*, vol. 29, no. 2, pp. 172-184.

Zembala, M. 2004, 'Electrokinetics Of Heterogeneous Interfaces', *Advances In Colloid And Interface Science*, vol. 112, no. 1-3, pp. 59-92.

Zhang, J., Duan, L., Jiang, D., Lin, Q. & Iwasa, M. 2005, 'Dispersion Of Tin In Aqueous Media', *Journal Of Colloid And Interface Science*, vol. 286, no. 1, pp. 209-215.

Zhang, L., Mizumoto, K., Sato, N., Ogawa, T., Kusumoto, M., Niiyama, H. & Tanaka, M. 1999, 'Quantitative Determination Of Apoptotic Death In Cultured Human Pancreatic

Cancer Cells By Propidium Iodide And Digitonin', *Cancer Letters*, vol. 142, no. 2, pp. 129-137.

Chapter 7: Three Dimensional, Polyelectrolyte Capsule For Contractility Assay - Proof of Concept

Contraction is a common biological process critical for the normal functioning of the vascular system. That is, smooth muscles, pericytes and endothelial cells on blood vessels need to be able to contract and relax according to the needs of the body to control blood pressure and perfusion as reviewed by Segal (1994; 2005), Procter and Park (2006) and Pournaras et al (2008). Inability to contract are often signs of pathological processes. For example, in Diabetes Mellitus, inability of the retinal micro-vasculature to contract and relax is one of the signs of Diabetic Retinopathy as shown by *in vitro* experiments (Gillies & Su 1993; Hughes et al. 2004; Kent, Light & Bailey 1985) and the *in vivo* prog-DR test (Martin & Markhotina 2003).

There are several ways to examine the contraction of vascular cells *in vitro*. The area of the cell may be measured over time to determine the relative contraction of the cell, however cell contraction and cell detachment or shrinkage cannot be distinguished in this manner and the force of the contraction cannot be quantified. To overcome this, substrates of known viscosity may be used, as the force required to deform the substrate is directly proportion to the force applied by the cell. For example, the number and length of wrinkles formed by cell contraction on silicone rubber substrates indicates the relative contractile force (Gillies & Su 1993; Harris, Wild & Stopak 1980), yet silicone may be cytotoxic. More sophisticated substrates may be utilized to measure contractile force, such as substrate that incorporate micro-pillars (du Roure et al. 2005) and micro-cantilevers (Park et al. 2005).

Although these substrates provide important information on vascular cell contractile force, cells are not in their native form, hence may not show their full/true contractile response. For example, it has been shown that bovine retinal pericytes and aortic endothelial cells grown in three dimensional systems have very different morphologies to when they are grown on two dimension glass coverslips (Kelly et al 1987). Preliminary results also show that retinal

cells in a three-dimensional, vessel-like format respond differently to glibenclamide and high potassium to cells in a monolayer (see Appendix C).

It would be ideal to assay vascular cell contraction in a three dimensional, lumen-containing tubular format which resemble the physiological environment of a blood vessel. The most commonly used 3 dimensional substrate for contraction assay is collagen (Elsdale & Bard 1972). Cells may be embedded or seeded onto collagen discs and the changes in size of the gel can be easily monitored over time to deduce the level of contraction (Kelley et al. 1987). However, this substrate is often expensive and specialized setup is required to manufacture lumen containing collagen tubes (ref).

Artificial blood vessel is the next best alternative and it has been shown that physiological mechanical properties such as stress, strain (Buttafoco et al. 2006), tensile strength (He et al. 2005), compression (Yang et al. 2005) can be achieved. However, the making of small diameter artificial blood vessels still remains a challenge for tissue engineers. Shen et al (2006) was able to engineer small vessels of 5mm diameter seeded with smooth muscle cells; Amiel et al (2006) was able to reduce the diameter to 3-4mm with viable HUVEC cells and Takei et al (2007) constructed collagen tubules consisted of two types of vascular cells (endothelial and smooth muscle cells) which can withstand physiological level of shear stress. Although these studies shows advances towards artificial capillaries, these vessels are still too large, the engineering processes involved are often very complex and more importantly, it has not been shown that the luminal size of these systems are reversibly tunable by cell contraction and relaxation.

Advances in nano and biomaterial research have gained considerable attention in the recent years and have shed light on potential new material and techniques which may be useful for tissue engineering. In particular, there has been a great deal of research published on polyelectrolytes (PE). The results reported in Chapters 6 and 7 as well as others have shown that PE are non-cytotoxic, and the terminating (basal lamina side) charge of the PE thin films can modulate cell behaviours such as actin distribution (Vautier et al. 2002) and proliferation (Boura et al. 2003). It has also been shown that PE capsules are

relatively stable, elastic and compressible (Dubreuil, Elsner & Fery 2003; Gao et al. 2001; Lulevich, Andrienko & Vinogradova 2004b). PE are also relatively affordable and can be deposited/coated on almost any surface from plastic, glass, latex, bacteria and red blood cells (Georgieva et al. 2004). The simple layer-by-layer assembly technique means that it is easy to tune the thickness and strength of the structure by varying the number of PE layers deposited. These interesting features suggests that PE may be the ideal material for a physiological-like (3 dimensional and with lumen) scaffold for contraction assays. This chapter explores the feasibility of using PE to engineer such a scaffold system to quantify the contractile force exerted by cells.

The design of the PE structures in this chapter was guided by the results reported in Chapters 6 and 7. Those chapters characterized the effects on cell behaviour using accessible 2D-based assays. Hence the anticipated effects on cell behaviour were known for PE chosen to construct the 3D structures reported in this chapter.

Method

7.1.1 Preparation of core material

Agarose cores were made by heating and dissolving 40ug agarose per mL of PBS and injecting/spinning the warm solution through a 18 gauge needle, into ice-cold PBS to produce gels in the form of long cylinders.

Chitosan cores were made in the forms of spheres and cylinders by dissolving 2% chitosan in 2% acetic acid overnight then diluting to 1.5% chitosan with ethanol. The solution was spun/dropped through a 27G needle into a warm bath of 5M NaOH:ethanol (1:1 ratio) using an syringe pump. The change in pH allowed the chitosan to cross-link and solidify to form either spheres or cylinders.

7.1.2 Preparation of the three dimensional, hollow scaffolds

Standard layer-by-layer (LBL) technique was used to adsorb PSS then PAH at 1mg/mL in 0.5M NaCl, onto the surface of the core material (either agarose or chitosan), to 7 to 9 layers of polyelectrolyte thin films. Agarose core was dissolved by DMSO heated to 80^{o}C overnight. The chitosan core was dissolved in 2% acetic acid overnight to form hollow 3 dimensional structures. These hollow structures were sterilized by washing with 70% ethanol three times, then with cell culture medium three to four times to remove all traces of ethanol.

Despite that procedure, it was found that PSS binds strongly to chitosan so that a thick layer of chitosan-PSS complex remained in the PE-PSS structures. To overcome this problem, the chitosan core was coated with PAH first (PE-PAH) and the feasibility of using different pH in the LBL process was explored. Briefly, PSS and PAH solutions in 0.5M NaCl in acidic, neutral and alkaline conditions were used to coat multi-well tissue culture dishes as described in previous chapters. The pH was indicated by phenol red and adjusted with 0.1M NaOH. These PE thin films were stained with 1% Coomassie blue for 1 hour, washed thoroughly and the absorbance at 595nm was measured by BioTek Synergy™ HT Multi-Mode Microplate Reader. The final modified solution for LBL on chitosan cores for the making of PE-PAH structures includes 1mg/mL of

polyelectrolyte in 0.5M NaCl, phenol red and the pH was adjusted with 0.1M NaOH until the solution is slightly red or pink.

7.1.3 Characterisation of the scaffolds

The scaffolds were characterized for size, morphology and ability for cells to grow on them using various microscopy techniques. Mechanical properties of the scaffolds were assessed using equipment built in-house as well as ultrasonic disruption.

7.1.1.1 Slit Lamp Microscopy

Capsules and chitosan beads were placed in a quartz cuvette with water and imaged on a slit lamp microscope connected to a digital video camera (DCM300, Hangzhou Huaxin IC Technology Inc). Image Pro Plus 5.0 was used to measure the size of these samples.

7.1.1.2 Confocal Microscopy

The Olympus FE300 Confocal Microscope with Fluoview 300 software was used to examine the core dissolution process, permeability of capsules and overall morphology of the PE coated tubes and capsules. For the core dissolution and permeability experiments, capsules were stained with FITC-dextran (Sigma, FD10S), at 1mg/mL for core dissolution and 500μg/mL for permeability experiments. For the permeability experiments, imaging started as soon as the 50μL of the dye was added. All images were taken with identical acquisition parameters (exposure time, photo-multiplier tube sensitivity levels, gains and offsets) to ensure comparability.

Optical sections of FITC-dextran stained capsules and physical sections of auto-fluorescent capsules was used to determine the approximate wall thicknesses of capsules (and sections) using the “thickness between curves” function of Image Pro Plus 5.0. In brief, portions of capsule were imaged on the confocal microscope, which are usually composed of 1-1.5mm lengths of the capsule wall. Note that the entire capsule could not be imaged due to the shear size of the capsule. The distance/thickness between the inner and outer circumference along these strips of capsule walls was then measured. Tubes

and rods were stained with 10ug/mL Rhodamine (Sigma, 83689) for morphological examinations.

7.1.1.3 Environmental Scanning Electron Microscope (ESEM)

PE coated tubes and capsules seeded with 3T3-L1, HEK-293 and RAW cells were fixed with 4% paraformaldehyde for 15-20 minutes. These cells were maintained in 10% FCS in DMEM (Sigma, D6429) in an incubator at 37^{o}C in a 5% CO_2 atmosphere, and passaged using Trypsin-EDTA (Sigma, T4299). The samples with and without cells were imaged and examined by and FEI Quanta 200 ESEM.

7.1.1.4 Fluorescent Microscopy

3T3-L1 cells were seeded on PE coated capsules (PE-PAH, PAH as the first inner layer) overnight and then stained with CFDA (Invitrogen, C1157), a long term fluorescent indicator for live cells. The cells were then fixed with 4% paraformaldehyde. The capsules with and without cells were first embedded in a plasma clot to form a cell block (a standard cytology method) which was then put through the auto tissue processors for sectioning. These sectioned samples were imaged under Olympus TE300 fluorescent microscope.

7.1.1.5 Transmission Electron Microscopy (TEM)

The sections of fixed PE-PAH capsules with 3T3-L1 cells mentioned were imaged under TEM.

7.1.1.6 Ultrasonic Treatment

Capsules in water were placed inside a glass test tube and into an ultrasonic bath. The capsules were subjected to 1 cycle (5 minutes) of ultrasound treatment (approximately 40Hz) and the numbers of broken and non-broken capsules were counted.

7.1.1.7 Capsule Compression

The mechanical strength and relative elasticity of the capsules was measured by applying stress to the capsule and measuring the deformation of the capsule. In this experiment, a piston connected to a micro-manipulator was used to compress the polyelectrolyte capsules contained in a cuvette with 1% methanol in water or HEPES buffered Saline (HBS). The cuvette was sitting on a jeweller's scale (accurate to 2 mg). The force (in grams) used to deform the capsules was measured using the jeweller's scale. The whole set up was mounted on a slit-lamp microscope connected to a digital video camera (DCM300, Hangzhou Huaxin IC Technology Inc), which allowed the deformation of the capsules to be monitored. A photograph of the set up is shown in Figure 7.1.

The piston was placed just on top of the capsules and the jeweler's scale was zeroed; the micromanipulator was then used to lower the piston to compress the capsule systematically until it burst, which is seen when the force applied drops dramatically or returns to zero.

The cross-sectional area of the capsules was used as the indicator of level of deformation, and was measured using Image Pro Plus 5.0. Force was calculated using the standard formula $Force = ma$, where *m* is mass and *a* is the gravitational acceleration of 9.80665 m/s². Microsoft ® Excel 2003 was used to run the least square regression (linear) on the force and deformation data.

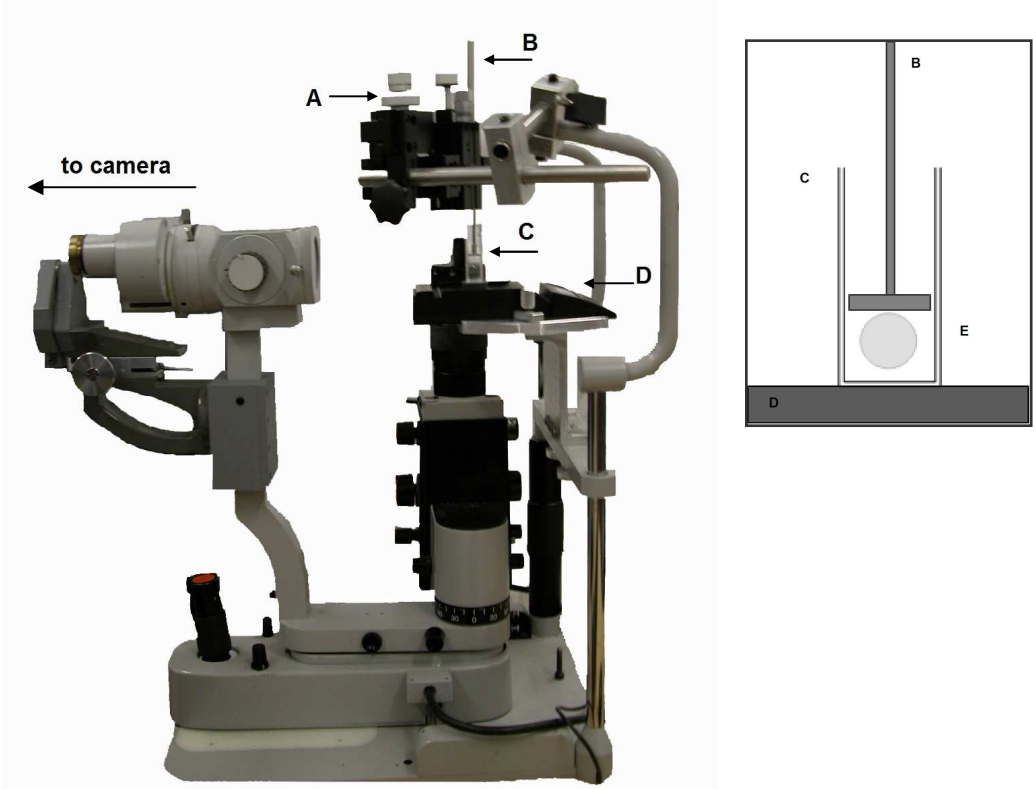

Figure 7.1: the Capsule Compression Equipment set-up. A: micromanipulator, B: piston, C: cuvette. D: jeweler's scale and E: capsule. Note that the inset image is not to scale.

7.1.4 Relaxation assay

3T3-L1 cells were seeded on polyelectrolyte capsules, that had been made using the chitosan core, and the area of the capsule was measured over 40 minutes on the dissecting microscope using Image Pro Plus 5.0 software from images captured using a digital camera (DCM300, Hangzhou Huaxin IC Technology Inc). The capsules with or without cells were either incubated in HBS, cell culture media, 10µm Forskolin or 10µM Cytochalsin D. The observation was carried out in a modified 35-mm petri dish, which had glass beads super-glued to form a chamber to stop the capsules from rolling around but permeable to bathing solutions. The data here were then compared to the results obtained in the capsule compression assay.

To ensure the effects seen on the capsules were the results of compressive force applied by the 3T3-L1 cells, the F-actin distribution of 3T3-L1 cells was characterised. Cells were seeded on coverslips at 50,000 cells per well of a 24 well plate overnight. Cells were incubated with 10μm Forskolin, 10μM Cytochalsin D or media at 37^{o}C for 20 minutes, then fixed with 4% paraformaldehyde for 20 minutes. Alexa-fluo 633 phalloidin (Invitrogen, A22284) was used to stain for F-actin after the cells were extracted with 1% Triton X-100 for 3 minutes and blocked 1% BSA 20 minutes. Images were taken by the Olympus TE300 fluorescent microscope under the x100 oil immersion objective.

7.1.5 Statistical Analysis

All statistical analysis was carried out with SPSS 15.0 using independent t-tests or ANOVA with Tukey-Kramer analysis. The results are considered significant when $p<0.05$. Least square regression was carried out using Microsoft ® Excel 2003.

7.2 Results

7.2.1 Feasibility of the LBL coating at different pH

There was a significant difference between the binding capabilities of PSS and PAH to 1% Coomassie blue as shown in Figure 7.2, where PAH and PAH terminating thin films have significantly higher absorbance at 595nm than PSS terminating thin films. However, there was no significant difference between the LBL constructions of these thin films made at different pH as measured by this method.

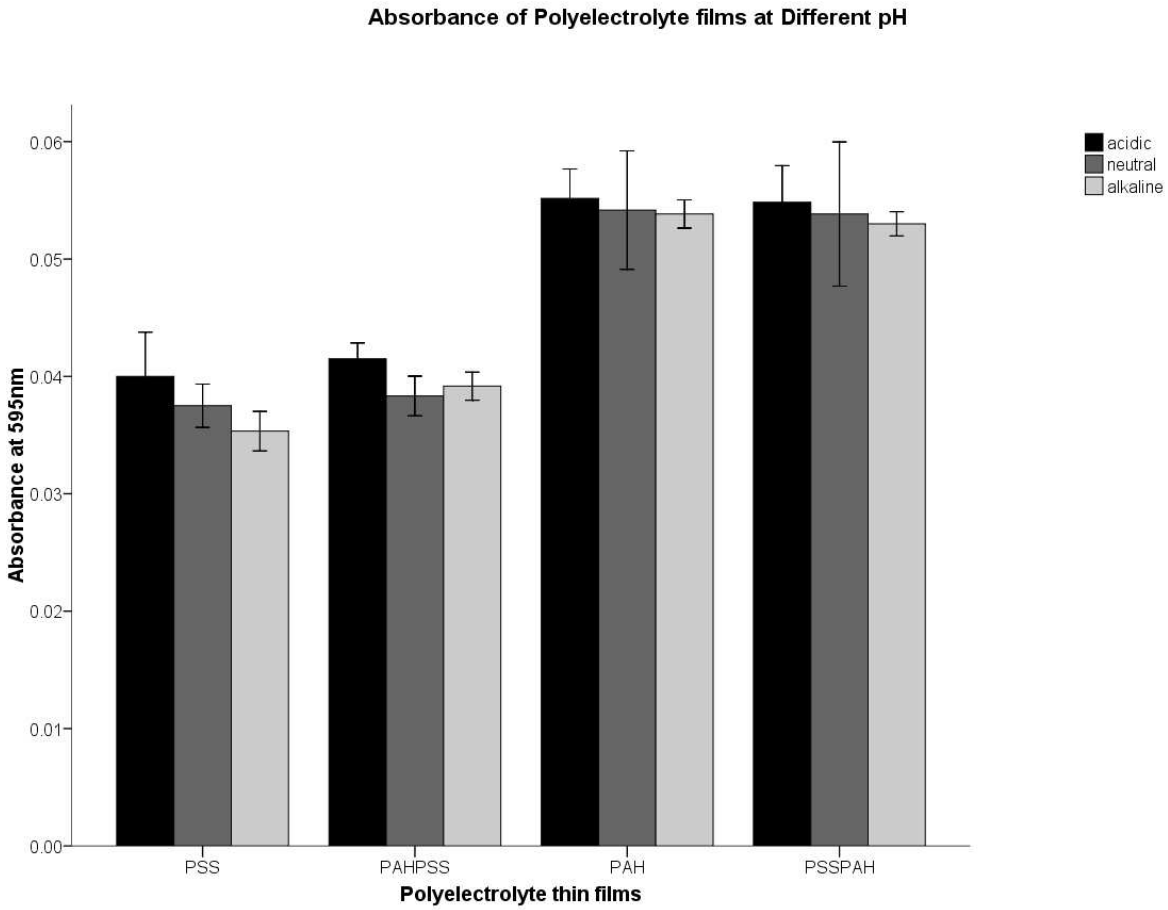

Figure 7.2: The absorbance of polyelectrolyte thin films made in different pH environment and stained with 1% Coomassie blue. Error bars represents the standard error.

7.2.2 Characterisation of PE scaffolds

The agarose-cored PE tubes were approximately 500μm in external diameter, but tend to vary up to millimeter in width. These tubes were stiff and able to stand vertically on without support. Chitosan-cored PE tubes were 150-300μm in external diameter and are much softer than the agarose-cored PE tubes. The characteristics of the chitosan-cored capsules are summarised in Table 7.1. The PE-PAH capsules, made by coating the chitosan core first with PAH in a neutral pH, are significantly larger than the PE-PSS capsules which are made by coating the chitosan core first with PSS in an acidic pH. These capsules can start to swell and even burst if store in milli-Q water for prolonged periods (over a week).

	PE-PSS	**PE-PAH**	**PE-PAH with core**
Diameter	2.05mm (0.04)	2.21mm (0.04)	1.77mm (0.04)
Surface Area	13.3mm^2 (0.5)	15.4mm^2 (0.6)	9.91mm^2 (0.5)

Table 7.1: Characteristics of chitosan-cored scaffolds. The average diameter and surface area of at least 16 PE-PSS and PE-PAH capsules and beads of PE-PAH before core dissolution. Standard errors are shown in brackets.

Chitosan-cored PE capsules and tubes also differed visually when different PE were used as the first coating material. PE-PSS capsules tend to be “whiter” and less translucent than PE-PAH capsules as shown in Figure 7.3.

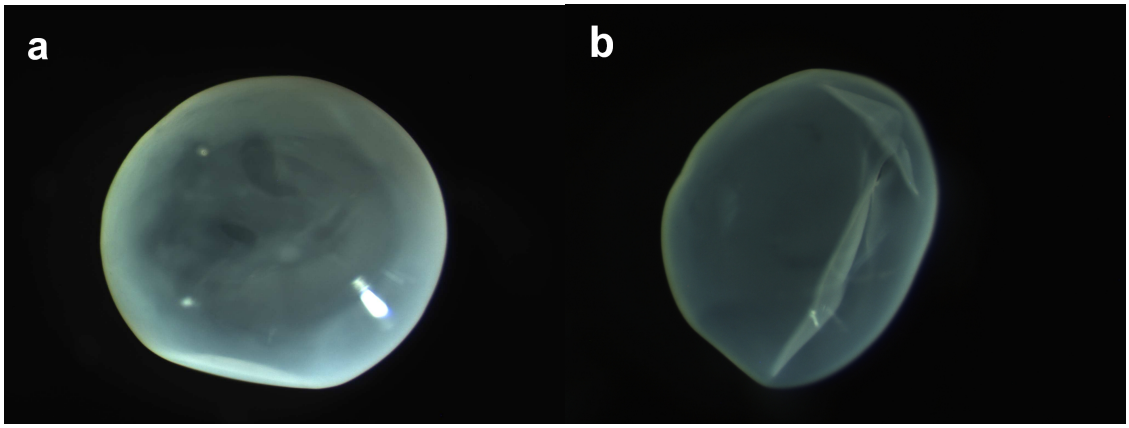

Figure 7.3: Chitosan-cored Polyelectrolyte capsules with PSS (a) and PAH (b) as the starting coating material. Image taken on the Leica dissecting microscope.

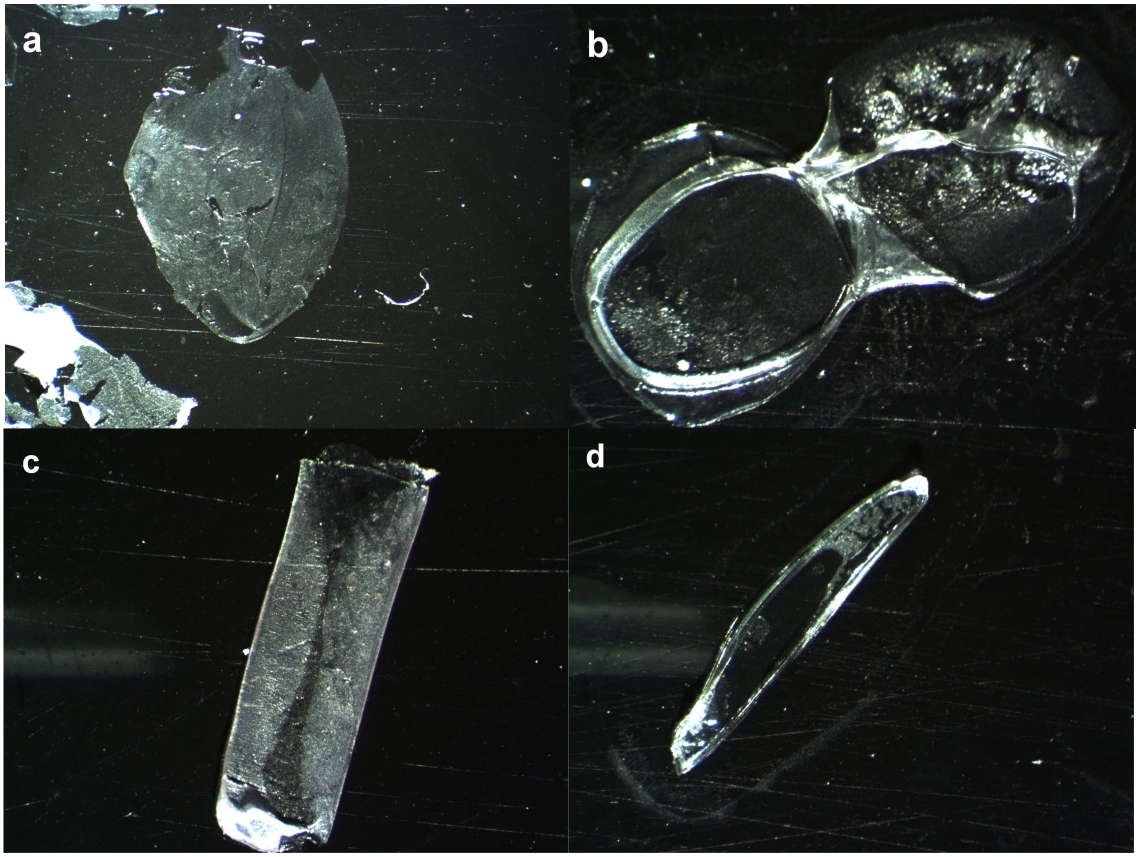

Figure 7.4: Collapsed polyelectrolyte capsules (a, b) and rods (c, d) made from chitosan cores with PSS (a, b) and PAH (b, d) as the start coating material. Images were made on Leica dissecting microscope, post ESEM imaging.

Figures 7.4 show the PE-PSS and PE-PAH rods and capsules post ESEM imaging, which have collapsed on to the black adhesive surface. It is clearly shown that the PE-PAH structures appear to be thinner or transparent whereas the PE-PSS structures are relatively white. The PE-PAH structures also appear to fold whereas the PE-PSS capsules did not.

7.2.2.1 Confocal microscopy

To ensure that the chitosan core dissolution was complete, PE capsules were stained with FITC-dextran. As show in Figure 7.5, the chitosan-cored PE capsules have a convoluted, sponge-like internal structure, and washing the capsule with 2% acetic acid, followed by overnight incubation with 1% acetic acid removed most of the core material. However, there was still a thick layer of chitosan incorporated in the wall of the capsule. This is evident by the micrometre range wall thickness (Figure in 7.5c) as compared to the nanometre

range thickness of 2 dimensional PE films (i.e. without core) prepared using the same LBL procedure.

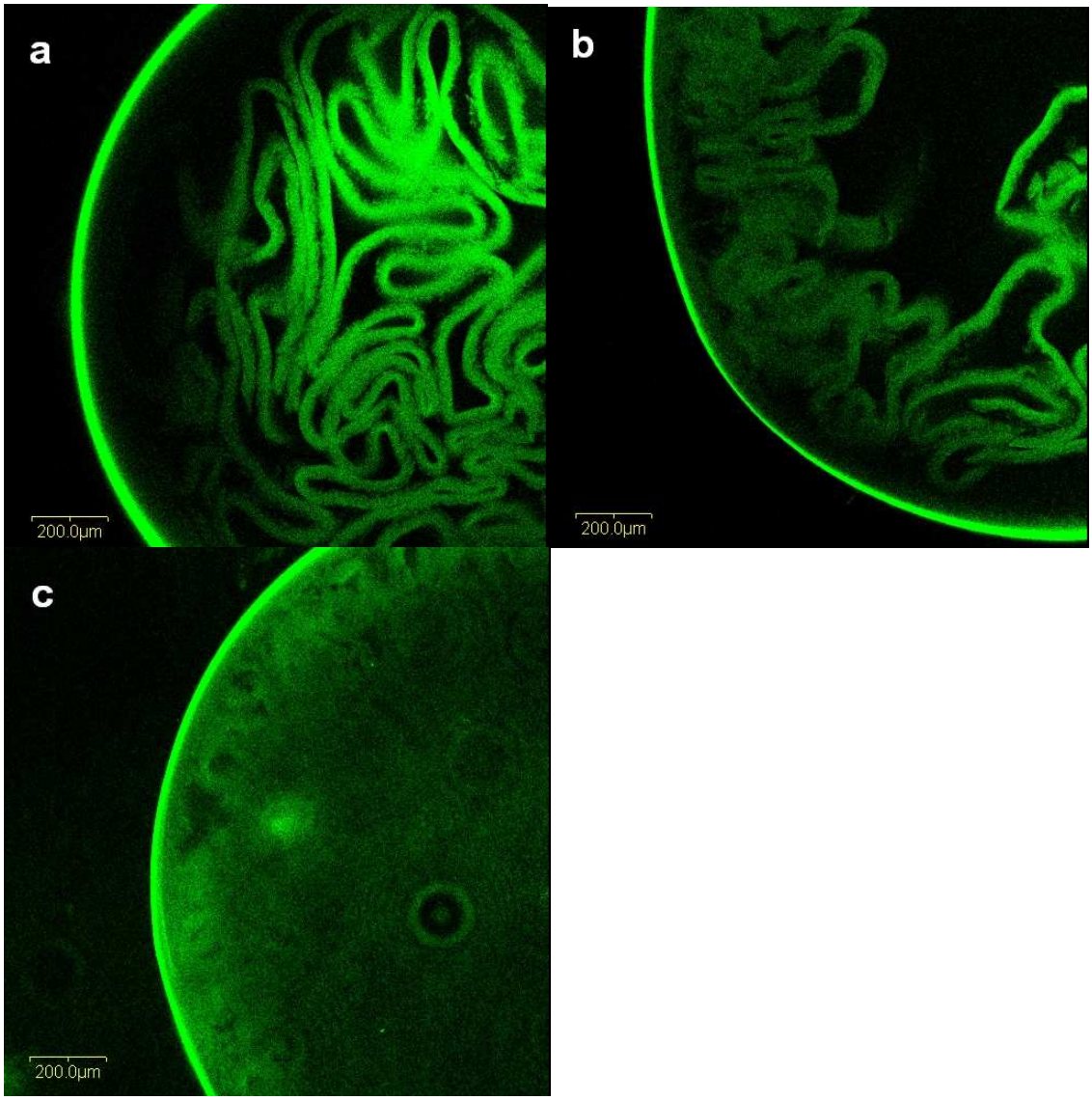

Figure 7.5: Confocal images of FITC-dextran stained chitosan-cored polyelectrolyte capsules with PAH as the start coating material in PBS (a), after washing with 2% acetic acid (b) follow by 1% acetic acid incubation overnight (c). Images were taken on the Olympus FE300 Confocal Microscope on the x10 objective.

To characterise the tubes, the PE tubes were stained with rhodamine. Under confocal microscopy, the rhodamine-stained walls of the tubes can be identified as shown in Figure 7.6. It is apparent that the walls of the open-ended PE-PSS tubes have two wall layers: a thick low-fluorescent inner wall and a high fluorescent, thin outer membrane. This PE-PSS tube is much thicker than the closed-end PE-PAH tubes. The PE-PAH tube has encapsulated rhodamine dye inside, but it has only one brightly stained layer. Similar can be said for the PE

capsules which were stained with FITC-dextran 10S as seen in Figure 7.7. The PE-PAH capsule has a defined wall structure whereas the PE-PSS capsule has a defined outer wall structure as well as another faintly stained inner ream.

The wall thickness was measured on the optical and physical sections of the capsules, using the confocal microscope and its software. Figure 7.8, show that there was no significant difference between optical and physical sections of capsules with PAH as starting coating material, but PE-PSS capsules have significant thicker walls.

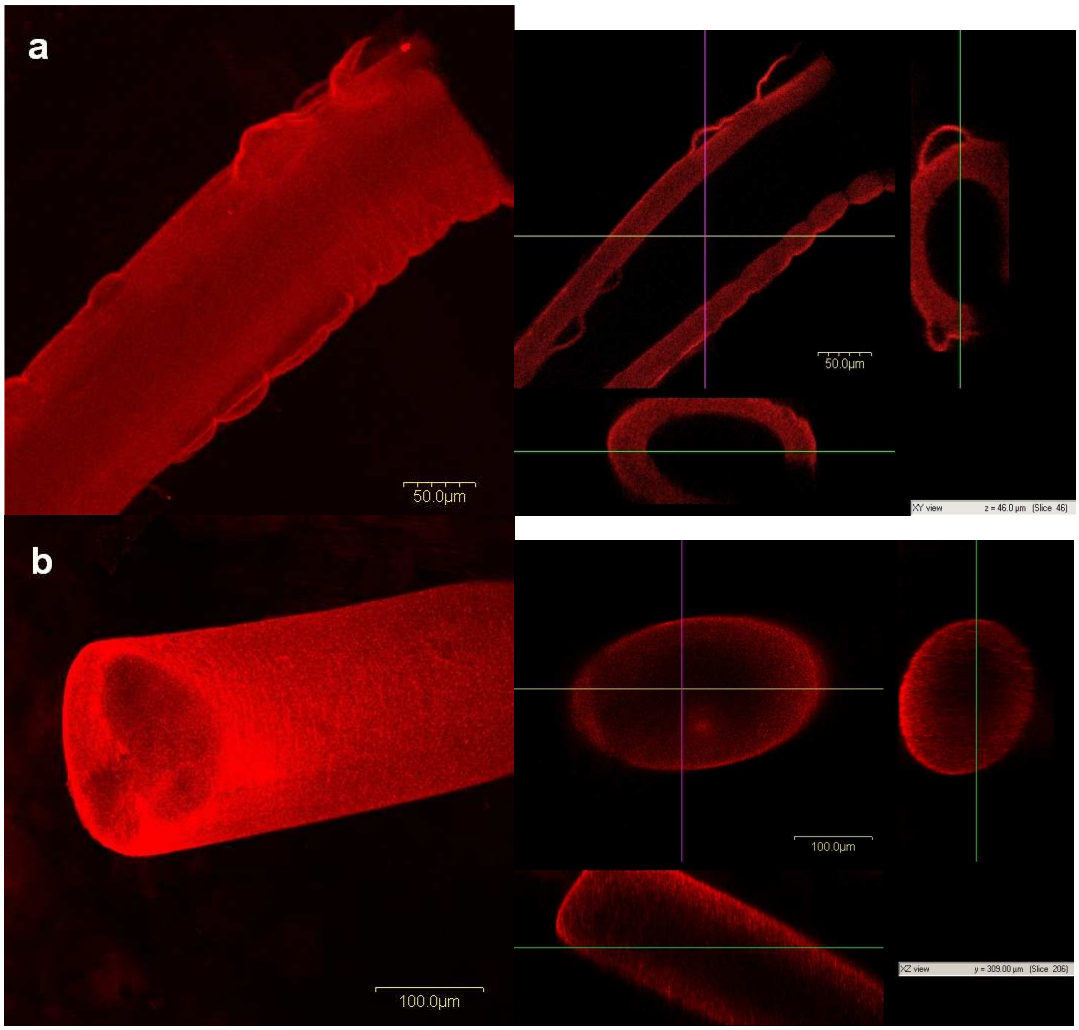

Figure 7.6: Confocal images of Rhodamine stained walls of chitosan-cored polyelectrolyte tubes with PSS (a) and PAH (b) as the starting coating material. The left panel shows the composite image of the z-stack taken on the confocal microscope and the right panel shows the cross sections. Note in (b) that the tube is sealed off or closed-end, thereby encapsulating the dye. Images were taken on the Olympus FE300 Confocal Microscope on the x10 objective.

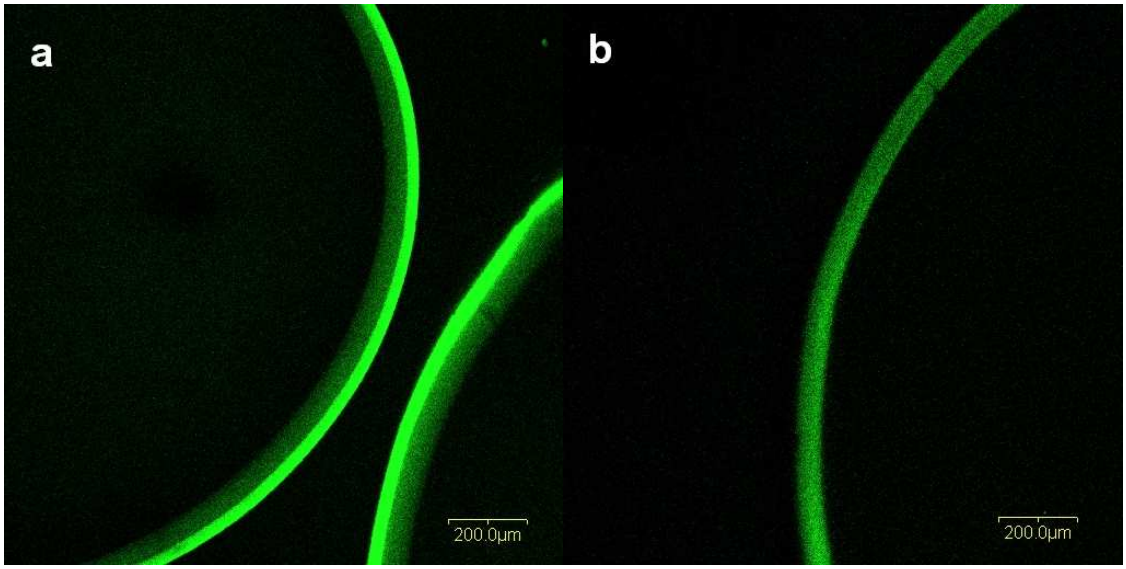

Figure 7.7: Confocal images of FITC-dextran stained walls of chitosan-cored polyelectrolyte capsules with PSS (a) and PAH (b) as the start coating material. Images were taken on the Olympus FE300 Confocal Microscope on the x10 objective.

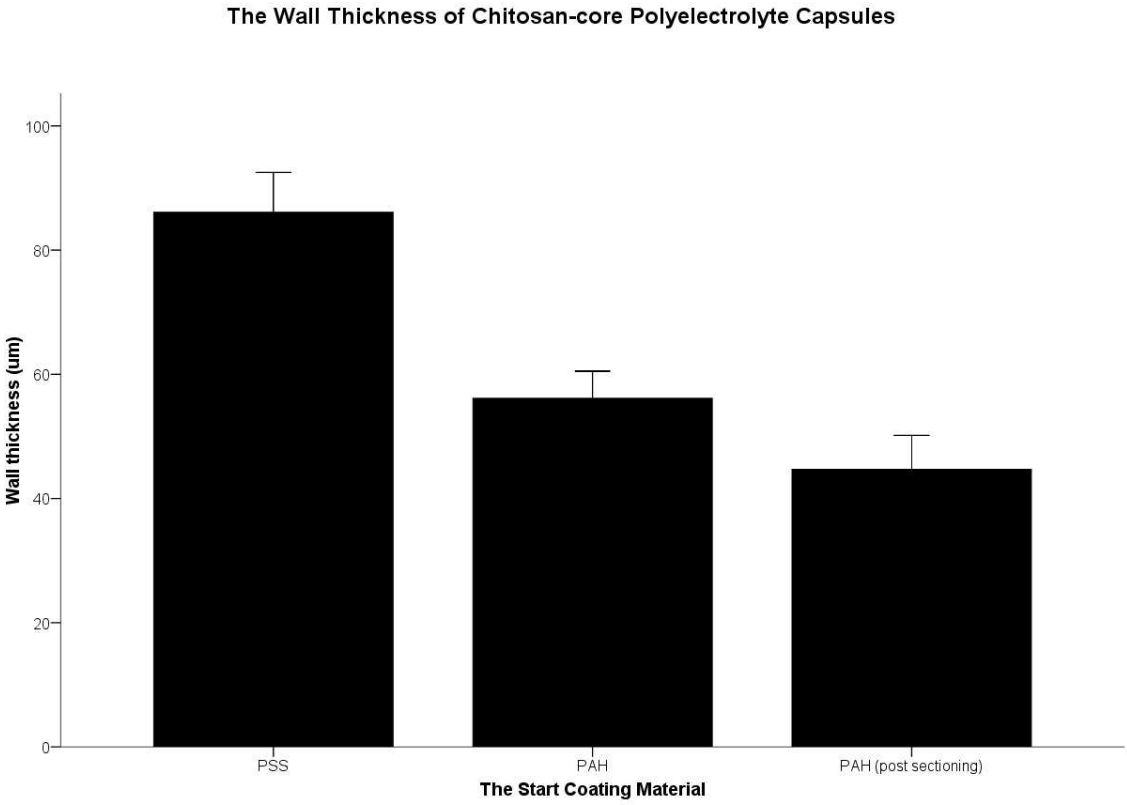

Figure 7.8: The wall thickness of capsules with PSS or PAH as the start coating material. Wall thickness of capsules with PSS and PAH as the start coating material were measured on their optical sections. PAH (post sectioning) show wall thickness of physical sections of PE-PAH capsules. Error bars represents standard error, n ≥ 9.

Figure 7.9 shows that both PE-PSS and PE-PAH capsules are permeable to FITC-dextran), albeit with different permeability coefficients. Over the time-scale of 600 seconds Figure 7.9 shows that the fluorescent intensity inside the PE-PSS capsule continue to increase whereas the fluorescent intensity inside the PE-PAH capsules plateaus fairly quickly. Although there were no significant differences in fluorescent intensities at the end of the experiment, there were significant differences at time zero as measured by independent t-test. Therefore, the permeability of PE-PSS and PE-PAH capsules are different.

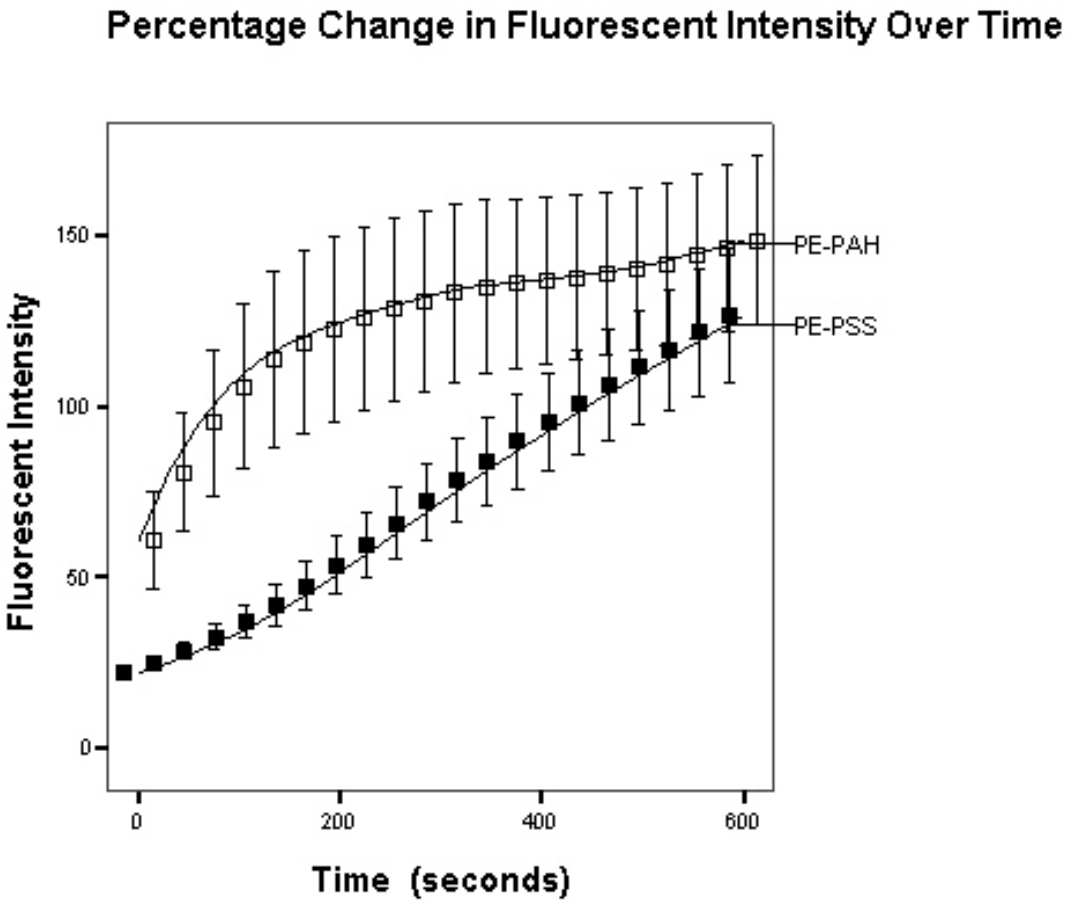

Figure 7.9: Permeability of polyelectrolyte capsules as measured by the change in fluorescent intensity over time, of capsule with PSS and PAH as the start coating material. The fluorescent intensity was measured using Olympus FE300 Confocal Microscope. Error bars represents standard error, n ≥ 8.

7.2.2.2 Fluorescent Microcopy

Physical sections of the capsules seeded with 3T3-L1 cells were obtained and viewed using fluorescent microscope as shown in Figure 7.10. The 3T3-L1 cells were live on these capsules, since CFDA is a fixable vital stain. Figure 7.11 also shows that the PE capsules have become brightly auto-fluorescent green and red, potentially due to absorption of excess metabolized CFDA or the sectioning process.

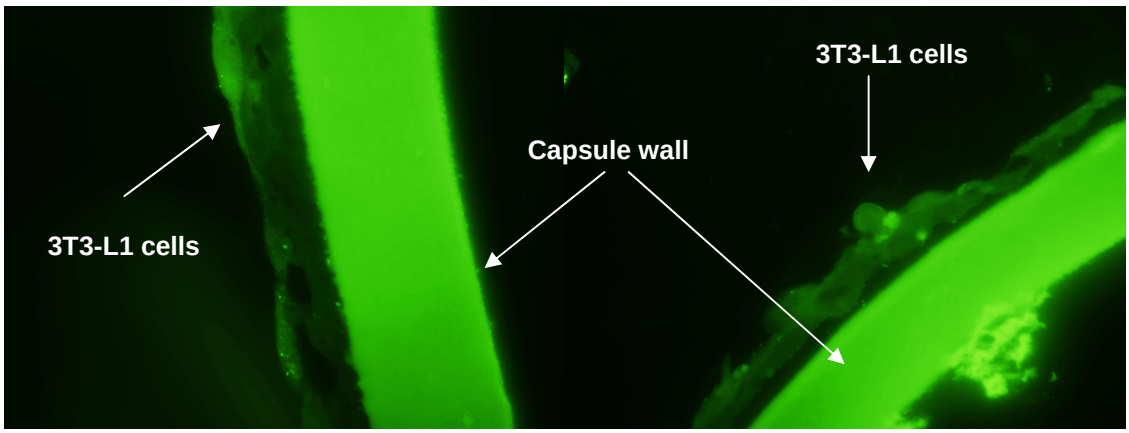

Figure 7.10: Chitosan-cored PE-PAH capsule with CFDA-stained 3T3-L1 cells. Images were made on Olympus TE300 fluorescent microscope under the x20 objective.

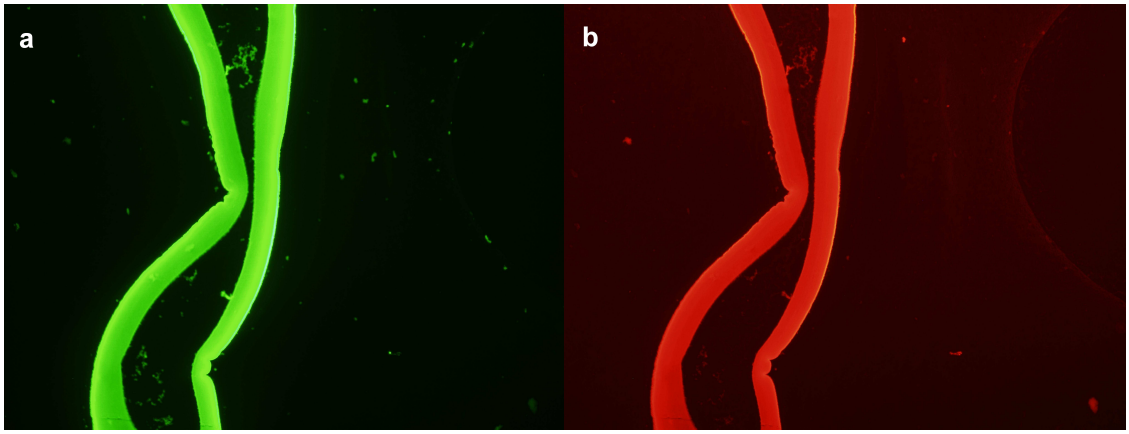

Figure 7.11: Chitosan-cored polyelectrolyte capsule autofluorescence in green (a) and red (b). Images were made on Olympus TE300 fluorescent microscope on the x10 objective.

7.2.2.3 ESEM

As shown in the ESEM images in Figure 7.12 and 7.13, cells can be seeded on PE tubes, and PE-PAH capsules in Figure 7.14b. Interestingly, the PE-PAH capsules collapsed during ESEM imaging as shown in Figure 7.14a.

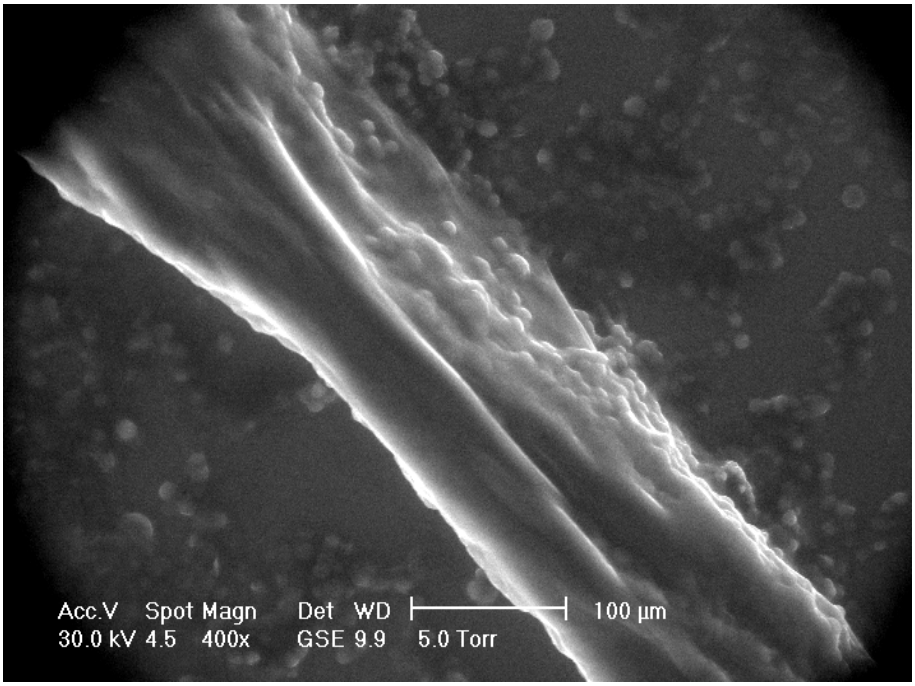

Figure 7.12: ESEM image of a polyelectrolyte tubes made from agarose cores seeded with RAW cells. The sample was fixed with paraformaldehyde as described in *Methods*.

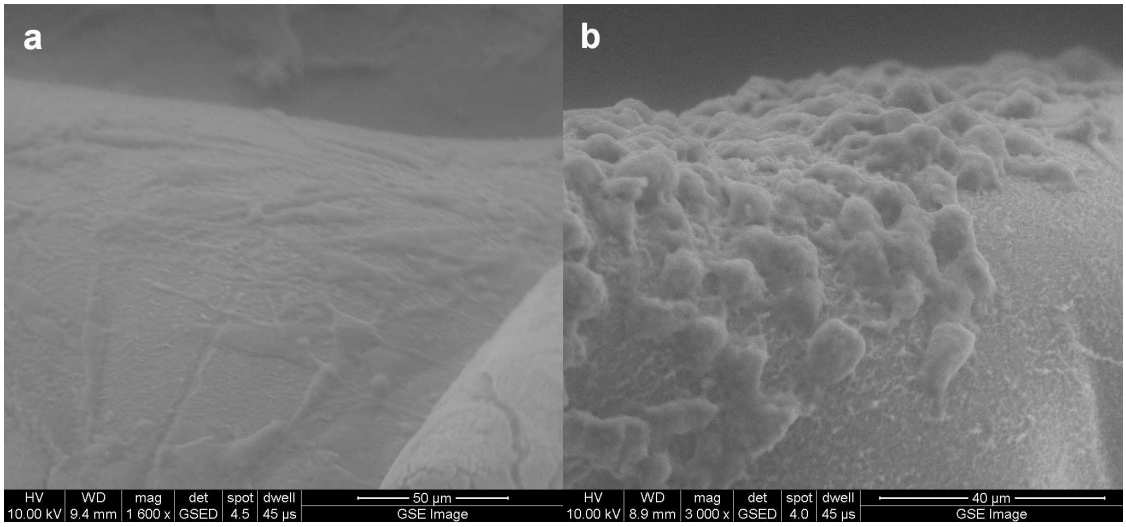

Figure 7.13: ESEM image of Polyelectrolyte tubes made from chitosan cores seeded with 3T3-L1 (a) and HEK-293 (b) cells. The sample was fixed with paraformaldehyde as described in *Methods*.

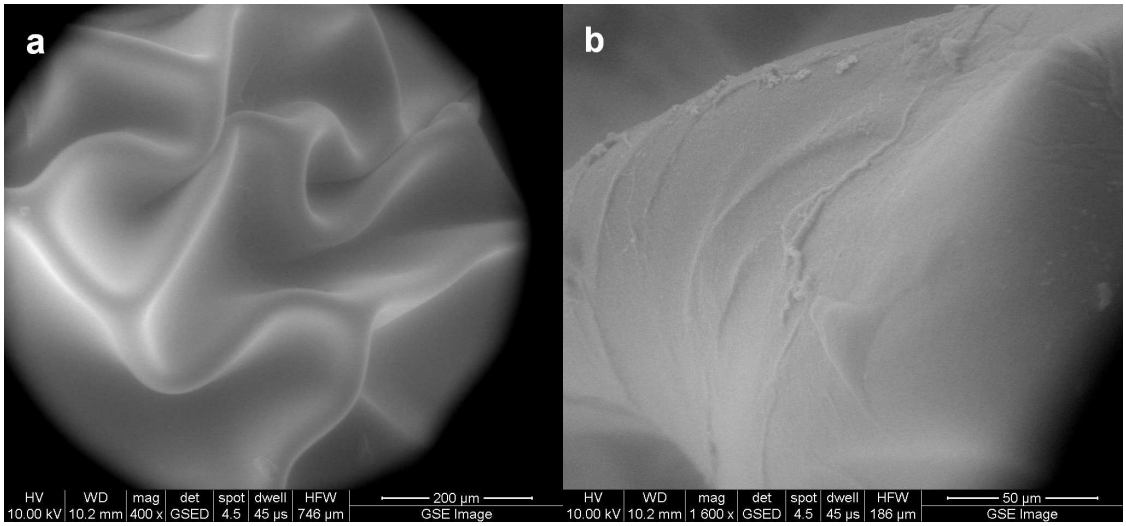

Figure 7.14: ESEM image of polyelectrolyte capsules made from chitsan spheres (PAH as the starting PE), collapsing under vaccum (a) and seeded with 3T3-L1 cells in (b). The sample was fixed with paraformaldehyde as described in *Methods*.

7.2.2.4 TEM

Figure 7.15 show the TEM images that 3T3-L1 cells grew on PE-PAH capsule, developed processes which anchor into the capsule wall. Interestingly, the thick capsule wall appears to be spongey or porous as shown in the pockets of dye.

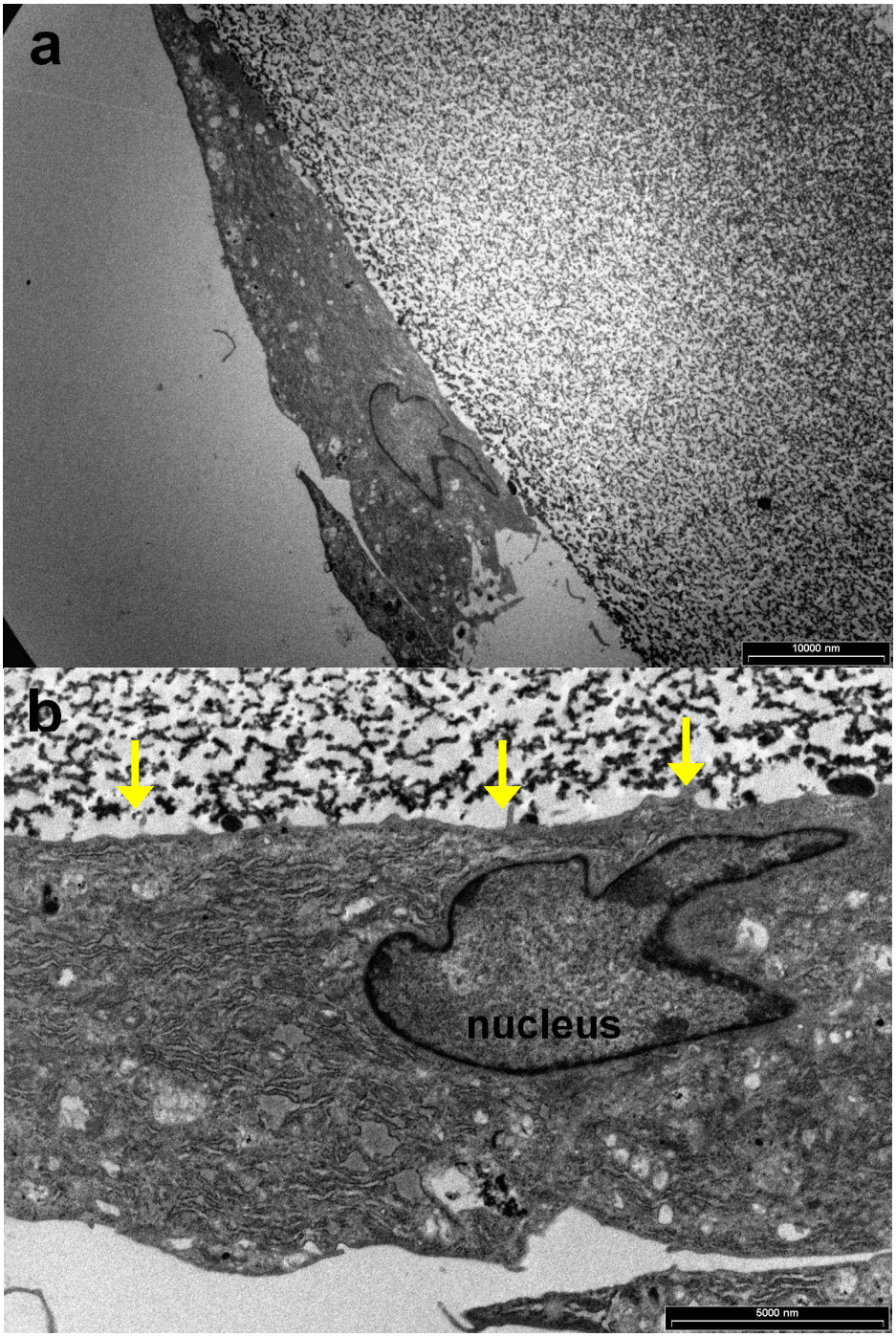

Figure 7.15: TEM image of 3T3-L1 cell on chitosan-cored PE-PAH capsule (a) and at higher magnification (b). Arrows point to protrusions from cell. The sample was fixed with paraformaldehyde and sectioned as described in *Methods*. Images kindly made by Dr Murray Killingsworth (South Western Area Pathology Service, Liverpool)

7.2.2.5 Mechanical Strength of Capsule

The mechanical strength of the PE-PSS and PE-PAH capsules was assessed by their ability to withstand 5 minutes of 40Hz disruption in an ultrasonic bath. Table 7.2 clearly shows that PE-PSS is more able to maintain its integrity in by such mechanical disruption.

	PE-PSS	**PE-PAH**
Percentage of broken capsules post ultrasonic treatment (40Hz)	3.03 (3.0)	51.52 (12.1)

Table 7.2: Mechanical strength of polyelectrolyte capsules as measured by ultrasonic treatment. The values are shown as the average and standard error from three independent experiments.

These initial observations using the ultrasonic bath were extended by the mechanical testing described in the following sections.

7.2.2.6 Relative Elasticity of Capsule

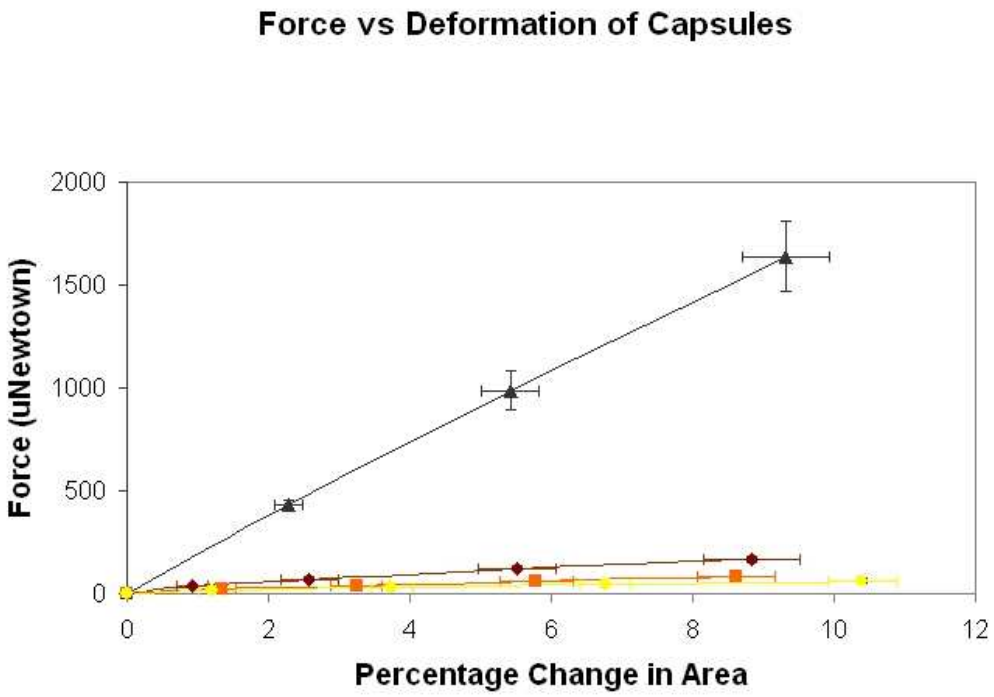

Figure 7.16: The force versus deformation graph of the ▲ PE-PAH capsule with the cores still intact, ◆ PE-PSS capsules, ■ PE-PAH capsules and ● PE-PAH capsules in buffer. The results are the average of fifteen samples and the error bars represents the standard error.

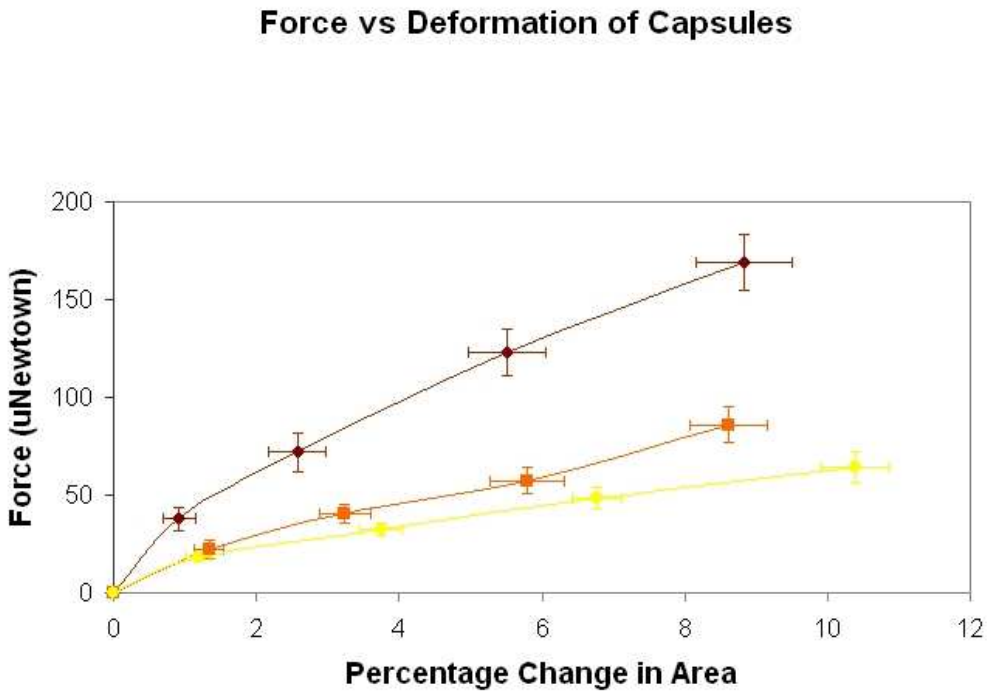

Figure 7.17: The force versus deformation graph of the ◆ PE-PSS capsules, ■ PE-PAH capsules and ● PE-PAH capsules in buffer. The results are the average of fifteen samples and the error bars represents the standard error.

As shown in Figure 7.16, the PE-PAH capsules with its core still intact are relative elastic but a lot firmer or "stiffer" than capsules with the chitosan core removed. In Figure 7.17, graphical information on the PE-PAH capsule with core was removed, to better illustrate the differences between the other capsules (with their cores removed). Figure 7.17 again shows that PE-PSS is again firmer that PE-PAH capsules, but PE-PAH in HBS is the softest of all four samples. For example, the force required to achieve a change in area of 6% was 120μN for the PE-PSS capsules and 50μM for the PE-PAH capsules.

Based on the same data set as Figures 7.16 and 7.17, the linear least square regression analysis on the force and deformation are shown in Table 7.3. The gradient interpreted as similar to a compressive modulus for the capsules. The stiffer capsules have a larger gradient ("compressive modules"). Note that the intercepts have been set to zero, as the capsules does not deform without force.

	PE-PAH with core	**PE-PSS**	**PE-PAH**	**PE-PAH in buffer**
Gradient	155.57 ± 14.4	18.97 ± 1.92	9.431 ± 1.31	6.522 ± 0.767
R^2	0.841	0.844	0.727	0.795

Table 7.3: The least square, linear regression of the force and deformation of PE-PAH before core dissolution, PE-PSS and PE-PAH capsules and PE-PAH in HBS buffer. The gradient of the equation reflects the relative elasticity of the sample, and data are shown with its 95% confidence level.

7.2.3 Relaxation Assay

The capsules were seeded with cells which grew to confluence as observed by microscopy. This relaxation assay measures the compressive force ("contractility") applied to the capsules by the cells from measurements of the area of the capsules after disrupting the F-actin cytoskeleton. Figure 7.18 shows the change in the area of capsule over time when incubated with different bathing solutions. The results are normalized to the initial area of the capsule before incubation of F-actin disrupting drugs. The average change in area was significantly different in the presence of actin disrupting drugs compared to capsules in buffer, culture media and capsules with no cells. The average change in area of the capsules after treating the cells with Cytochalasin D was approximately 7%. The average change in area after treatment with Forskolin was approximately 3%. It is clear that the Cytochalasin D induced a greater effect on the contractility of the cells that did Forskolin.

Figure 7.19 depicts the F-actin distribution of 3T3-L1 cells in culture media and in the presence of actin disrupting drugs. In culture medium, actin filaments in the 3T3-L1 cells are obvious and distributed throughout the cells. Exposure to F-actin disrupting drugs has localized the F-actin to the body of the cell and filaments become diffused. Whilst some filaments are still visible upon exposure to 10μM Forskolin, the actin filaments have become segmented with 10μM Cytochalasin D.

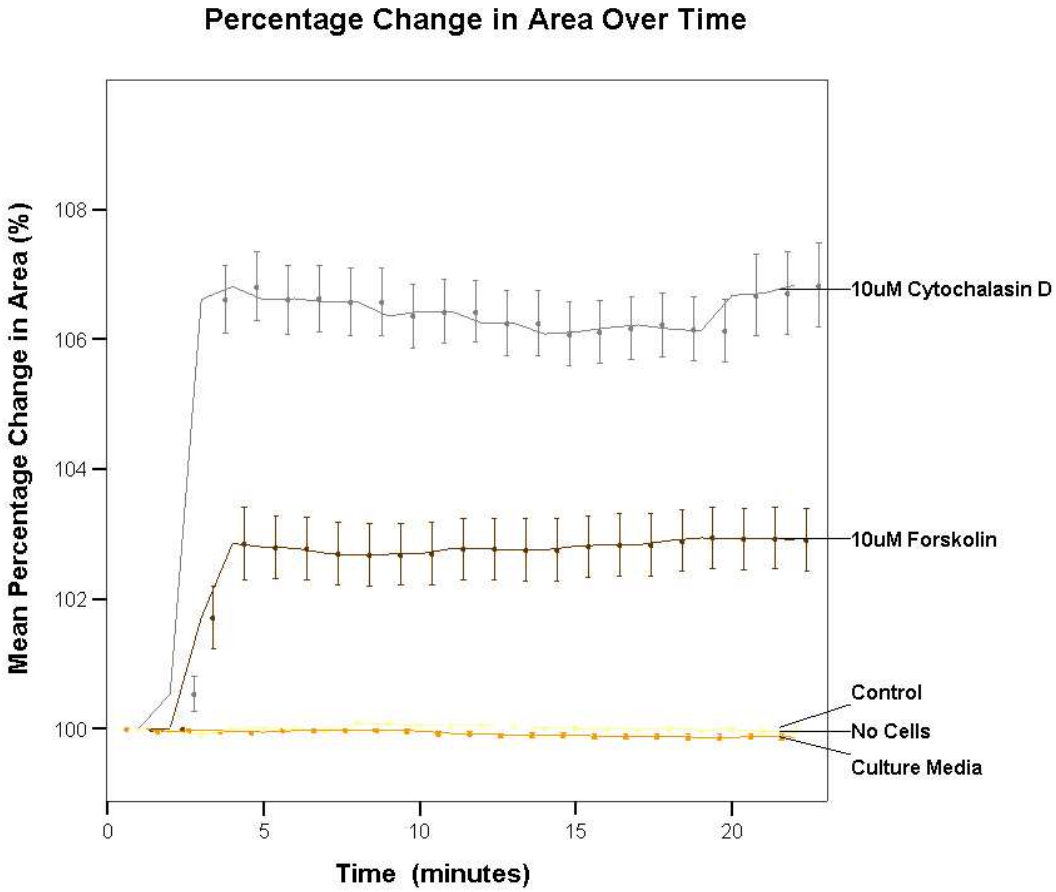

Figure 7.18: The mean change in area over time of 3T3-L1 seeded polyelectrolyte capsules. Results normalized to the area of the capsule before drug incubation as measured on Leica dissecting microscope. The result represents the average of at least six independent experiments and the error bars represents the standard error.

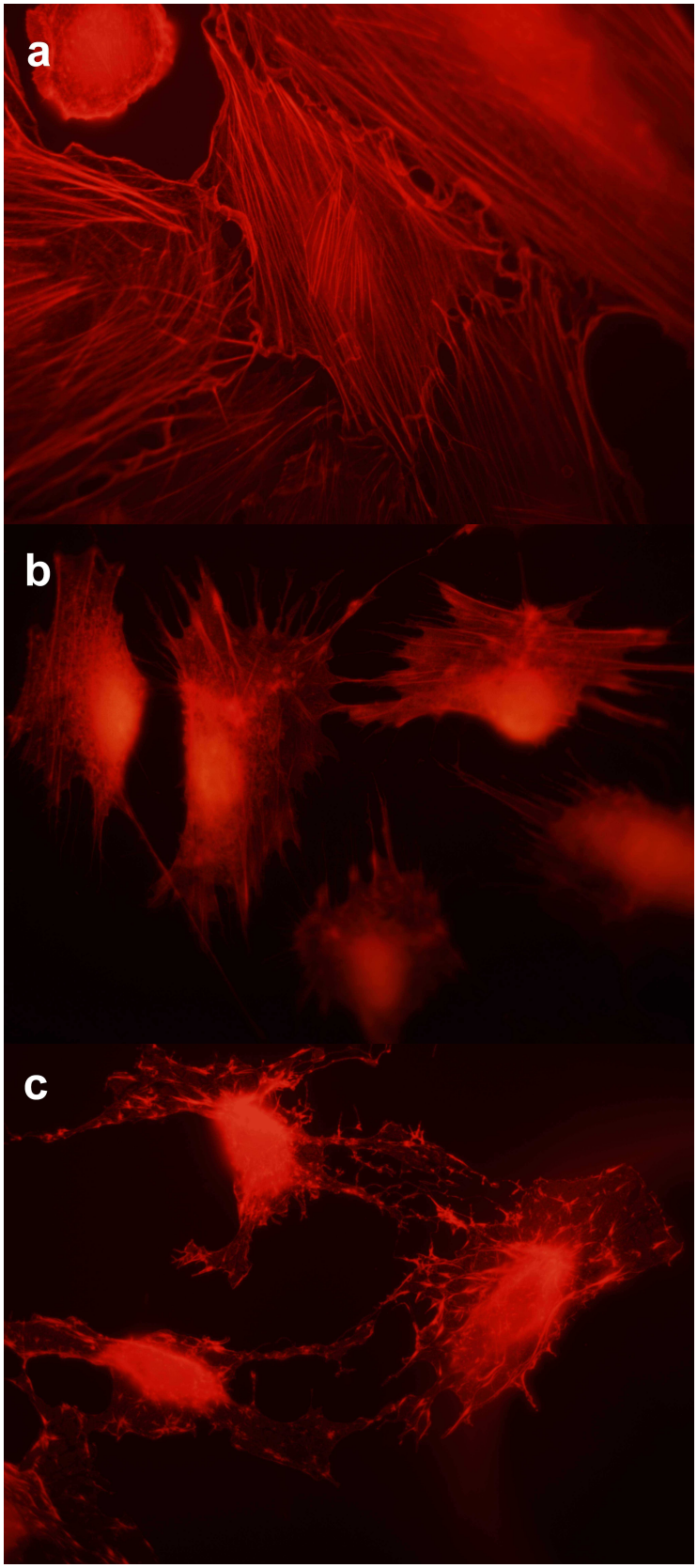

Figure 7.19: The actin distribution of 3T3-L1 cells in culture media (a) and post 20minutes exposure to 10μM Forskolin (b) and 10μM Cytochalasin D (c). 3T3-L1 cells were fixed and stained with alexa fluo 633 phalloidin. Images were made on Olympus TE300 fluorescent microscope under the x100 oil immersion objective.

As shown in Figure 7.18, 10μM Forskolin and 10μM Cytochalasin D caused a 3% and 7% change in the area of the PE-PAH capsules. Using the force and deformation information as shown in Table 7.3, the known surface area of these capsules and an estimated cell density, the average force exerted by the 3T3-L1 cells on PE-PAH capsules in HBS buffer was be estimated. It should be noted however, that the cell density 1000/mm^2 assumes that the 3T3-L1 cells do grow on top of each other (i.e. not just in a monolayer).

	Level of Deformation	
	3%	**7%**
Force required (uN)	15.56 ± 2.30	45.66 ± 2.30
Surface Area (mm^2)	15.4 ± 1.16	
Assume the cell density is at maximal of 1000/mm^2		
Force exerted per cell (nN)	1.27 ± 0.06	2.96 ± 0.14

Table 7.4: calculation of the force exerted per cell to reach the level of deformation shown by actin disruption using 10μM Forskolin (3%) and 10μM Cytochalasin D (7%). The average and 95% confidence intervals are shown.

7.3 Discussion

The aim of the physiological aspect of this project was to develop an improved alternative scaffold to construct an assay for cell contractility. This scaffold must be similar to the vascular physiological environment (3 dimensional and with lumen), support the cellular contraction and of course be non-cytotoxic. The results in chapters 6 and 7 indicate that PSS and PAH polyelectrolytes were appropriate for the surface material as they can fulfill these requirements. In confirmation of the results reported in chapters 6 and 7, it has been shown that PSS and PAH films are not cytotoxic to endothelial cells (Boura et al. 2003), osteoblast-like cells (Tryoen-Tóth et al. 2002) as well as the 3T3-L1 cells used in this study (Lin et al. 2006). PSS and PAH films (Mermut et al. 2003a) and capsules (Heuvingh, Zappa & Fery 2005a; Lulevich, Andrienko & Vinogradova 2004a) have also been show to be elastic. The simple LBL technique used to construct these PE films is also versatile, so that almost any surface or core material may be used to construct a three dimensional and hollow scaffold.

7.3.1 Optimise core material

As reviewed by Antipov and Sukhorukov (2004), the choice of core material can have varying effects on the properties of end PE capsules, as the core material is rarely completely eliminated and some of the solvents used to dissolve the core may crosslink PE chains. The ideal core material should be affordable, easy to make and remove. In the case where there are remnants of the core material, the level should be low, non-cytotoxic and does not affect the elasticity of the capsule.

Common cores used for PE scaffolds are melamine formaldehyde (Decher 1997) and calcium carbonate (Antipov et al. 2003), however, these cores are too small for cells to grow on (nanometer to 10μm in diameter). Both agarose and chitosan are natural materials: agarose is derived from agar (seaweed) and chitosan is extracted from crustaceans. These are abundant, non-cytotoxic, biodegradable and biocompatible which makes agarose and chitosan suitable

candidates as core material for larger capsules on which to grow cells for the contractility assay.

The manufacturing of the cores requires spinning of the core material through a needle into the cross-linking solution. The inner diameter of a 27 gauge needle is approximately 200μm in diameter and 800μm for a 18 gauge needle. However, the agarose and chitosan cylindrical cores are often smaller than this because as the cylindrical cores enter into the cross-linking solution the spinning process stretches the cylinders of chitosan or agarose before solidification.

The variations in the cores sizes were particularly substantial with the melt spinning of agarose because it was difficult to keep many of the parameters constant. Agarose gels quickly at room temperature and keeping the solution at high temperature creates evaporation, hence the injection needed to be done quickly by hand and with a needle with a wide bore. This means that it is difficult to keep temperature, injection rate and agarose concentration constant, thereby making it difficult to make consistent agarose cores.

The use of chitosan as the core material overcame some of these difficulties, as it gels with the change in pH as opposed to temperature, therefore a constant injection rate, chitosan concentration and a smaller needle (27 gauge) can be used. Despite being able to keep most parameters constant, the diameter of the chitosan spheres is much larger (1-2 mm in diameter) than the tubes/cylinders (150-300μm in diameter) because chitosan solution had to be dropped into solution as oppose to spun in the making of spheres. That is, droplets of chitosan solution gather at the tip of the needle and falls into the cross-linking solution. As the manufacturing process proceeds, tip of the needle becomes wet with the result that more chitosan solution can accumulate in the droplet forming at the tip of the needle before becoming too heavy and dropping into solution. The distance between the needle tip and the cross-linking solution increases as the cross-linking solution evaporates (since ethanol is volatile), allowing more chitosan solution to gather before hitting the cross-linking solution. Although the distance was adjusted regularly, those effects contribute to variable sizes of the chitosan spheres.

During the handling of the agarose-cored and chitosan-cored PE tubes, it was obvious that there were remnants of core material in the structure. This was particularly apparent with the PE made from agarose cores as the tubes were stiff and are able to stand vertically without support during ESEM imaging, whilst the tubes made from chitosan cores had to lie flat. Different methods were used to dissolve the agarose remnants such as with 1-10M HCl, trypsin, DMSO as well as heating to 80^{o}C with these solvents overnight; however, the agarose remnants remained. Therefore, it was decided that is not the suitable core matieral, as it was difficult to control the manufacturing process and the level of remnants are high.

Confocal microscopy was used to monitor the wall thickness of chitosan cored PE structures as seen in Figures 7.6 and 7.7. Although both capsules and tubes with PSS and PAH as the start coating material had remnants of chitosan in its structure, it has been shown that chitosan hollow fiber membranes are relatively elastic (Modrzejewska & Eckstein 2004) and Figure 7.16 also show in that capsules with chitosan core still intact are elastic. Therefore, chitosan appears to be the more preferred core material, as there seem to be less remnants, it was easier to make, its solvent (acetic acid) is not cytotoxic, and it is relatively elastic.

To fully optimise the polyelectrolyte contractile scaffolds for this assay, cores which yield even less remnants and a smaller scaffold (but large enough for cells to grow on) would be preferable. This is because a smaller scaffold (by using a smaller core) would allow confocal microscopy to be used to monitor and record any three dimensional changes or deformation by cell contractions. A lower level of remnants may also enhance the compressibility and elasticity of the scaffold therefore allowing lower levels of contractile force to be detected and measured.

7.3.2 Optimised manufacturing process

The ideal scaffold should be vessel-like in order to imitate the physiological environment of vascular cells, be strong enough to allow handling of the scaffold, and be sufficiently elastic and deformable by cells contraction. Of course, cells must be able to adhere and grow on the scaffold material.

An open-ended, tubular format such as seen in the PE-PSS tube in Figure 7.6a seems to be the most vessel-like, however, when the level of core remnant was reduced such as in the PE-PAH tube, the lack of internal support collapses and flatten the structure. An alternative closed-ended rod format was also trialled in the hope that the fluid trapped inside the PE-PAH rod would give sufficient support such as in Figure 7.6b, however, these often collapses also. Therefore, a PE thin shell structure (base on the chitosan spheres) was chosen to provide a stable vessel-like structure with a lumen that did not collapse.

7.3.2.1 Feasibility of LBL coating at different pH

The LBL technique of alternating coatings of PSS and PAH is the standard approach to the building of PE structures. As already mentioned, there were chitosan remnants in the structure, and minimizing the level of remnants cab improved the elasticity or deformability of the scaffold. It was suspected that the poly-anion, PSS formed strong ionic bonds with chitosan because the amino group on the chitosan polymer carries a positive charge, it can form a stable complex with PSS which cannot be removed from the capsule wall. Therefore, it was considered that by having PAH in between PSS and chitosan, the level of chitosan remnants may be reduced.

However, since both chitosan and PAH are positively charged polymers, it is likely that the PAH would repel the chitosan core rather than adsorb on to it. A closer examination into the chemical properties of these polymers revealed that the acid dissociation constant (pKa) of chitosan is approximately 6.5 whilst it is 8.5 for PAH, so PAH is still strongly charged at pH 7 (Mermut et al. 2003b). Therefore, for the further construction of the vessel-like scaffolds an above neutral pH was chosen for the adsorption of PAH on to chitosan.

A very acidic pH is usually used for the LBL, hence the feasibility of using PE solutions at different pH was verified by examining the adsorption of PSS and PAH on to tissue culture plastic. Conventionally, PE adsorption is confirmed by determining the zeta potential of the thin film surface through streaming potential measurements, determining the film thickness through ellipsometry or identified by the alternation of water contact angle with each deposition (PAH have a higher water contact angle). In this thesis however, a much easier and less complicated method was developed.

This simple method involved the staining of the PE films with 1% Coomassie blue. Coomassie blue which has a slight negative charge will bind with PAH more so than to PSS, therefore, a high absorbance at 595nm would indicate the presence of the positively charged surface (PAH) whereas a low absorbance indicate a negatively charged surface (PSS).

As shown in Figure 7.2 that there were no significant differences between LBL coatings at different pH. Hence, PE-PAH capsules were made in a neutral environment and the suitability of this “improved” capsule was compared to the original PE-PSS capsules. Note that phenol red was used as the pH indicator as oppose to a pH measurement electrode, because the polyelectrolyte might coat and thereby damage the electrode with long term usage.

7.3.3 Characterisation of PE-PSS and PE-PAH Capsules

PE-PSS capsules made by conventional LBL adsorption in an acidic environment are significantly different to PE-PAH capsules as assessed by morphology, wall thickness, permeability and mechanical strength.

Just by visual observation, the PE-PAH capsules are less white and more translucent than PE-PSS capsules (Figure 7.3). Such differences can also be seen in the post-EMEM, collapsed capsules and rods (Figures 7.4). Confocal microscope was used to obtain optical sections of capsules stained with FITC-dextran 10S, and the average wall thickness was measured. However, there are inherent issues with using confocal images to quantify the sizes of samples, because the images generated are dependent on fluorescence. That is, material with similar thickness might appear very different if there is significant

difference in dye absorption. Therefore, physical sections were also used to ensure that the wall thickness measurements on the confocal images are real. The results in Figure 7.8 show that there was no significant difference between the wall thickness of optical and physical sections of PE-PAH capsules, but the PE-PSS capsule wall were significantly thicker.

Confocal microscopy shows that there was a difference in permeability between the PE-PSS and PE-PAH capsules (Figure 7.9). Although there was no significant difference between the fluorescent intensity after 5 minutes of incubation with FITC-dextran 10S, the immediate fluorescent intensity of PE-PAH capsules upon the dye addition is significantly higher. This may be attributed to the thicker wall of the PE-PSS capsules stopping the infiltration of the dye.

The mechanical properties between the PE-PSS and PE-PAH capsules also differ, with significantly more PE-PSS capsules surviving 1 cycle of ultrasonic treatment than the PE-PAH capsules (Table 7. 2). In order to estimate the elasticity of the capsules, osmotic stress is one of the simplest ways to apply a measurable stress on the capsules. Sucrose (Baumler et al. 2000) and PSS (Gao et al. 2001) had been used to create such stress as these are impermeable to most PE capsules. However, these were both permeable to the chitosan-core PE capsules, therefore unsuitable for elasticity measurements.

The compression – deformation curves shown in Figure 7.16 and 7.17 illustrate that the PE-PAH capsules are less firm than the PE-PSS capsules. This means that it would be easier for cells to deform PE-PAH than the PE-PSS capsules. The salt softening effect seen in other polyelectrolyte capsules (with melamine formaldehyde as core) (Heuvingh, Zappa & Fery 2005b; Lebedeva et al. 2005) were also observed in the PE-PAH capsules in HBS buffer.

Therefore, by coating the chitosan bead in a pH neutral environment and using PAH as the start coating material, relatively elastic PE-PAH capsules with significantly larger diameter, smaller wall thickness, higher permeability, lower mechanical strength were engineered.

7.3.4 Cell attachment or growth on PE-PAH capsule

Figures 7.12 and 7.13 show by ESEM that RAW cells ((Mouse leukaemic monocyte macrophage cell line) attached on to the agarose-core PE tubes, and 3T3-L1 and HEK-293 cells adhered to chitosan-core PE tubes. We expected to see similar for the PE-PAH capsules, however these collapsed whilst being imaged on the ESEM as shown in Figure 7.14a. This may be due lower internal pressure created by removing the internal fluid of the capsules, therefore imploding the thin-shell structure. Also the high voltage electron beam probably disintegrated the chitosan remnant. Although it looks like there may be cells on the PE-PAH capsules in Figure 7.14b, alternative methods were necessary to confirm the presence of cells.

Fluorescent and TEM images were taken on the physical sections of the capsules. Figure 7.15 show the TEM images of a 3T3-L1 cell seeded on the capsule and the high magnification image seem to show that there might be cell processes extending into the capsule wall. The TEM images also show that the capsule wall is porous and potentially spongy.

The 3T3-L1 cells seeded on the PE-PAH capsules were stained with a fixable vital stain, CFDA, and images from fluorescent microscopy clearly showed that the cells were live on the PE-PAH capsules. Surprisingly, it also shows that the walls of the PE-PAH capsules became auto-fluorescent during the sectioning process as shown in Figure 7.11.

7.3.5 PE-PAH capsule as a contraction scaffold

For an ideal contraction scaffold, cells contraction should be reflected by a reduction in area or preferably, volume, quantifiable over time. Ideally, contractile vascular cells such as smooth muscle and endothelial cells should be used. However, such cells were not available, hence the 3T3-L1 cells (sub-strain of the swiss 3T3 cell line) were used to establish and test the contractility assay method. It was reported that those fibroblast contract when stimulated with fetal bovine serum (FBS) (Nobe et al. 2003; Obara et al. 1995).

It was expected that as cells proliferate and contracts, we can observe a reduction in the area of the capsule over time. However, due to the large size of the capsules and the time it takes for the effects to be apparent, it was very difficult to image the capsules on the same focal plane. Therefore, a relaxation assay was pursued. It was expected that when the stress or contractile force exerted by cells on the capsules were removed, there would be an increase in the cross-sectional area of the capsule.

Two F-actin disruption drugs, forskolin and cytochalasin D were used to remove the stress exerted by the cells on the capsules. As shown in Figure 7.18, exposure to the F-actin disrupting drugs did increase the area of the capsules. However, it was noted that the two drugs exerted two significantly different magnitude of relaxation.

Fluorescent microscopy was used to examine the F-actin distribution upon exposure to the two different F-actin disruption drugs and and the results showed that forskolin and cytochalasin D have different effects on 3T3-L1 cells. Since cell contraction is dependent on the pull of actin filaments connected to the substrate, the segmentation of actin filaments induced by cytochalasin D (Figure 7.19c) obliterated the contractile force the 3T3-L1 cells exerted on the PE-PAH capsules. Although the F-actin filaments became diffused with 10μm forskolin incubation, some filaments can still be seen in Figure 7.19b. This suggests that the contractile force exerted by the 3T3-L1 cells were not completely obliterated therefore the “relaxation” of the capsules were not as high as Cytochalasin D.

Based on the change in area of the capsules elicited by the cells and the mechanical properties previously measured, it was estimated that the “relaxation” of the cells with 10μM forskolin and 10μM cytochalasin D relieved the capsules of 15.56±2.30μN and 45.66±2.30 μN of contracted force respectively. This equates to approximately 1.27±0.06nN and 2.96±0.14nN of force exerted by each cells, which are within the range (0.1nN-50nN) reported in the literature (Delvoye et al. 1991; Eastwood, McGrouther & Brown 1994; Freyman et al. 2001; Kasugai et al. 1990).

In conclusion, the contractility assay developed in this chapter is sufficiently sensitive to quantify the differential disruption to the actin cytoskeletin induced by forskolin compared to cytochalasin D.

7.4 References

Amiel, G.E., Komura, M., Shapira, O., Yoo, J.J., Yazdani, S., Berry, J., Kaushal, S., Bischoff, J., Atala, A. & Soker, S. 2006, 'Engineering Of Blood Vessels From Acellular Collagen Matrices Coated With Human Endothelial Cells', *Tissue Engineering*, vol. 12, no. 8, P. 2355.

Antipov, A.A., Shchukin, D., Fedutik, Y., Petrov, A.I., Sukhorukov, G.B. & Möhwald, H. 2003, 'Carbonate Microparticles For Hollow Polyelectrolyte Capsules Fabrication', *Colloids And Surfaces A: Physicochemical And Engineering Aspects*, vol. 224, no. 1-3, pp. 175-183.

Antipov, A.A. & Sukhorukov, G.B. 2004, 'Polyelectrolyte Multilayer Capsules As Vehicles With Tunable Permeability', *Advances In Colloid And Interface Science Plenary And Invited Lectures From The Xvith European Chemistry At Interfaces Conference, Vladimir, Russia, May 2003*, vol. 111, no. 1-2, pp. 49-61.

Baumler, H., Artmann, G., Voigt, A., Mitlohner, R., Neu, B. & Kiesewetter, H. 2000, 'Plastic Behaviour Of Polyelectrolyte Microcapsules Derived From Colloid Templates', *Journal Of Microencapsulation*, vol. 17, no. 5, pp. 651-655.

Boura, C., Menu, P., Payan, E., Picart, C., Voegel, J.C., Muller, S. & Stoltz, J.F. 2003, 'Endothelial Cells Grown On Thin Polyelectrolyte Mutlilayered Films: An Evaluation Of A New Versatile Surface Modification', *Biomaterials*, vol. 24, no. 20, pp. 3521-3530.

Buttafoco, L., Boks, N., Engubers-Buijtenhuijs, P., Grijpma, D.W., Poot, A., Dijkstra, P., Vermes, I. & Feijen, J. 2006, 'Porous Hybrid Structures Based On P(DLLA-*Co*-TMC) And Collagen For Tissue Engineering Of Small Diameter Blood Vessels', *Journal Of Biomedical Materials Research Part B: Applied Biomaterials*, vol. 79, no. 2, pp. 425-434.

Decher, G. 1997, 'Fuzzy Nanoassemblies: Toward Layered Polymeric Multicomposites', *Science*, vol. 277, no. 5330, pp. 1232-1237.

Delvoye, P., Wiliquet, P., Leveque, J.-L., Nusgens, B.V. & Lapiere, C.M. 1991, 'Measurement Of Mechanical Forces Generated By Skin Fibroblasts Embedded In A Three-Dimensional Collagen Gel', vol. 97, no. 5, pp. 898-902.

Du Roure, O., Saez, A., Buguin, A., Austin, R.H., Chavrier, P., Silberzan, P. & Ladoux, B. 2005, 'Force Mapping In Epithelial Cell Migration', *Proceedings Of The National Academy Of Sciences Of The United State Of America*, vol. 102, no. 7, pp. 2390-2395.

Dubreuil, F., Elsner, N. & Fery, A. 2003, 'Elastic Properties Of Polyelectrolyte Capsules Studied By Atomic-Force Microscopy And RICM', *Soft Matter And Biological Physics*, vol. 12, no. 2, pp. 215-221.

Eastwood, M., Mcgrouther, D.A. & Brown, R.A. 1994, 'A Culture Force Monitor For Measurement Of Contraction Forces Generated In Human Dermal Fibroblast Cultures: Evidence For Cell-Matrix Mechanical Signalling', *Biochimica Et Biophysica Acta (BBA) - General Subjects*, vol. 1201, no. 2, pp. 186-192.

Elsdale, T. & Bard, J. 1972, 'Collagen Substrata For Studies On Cell Behaviour', *Journal Of Cell Biology*, vol. 54, no. 3, pp. 626-637.

Freyman, T.M., Yannas, I.V., Yokoo, R. & Gibson, L.J. 2001, 'Fibroblast Contraction Of A Collagen-GAG Matrix', *Biomaterials*, vol. 22, no. 21, pp. 2883-2891.

Gao, C., Donath, E., Moya, S., Dudnik, V. & Mohwald, H. 2001, 'Elasticity Of Hollow Polyelectrolyte Capsules Prepared By The Layer-By-Layer Technique', *The European Physical Journal E: Soft Matter And Biological Physics*, vol. 5, no. 1, pp. 21-27.

Georgieva, R., Moya, S., Donath, E. & Baumler, H. 2004, 'Permeability And Conductivity Of Red Blood Cell Templated Polyelectrolyte Capsules Coated With Supplementary Layers', *Langmuir*, vol. 20, no. 5, pp. 1895-1900.

Gillies, M. & Su, T. 1993, 'High Glucose Inhibits Retinal Capillary Pericyte Contractility In Vitro', *Investigative Ophthalmology & Visual Science*, vol. 34, no. 12, pp. 3396-3401.

Harris, A., Wild, P. & Stopak, D. 1980, 'Silicone Rubber Substrata: A New Wrinkle In The Study Of Cell Locomotion.' *Science*, vol. 208, no. 4440, pp. 177-179.

He, W., Ma, Z., Yong, T., Teo, W.E. & Ramakrishna, S. 2005, 'Fabrication Of Collagen-Coated Biodegradable Polymer Nanofiber Mesh And Its Potential For Endothelial Cells Growth', *Biomaterials*, vol. 26, no. 36, pp. 7606-7615.

Heuvingh, J., Zappa, M. & Fery, A. 2005a, 'Salt Softening Of Polyelectrolyte Multilayer Capsules', *Langmuir*, vol. 21, pp. 3165-3171.

Heuvingh, J., Zappa, M. & Fery, A. 2005b, 'Salt Softening Of Polyelectrolyte Multilayer Capsules', *Langmuir*, vol. 21, no. 7, pp. 3165-3171.

Hughes, S.-J., Wall, N., Scholfield, C.N., Mcgeown, J.G., Gardiner, T.A., Stitt, A.W. & Curtis, T.M. 2004, 'Advanced Glycation Endproduct Modified Basement Membrane Attenuates Endothelin-1 Induced [Ca2+]I Signalling And Contraction In Retinal Microvascular Pericytes', *Molecular Vision*, vol. 10, pp. 996-1004.

Kasugai, S., Suzuki, S., Shibata, S., Yasui, S., Amano, H. & Ogura, H. 1990, 'Measurements Of The Isometric Contractile Forces Generated By Dog Periodontal Ligament Fibroblasts In Vitro', *Archives Of Oral Biology*, vol. 35, no. 8, pp. 597-601.

Kelley, C., D'Amore, P., Hechtman, H. & Shepro, D. 1987, 'Microvascular Pericyte Contractility In Vitro: Comparison With Other Cells Of The Vascular Wall', *Journal Of Cell Biology*, vol. 104, pp. 483-490.

Kent, M., Light, N. & Bailey, A. 1985, 'Evidence For Glucose-Mediated Covalent Cross-Linking Of Collagen After Glycosylation In Vitro', *Biochemistry Journal*, vol. 25, no. 3, pp. 745-752.

Lebedeva, O.V., Kim, B.-S., Vasilev, K. & Vinogradova, O.I. 2005, 'Salt Softening Of Polyelectrolyte Multilayer Microcapsules', *Journal Of Colloid And Interface Science*, vol. 284, no. 2, pp. 455-462.

Lin, Y., Wang, L., Zhang, P., Wang, X., Chen, X., Jing, X. & Su, Z. 2006, 'Surface Modification Of Poly(L-Lactic Acid) To Improve Its Cytocompatibility Via Assembly Of Polyelectrolytes And Gelatin', *Acta Biomaterialia*, vol. 2, no. 2, pp. 155-164.

Lulevich, V., Andrienko, D. & Vinogradova, O. 2004a, 'Elasticity Of Polyelectrolyte Multilayer Microcapsules', *Journal Of Chemical Physics*, vol. 120, no. 8, pp. 3822-3826.

Lulevich, V.V., Andrienko, D. & Vinogradova, O.I. 2004b, 'Elasticity Of Polyelectrolyte Multilayer Microcapsules', *The Journal Of Chemical Physics*, vol. 120, no. 8, pp. 3822-3826.

Martin, D.K. & Markhotina, N. 2003, *novel Screens To Identify Agents That Modulate Retinal Blood Vessel Function And Pericyte Function And Diagnostic And Therapeutic Application Therefor*, no WO03103771, World.

Mermut, O., Lefebvre, J., Gray, D. & Barrett, C. 2003a, 'Structural And Mechanical Properties Of Polyelectrolyte Multilayer Films Studied By AFM', *Macromolecules*, vol. 36, pp. 8819-8824.

Mermut, O., Lefebvre, J., Gray, D.G. & Barrett, C.J. 2003b, 'Structural And Mechanical Properties Of Polyelectrolyte Multilayer Films Studied By AFM', *Macromolecules*, vol. 36, no. 23, pp. 8819-8824.

Modrzejewska, Z. & Eckstein, W. 2004, 'Chitosan Hollow Fiber Membranes', *Biopolymers*, vol. 73, no. 1, pp. 61-68.

nobe, H., nobe, K., Fazal, F., De Lanerolle, P. & Paul, R.J. 2003, 'Rho Kinase Mediates Serum-Induced Contraction In Fibroblast Fibers Independent Of Myosin LC20 Phosphorylation', *American Journal Of Physiology: Cell Physiology*, vol. 284, no. 3, pp. C599-606.

Obara, K., Nikcevic, G., Pestic, L., nowak, G., Lorimer, D.D., Guerriero, V., Jr., Elson, E.L., Paul, R.J. & Lanerolle, P.D. 1995, 'Fibroblast Contractility Without An Increase In Basal Myosin Light Chain Phosphorylation In Wild Type Cells And Cells Expressing The Catalytic Domain Of Myosin Light Chain Kinase', *Journal Of Biological Chemistry*, vol. 270, no. 32, pp. 18734-18737.

Park, J., Ryu, J., Choi, S.K., Seo, E., Cha, J.M., Ryu, S., Kim, J., Kim, B.-S. & Lee, S.H. 2005, 'Real-Time Measurement Of The Contractile Forces Of Self-Organized Cardiomyocytes On Hybrid Biopolymer Microcantilevers', *Analytical Chemistry*, vol. 77, no. 20, pp. 6571-6580.

Pournaras, C.J., Rungger-Brändle, E., Riva, C.E., Hardarson, S.H. & Stefansson, E. 2008, 'Regulation Of Retinal Blood Flow In Health And Disease', *Progress In Retinal And Eye Research*, vol. 27, no. 3, pp. 284-330.

Proctor, D.N. & Parker, B.A. 2006, 'Vasodilation And Vascular Control In Contracting Muscle Of The Aging Human', *Microcirculation*, vol. 13, no. 4, pp. 315-327.

Segal, S.S. 1994, 'Cell-To-Cell Communication Coordinates Blood Flow Control', *Hypertension*, vol. 23, no. 6, pp. 1113-1120.

Segal, S.S. 2005, 'Regulation Of Blood Flow In The Microcirculation', *Microcirculation*, vol. 12, no. 1, pp. 33-45.

Shen, J.Y., Chan-Park, M.B., He, B., Zhu, A.P., Zhu, X., Beuerman, R.W., Yang, E.B., Chen, W. & Chan, V. 2006, 'Three-Dimensional Microchannels In Biodegradable Polymeric Films For Control Orientation And Phenotype Of Vascular Smooth Muscle Cells', *Tissue Engineering*, vol. 12, no. 8, P. 2229.

Takei, T., Yamaguchi, S., Sakai, S., Ijima, H. & Kawakami, K. 2007, 'novel Technique For Fabricating Double-Layered Tubular Constructs Consisting Of Two Vascular Cell Types In Collagen Gels Used As Templates For Three-Dimensional Tissues', *Journal Of Bioscience And Bioengineering*, vol. 104, no. 5, pp. 435-438.

Tryoen-Tóth, P., Vautier, D., Haikel, Y., Voegel, J.-C., Schaaf, P., Chluba, J. & Ogier, J. 2002, 'Viability, Adhesion, And Bone Phenotype Of Osteoblast-Like Cells On Polyelectrolyte Multilayer Films', *Journal Of Biomedical Materials Research*, vol. 60, no. 4, pp. 657-667.

Vautier, D., Karsten, V., Egles, C., Chluba, J., Schaaf, P., Voegel, J.-C. & Ogier, J. 2002, 'Polyelectrolyte Multilayer Films Modulate Cytoskeletal Organization In Chondrosarcoma Cells', *Journal Of Biomaterials Science, Polymer Edition*, vol. 13, pp. 712-731.

Yang, J., Motlagh, D., Webb, A.R. & Ameer, G.A. 2005, 'novel Biphasic Elastomeric Scaffold For Small-Diameter Blood Vessel Tissue Engineering', *Tissue Engineering*, vol. 11, no. 11-12, pp. 1876-1886.

Chapter 8: Conclusion and Future Perspective

The underlying theme of this thesis is cellular contractility. As was suggested in the introduction, this thesis reports an investigation conducted from the perspective of the "bedside" to the "bench". That is, from an economic evaluation of a medical intervention to basic research and development of a contractility assay. The thesis was stimulated by our laboratory's work in the microvascular complications of diabetic retinopathy.

8.1 Health Economic Perspective

The health economic perspective of this thesis aimed to determine whether the prog-DR test is worthwhile. It involved Markov modelling of DR progression, costs and utility as shown in Chapter 3. The results (reported in Chapter 4) showed that early DR diagnosis, such as would be achieved with the use of the prog-DR test would improve the number of life years, sight years and quality – adjusted life years of screened subjects. The prog-DR test would be cost effective relative to the benchmark of annual or bi-annual DR screening (Vijan, Hofer & Hayward 2000); with incremental cost effectiveness ratios (ICERs) within an acceptable range (above the $50,714 threshold and below the $91,705 reject cut-off) as determined by decisions made by PBAC (George, Harris & Mitchell 2001) and comparable to the ICERS for average medical interventions submitted to PBAC for review and recommendation (Harris et al. 2008). Scenario and sensitivity analysis also showed that the cost effectiveness of the prog-DR test would be improved by i) better blood glucose management post prog-DR test, (ii) targeted screening (as opposed to population-wide screening) and (iii) reduced costs of both screening and management of DM and DR.

Although the results presented here are very encouraging, it is important to note the limitations of the Markov model and that further research is necessary (namely, a randomised clinical trial). An RCT to assess the safety and clinical efficacy of the prog-DR test would be essential before it could be made available to the public. Information collected through an RCT can also be used to "fill in the gaps" of the model. For example, such information could be used

to update the DR progression data which were based on reports published prior to 2000 as well as use information about quality of life of directly collected from research subjects as opposed to using the QoL scores collected from subjects in other research studies which were used in the model.

The adoption and implementation of the prog-DR test by service providers will depend on various factors. The Markov model for DR progression shows that the patient's condition will be improved; therefore it may be assumed that ophthalmologists and optometrists will accept that the screening test is efficacious. However, acceptance of efficacy does not equate to immediate implementation. For example, the majority of ophthalmologists and optometrists agree that the NHMRC Clinical Practice Guideline for the Management of Diabetic Retinopathy (National Health and Medical Research Council 1997) was just right (McCarty et al. 2001), yet a large percentage of ophthalmologists had not completely read the guideline more than a year after its implementation. This is because the problem confronting providers faced with new technology may not be whether to adopt the new technology or not, but whether to defer adoption or not (Hall & Khan 2003). Unfortunately, the diffusion of new technology "usually appears as a continuous and rather slow process" (Hall & Khan 2003).

The accessibility of the prog-DR test by patients will be dependent on the availability and number of ophthalmologist and optometrists in Australia. There are over 1500 optometry businesses (McLennan 1999) and over 700 ophthalmology practicing sites in Australia and most of these are in capital cities (Australian Medical Workforce Advisory Committee 1996) which people can access. However, there are only 2.3 ophthalmologists (Trewin 2003) and 15.7 optometrists per 100,000 people in Australia (McLennan 1999). The average number of consultations for optometrist is around 40 per week (McLennan 1999), which approximate to 2000 consultations each year and ophthalmologists perform roughly 3945 services each year (Australian Medical Workforce Advisory Committee 1996). Although 3800 per 100,000 are diagnosed diabetics and 0.8% or 800 per 100,000 are partially or completely blind, there are obviously not enough optometrists and ophthalmologists to

service and screen the whole of the Australian population especially when the demand for medical attention is expected to increase with the aging of the population. Therefore, this novel prognostic test may have to be used as a supplementary diagnostic tool unless the number of ophthalmologists and optometrists is increased.

In conclusion, a Markov model of DR progression was built. It can be used to predict the progression of DR, quality of life, and costs and to assess the relative cost-effectiveness and cost-utility of alternative strategies for the prevention and treatment of DR. The economic evaluation of the Prog-DR test showed that early diagnosis of DR increases the quantity and quality of the life of subjects who are at risk of developing DM and DR. Although there are uncertainties surrounding making this novel prognostic test available to the Australian population, the results thus far are encouraging.

8.2 Physiological Perspective

The physiological perspective of this thesis aimed to develop a cell contractility assay that utilised a 3D scaffold in order to more closely model the physiological conditions, so that the attenuated contractile response observed by the prog-DR test can be fully elucidated.

Chapter 6 investigated the cyto-biocompatibility of the scaffold material candidates PSS and PAH, with Ti and TiN thin films as comparators, on 3T3-L1, HEK-293 and SaOS-2 cells and can be used to further research in the area of biomaterial and bio-mimetic. Specifically, the work with Ti and TiN thin films may be most useful in the development of dental and osteo implants.

In Chapter 7, a 3D, hollow scaffold (PE-PAH capsule) was constructed and the feasibility to use this scaffold as a contractility assay was investigated. The development of this scaffold involved (i) the selection of the optimal core material, (ii) optimisation of the manufacturing process, (iii) characterisation of the scaffold and (iv) ensuring that cells can be grown on it. The contractility assay was sufficiently sensitive to discriminate the change in force due to disruption of the actin cytoskeleton by forskolin and cytochalasin D

Although an adequate scaffold was engineered for the contractility assay, further work is still necessary to improve and optimise the system. The PE-PAH capsules developed were millimetre in diameter so that it can only be observed on standard 2-dimensional microscopy under low magnification, whereas it would be preferable to utilise a 3-dimensional system such as a confocal microscope. It would be preferable for these PE-PAH capsules to be smaller (e.g. up to 100μm in diameter but large enough for cells to grow on) so that cell contraction and deformation of the capsule can be observed by confocal microscopy in three dimensions or even by flow cytometry. It would also be ideal if the scaffold resembled a capillary, that is, tubular and hollow in structure, for microvascular cell research. The PE-PAH capsule contractility assay presented here is affordable, easy to make and quantifiable. The results shown in this thesis also proves that it is feasible to use PE to engineer such a system, and has set the groundwork for optimising the assay for microvascular cell contraction research.

Once this contraction assay is finally optimised, it can be use to investigate the contraction and relaxation of a range of cell type. Specifically for the application for the prog-DR test, the response of vascular cells (pericytes, endothelial and smooth muscle cells) to a range of drugs may be screened to identify the most appropriate stress drug, which may be the most potent drug or the drug which elicit the most dramatic response. The sensitivity of the vascular cells to different level of glucose concentration can also be assessed, to identify the threshold and or pathways by which high glucose concentration damages the contractile function of the cells.

In conclusion, the effects of polyelectrolyte thin films on a range of cell lines were characterised. This information is useful in the field of biomaterial research and was used to develop a 3D, hollow scaffold for the use as a contractility assay. Although this contractility assay requires optimisation, the results thus far are encouraging and the application of this assay will be very useful in the understanding of vascular cell contraction and relaxation and important for the advancement of the prog-DR test.

8.3 References

Australian Medical Workforce Advisory Committee 1996, *The Ophthamology Workforce In Australia*, Sydney.

George, B., Harris, A. & Mitchell, A. 2001, 'Cost-Effectiveness Analysis And The Consistency Of Decision Making: Evidence From Pharmaceutical Reimbursement In Australia (1991 To 1996)', *Pharmacoeconomics*, vol. 10, no. 11, pp. 1103-1109.

Hall, B. & Khan, B. 2003, *Adoption Of New Technology*, Berkeley.

Harris, A.H., Hill, S.R., Chin, G., Li, J.J. & Walkom, E. 2008, 'The Role Of Value For Money In Public Insurance Coverage Decisions For Drugs In Australia: A Retrospective Analysis 1994-2004.' *Medical Decision Making*, vol. 28, no. 5, pp. 713-723.

Mccarty, C.A., Taylor, K.I., Mckay, R. & Keeffe, J.E. 2001, 'Diabetic Retinopathy: Effects Of National Guidelines On The Referral, Examination And Treatment Practices Of Ophthalmologists And Optometrists', *Clinical And Experimental Ophthalmology*, vol. 29, no. 2, pp. 52-58.

Mclennan, W. 1999, *Optometry And Optical Dispensing Services*, Australian Bureau Of Statistics, Canberra.

National Health And Medical Research Council 1997, *Management Of Diabetic Retinopathy*.

Trewin, D. 2003, *Australian Social Trend 2003*, The Australian Bureau Of Statistics, Canberra.

Vijan, S., Hofer, T.P. & Hayward, R.A. 2000, 'Cost-Utility Analysis Of Screening Intervals For Diabetic Retinopathy In Patients With Type 2 Diabetes Mellitus', *Journal Of The American Medical Association*, vol. 283, no. 7, pp. 889-896.

Appendices

Appendix A: Univariate sensitivity analysis on health outcomes and costs

	LY	SY	QALY	Cost
Prevalence				
Pre-DM	-8.33 (8.33) *	-8.44 (8.44) *	-8.38 (8.38) *	-4.04 (4.04)
DM	-1.67 (1.67)	-1.56 (1.56)	-1.62 (1.62)	-4.19 (5.88)
Obesity	0.03 (-0.03)	0.06 (-0.06)	0.04 (-0.04)	0.15 (-1.55)
Rate for				
Laser treatment need	-0.00 (0.00)	0.01 (-0.01)	-0.00 (0.00)	-0.10 (0.14)
Laser treatment success	0.00 (0.00)	-0.00 (0.00)	0.00 (0.00)	0.86 (0.83)
DM diagnosis	-0.00 (0.00)	-0.01 (0.01)	-0.03 (0.03)	-0.28 (2.0)
Costs				
Blood glucose management				-1.57 (1.63)
Eye examination				0.45 (1.23)
Laser Treatment				0.84 (0.85)
Blindness				-7.15 (8.84) *
Total costs				-9.96 (10.02) *

Table A.1: Univariate Sensitivity Analysis on health outcomes and costs. Table shows the percentage change in health outcomes or costs, with a 10% increase or decrease (in brackets) in parameters. * indicates elasticity.

Appendix B: Sensitivity analysis on health outcomes, costs and incremental cost effectiveness ratio

Parameters	Level of Change	The change in				
		LY gained	SY gained	QALY gained	Cost ('000,000)	Cost per QALY
Prevalence of pre-DM	+10%	10,614	27,166	38,144	1,879	49,262
	-10%	9,332	24,077	34,058	1,677	49,247
Prevalence of DM	+10%	10,304	26,620	37,645	1,849	49,103
	-10%	9,651	24,633	34,559	1,740	50,341
Prevalence of Obesity	+10%	10,332	26,307	36,672	1,799	49,054
	-10%	9,599	24,944	35,518	1,789	50,364
Need for laser treatment	+10%	9,918	25,733	35,951	1,879	52,277 *
	-10%	9,935	25,484	36,183	1,885	52,085 *
Blindness QoL scores	0.26	-	-	42,044	-	42,958
Discount rate	5%	8,655	22,301	31,583	1,745	55,252 *
	7%	7,555	19,493	27,762	1,556	56,032 *
Laser Treatment Success rate	+10%	9,957	25,647	36,090	1,806	50,038
	-10%	9,946	25,596	36,076	1,806	50,074
Diabetes Diagnosis rate	+10%	9,825	25,196	34,724	1,747	50,322
	-10%	10,118	26,083	37,545	1,842	49,073

Table B.1: Summary of the percentage change in life years, sight years, QALYs, costs and cost per QALY with a 10% change in parameters (unless otherwise indicated). A positive reading indicates an increase whereas a negative reading indicates a decrease in the outcome measure. * indicates the cost per QALY is above the lower limit of the implicit PBAC threshold ($50,714). There was no cost per QALY values above the higher limit of the implicit PBAC threshold ($91, 7268) and significant decrease in the probability of acceptance (6% or more) by PBAC. Numbers are rounded to five significant figures.

Parameters	**Level of Change**	**The change in Cost per QALY**
Annual total cost	+10%	57,373 * #
	-10%	46,942
Pre-DR screening cost	+10%	50,809 *
	-10%	48,598
Blood glucose control cost	+10%	56,989 * #
	-10%	47,326
Routine eye examination costs	+10%	49,866
	-10%	49,541
Laser Treatment costs	+10%	49,705
	-10%	49,702
Blindness costs	+10%	48,817
	-10%	50,589 *

Table B.2: Summary of the percentage change in cost per QALY with a 10% change in cost parameters. A positive reading indicates an increase whereas a negative reading indicates a decrease in the outcome measure. * indicates the cost per QALY is above the lower limit of the implicit PBAC threshold ($50,714). There was no cost per QALY values above the higher limit of the implicit PBAC threshold ($91, 7268). # indicates the cost per QALY would significant decrease in the probability of acceptance (6% or more) by PBAC. Numbers are rounded to five significant figures

Appendix C: Stimulation of microvascular cells

Microvascular cells were stained for intracellular free calcium with calcium orange.AM (Invitrogen C-3015) which is important for cellular contraction and monitored confocal microscopy (FE300, Olympus). As shown in Figure A.1, upon stimulation with buffer with high (100mM) potassium levels at 0 second, the calcium level rises immediately, plateaus and then drops in cells in the vascular/tubular format, whereas in cells in monolayers, the calcium levels fluctuate before rising and falling.

Upon stimulation with 10μm Glibenclamide as shown in Figure A.2, the calcium levels slowly rises in cells in the vascular/tubular format whereas it falls before rising in cells in monolayers. The level of intracellular calcium also maintain at a higher levels in cells in the vascular/tubular format as compared to cells in monolayers.

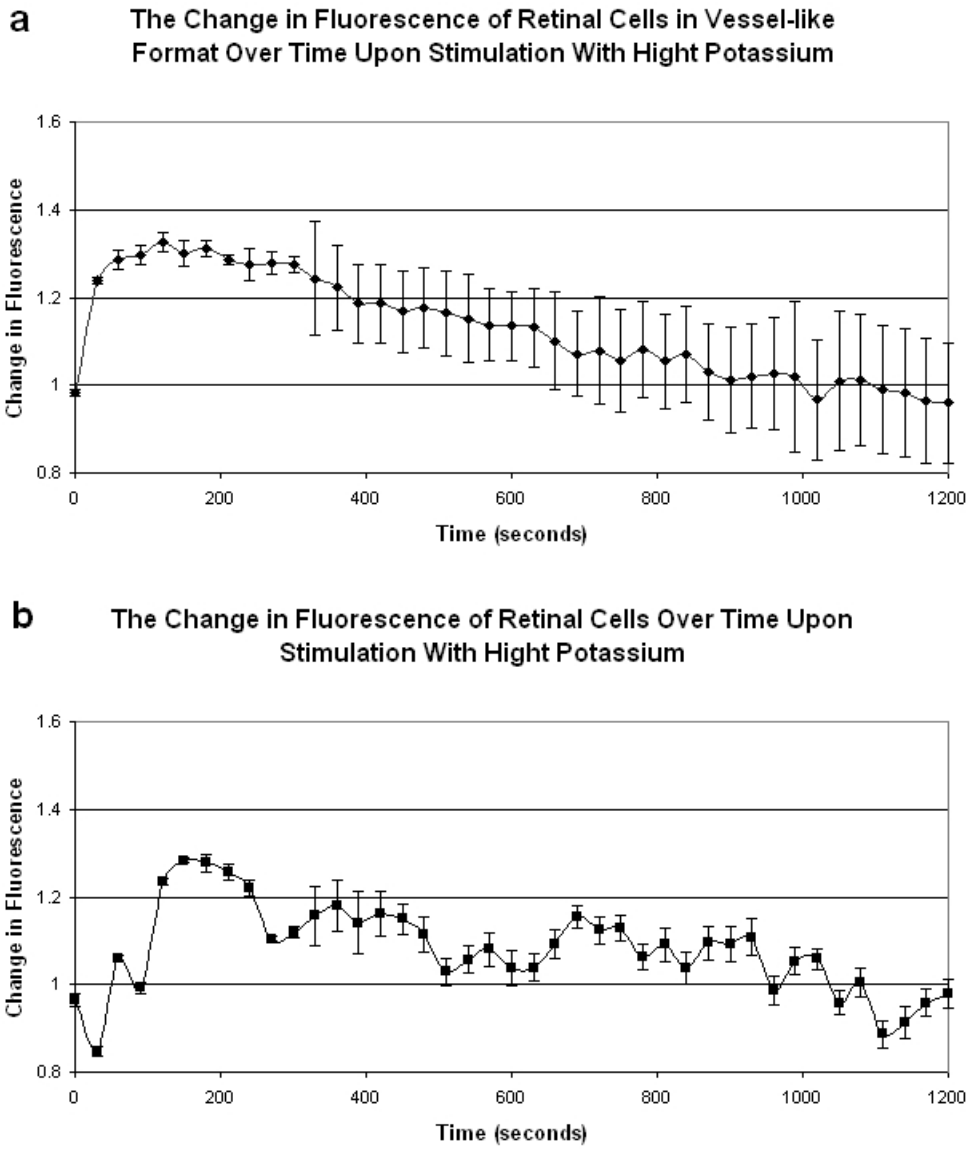

Figure C.1: The change in free intracellular calcium levels upon high potassium in retinal microvascular cells over time. The change in intracellular free calcium is reflected by the change in fluorescence intensity of calcium orange. It was monitored by the Olympus FE300 confocal microscope and the fluorescence intensity was measured using Olympus Fluoview 300. Error bars represents standard error.

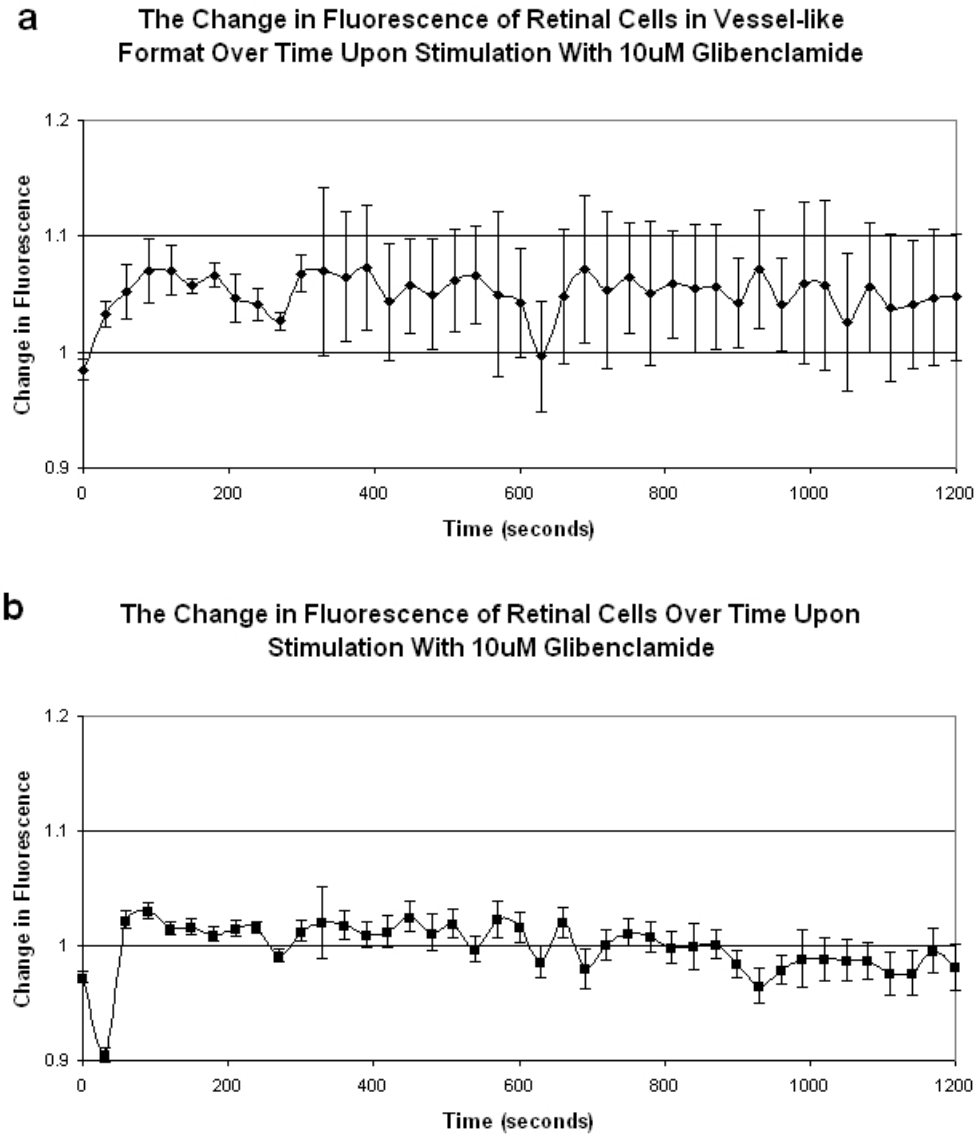

Figure C. 2: The change in free intracellular calcium levels upon 10μm Glibenclamide in retinal microvascular cells over time. The change in intracellular free calcium is reflected by the change in fluorescence intensity of calcium orange. It was monitored by the Olympus FE300 confocal microscope and the fluorescence intensity was measured using Olympus Fluoview 300. Error bars represents standard error.

Appendix D: The costs of a contraction assay composed of collagen as compared to polyelectrolyte

	Collagen	poly(sodium 4-styrene sulfonate) (PSS)	Poly(allylamine hydrochloride) (PAH)
Source (Sigma Aldrich)	C9791-250mg	243051-100g	283215-5g
Price per 100g	$1476	$0.59	$25.6
Price per assay	$2.95 - $5.90 [a]	$0.42 [b]	

Table D.1: The prices of collagen and polyelectrolyte. [a] Based on the assumption that the collagen concentration used range from 1-2mg/mL and the collagen substrate is 2mL in volume (Chen et al. 2007). [b] Based on the assumption that the core material is 2mL in volume and polyelectrolyte solution of twice this volume was used per coating and a total of 8 polyelectrolyte layers was adsorbed.

Appendix E: Cell cycle analysis of 3T3-L1 and HEK-293 cells

Cells were seeded at 250,000 cells per 25cm^2 tissue culture flasks and grown for 2 days. Cells were then lifted by Trypsin-EDTA (Sigma T4299) treatment and stained with a cell cycle analysis solution for at least 1 hour (40µg/mL PI, 0.1% triton X-100, 10µg/mL RNAse and 0.1% BSA in PBS). BD FACSCalibur^{TM} flow cytometer was used scan and collect the cell data. The WinMDI 2.8 software was used to generate flow cytometry data and the Cylchred 1.0.2 software was used to estimate the proportion of cells in the different cell cycle stages.

Cell cycle of the 3T3-L1 and HEK-293 cells were measured by flowcytometry on day 3, and there were no significant differences found between the tissue culture plastic (TCP), PSS and PAH thin films as shown in Figure B.1.

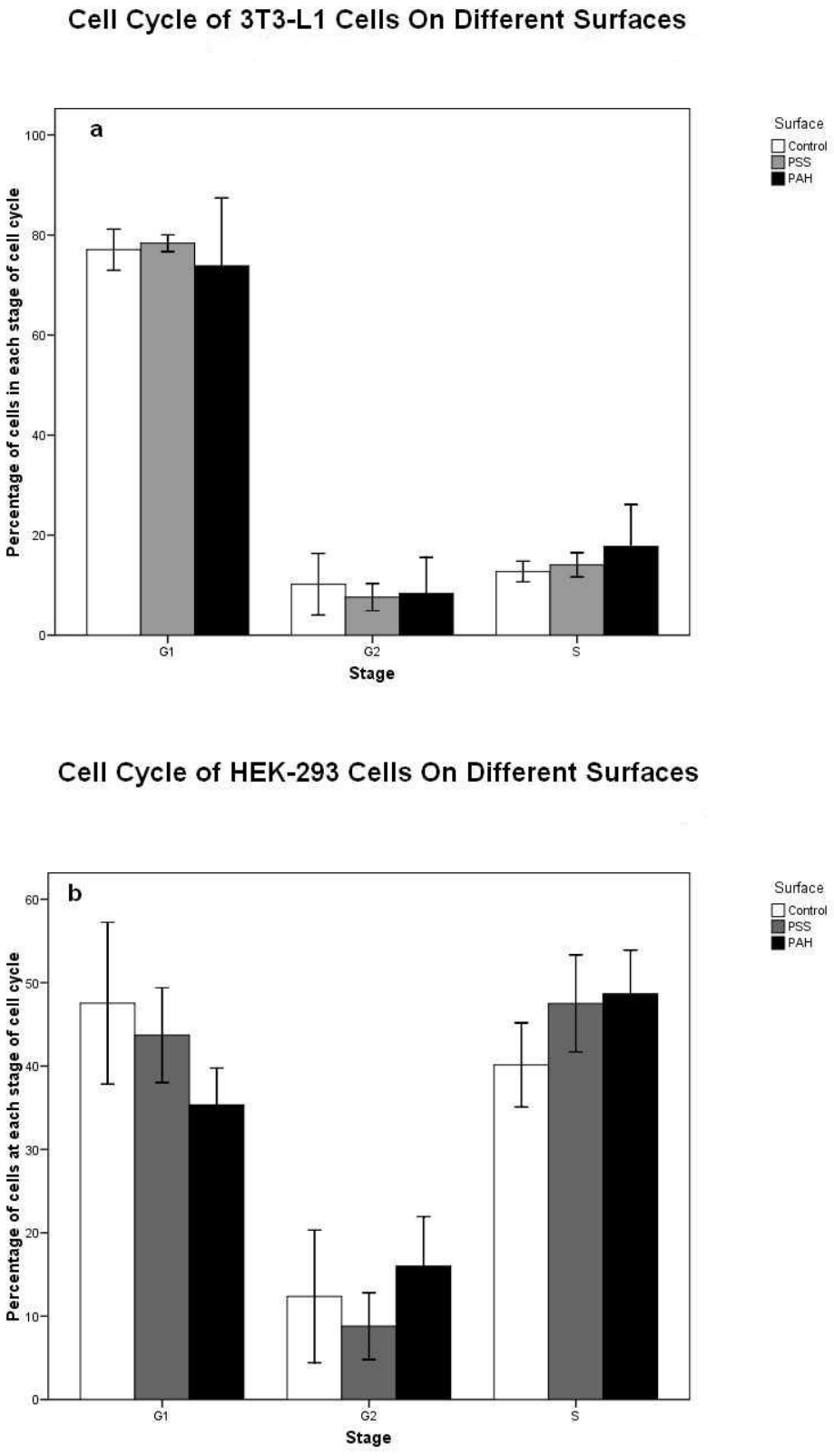

Figure E.1: The proportion of 3T3-L1 (a) and HEK-293 (b) cells at different stages of cell cycle on TCP, PSS and PAH thin films on day 3 as measured by flowcytometry. Error bars represents the standard error.